

# **Developing a Framework for Improving the Accuracy of Process-based LCA for Energy Pathways**

by

Giovanni Roberto Di Lullo

A thesis submitted in partial fulfillment of the requirements for the degree of

Doctor of Philosophy

in

Engineering Management

Department of Mechanical Engineering

University of Alberta

© Giovanni Roberto Di Lullo, 2022

## Abstract

Life cycle assessment (LCA) is becoming a popular tool to quantify environmental impacts including greenhouse gas (GHG) emissions. Because of the high number of assumptions and low quality of available data, the results of LCA are often viewed with skepticism. It is common for studies to provide deterministic point estimates and a limited sensitivity analysis and not account for uncertainty in the data and assumptions used, which can also lead to a lack of confidence in the results. In order to further increase the usefulness of LCA results for decision makers, a robust methodological framework that can be used to accurately quantify uncertainties and communicate results is needed. Furthermore, obtaining accurate data of certain industrial activities requires complex engineering models that have long computing times, are difficult for non-experts to use, and may contain confidential data. Proxy modeling is investigated here to create an accurate, easy-to-use, black-box model that can be easily shared.

A survey of the existing literature was performed to examine how practitioners are currently implementing sensitivity and uncertainty. The survey found sensitivity and uncertainty analyses were inconsistent and basic, and the methods/assumptions lacked proper justification. Multiple sensitivity and uncertainty methods were investigated, leading to the development of the Regression, Uncertainty, and Sensitivity Tool (RUST) and framework. The Morris and Sobol global sensitivity methods used in RUST were examined to determine whether they can accurately identify the key inputs that have the largest effect on overall output variance. RUST was validated using the previously published **FUNdamental ENgineering PrinciplEs-based Model for Estimation of GreenHouse Gases in Conventional Crude Oils and Oil Sands**

(FUNNEL-GHG-CCO/OS) and FUNNEL-GHG-Natural Gas Transmission Lines (NGTL) as case studies. After reviewing multiple proxy modeling methods, quadratic and artificial neural network (ANN) regression proxy models were investigated to create an accurate, easy-to-use black-box model that can be easily shared. Generating target values needed for training from the engineering software can be time consuming; hence, adaptive sampling methods were examined (random, spread, high error, and 50/50 random/high error).

It was found that while both the Morris and Sobol methods can identify the key parameters, the Morris method requires fewer than 1/100<sup>th</sup> as many model evaluations as Sobol. RUST and the corresponding framework can be used to improve the quality of the LCA and reduce the time required by the practitioner. Quadratic proxy modeling works well for models that exhibit nearly linear behavior, but the ANN proxy models are superior for iterative non-linear models.

The results found that ANN proxy models are more accurate than quadratic regression, and the high error sampling method reduced the maximum error but increased the average error. Because of uncertainty in LCA input values, reducing average error is less valuable than reducing extreme errors. The regression model can be easily published, it does not require a large effort to make a user-friendly version of the model, and it conceals confidential data if necessary. The simplified model makes it easy for policy makers to investigate how changes in critical parameters affect LCA results without having to learn how to use the full complex model.

## Preface

This dissertation is original work by Giovanni Di Lullo under the supervision of Dr. Amit Kumar.

Chapter 2 and Appendix A were submitted as Di Lullo, Gemechu, Oni and Kumar, “A survey of how practitioners implement sensitivity and uncertainty analysis in life cycle assessments of energy systems.” Submitted to *International Journal of Life Cycle Assessments* Oct 25, 2021.<sup>1</sup>

Work published as Di Lullo, Gemechu, Oni and Kumar, “Extending sensitivity analysis using regression to effectively disseminate life cycle assessment results.” *International Journal of Life Cycle Assessments*. **2019**, 25, 222-239. DOI: 10.1007/s11367-019-01674-y was split between Chapters 3 & 4 and Appendix C.<sup>2</sup>

Work published as Di Lullo, Oni, Gemechu and Kumar, “Developing a greenhouse gas life cycle assessment framework for natural gas transmission pipelines.” *Journal of Natural Gas Engineering*. **2020**, 75, 103136. DOI: 10.1016/j.jngse.2019.103136, Di Lullo, Oni and Kumar, Blending blue hydrogen with natural gas for direct consumption: Examining the effect of hydrogen concentration on transportation and well-to-combustion greenhouse gas emissions. *International Journal of Hydrogen Energy* **2021**, 46, (36), 19202-19216. DOI:10.1016/j.ijhydene.2021.03.062, and <sup>3</sup> were used in Chapter 3 and Appendix B.<sup>4,5</sup>

Chapter 5 and Appendix D will be submitted to *Energy Conversion and Management* as Di Lullo, Oni and Kumar, “Using proxy models and adaptive sampling to integrate complex engineering models into life cycle assessments of energy systems.”

Giovanni was responsible for the concept formulation, data collection, model development and validation, and manuscript composition. Dr. Abayomi Olufemi Oni and Dr. Eskinder Gemechu contributed to model validation, assessment of results, and manuscript edits. Dr. Amit Kumar was the supervisory author and was involved with concept formulation, evaluation, assessment of results, and manuscript edits.

## **Dedication**

This dissertation is dedicated to the memory of Nonna Anna Di Lullo who taught me the importance of taking care of those around you and not letting personal hardships blind you to the suffering of others.

For my father who encouraged curiosity and a joy for science. I will always remember building a hovercraft for the elementary school science fair. For my mother for teaching me the joy of reading and hard work.

This dissertation is also dedicated to my wife Elianna who encouraged me to pursue my dreams and was a constant support throughout my degree. When I stumbled, she was always there to encourage me to keep going.

## Acknowledgments

I would like to thank the following people who have helped me undertake this research:

Prof. Amit Kumar for his guidance and support through my graduate degree and in helping me explore different potential career paths. I appreciate the multiple opportunities I have had to engage with industry and government representatives through his research projects.

Postdoctoral fellow Dr. Abayomi Olufemi Oni for his advice and guidance throughout my degree. He has helped me get back on track after getting stuck on a problem or having a hard time figuring out how to present my findings. His encouragement and support have helped me share my knowledge with my research group and industry, increasing the impact of my work.

Postdoctoral fellow Dr. Eskinder Gemechu for his advice and guidance on how to frame my writing and analyses for different audiences. Our differing academics backgrounds helped me see our work from a different perspective.

Astrid Blodgett for editorial assistance and for helping improve my writing over the years.

I would like to acknowledge my colleagues at the University of Alberta for their feedback, advice, and support.

I thank the NSERC/Cenovus/Alberta Innovates Associate Industrial Research Chair in Energy and Environmental Systems Engineering and the Cenovus Energy Endowed Chair in Environmental Engineering for providing financial support for this project. As a part of the University of Alberta's Future Energy Systems research initiative, this research was made possible in part thanks to funding from the Canada First Research Excellence Fund. I also received financial scholarship support from the Natural Sciences and Engineering Research Council of Canada (NSERC) in the form of a postgraduate doctoral scholarship.

Cette recherche a été financée par le Conseil de recherches en sciences naturelles et en génie du Canada (CRSNG).

# Table of Contents

Abstract.....	ii
Preface.....	iv
Dedication.....	v
Acknowledgments.....	vi
Table of Contents.....	vii
List of Tables .....	x
List of Figures.....	xi
1 Introduction.....	1
1.1 Background and Motivation.....	1
1.2 Research Gaps .....	3
1.3 Objectives.....	5
1.4 Scope, Challenges, and Limitations .....	6
1.5 Organization of the Report.....	8
2 A Survey of How Practitioners Implement Sensitivity and Uncertainty Analysis in Life Cycle Assessments of Energy Systems.....	10
2.1 Introduction .....	10
2.2 Background .....	13
2.2.1 Terminology clarification .....	13
2.2.2 Local vs. global sensitivity .....	15
2.2.3 Uncertainty analysis.....	16
2.3 Literature Survey Method .....	18
2.4 Results and Discussion.....	21
2.4.1 Sensitivity analysis.....	22
2.4.2 Uncertainty analysis.....	24
2.4.3 Limitations and areas for improvement in current work .....	32
2.5 Conclusion.....	49
3 Development of the Regression, Uncertainty, and Sensitivity Tool (RUST).....	51
3.1 Introduction .....	51
3.2 Method .....	52
3.2.1 Sensitivity screening methods.....	53
3.2.2 Case studies.....	58
3.3 The general flow equation is used to calculate the pressure drop along the pipeline from friction and elevation losses. <sup>157, 158</sup> The flow rate split between parallel pipes uses the Newton-Raphson method; hence, the partial derivative of pressure drop with respect to the flow rate is also calculated. An iterative approach is used to calculate the average temperature, pressure, and compressibility factors. The average temperature is calculated by accounting for heat loss to the ground and the effect of expansion cooling. See Appendix B for additional details on the calculations used. The NGTL paper examined the Alliance and Prince Rupert transmission	

pipelines, see Chapter 3.3.5.3 for a description of the two pipeline systems. <sup>4</sup> Results and Discussion .....	61
3.3.1 Application of Morris method .....	61
3.3.2 Application of the Sobol method .....	62
3.3.3 Morris vs. Sobol for screening purposes.....	63
3.3.4 RUST summary .....	65
3.3.5 Qualitative results .....	66
3.4 Conclusion.....	75
4 Development of Proxy Models with Linear Regression.....	76
4.1 Introduction .....	76
4.2 Method .....	77
4.2.1 Identifying critical parameters .....	78
4.2.2 Developing the regression model.....	78
4.2.3 Validating the regression model .....	81
4.2.4 Developing and validating the regression model process.....	82
4.2.5 Model template .....	83
4.2.6 Case study .....	84
4.3 Results and Discussion.....	84
4.3.1 Validating the regression model form.....	86
4.3.2 High-level checks.....	87
4.3.3 Overfitting checks .....	88
4.3.4 Checking model response .....	89
4.3.5 Final regression models .....	90
4.4 Conclusion.....	91
5 Development of Artificial Neural Network-based Proxy Models for Life Cycle Assessment of Energy Pathways .....	93
5.1 Introduction .....	93
5.2 Methods.....	95
5.2.1 Case studies.....	96
5.2.2 Standardized validation set .....	96
5.2.3 Defining model accuracy .....	97
5.2.4 Regression methods .....	97
5.2.5 Evaluation methods.....	98
5.2.6 Experimental methods .....	100
5.2.7 Sampling methods.....	100
5.3 Results and Discussion.....	105
5.3.1 Quadratic regression .....	105
5.3.2 ANN regression .....	106
5.3.3 Time required.....	115

5.3.4	Future improvements .....	117
5.4	Conclusion.....	118
6	Conclusions and Recommendations for Future Work .....	120
6.1	Novelty.....	126
6.2	Recommendations for Future Work.....	126
	Bibliography .....	128
	Appendix A: Surveyed Papers .....	150
A.1.	Scopus Survey Filter .....	150
A.2.	Surveyed Work.....	151
	Appendix B: NGTL Functions .....	158
B.1.	Natural Gas Viscosity <sup>4</sup> .....	158
B.2.	Peng-Robinson .....	159
B.3.	Compressor Power .....	162
B.3.1.	Compressor power calculation updates .....	164
B.4.	Pipeline Pressure Drop.....	165
B.4.1.	Pipe pressure drop calculation update.....	168
B.5.	Updated Natural Gas and Hythane Viscosity.....	169
	Appendix C: RUST Demonstration and Input Ranges.....	175
C.1.	Rust Demonstration.....	175
C.2.	Original Input Ranges .....	182
C.3.	Refined Input Ranges .....	187
	Appendix D: Proxy Modeling Supplementary Results and Algorithms.....	189
D.1.	Quadratic Regression Results.....	189
D.2.	ANN Regression Results.....	191
D.3.	ANN Results vs. Sample Size and Method.....	194
D.4.	Computing Time Required.....	197
D.5.	Summary of High Error and Combo Sampling Methods for NGTL .....	200
D.6.	Sampling Algorithms Explained .....	201
D.6.1.	Brute force spread algorithm .....	201
D.6.2.	Optimized spread algorithm (S-Opt1) .....	202
D.6.3.	Optimized spread algorithm, preventing edge clustering (S-Opt2&3).....	204
D.7.	MATLAB code modifications .....	207

## List of Tables

Table 2.1: Frequency of sensitivity and uncertainty analysis in LCAs over time .....	22
Table 3.1: Overview of Alliance and Prince Rupert Pipelines <sup>4</sup> .....	67
Table 4.1: Maya range of residual variance (max – min) with 4th level interactions, ranges from 100 runs with 1,000 samples each (the same overfit check samples were used in every scenario) .....	89
Table 4.2: Verifying the regression model response using Morris .....	89
Table 4.3: Regression summary for Maya nitrogen injection, Bow River water flood and Athabasca mined bitumen.....	90
Table 5.1: Experimental data recorded .....	99
Table 5.2: Change in the number of coefficients, average absolute error, and maximum absolute error from using ANN (random sampling) compared to the best performing quadratic regression proxy model .....	110

## List of Figures

Figure 1-1: Overview of LCA types included (black) and excluded (red) in the study .....	8
Figure 1-2: Report organization.....	9
Figure 2-1: Journal paper filtering process .....	20
Figure 2-2: Distributions used in the 13 Monte Carlo Studies (4 of the studies in this work did not specify what distribution was used, but it is expected they used lognormal as that is the ecoinvent/SimaPro default).....	28
Figure 2-3: Uncertainty presentation methods.....	29
Figure 2-4: Morris plot created using RUST <sup>2</sup> .....	35
Figure 2-5: Example of a Classification and Regression Tree (CART) generated using R <sup>133</sup> .....	46
Figure 2-6: Summary characteristics of a basic vs. detailed analysis.....	49
Figure 3-1: Overview of RUST framework and process flow diagram.....	53
Figure 3-2: Example of Morris sampling with three parameters ( $k$ ), two OAT designs ( $r$ ), and four levels ( $p$ ).....	55
Figure 3-3: Sobol sample generation .....	57
Figure 3-4: FUNNEL-GHG-CCO/OS model boundary .....	59
Figure 3-5: FUNNEL-GHG-NGTL model boundary.....	60
Figure 3-6: Variation in Morris mean over 50 runs for different levels ( $p$ ) and approaches ( $r$ )...	62
Figure 3-7: Sobol index accuracy as a function of sample size: 1st order (left) and total (right).	63
Figure 3-8: Sobol index rank vs. sample size for Alliance (top) and Maya (bottom); each line represents an input .....	63
Figure 3-9: Variations in parameter rank for Maya: OAT (left), Sobol (right) (+ means the OAT/Sobol rank's parameter is less important than the Morris method's).....	65
Figure 3-10: Effect of dependency in differential analysis for 50 million m <sup>3</sup> /d Alliance .....	70
Figure 3-11: Uncertainty in cost results of blue hydrogen production technologies (from Oni et al. <sup>168</sup> ) .....	72
Figure 3-12: Comparative analysis of cost production for blue hydrogen technologies (from Oni et al. <sup>168</sup> ) .....	72

Figure 3-13: The influence of economic parameters on the hydrogen cost from (A) SMR-52%, (B) SMR-85% (C) ATR, and (D) NGD.....	73
Figure 3-14: Sobol results for the differences between SMR-52% - ATR-CCS (left) and SMR-85% - NGD-CCS (right).....	74
Figure 4-1: Regression framework .....	77
Figure 4-2: Regression verification example with a poor fit (left) and a better fit (right).....	82
Figure 4-3: RUST background process flow diagram .....	84
Figure 4-4: Morris screening of the FUNNEL-GHG-CCO/OS Maya pathway .....	86
Figure 4-5: The effect of levels of interaction used (left) and number of terms included in the final regression model (right) on the residual (both use 5,000 samples in training data; right plot uses 5th level interactions).....	87
Figure 4-6: Regression residual verification for FUNNEL-GHG-CCO/OS Maya pathway .....	88
Figure 5-1: High level proxy modeling method .....	96
Figure 5-2: Optimized method to increase distance to nearest neighbour (dNN) by moving the candidate point (CN: closest neighbour, NN: nearest neighbour, Cand: candidate point, dMM: max movement distance, dCut: cut-off distance required).....	102
Figure 5-3: High error sampling method (SS: subsample, MD: max disagreement, PCS: potential candidate set, dCut: cut-off distance required, dNN: distance to nearest neighbour, Pcand: candidate point).....	105
Figure 5-4: Maya quadratic regression absolute residual results: L=Linear, NL=Non-linear, O#=Order of interactions .....	106
Figure 5-5: Maya ANN regression absolute residual results: N=Nodes in hidden layer of ANN .....	108
Figure 5-6: Overfit check for Maya (top) and NGTL (bottom) using random sampling (test MSE>>train MSE indicates overfitting); error bars represent 90% CI .....	109
Figure 5-7: Absolute residual results (Maya, Bow, NGTL use 10,000 samples; MB uses 7,000 samples) NL_O5 =nonlinear quadratic with 5 <sup>th</sup> order interactions, Rand 50N= 50 node ANN with random sampling, HE 50N = 50 node ANN with high error sampling .....	109
Figure 5-8: NGTL accuracy vs. # of coefficients (50,000 random samples, 26 inputs).....	111

Figure 5-9: NGTL 50N ANN MSE and max absolute error using external validation set (p-value >5% implies the difference in means is not statistically significant; <i>p</i> values <5% are not shown); error bars represent 90%CI (Rand: random sample, HE: high error sample).....	113
Figure 5-10: NGTL 50N ANN MSE using internal and external validation samples (Rand: random sample, HE: high error sample).....	113
Figure 5-11: Cumulative time to produce proxy models for NGTL 50-node ANN (Rand: random sample, HE: high error sample) .....	116
Figure 5-12: One-shot random sampling vs. cumulative high error (HE) and combo sampling (k: thousand samples).....	117
Figure 6-1: Summary characteristics of a basic vs. detailed analysis.....	121
Figure 6-2: Overview of RUST framework and process flow diagram.....	122
Figure 6-3: Quadratic Regression framework.....	123
Figure 6-4: High level ANN proxy modeling method.....	124
Figure 6-5: Absolute residual results: Maya, Bow, NGTL use 10,000 samples; MB uses 7,000 samples (NL_O5 =nonlinear quadratic with 5 <sup>th</sup> order interactions, Rand 50N= 50 node ANN with random sampling, HE 50N = 50 node ANN with high error sampling).....	125
Figure 6-6: NGTL 50N ANN MSE and max absolute error using external validation set (p-value >5% implies the difference in means is not statistically significant; <i>p</i> values <5% are not shown); error bars represent 90%CI .....	126

# 1 Introduction

## 1.1 Background and Motivation

Life cycle assessment (LCA) is a popular tool used to quantify environmental impacts including greenhouse gas (GHG) emissions.<sup>6</sup> LCA publications in the fields of energy, engineering, and environmental science have grown from fewer than 20 per year in 1990 to more than 2,700 in 2020 (Scopus search). Several jurisdictions have used LCA to develop GHG emission reduction policies; the Canadian Clean Fuel Standard (CFS),<sup>7</sup> the California Low Carbon Fuel Standard (LCFS),<sup>8</sup> and the European Union Renewable Energy Directive<sup>9, 10</sup> are a few examples. Though LCA is the most widely used environmental assessment tool, there is concern over the robustness of LCA results. This research focuses on theory-driven, process-based LCA of complex systems. In theory-driven LCA, inventory values are often generated using rigorous fundamental engineering-based models and calculations, which include complex interactions between the various model inputs. These complex interactions make it difficult for practitioners to understand the effect of each input value and assumption on the final output. *Because of the large number of assumptions and low quality of available data, the results of LCA are often viewed with skepticism.*<sup>11</sup> For example, LCAs of transportation fuels from various crude oils have been conducted by several groups (Jacobs,<sup>12</sup> TIAX,<sup>13</sup> Oil Climate Index<sup>14</sup>) and produced a wide range of results. The differences in results make conclusions about which crudes have lower emissions unreliable. All the LCAs provided deterministic point estimates and a limited sensitivity analysis but did not account for uncertainty in the data and assumptions used, which can lead to a lack of confidence in the results.<sup>15</sup> *In order to further increase the usefulness of LCA results for decision makers, a robust methodological framework that can be used to accurately quantify uncertainties and communicate results is needed.* Moreover, LCA models of complex energy systems (such as oil refineries) need to be made more accessible to non-experts by simplifying them while maintaining adequate accuracy. This thesis, therefore, aims to provide a novel contribution to the scientific community by addressing those two broad challenges.

While ISO 14040/44 recommend performing sensitivity and uncertainty analysis (SUA) for LCA, they provide no guidance or formal requirements.<sup>16, 17</sup> Currently, there is no standard framework or guideline for performing SUA. The quality of SUAs observed in our survey

(discussed further in Chapter 2) is inconsistent, and the SUAs generally have a narrow scope. Igos et al. examined how to treat uncertainty in LCA and discussed types of uncertainty along with the advantages and disadvantages of the various methods and how to communicate uncertainty results.<sup>18</sup> That research built on the work of Heijungs and Huijbregts,<sup>19</sup> Lloyd and Ries,<sup>20</sup> Uusitalo,<sup>21</sup> and Refsgaard et al.<sup>22</sup> Igos et al. suggest using global sensitivity methods such as Morris and Sobol, rather than the local one-at-a-time (OAT) method, which is currently used; the local methods fail to account for interaction and non-linear effects. These review papers are excellent sources of information for practitioners looking to implement SUA into their LCAs because they provide a blueprint of how SUA should be done.

Ross et al. reviewed 30 LCA studies published between 1997 and 2002, in particular examining how published LCAs currently handle SUAs.<sup>23</sup> The review provides a deep examination of issues facing LCA practitioners attempting to implement SUA. Similar review studies (i.e., by Tu et al.,<sup>24</sup> Byrne et al.,<sup>25</sup> Ferretti et al.,<sup>26</sup> Lloyd and Ries,<sup>20</sup> and Budzinski<sup>27</sup>) also discuss the implementation of SUA in LCA. The results of these reviews highlight that *a structured, methodical framework for performing and linking sensitivity and uncertainty analysis is required. Moreover, an up-to-date, deep review of how LCA practitioners address sensitivity and uncertainty is needed in order to identify areas for improvement.*

Conducting LCA can be expensive and time consuming,<sup>11</sup> especially when dealing with a complex product system. *One possible solution is proxy modeling.* Proxy modeling/metamodeling regression techniques include linear, polynomial, multivariate adaptive splines, kriging, radial bias function, support vector machine, and artificial neural network (ANN).<sup>28</sup> Agricultural LCA has used ANN models rather than analytical models to estimate crop yields based on field data for rice<sup>29, 30</sup> and wheat.<sup>31, 32</sup> Field-collected data has also been used to estimate energy and emission intensities.<sup>30, 33</sup> When we perform a comparative LCA, we need accurate results in order to confidently state that one pathway is better than another. *Obtaining accurate results for a complex process can be difficult, especially when good quality data is unavailable.* For example, an LCA of transportation fuels from various crudes requires an accurate refinery model to compare the GHG intensity of the crudes. The current procedure is to use a simplified or a rigorous model. A simplified model is easier to use by non-experts but provides less accurate results. Rigorous models are more accurate but can require specialty

software, contain confidential data, and require expert knowledge to use. In the building design industry, for instance, ANN proxy models are used to overcome the high computational times of rigorous models in order to optimize LCA emissions and costs and produce a simplified model that can be used by non-experts.<sup>34-36</sup> *In order to reduce modeling error while keeping models simple and easy to use, proxy modeling could be used in the energy industry.* Additionally, rigorous models can have long computing times, making it difficult to perform alternative scenario analysis and more rigorous uncertainty analysis methods. Therefore, *computationally efficient proxy models can be used instead, allowing policy makers to quickly examine alternative scenarios.*

Proxy modeling, also known as metamodeling, comes in various forms depending on the complexity of the true model.<sup>28</sup> Training a proxy model requires generating a training data set. This can be done through a classical design of experiments (DOE), space-filling methods, importance sampling, and sequential/adaptive sampling.<sup>28</sup> Current research on adaptive sampling is focused on kriging models;<sup>37</sup> however, kriging models are complex and not as accurate and flexible as ANNs.<sup>38</sup> For rigorous models with moderate to long computing times, it is ideal to minimize the number of samples required for the training set through adaptive sampling. However, few high-dimensional proxy models that require large samples sizes have been developed.<sup>28</sup> *A proxy-modeling framework is needed to represent complex, high-dimensional, and moderate computing time models.*

A detailed literature review is provided in Chapter 2. Based on this literature review, the Chapter on research gaps was developed.

## **1.2 Research Gaps**

In order to increase the robustness of LCA results so that they better support decision-making, methods of quantifying SUA need to be improved. Furthermore, complex LCA models need to be made more accessible to non-experts by simplifying them while still maintaining accuracy. In this context, the thesis attempts to address several gaps.

- Current LCA publications lack consistency in their sensitivity and uncertainty analyses as there is no accepted framework. While there are a number of reviews on sensitivity and uncertainty analyses, the reviews mainly provide a blueprint on how SUA should be done. They fail to examine how SUA is actually being implemented in current LCA practice.<sup>18-21</sup> However, these reviews are excellent sources of information for practitioners planning to implement SUA. A few reviews examine the frequency and quality of SUA in LCA studies. Reviews on the limitations of SUA are necessary to identify shortcomings in the current studies and to produce a practical guide of mistakes to avoid. These reviews aim to provide a deeper examination of issues facing LCA practitioners attempting to implement SUA in their work. LCA reviews on the implementation of SUA are outdated<sup>23</sup> or have a narrow focus.<sup>24-26</sup> An updated survey is needed to identify the current quality and limitations of sensitivity and uncertainty analysis in published LCA studies. Once the shortcomings in the current work are identified, recommendations for improvements can be made.
- The common LCA and Excel add-in software support Monte Carlo simulation only.<sup>39-42</sup> Including sensitivity methods such as Morris or hybrid methods such as CART could allow the underlying data to be further explored. While these methods are available in programs such as MATLAB and R, they require programming knowledge to use. To encourage the use of alternative sensitivity and uncertainty methods, an open source, easy-to-use tool is needed.
- Adapting LCA results for specific case studies is time consuming and expensive, especially for policy and decision makers who lack a strong background in LCA.<sup>11</sup> Published models for complex energy systems that can be used to generate LCA inventory data are either rigorous models that provide a high level of accuracy but are difficult to use by non-experts and may contain confidential data or require specialty software; or simplified models that are easy to use but are less accurate.
  - While proxy models can be used to provide a simple, easy-to-use model, current proxy modeling approaches are limited to a small number of inputs or require large sample sizes.

- A standardized method to communicate uncertainty is needed. Understanding the uncertainty and limitations of LCA models is difficult given the limited information provided in current LCA studies.

### 1.3 Objectives

The goal of this research is to create a framework aimed at further improving the quality of LCA results so they can be used as reliable information to support decision-making in environmental protection and GHG emission reductions strategies in the energy sector. This goal will be achieved through the following sub-objectives:

- 1) The development of a framework for improving the quality of LCA sensitivity and uncertainty analysis using a methodical, structured approach to improve end-user confidence in the model results by:
  - a) Identifying the quality of sensitivity and uncertainty analyses in recently published LCAs by carrying out a detailed literature survey and identifying areas for improvement;
  - b) Determining the ability of the Morris screening method to quickly and effectively identify key inputs and perform a case study;
  - c) Developing an open-source tool to make performing sensitivity and uncertainty analysis easier for non-technical users to encourage broader use of sensitivity and uncertainty analysis;
  - d) Developing a framework for effectively communicating sensitivity, uncertainty, and the limitations of an LCA's results.
- 2) The development of natural gas framework to improve the accessibility of LCA results for use by non-experts while maintaining a high level of accuracy using proxy models. This involves:
  - a) Conducting a literature review and examining the different types of proxy models available;
  - b) Developing a framework and demonstrating how linear regression can be used to create proxy models for simpler processes and performing a case study using the **FUNDamental Engineering PrincipleS-based Model for Estimation of GreenHouse Gases** in

Conventional Crude Oils and Oil Sands (FUNNEL-GHG-CCO&OS) model and the Natural Gas Transmission Pipeline (FUNNEL-GHG-NGTL) model;

- c) The development of a framework and demonstrating how artificial neural networks (ANNs) can be used to create proxy models for complex processes;
- d) The identification of optimal sampling strategies to reduce the number of training samples needed.

## 1.4 Scope, Challenges, and Limitations

There are many types of LCA, as summarized in Figure 1-1. The sensitivity, uncertainty, and proxy modeling methods can be applied to all types of LCA but this work specifically focused on process-based, theory-driven carbon footprinting LCA as this is what is currently being used in the energy industry. A brief background on the implications of this restriction is provided.

LCA methods include process-based, economic input-output-based, and hybrid-based methods. The economic input-output (EIO) method uses aggregated industrial sector transaction data to estimate emission changes due to industrial growth and large-scale industrial transitions.<sup>43</sup> Because of EIO's aggregated nature, it typically has a wide scope, as it captures all the major economic sectors. Process-based methods determine input and output mass and energy balances for each step along a product's life to determine its impact.<sup>43</sup> Because of process LCA's detailed nature, it can be used to compare alternative technology pathways<sup>44</sup> and examine future technologies as required by the CFS.<sup>45</sup> However, the level of detail required can make scope and boundary identification difficult and create cut-off errors, resulting in the underestimation of the true emission intensity.<sup>46</sup>

Life cycle inventory analysis (LCIA) involves quantifying the input and output material and energy flows for each process along a product's life. In a data-driven model, extensive data from industry and various databases are used to determine inventory values for each process. Data available to the LCA practitioner is typically aggregated, reducing the resolution and accuracy of the LCA model.<sup>47</sup> Additionally, data may not be available for the specific process desired, so data from a similar process may need to be used, introducing additional sources of error.<sup>21, 46, 48,</sup>

<sup>49</sup> A theory-driven approach uses engineering fundamentals, computer simulations, and analytical calculations to determine mass and energy flows. For example, a rigorous Aspen

HYSYS model could be used to model a refinery using chemical kinetics and thermodynamics to determine the product yields, hydrogen consumption, and energy required.<sup>50</sup> A theory-driven approach often requires less data from industry and can be used to model and compare alternative pathways, as required by the CFS, which would not be possible using aggregated data. However, a theory-driven approach also includes additional sources of uncertainty associated with the modeling process' used and assumed operating conditions.<sup>51</sup> Theory-driven LCA can also contain complex models that can benefit from proxy modeling. Typically, LCIA uses a combination of theory- and data-driven methods for different processes or data levels (foreground vs background) based on the information available. The purpose of an LCA varies; two common LCAs are hotspot identification and comparative LCA. Hotspot identification is used to identify which stage of the LCA is responsible for most of the emissions and is used to guide reduction efforts. Comparative LCA is used to compare the impacts of alternative products/pathways. Hotspot identification LCA requires less accuracy and can still be useful if aggregated data is used. However, comparative LCA requires a deeper examination of alternative pathways and a higher accuracy to make confident conclusions about which pathway and is therefore the focus of this study.<sup>15, 52</sup>

LCA impact assessments can focus on a single impact factor or a combination of impact factors. These impact factors can then be grouped as mid-point categories (human toxicity, respiratory effects) and end-point categories (human health). Various methods exist for quantifying mid-point and end-point impact categories such as CML, Eco-indicator 99, Eco-Scarcity, and ReCiPe.<sup>53</sup> Alternatively, LCA can be performed with a narrower scope, focusing on a single or a subset of impact categories. For example, the Clean Fuel Standard,<sup>54</sup> GREET,<sup>55</sup> and FUNNEL<sup>44</sup> focus only on greenhouse gas (GHG) emissions (also known as carbon footprinting). Agrawal et al. performed a GHG and water footprinting LCA of the electricity sector.<sup>56</sup> Single impact carbon footprinting LCAs are used to reduce computational resources needed for data collection, LCA interpretation, and proxy modelling.

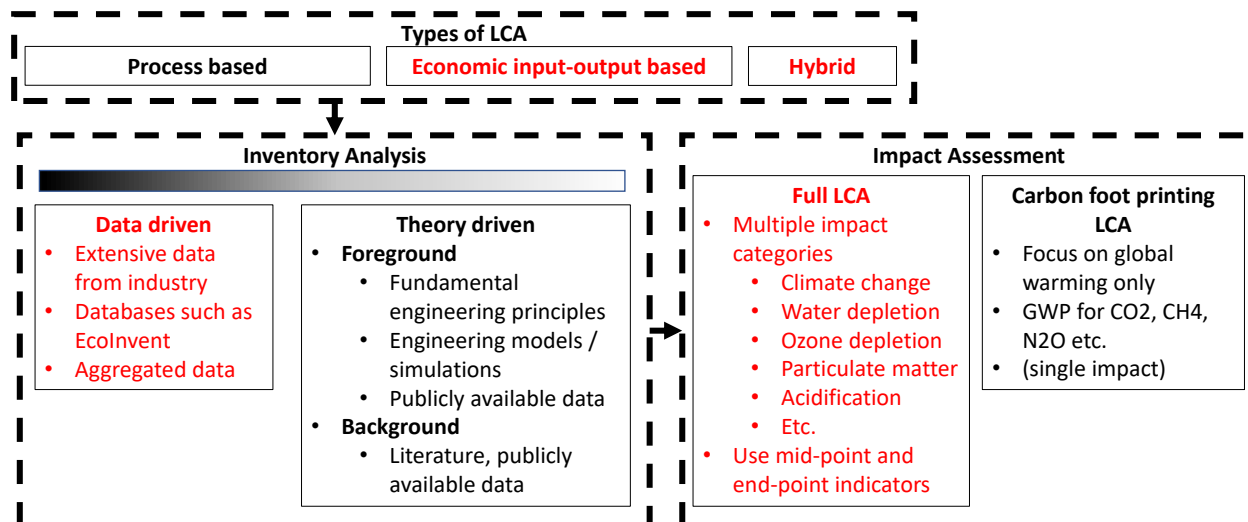


**Figure 1-1: Overview of LCA types included (black) and excluded (red) in the study**

The end goal of the proxy modeling effort is to create a simple-to-use upgrader and refinery model. However, as the Aspen upgrader and refinery models are still under development, the proxy modeling framework will be developed using a natural gas transmission pipeline model (NGTL). The NGTL model is like the upgrader model in that it has many inputs and uses an iterative non-linear solver; however, the NGTL model has a shorter calculation time and is easier to link to MATLAB, allowing for easier testing of alternative methods.

## 1.5 Organization of the Report

A visual of the report organization is provided below in Figure 1-2. The current chapter (i.e., Chapter 1) provides background on the research and lists the objectives. Chapter 2 is a review of sensitivity and uncertainty implementation. Implementation reviews survey published LCA studies, examine how LCA practitioners perform SUA, and ask questions like: what methods were used, what is the quality of the analysis, etc. Chapter 3 describes the development of the Regression, Uncertainty, and Sensitivity Tool (RUST). The aim of RUST is to encourage wider use of various sensitivity and uncertainty methods in LCA. The chapter includes a case study illustrating how RUST can be used on both linear and non-linear models. Chapters 4 and 5 discuss the practicality of using proxy modeling to produce an easy-to-use, computationally efficient, and sufficiently accurate alternative model. Chapter 4 describes simpler linear regression models including interaction, squared, and cubed terms. A case study examining the

accuracy of proxy models for linear and non-linear models is included. Chapter 5 describes the use of artificial neural networks (ANNs) to develop proxy models for complex processes. Since generating training data is time consuming, sampling strategies are explored in depth. A case study using a natural gas transmission line is used to evaluate the various ANNs and sampling strategies. Chapter 6 provides an overview of future work.

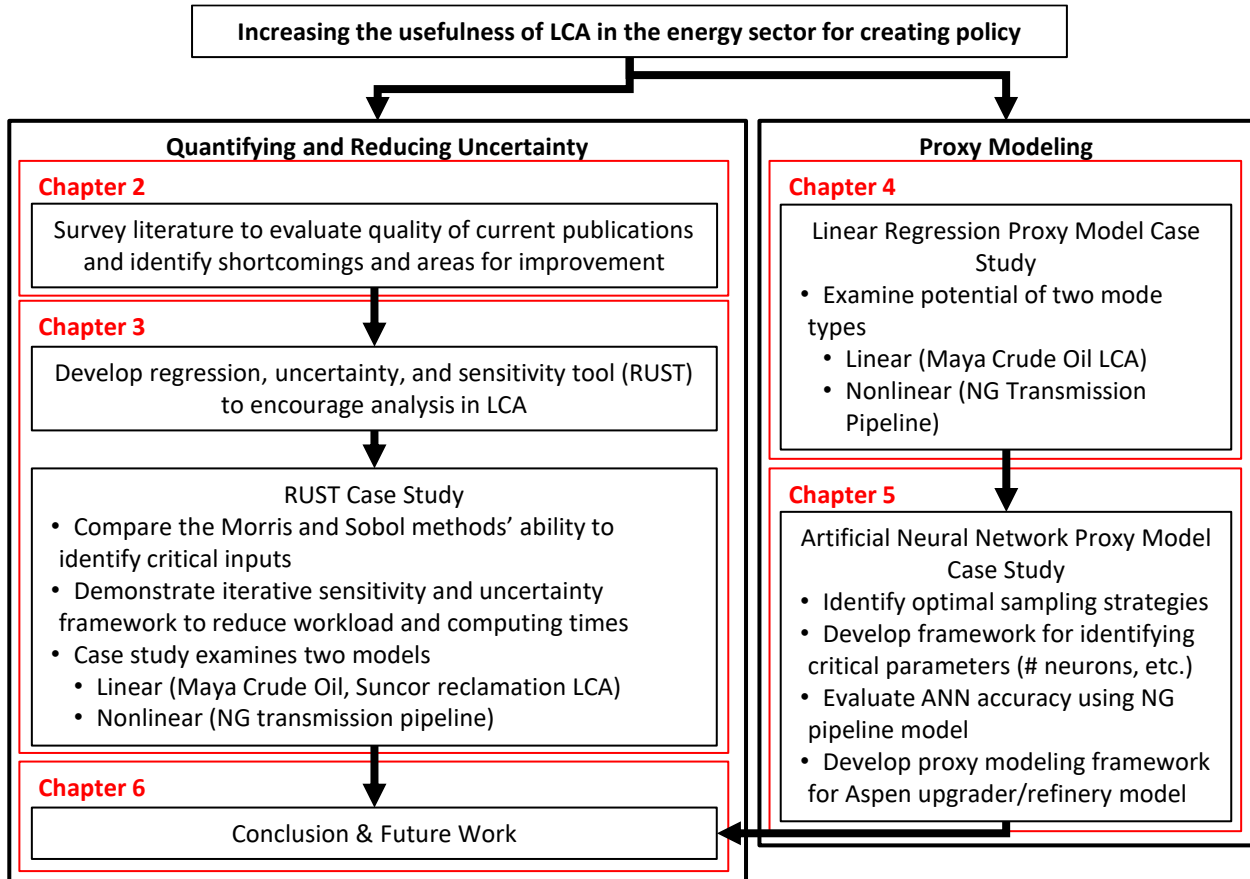


**Figure 1-2: Report organization**

## 2 A Survey of How Practitioners Implement Sensitivity and Uncertainty Analysis in Life Cycle Assessments of Energy Systems\*

### 2.1 Introduction

Life cycle assessment (LCA) uses either a bottom-up or top-down approach. A bottom-up approach is a process-based LCA that uses process-specific data based on engineering fundamental principles or operation data to calculate energy and mass balances for each major process unit. Aggregated generic databases can also be used for background systems. Top-down LCA uses aggregated economic data to estimate emissions of a particular product system but lacks the depth required to assess the effects of process changes and identify areas for improvement. Uncertainty can manifest in different forms such as parameter, normative, or model uncertainty. Parameter uncertainty can result from measurement or data uncertainty. Top-down studies are more likely to suffer from aggregation error, while bottom-up studies suffer uncertainty in parameter values. Normative uncertainty is due to subjective decisions made by the practitioner such as what time horizon to use. Simplification and approximation result in modeling error.<sup>19</sup> Typically, it is not possible to validate process-based LCA models because of the severe lack of data or because they are modeling technology that has not been implemented yet. Differences in results across numerous studies and unclear or unsupported assumptions lead to a lack of confidence in LCA results. Therefore, uncertainty needs to be quantified.

While a common output of an uncertainty analysis is a range of values, it should not be the sole purpose of the analysis. By performing SUA, practitioners are forced to examine the limitations in their data, model structure, and understanding of the problem, and this can lead them to adjust their course of action and make a higher quality assessment. Furthermore, performing sensitivity

---

\*This chapter is based on Di Lullo, Gemechu, Oni and Kumar, "Investigation and discussion of how practitioners currently implement sensitivity and uncertainty analysis in estimation of GHG in life cycle assessments of energy systems and improvements needed". *Submitted to Int. J. Life Cycle Assess. Oct 25, 2021.*

analysis on preliminary versions of a model (and identifying insignificant processes, for instance) can reduce the time spent on data collection and model development.

In this study, we discuss two types of reviews, method and implementation reviews. Method reviews examine the various methods available to perform sensitivity or uncertainty analysis and summarize the methods' fundamental principles, strengths, and weaknesses along with a high-level discussion of the limitations in performing SUA in LCA. Implementation reviews survey published LCAs and examine how SUA is performed by LCA practitioners, asking what methods the practitioners use, what the quality of the analysis is, etc. In summary, method reviews look at how practitioners can perform SUA, while implementation reviews look at how practitioners implement SUA.

The most current method review, by Igos et al., examines how to treat uncertainty in LCA and discusses types of uncertainty, advantages and disadvantages of the various methods, and how to communicate uncertainty.<sup>18</sup> Igos et al. built on the work of Heijungs and Huijbregts,<sup>19</sup> Lloyd and Ries,<sup>20</sup> Uusitalo,<sup>21</sup> and Refsgaard et al.<sup>22</sup> While these method reviews are excellent sources of information for practitioners who are looking to implement SUA into their LCAs, they only provide a blueprint of how SUA should be done without examining how SUA is actually being done. An implementation review is necessary to identify shortcomings in the current studies and to produce a practical guide of mistakes to avoid. An implementation review aims to provide a deeper examination of issues facing LCA practitioners attempting to implement SUA in their work. Ross wrote an implementation review that assessed 30 LCA studies published between 1997 and 2002 to determine how SUA was being handled.<sup>23</sup> We found additional implementation reviews/data, but they had a narrow focus and provided a limited analysis. Tu et al. examined 54 algae biofuel papers published between 2009 and 2016 and examined only whether they included a quantitative sensitivity or an uncertainty analysis; the authors did not analyze the methods used.<sup>24</sup> Byrne et al. examined 256 LCAs of urban water systems published between 1998 and May 2017 and performed a word search for sensitivity to estimate how many included sensitivity analysis.<sup>25</sup> Ferretti et al. performed a broad assessment of 66 papers published between 2005 and 2014 that included the term “sensitivity analysis” to examine trends in sensitivity analysis but did not examine uncertainty.<sup>26</sup> Lloyd and Ries examined 24 LCA

studies published between 1996 and 2004 that included uncertainty.<sup>20</sup> Budzinski examined 17 LCA studies published between 2008 and 2011 that included Monte Carlo simulations.<sup>27</sup>

Computer software and hardware have improved significantly over the last decade, allowing us to improve upon the previous implementation reviews both by looking at research from 2017 and by providing a broader and deeper analysis than the previous implementation reviews.

Furthermore, unlike the more current method reviews that examined what methods are available, this study performs an implementation review and takes a deeper look to examine the quality of analysis currently being published with the aim of answering the following questions:

- How frequently do LCAs include SUA?
  - Are ISO standards referenced?
  - Is the rate of implementation improving?
- When included, is the SUA rigorous or simplistic?
  - How many inputs/assumptions are examined?
  - What types of uncertainty are examined?
  - How are results communicated?
  - Are non-linear or interaction effects examined?
  - Are correlation and dependency discussed or included?
- What methods of SAU are most common and why?
  - What software is available?
- What issues/limitations are observed?
- How can the current works be improved?

As a result of this work, for Excel-based LCA models, I have recently created an open source template that uses R to generate the samples and process the results and Excel macros to generate the output file and link the Excel and R codes.<sup>2</sup> The template is called the Regression, Uncertainty, and Sensitivity Tool (RUST) and has been used in studies that have resulted in seven journal articles in the last three years.<sup>57-64</sup>

This chapter begins with high-level background information. To keep the chapter concise and avoid repeating information from the earlier method reviews, background data is provided as

needed to facilitate discussion (in Chapter 2.2). References for supplementary background information are provided as needed throughout the paper for interested readers. The screening method used to identify papers for the survey and the evaluation methods used are discussed in Chapter 2.3. In Chapter 2.4, the results of the survey, followed by the limitations observed in the current work, are discussed. Finally, Chapter 2.5 discusses recommendations for improving the quality of sensitivity and uncertainty in LCA. Appendix A includes a full list of the studies examined in this paper as well as a summary of the methods used in each paper.

## **2.2 Background**

High-level background on terminology and types of SUA are provided here. More detailed background information is provided throughout the paper as needed. For a review of sensitivity and uncertainty methods available, the review by Igos et al. is well cited in the literature and is a good start for the current analysis.<sup>18</sup>

### **2.2.1 Terminology clarification**

We discuss three analysis methods for understanding the results of LCA models: contribution to variance, sensitivity, and uncertainty. Due to the overlap in methods to determine sensitivity and uncertainty, the two are often used interchangeably and this can lead to a great deal of confusion. The primary difference between them is the end goal. The goal of a sensitivity analysis is to identify which model inputs are important and to determine how a change in the input value will affect the output. The goal of an uncertainty analysis is to determine an output probability/possibility distribution, given ranges for each input value.<sup>65, 66</sup> The primary difference between sensitivity and uncertainty is that a sensitivity analysis does not include a probability/possibility distribution, only a range.

The difference between sensitivity and contribution to variance analyses is that the former examines how each input affects the output value, while the latter determines how each input contributes to the output variance. The inputs in a contribution to variance analysis use the same probability/possibility distributions as the uncertainty analysis.

A source of confusion during our literature survey was the use of the terms “pathway” and “scenario”.<sup>67</sup> For clarity, in this paper “pathway” is used to describe a unique product or

production process for which an impact assessment is required; it is not related to a sensitivity or uncertainty analysis. For example, an LCA comparing lithium ion (Li-ion) and nickel-metal hydride (NiMH) batteries would have two pathways, one for the Li-ion and one for the NiMH batteries. In this paper, “scenario” is used to describe the use of alternative input values, assumptions, and/or boundaries, and is related to sensitivity or uncertainty analysis. Another source of confusion comes when scenarios are used to perform either a sensitivity or uncertainty analysis. Normally in a sensitivity analysis, several scenarios are considered and different inputs are changed in each scenario. A one-at-a-time (OAT) sensitivity analysis uses scenarios in which only one input is changed at a time and the remaining inputs retain their base case values. Scenarios that change several inputs simultaneously can be used to explore the interaction effects between the parameters; this is still a sensitivity analysis. If all the scenarios change the same inputs, it is an uncertainty analysis, as the goal is to determine a reasonable range of output values for, for example, base case, best case, and worst-case scenarios.

We realized during the survey that whether an alternative should be classified as a pathway or scenario also depend on the hypothesis being tested. For example, when performing an LCA of a single product that can be produced by several methods, whether the method is a scenario or pathway depends on the end goal of the analysis. If the goal is to compare the life cycle impact of the methods, each method is a pathway. If the goal is to determine the average life cycle impact of the product, then the method is part of a scenario. For example, one could perform an LCA of crude extraction in Northern Alberta (a province in Canada) using steam assisted gravity drainage (SAGD) with and without cogeneration. If the goal is to compare the GHG emission intensity of SAGD with or without cogeneration, each process is a pathway. However, if the goal is to compare the GHG emission intensity of SAGD-extracted crude with conventional crude, knowing SAGD is used with and without cogeneration allows us to assess scenarios with different cogeneration capacities as part of a sensitivity or uncertainty analysis. These definitions are not definitive or standardized but are used in this paper to help avoid confusion during the discussion of uncertainty approaches. Scenarios can also be used to describe future outcomes and trends; however, that definition is not used in this study as forecasting LCAs are outside the current scope.

### 2.2.2 Local vs. global sensitivity

Sensitivity is simply a partial derivative; in other words, it looks at how the model output changes because of a change in the specified input. The partial derivative value for input  $x_i$  can depend on the value of  $x_i$  itself (non-linear effect) or the values of the other model inputs  $x_i * x_j$  (interaction effects). There are two main types of sensitivity analysis, local and global. A local sensitivity analysis, also known as one-at-a-time (OAT) or one-factor-at-a-time (OFAT), is centered on a base case and only examines the sensitivity of individual parameters. OAT is often used since it is simple and does not require an algorithm to generate samples. The base case is used as a reference and each input is varied separately. The minimum number of model evaluations required is  $N=2*k+1$ , where  $k$  is the number of inputs.<sup>68</sup> Alternatively, rather than using a single minimum and maximum value for each input, several values can be used to determine whether the model has a non-linear response. The OAT method does not examine interaction effects and therefore is only recommended for simple linear models with minimal interactions between inputs. Global methods such as the factored approach (also known as design of experiments [DOE]) examine the entire parameter space. A factored approach overcomes the OAT method's limitations by allowing the possible interaction effects between inputs. However, a full factored approach requires  $N = L^k$ , where  $L$  is the number levels and represents the number of unique values each parameter can take and  $k$  is the number of inputs examined. Generally, a full factorial approach is only used with two or three inputs and two levels, otherwise the number of model evaluations becomes overwhelming. Using only two levels is acceptable for linear models but can be misleading for non-linear models, especially if they are non-monotonic. Partial fractional designs can be used to reduce the number of samples required but at the expense of clarity.<sup>69</sup>

Consider a model base case in which 5% of heat demand is supplied from a cogeneration unit and the rest from a conventional boiler; the actual share from cogen can range from 0% to 50%. With a local approach, the cogen unit efficiency would appear to be insensitive, while the boiler efficiency would appear to be sensitive. However, as the share of heat produced from the cogen unit increases, so would the sensitivity of the cogen unit efficiency. The global method accounts for variations in the inputs' sensitivity because of non-linear and interaction effects, hence, it would prevent the underestimation of the cogen unit efficiency sensitivity by accounting for its

interaction with the “share of heat from cogen” input. Chapter 2.2.2 provides further discussion on local vs. global sensitivity. Reviews by Norton,<sup>68</sup> Groen et al.,<sup>70</sup> Iooss and Lemaitre,<sup>71</sup> and Ravalico et al.<sup>72</sup> provide additional background on sensitivity methods.

### 2.2.3 Uncertainty analysis

There is no standard way of classifying uncertainty (i.e., sources or types of uncertainty). Heijungs and Huijbregts examined six studies, all of which used different uncertainty classifications.<sup>19</sup> Ascough et al. attempted to group uncertainty into knowledge (epistemic or reducible), variability (aleatory or irreducible), and linguistic.<sup>48</sup> Uusitalo et al. further divided epistemic and aleatory uncertainty into 6 classes: inherent randomness, measurement error, systematic error, natural variation model uncertainty, and subjective judgement.<sup>21</sup> Williams et al. examined uncertainty in LCA inventories and defined 5 uncertainty categories: data, cut-off, aggregation, geographic, and temporal.<sup>47</sup>

Lloyd and Ries created a combined uncertainty topography table.<sup>20</sup> The columns, taken from the United States Environmental Protection Agency (US EPA), show the parameter (input data), scenario (normative choices), and model (mathematical relationships).<sup>73</sup> The rows, taken from Morgan and Herion, show random error and statistical variation, systematic error and subjective judgement, linguistic imprecision, variability, inherent randomness and unpredictability, expert uncertainty and disagreement, and approximation.<sup>46</sup> This study groups uncertainty into parameter, normative, and model uncertainty. “Normative” is used instead of “scenario” to avoid confusion with the definitions of scenario vs. pathway given in Chapter 2.2.1.

Lloyd and Ries’s table incorporates the various sources of uncertainty discussed in earlier studies such as spatial, variations due to location or time scale, temporal, measurement/data, error due to inaccuracies in the measuring or data collection process, natural variation/randomness, and aleatory variation due to inherent randomness primarily under parameter uncertainty.<sup>21, 46-49</sup> Normative uncertainty includes cut-off,<sup>47</sup> allocation rules, and selecting distribution types (uniform vs. triangle).<sup>20</sup> Modeling uncertainty includes using simplified models/correlations, measurement error in physical constants, numerical error (model convergence), and extrapolating

relationships to similar processes.<sup>20</sup> Disagreement between experts can affect parameter, normative, and model uncertainty; many standards exist for developing uncertainty distributions from experts examining issues such as bias, weighting, and how to phrase the inquiry properly.<sup>74-76</sup>

Once uncertainty has been identified, probability distributions can be determined. Different types of distribution functions are used in Monte Carlo simulations including uniform, triangular, normal, log normal, and project evaluation and review technique (PERT). Uniform distribution is the simplest; it requires estimates of the minimum and maximum values only and assumes an equal probability for all intermediate values.<sup>77</sup> It should be used when minimal information is available on the probabilities. Uniform distributions provide a conservatively wide output distribution. When a most likely or typical value is also known, triangle, PERT, or modified PERT distributions may be used. Typically, it is easier for experts and practitioners to estimate the minimum, maximum, and most likely values rather than the mean and standard deviations of a normal distribution.<sup>78</sup> PERT and modified PERT distributions approximate the normal distribution, producing bell curves. The modified PERT's optional factor, gamma, adjusts the shape of the bell curve. Large gamma produces a tall skinny bell with long tails, and low gamma produces a fatter bell. A gamma factor of 4 produces the basic PERT distribution. The main difference between the three distributions is how they handle the tails and the mean. The triangle distribution provides higher probabilities for the tails and a larger standard deviation, which produces a more conservative, wide output distribution. The PERT and modified PERT, with large gamma values, produce higher probabilities for the values closer to the mean. When a symmetric distribution is used, the mode value for all three distributions will be the most likely value. However, when asymmetric distributions are used, the mean value deviates significantly from the most likely value and can produce a skewed output distribution. When used in project planning, this can result in overly conservative project completion time estimates. The PERT and modified PERT calculate the mean as  $\mu = (a + \gamma c + b)/(\gamma + 2)$ , where  $a$ ,  $b$ , and  $c$  are the min, max, and most likely values, respectively. The basic PERT uses  $\gamma=4$ , which means the most likely value is four times as influential to the mean as the min and max values are. Hence, if triangle distributions are used instead of PERT, the output distribution can be significantly skewed, leading to over/underestimation bias. This problem is further amplified in non-linear

models. Therefore, it is important to consider the impact of using a triangle distribution when the tails are severely asymmetrical; uniform distributions that are not symmetrical relative to the base case will also lead to bias issues.

The normal distribution is often used since natural variation tends to follow a normal distribution. Two limitations of a standard normal distribution are that they must be symmetrical and are unbounded. Unbounded distributions can cause calculation errors within the model that can be avoided by truncating the distribution. A parameter  $X$  is lognormally distributed if  $Y=\ln(X)$  is normally distributed. Lognormal distributions are typically used as they produce long tails; they are the default distribution used in ecoinvent v2.<sup>79</sup> While ecoinvent deals primarily with linear models, care should be taken when using lognormal distributions for highly non-linear models as the extreme tails can lead to calculation errors or unrealistic scenarios.

### **2.3 Literature Survey Method**

The goal of the survey is to examine how practitioners executing an LCA address SUA. Therefore, in this review, we focus on research that performs LCA. Review papers or papers focused only on evaluating a new type of sensitivity or uncertainty analysis in a pre-existing LCA were not included. To reduce the number of papers selected, this survey focused on energy- and fuel-based LCA. A Scopus search for [“life cycle assessment,” “life cycle analysis,” or “LCA”] and [“energy” or “fuel”] in the title, abstract, or keywords and published in 2017 resulted in 1630 papers. To further refine the search, [“greenhouse” or “global warming”] were added as required keywords. Because of the unique characteristics of medical studies and our desire to focus on energy-related studies, we excluded articles from the subject areas of medicine; biochemistry, genetics and molecular biology; immunology and microbiology; pharmacology, toxicology and pharmaceuticals; and veterinary. Articles on economics were also excluded, as these are specialized analyses that build on conventional LCAs. The final Scopus search string resulted in 331 articles and is provided in the SI. The abstracts were reviewed and studies were eliminated that focused on LCA of building materials, waste disposal not focused on energy production, food crops and agricultural waste not focused on bioenergy production, forecasting future scenarios, and primarily economic-based analysis; once these studies were eliminated, 74 were left (Figure 2-1). The studies included in the survey are listed in Table A1.

One of the limitations of this approach is that it does not capture all of the LCA papers, and any conclusions drawn cannot be applied to LCAs in different fields. However, the filtering criteria were selected to reduce the number of papers to a reasonable level so that each may be read in detail.

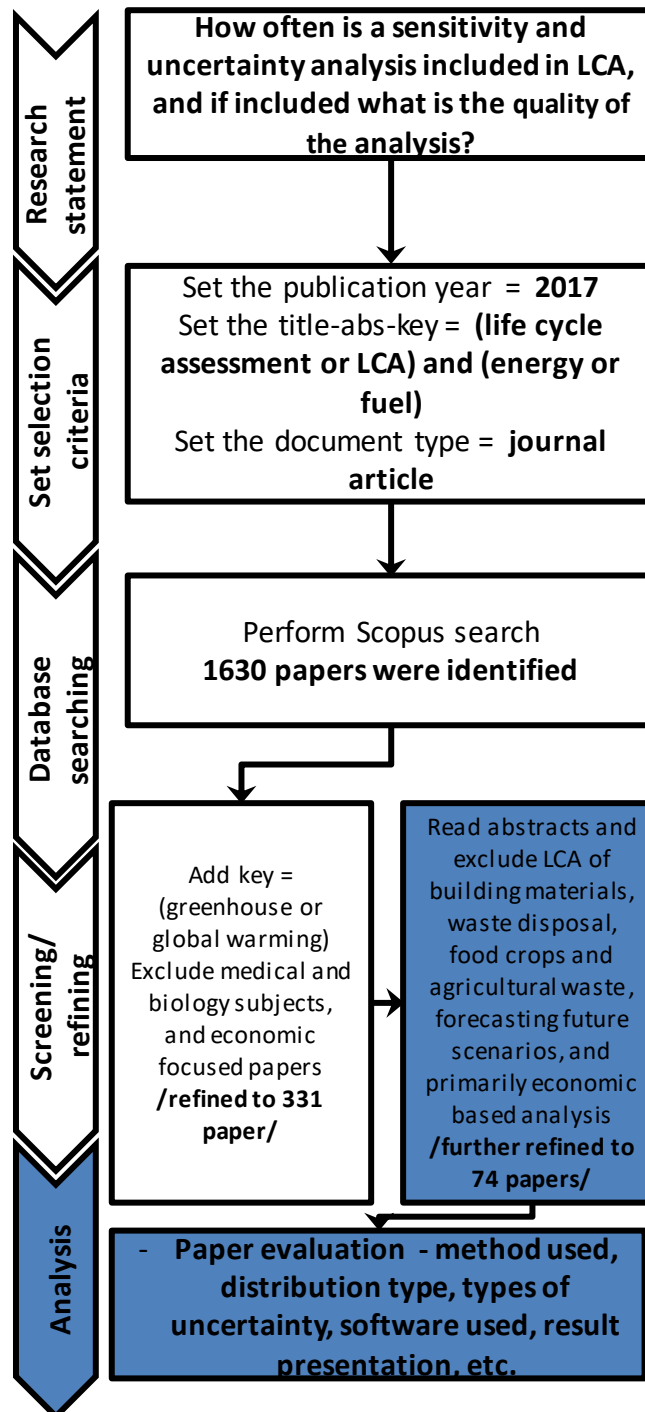


Figure 2-1: Journal paper filtering process

In addition to a key term word search, each paper was reviewed to determine the analysis that was performed. All the supplementary information included in the papers were also reviewed. A full list of searched terms is included in the Supplementary Information (SI). The search words

include sensitivity, uncertainty, various software names, and common analysis names (fuzzy, Morris, etc.).

For each paper, there was detailed focus on the methods and distributions, whether the distributions were justified, what types of uncertainty were included (parameter, normative, model), whether key statistics were mentioned, what software was used, whether correlation or dependency was mentioned, how results were presented, and whether the analysis was basic, moderate, or advanced, among others. In some cases, the authors of a paper were contacted to clarify information.

## **2.4 Results and Discussion**

First, the papers were searched to see whether they referenced ISO 14040<sup>80</sup> or 14044<sup>17</sup> standards. In 2002, Ross' implementation review assessed 30 LCA studies published between 1997 and 2002 to determine how they handled sensitivity and uncertainty.<sup>23</sup> Ross determined that only 63% of the studies followed the ISO standards. Our review found that in 2017, 61% (45) of the examined studies referred to ISO 14040/14044 standards directly, showing a negligible change in 15 years.

The use of sensitivity and uncertainty analyses has also increased. For example, in 2002, Ross assessed 30 LCA studies and found that while 47% of the studies reported uncertainty, only 13% explicitly discussed uncertainty in the results. Furthermore, only one of the studies included a quantitative uncertainty analysis and two included a qualitative analysis.<sup>23</sup> Later, Tu et al. examined 54 algae biofuel papers published between 2009 and 2016 and found that 15% included a quantitative uncertainty analysis, while 36% included a quantitative sensitivity analysis.<sup>24</sup> Byrne et al. examined 256 LCAs of urban water systems published between 1998 and May 2017 and found that 40% included a sensitivity analysis.<sup>25</sup> Byrne's results may be conservative as they simply searched the document for the words "sensitiv" and "sensitivity"; some of the studies may not have actually performed a sensitivity analysis. The trend suggests that SUA might be becoming more common, but improvement is still needed to meet ISO standards. Of the 74 studies included, 76% (56) include either a sensitivity or an uncertainty analysis, 69% (51) include a sensitivity analysis, and 27% (20) include an uncertainty analysis. The key figures from these implementation reviews are summarized in Table 2.1. The remainder

of this Chapter provides critical views on the implementation of SUAs in the 74 papers chosen in terms of method used, inputs distribution, and results presentation. Background information relevant to the discussion is provided as needed.

**Table 2.1: Frequency of sensitivity and uncertainty analysis in LCAs over time**

<b>Paper</b>	<b>Surveyed years</b>	<b># of Papers surveyed</b>	<b>Sensitivity</b>	<b>Uncertainty</b>
<b>Ross et al.<sup>23</sup></b>	1998-2002	30	N/A	13% (47%)
<b>Byrne et al.<sup>25</sup></b>	1998-2017	256	40%	N/A
<b>Tu et al.<sup>24</sup></b>	2009-2016	54	36%	15%
<b>This Work</b>	2017	74	69%	29%

### 2.4.1 Sensitivity analysis

Of the 74 surveyed studies, 51 (69%) included a quantitative sensitivity analysis, which is a significant increase from the surveys by Tu et al. and Byrne et al., who found that only 36% and 40%, respectively, included sensitivity.

This work found that 78% (40) of the papers performed a one-at-a-time (OAT), 33% (17) a factorial approach, and 12% (6) included both. Ferretti et al. performed a broad assessment of 66 papers that included the term “sensitivity analysis” published in either *Science* or *Nature* journals between 2005 and 2014 to examine trends in sensitivity analysis.<sup>26</sup> Ferretti et al. determined that 59% used a simple OAT approach, while the remaining 41% used global sensitivity methods. Global vs. local sensitivity is further discussed in Chapter 2.2.2.

#### 2.4.1.1 Sensitivity background

As OAT and factored sensitivity were the only methods used in the surveyed work, a quick background is provided in Chapter 2.2 to aid in discussion. See Iooss et al.<sup>71</sup>, Ferretti et al.<sup>26</sup>, and Groen et al.<sup>70</sup> for reviews of other methods.

#### 2.4.1.2 Inputs examined

The OAT and factored approaches are used to examine both parameter and normative inputs. While advances in computing have made sensitivity analysis easier to perform, especially for

parameter inputs, most studies are still limited in scope; 28% of the OAT analyses examined only a single parameter of interest and 58% included three or less. Only 15% of the OAT analyses included 10 or more inputs. Since factored analysis requires more model runs, it is understandable that 76% examined four or fewer inputs. None of the studies assessed model inputs. Of the OAT studies, 68% assessed parameter inputs, 78% assessed normative inputs (45% assessed both). Of the factored studies, 82% assessed parameter inputs, 45% assessed normative inputs (47% assessed both).

The normative inputs generally assessed in the surveyed papers include alternative allocation methods, boundary expansion scenarios, and alternative technology and implementation pathways. The parameter inputs in the surveyed papers include unit efficiencies, emission factors, consumption and production rates, and fuel properties.

Further analysis found that 22% of the sensitivity analyses use identical generic ranges for all inputs,<sup>81</sup> rather than parameter-specific ranges. Sensitivity analysis should avoid using a generic  $\pm x\%$  for every input as this may lead to incorrect conclusions on significance (discussed further in Chapter 2.4.3.2).

#### *2.4.1.3 Presenting results*

Sensitivity in the surveyed studies is presented using bar charts/scatter plots (49%), tables (33%), tornado plots (16%), spider plots (16%), and error bars (8%). Tornado and spider plots are easy-to-read, compact charts that present OAT results effectively. The more complex factored sensitivity results are usually presented with many grouped bar charts and error bars, which add several dimensions to a single figure and can be overwhelming for the reader.<sup>82</sup> When there is more than one output, radar plots can be used in place of spider plots.<sup>83</sup>

Factored designs can help us examine the effect of input interactions, but (as noted above) these produce an overwhelming number of outputs and are difficult to communicate properly.<sup>82</sup> Results are presented for each factored design, but the importance of each parameter or interaction effect is not ranked or quantified in the surveyed work; their analysis only looked for obvious trends.<sup>84</sup>

## 2.4.2 Uncertainty analysis

Many studies examine uncertainty in LCA. This work found that uncertainty analysis is becoming more common. 27% of the surveyed studies include uncertainty compared to 13% and 15% found by Ross et al.<sup>23</sup> and Tu et al.<sup>24</sup>, respectively. Other reviews have examined LCAs that specifically include uncertainty analysis to determine which method is used. Lloyd and Ries examined 24 LCA studies published between 1996 and 2004 that include uncertainty.<sup>20</sup> Budzinski examined 17 LCA studies published between 2008 and 2011 that include Monte Carlo simulations.<sup>27</sup>

Of the 24 LCAs that include quantitative uncertainty analysis, Lloyd and Ries determined that 67% used Monte Carlo, 29% used scenarios, 17% used fuzzy data sets, 8% used interval calculations, 8% used uncertainty propagation, and 4% were unspecified.<sup>20</sup> This study found that 65% of the uncertainty papers reviewed used Monte Carlo, and 35% used scenario analysis. The increase in MC analysis may be a result of LCA software such as SimaPro and GaBi integrating MC simulations into their programs (see Chapter 2.4.2.1).<sup>42, 85</sup> That said, scenario analysis is easy and does not require any specialized software for simple monotonic models.

### 2.4.2.1 Software currently used

SimaPro<sup>86-89</sup>, ModelRisk<sup>44, 90</sup>, @Risk<sup>67, 91</sup>, GaBi<sup>92</sup>, and Crystal Ball<sup>93</sup> are the main software programs used for Monte Carlo Simulations. ModelRisk, @Risk, and Crystal Ball are commercial Excel add-in programs.<sup>39-41</sup> SimaPro and GaBi are commercial LCA programs; SimaPro and GaBi typically use the ecoinvent database.<sup>42, 53, 85</sup> Overall, user-friendly software like SimaPro/ecoinvent and Excel add-ins make it easier to perform Monte Carlo simulations, which may explain Monte Carlo's growing popularity among LCA practitioners. Ecoinvent also comes with default uncertainty distributions, further reducing the workload of a Monte Carlo simulation.

The common LCA and Excel add-in softwares support Monte Carlo simulation only.<sup>39-42</sup> The inclusion of sensitivity methods such as Morris or hybrid methods such as classification and regression trees (CART) could allow further exploration of the underlying data (discussed further in Chapter 2.4.3.9.3). For users interested in performing other methods, R/MATLAB libraries are

available for sample generation and output processing that can be linked to SimaPro through scripts or to Excel through macros, but these require basic programming knowledge to use. SimLab has created an open source user interface that uses the R algorithms and does not require coding experience if the model is created inside its interface.<sup>94</sup> For Excel-based LCA models, I have recently created an open source template that uses R to generate the samples and process the results and Excel macros to generate the output file and link the Excel and R codes.<sup>2</sup> GaBi currently does not support automation.

#### 2.4.2.2 *Uncertainty method background*

Because the papers that were surveyed use either Monte Carlo or scenario analysis, background information on these have been provided; Igos et al. describe other uncertainty analysis approaches.<sup>18</sup>

One begins a Monte Carlo simulation by defining probability distributions for each parameter.  $N$  samples are generated for each input from their probability distribution and the model is run with each sample. The outputs are then displayed as a histogram or cumulative distribution function (CDF). Due to the random nature of Monte Carlo simulations, the resulting mean will vary between simulation runs; the variation is known as the sampling error (SE) and can be approximated as  $SE = 2.96 * \sigma / \sqrt{N}$ , where  $\sigma$  is the output standard deviation and  $N$  is the number of samples.<sup>95</sup> Modern computing allows large sample sizes and therefore sampling error is generally negligible.

The best/worst case (BWC) method requires only min/max or best/worst values for each input and no information on probabilities.<sup>96</sup> Additionally, for a monotonic model, only three model evaluations are required; these can be performed manually without the need to write automation code to perform thousands of iterations. However, an optimization approach is required for non-monotonic models. The obvious disadvantage of the BWC method is that the calculated output range may be excessively large; furthermore, unlike a Monte Carlo simulation, no information on parameter importance is available.

### 2.4.2.3 Monte Carlo in the survey results

This study determined that Monte Carlo is the most common form of uncertainty analysis used in LCA. The 13 Monte Carlo LCA studies from the survey were examined to determine the current state of research. Tu et al. gathered all the required information for distributions but did not actually execute the simulation.<sup>24</sup> But their work has been included in this survey as the analysis was done well and the MC simulation will be part of their next study. Only 46% (6) of the studies provided adequate information about the Monte Carlo simulations;<sup>44, 67, 88, 90, 97, 98</sup> this includes information on the number of samples, input distribution selection, justification for input distribution values, justification for which parameters are included in the simulation, and explanation of error bar values (min/max or percentiles).

#### 2.4.2.3.1 Sampling error and method

Because of the random nature of Monte Carlo simulations, sampling error causes the results to differ between runs. Only 15% (2) of the survey studies mention sampling error and justify the number of samples used.<sup>44, 90</sup> 23% (3) do not provide the number of samples used;<sup>67, 91, 92</sup> hence, sampling error cannot be approximated. However, since the number of samples used in the surveyed simulations ranged from 1,000 to 100,000, sampling error is likely minimal.

Monte Carlo samples are generated randomly or using a Latin hypercube sample (LHS). While the most used Monte Carlo software uses random sampling (ModelRisk<sup>39</sup>, SimaPro<sup>85</sup>, GaBi<sup>42</sup>, and Crystal ball<sup>41</sup>), it can be inefficient and result in points that are either clustered too closely together or spread too far apart. The LHS method splits the sample space into subChapters and ensures that each subChapter is adequately sampled and that a well-spaced sample is produced. If model evaluations are computationally expensive, the LHS method can be used, as its sampling error is  $O(1/N)$ , much lower than Monte Carlo's  $O(1/\sqrt{N})$ .<sup>99</sup> While the LHS improves the sampling of a single distribution, it does not ensure input combinations are adequately sampled; therefore, LHS loses its advantage as the number of *significant* inputs increases. A model may contain hundreds of inputs, but if the output uncertainty is dominated by a single input, then the error in output distribution will be dominated by the error in the single input's distribution.<sup>99</sup> None of the studies mentions the use of a Latin hypercube sample. While the software used by the studies relies on random sampling, only four studies specifically

mention that random MC was used.<sup>44, 86, 89, 90</sup> Overall, the more complex LHSs are only needed for computationally expensive models where small sample sizes are desired or where highly skewed distributions significantly affect the output distribution.

#### *2.4.2.3.2 Types of distributions used and their justifications*

When it came to justifying which Monte Carlo distributions were used and their key values (Figure 2-2), Budzinski, and Lloyd and Ries, found that 18% and 17% of the studies assessed, respectively, provided no information; in the papers that were reviewed, 23% used the SimaPro/ecoinvent defaults but provided no further explanation or justification.<sup>86, 87, 92</sup> This review found that 23% of the studies used identical generic distributions for all parameters; two used normal distributions with a standard deviation of 5% and 10% of the mean<sup>91, 93</sup> and one used GaBi, stating the uncertainty analysis results were produced using “Monte Carlo analysis (with a 20% variation rate).”<sup>92</sup> Using identical generic distributions is at best a simplistic sensitivity analysis, not an uncertainty analysis (see Chapter 2.4.3.2). Only 23% (3) of the studies used a sensitivity analysis to screen key inputs to be included in the Monte Carlo simulation.<sup>44, 90, 97</sup> The other studies either arbitrarily included life cycle inventory (LCI) parameters with the distributions available<sup>86, 87</sup> or specified key inputs based on author judgement.<sup>24, 67, 88, 98</sup>

#### *2.4.2.3.3 Distributions used*

In studies that used multiple distributions, the uniform and triangle distributions were the most common (Figure 2-2). The popularity of the lognormal distribution is most likely because SimaPro/ecoinvent, used in 46% (6) of the studies, defaults to lognormal distributions. Lognormal distributions are also commonly used with data quality indicators (DQI) (further discussed in Chapter 2.4.3.3). Budzinski found lognormal distributions used in 65% of the studies examined, and these studies primarily used SimaPro/ecoinvent.<sup>27</sup> This study determined that error, Johnson, Weibull, and skew normal distributions were used in 8% of the studies. Uniform, triangle, PERT, normal, and lognormal distribution background information can be found in Chapter 2.2.3.

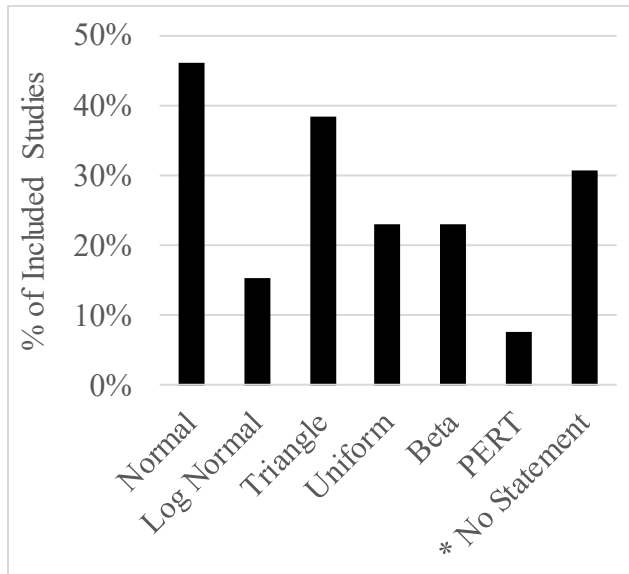


**Figure 2-2: Distributions used in the 13 Monte Carlo Studies (4 of the studies in this work did not specify what distribution was used, but it is expected they used lognormal as that is the ecoinvent/SimaPro default)**

#### 2.4.2.3.4 Presenting results

The Monte Carlo results are presented primarily with error bars, 38% (5),<sup>86, 87, 91-93</sup> histograms, 23% (3),<sup>67, 97, 98</sup> comparison charts/tables, 23% (3),<sup>24, 88, 89</sup> and box and whisker plots, 15% (2) (Figure 2-3). Error bars reflect either a specified confidence interval<sup>86, 92, 93</sup> or standard deviation;<sup>87</sup> in one case, it was unclear what the error bars represented.<sup>91</sup> Both 90% and 95% confidence intervals were most commonly used for the box and whisker and the error bar plots. Confidence interval should be used over standard deviation when the output distribution is skewed. Comparison bar charts show the percentage of samples where pathway A=>B. The number of comparisons is equal to the combination (p,2), where p is the number of pathways; this number can become overwhelming when more than 3 pathways are compared. Additionally, the comparison charts only show whether A=>B, but not how much greater A is than B. Tables and in-text discussion are also used to communicate key results. Manadhar and Shah, and Nimana et al. extend their analysis by determining the cross-over point between two pathways based on a critical input such as distance or system capacity.<sup>90, 98</sup>

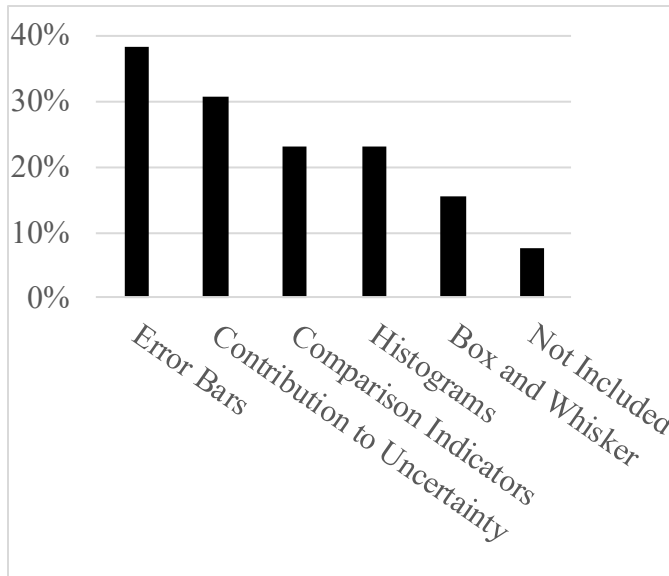


**Figure 2-3: Uncertainty presentation methods**

#### 2.4.2.3.5 Correlation and dependence

LCA is commonly used to compare two or more alternatives. When conducting an uncertainty analysis for comparative LCA, it is important to consider dependency; however, 54% of the papers surveyed did not do so. Of the six studies that accounted for parameter correlations, three specifically included correlated inputs<sup>44, 67, 90</sup> and three used a differential analysis to account for multiple pathways sharing random inputs.<sup>86, 88, 89</sup> Consider an LCA of two technology alternatives A and B. While there may be uncertainty in the electricity carbon intensity (CI) if both projects are being considered for the same location and would use the same grid, it would not be appropriate to compare alternative A using low CI and alternative B using high CI electricity. In order to get an accurate comparison, the uncertainty for each model should be run simultaneously and the output should be the difference between the two alternatives. Not all inputs will be dependent, and some may be only partially dependent. For example, if alternatives A and B are located in different regions, their electricity CI would be independent. The issue of dependency in comparative LCA has been examined by Henriksson et al., who recommend performing statistical tests on the difference between pathways to determine if the results are statistically significant.<sup>100</sup>

Dependency within ecoinvent, a commonly used LCA database, is currently being debated. Qin and Suh examined the possibility of using pre-calculated distributions for the ecoinvent database

to reduce computational times.<sup>101</sup> Henriksson commented that the use of pre-calculated uncertainties cannot be used in comparative LCA as they do not account for dependency and will therefore overestimate uncertainty.<sup>102</sup> Qin and Suh responded by examining the probability of a decision being reversed (from  $a > b$  to  $b > a$ ) or moderated (from  $a > b$  to  $a \approx b$ ) if fully dependent samples are used instead of pre-calculated distributions. Their results indicated that no results were reversed and only 10.5% were moderated for similar processes.<sup>103</sup> They further performed an empirical analysis of 100ecoinvent processes to determine if the ratio of geometric standard deviation (GSD) with dependent sampling over pre-calculated distribution sampling was less than one, which would indicate that using pre-calculated distributions overestimates uncertainty.<sup>104</sup> Their results indicated the GSD ratio ranged from 1.0681 to 1.0696 with a 95% confidence interval, indicating that using pre-calculated distributions will more likely result in a slight underestimation of uncertainty. While Qin and Suh's work suggests that using pre-calculated uncertainties will not result in inaccurate uncertainty estimations, their pre-calculated distributions were developed using dependent sampling and are therefore partially dependent. When users supply foreground data or their own uncertainty distributions for background data, it is up to them to ensure dependent sampling is accounted for. Furthermore, Qin and Suh found that the error associated with pre-calculate distributions is small 95% of the time but in a small number of cases could be significant ( $0.8 > \text{GSD ratio} > 1.5$ ). It is therefore suggested that a sensitivity/screening analysis be used to identify potential risk. If uncertainty is dominated by the foreground data, then, even if there is an error in the background uncertainty due to dependency, it will have a negligible effect on the results. On the other hand, highly sensitive background inputs that are dependent indicate further investigation may be required.

One of the largest challenges in assessing pathways with dependent inputs is the requirement to perform pairwise comparisons. As the number of pathways increases, interpreting and displaying results can become complicated (see Chapter 2.4.3.9 for further discussion).

#### *2.4.2.3.6 Contribution of variance*

Only one the papers calculated the contribution to variance (COV) of the uncertain inputs; however, no information on the method used was provided.<sup>93</sup> Two papers used conditional mean

tornado plots derived from the Monte Carlo simulation data to rank each input's impact on the mean value.<sup>44, 90</sup> A contribution of variance analysis allows the practitioner to identify which inputs need to be further examined in order to improve the accuracy of the results. Unlike sensitivity analysis, COV uses probability distributions. While a COV analysis can provide additional insight, it is not a requirement, can be time consuming to perform, and, for simple models, can be redundant if a sensitivity analysis has already been done; therefore, its absence from the majority of uncertainty studies is not a critical flaw.

#### *2.4.2.4 Best/worst case scenarios in survey*

None of the seven best/worst case scenario (BWCS) studies used optimization to identify extreme scenarios and simply assumed the models are monotonic. The inputs included in the surveyed assessments were selected by the author's judgement, and data ranges were selected from the literature. Commonly included inputs were use factors, production rates, efficiencies, and product lifetimes.<sup>81, 96, 105</sup> Since a subjective approach was used to select the parameters included, the uncertainty may be underestimated if excluded parameters have a significant effect.

All of the studies in this review examined parameter uncertainty using the BWCS method alone; however, alternative pathways,<sup>106</sup> OAT,<sup>96</sup> and factored sensitivity<sup>107</sup> were used in combination with BWCS to examine the effect of normative choices as well. Of the BWCS studies, three assessed over ten parameters<sup>105, 106, 108</sup> and the remaining four assessed only 2-5 parameters.<sup>81, 96, 107, 109</sup> The results are primarily presented using bar charts,<sup>96</sup> error bars,<sup>106</sup> and tables.<sup>81</sup>

BWCSs are not as rigorous as a Monte Carlo simulation. However, if resources are unavailable to perform a Monte Carlo simulation, BWCS can still be valuable. Using BWCS in combination with OAT or factored sensitivity can provide useful insight into the model's behavior with minimal computational power, assuming the model is monotonic, as only a small number of samples are needed compared to Monte Carlo simulations. Additionally, given the small number of samples required, the analysis can be run manually and does not require specialty software or scripts.

### 2.4.3 Limitations and areas for improvement in current work

This Chapter provides a review of the limitations observed in the current literature and includes recommendation for improvement.

#### 2.4.3.1 *Global vs. local sensitivity methods*

As mentioned in Chapter 2.2.2, sensitivity analysis can use either a local or a global approach. A majority (73%) of the papers examined used a limited local sensitivity analysis. Saltelli and Annoni suggest that local sensitivity methods are favored as the base case is seen as the best estimate. Additionally, the model may become less accurate and even unstable/invalid for input combinations far away from the base case, and when the model does fail it is easier to identify the cause of failure when an OAT approach is used. OAT methods do not include noise, eliminating the possibility of type I errors.<sup>110</sup> Saltelli and Annoni used a geometric proof to illustrate that as the number of parameters in the model increases, the fraction of the parameter hyperspace explored using an OAT rapidly approaches zero. Global approaches provide a better representation of sensitivity by accounting for non-linear and interaction effects.

While a global method provides more detailed results that account for non-linear and interaction effects, the additional effort may not be required for simpler models. For example, consider an LCA of a crude oil pipeline. In model A, aggregated data is used to determine the carbon intensity (CI), and the model simply adds the aggregated CI from various stages ( $Y = X_1 + X_2 + \dots + X_n$ ). In model B, a rigorous bottom-up approach based on engineering first principles is used. In model A, there is no benefit in running a global method over a local one as there are no interactions or non-linear effects. However, in model B, where complex calculations are performed, an input such as the pipeline diameter will propagate throughout the model and interaction effects could be significant. Therefore, a global approach will be beneficial. Furthermore, some models may lack sufficient depth to benefit from a global sensitivity method. For example, in a natural gas pipeline, several gas and fluid flow properties depend on both the gas temperature and the composition. In a model where the gas/fluid properties are provided by the user, rather than calculated based on the gas temperature and composition, the global approach would not be able to properly quantify the sensitivity of the gas temperature and composition. In this case, the benefit of using a global method over a local one is reduced. For

non-linear models, the sensitivities may be overestimated because of large sensitivities calculated at the extreme points dominating the analysis (when a small number of samples is used). Alternatively, local methods may underestimate parameter sensitivities by failing to account for non-linear and interaction effects.

A factored approach using multiple levels provides a better estimate than the OAT approach and does not assume linearity. However, it still provides only a limited exploration of the parameter hyper-space.<sup>110</sup> Linear regression can be used to calculate sensitivities via the predicted coefficient for each input. The advantages of linear regression include the ability to examine the averaged effect for each input over its entire range and to provide the sign of the effect on the output. However, the accuracy of the linear regression method is affected by the  $R^2$  value of the model. The parameter coefficients cannot be used to rank input sensitivities for a poorly fitted model (low  $R^2$  value). The regression sample can be used later by the Monte Carlo simulation to reduce computation times.<sup>110</sup> While, like the local OAT method, linear regression is best used for purely additive models, it at least provides an indicator on non-additivity and non-linearity through the  $R^2$  value.<sup>110</sup> Variance-based methods such as Sobol (Chapter 2.4.3.6) can be used as a sensitivity method; however, they require a large number of model evaluations, limiting their use to a small number of inputs and models with short computation times.

To overcome local methods' inability to identify interaction effects and the large sample requirements of the factored approach, the Morris method can be used. The Morris method (or elementary effect method) is a versatile and efficient global method that can be used for screening purposes. It works for non-linear and non-monotonic models. The Morris method uses an OAT approach but is not centered at the base case scenario. Each input is changed OAT, but instead of returning to the base case after each step, the next input is changed immediately; this results in a trajectory that randomly moves through the parameter hyperspace. After each input has been changed, a new starting point is selected and the process repeats. Therefore, within each trajectory a partial derivative is calculated for each input. As the number of trajectories used increases, the portion of the hyperspace explored increases, at the cost of additional model evaluations. The number of model evaluations required is  $N=r*(k+1)$ , where  $r$  is the number of trajectories and  $k$  is the number of parameters. Saltelli and Annoni suggest that good but not quantitative estimates for screening purposes can be obtained using only 4 to 10 trajectories.<sup>110</sup>

The number of trajectories required depends on the model complexity; highly non-additive and non-linear models will require additional trajectories. In another study, it was found that there is negligible benefit in increasing the number of approaches above 60.<sup>2</sup> While the number of model evaluations required is larger than OAT ( $N=2k+1$ ), it is still significantly smaller than the samples required for the factored, linear regression, and Sobol approaches. It was also found that adequate estimates of parameter sensitivities obtained using Morris required fewer than 1/100<sup>th</sup> as many samples as those obtained using the Sobol method.<sup>2</sup> Campolongo et al. developed an algorithm to select a small number of optimal approaches that provides the best coverage of the parameter space, rather than using randomly selected approaches, for situations when the number of model executions needs to be minimized.<sup>111</sup>

The average and standard deviations (SD) of the  $r$  partial derivatives taken for each parameter are plotted on the Morris plot. The Morris average uses absolute values to ensure non-monotonic responses are accounted for. A higher Morris average indicates a greater sensitivity, while a high Morris standard deviation implies the sensitivity of the given parameter varies across the parameter hyper-space. The Morris SD can be thought of as the variation in the Morris mean (parameter sensitivity). To highlight the benefit of using the Morris over the commonly used OAT method, consider a scenario shown in Figure 2-4 for parameter X11. Depending on what value is used for the base case in an OAT approach, parameter X11 could be considered insensitive (point 1) or highly sensitive (point 2). The Morris method, however, shows that the sensitivity of parameter X11 varies widely, either because of a non-linear response or an interaction effect. Unlike OAT, the Morris method can account for global sensitivity while using fewer samples than a factored approach. The limitation of the Morris method is that it cannot differentiate between non-linear and interaction effects but can only indicate if neither occur (zero standard deviation). Technical details for the Morris method can be found in works by Campolongo et al. and Morris.<sup>111-113</sup>

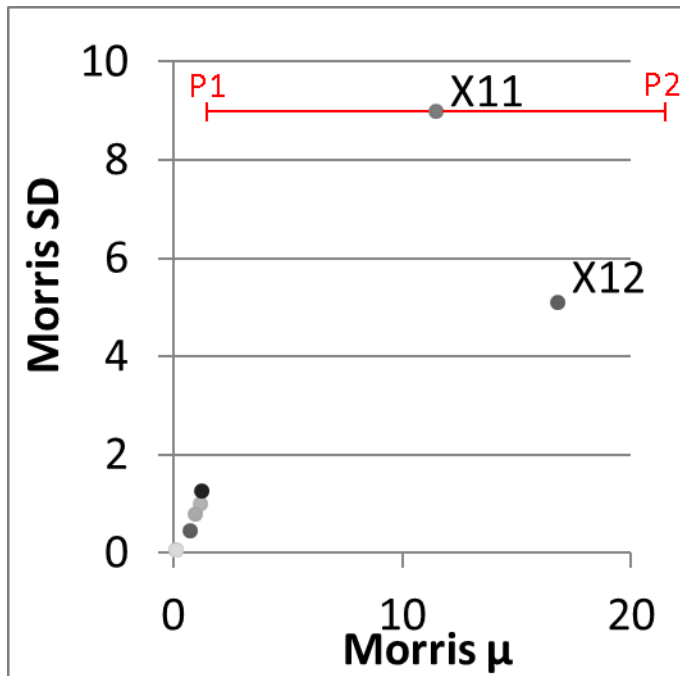


**Figure 2-4: Morris plot created using RUST<sup>2</sup>**

#### 2.4.3.2 Sensitivity scope and quality

As mentioned in Chapter 2.4.3.1, the use of a local sensitivity analysis may lead to sensitive inputs being misclassified as insensitive. Another cause of misclassification is the use of generic sensitivity ranges, as seen in 22% of the surveyed papers that performed sensitivity. While it is easier to simply change each input by  $\pm 10\%$  to perform a sensitivity analysis, doing so may lead to faulty conclusions. For example, pipeline operating emissions depend on pump efficiency and pipe relative roughness. If a generic  $\pm 10\%$  range is used for the sensitivity analysis, the pump efficiency would appear to be significant, while relative roughness appears insignificant. However, the relative roughness can vary by an order of magnitude and be significant.<sup>4</sup> While the use of generic ranges in a sensitivity analysis could be defended as a simple exploratory approach, it cannot be applied to uncertainty analysis. Unless justification is used, applying generic distributions to a Monte Carlo simulation produces a meaningless output distribution, communicates a false sense of confidence in the results, and should not be performed for the sole purpose of adding error bars to the results. The Monte Carlo results could be used as a basic sensitivity analysis if they are analyzed using a conditional mean tornado plot, for example; however, the output histogram would be meaningless.

In the surveyed literature there was a notable lack of justification on which parameters were included/excluded in the sensitivity analysis (Chapter 2.4.3.2). Since the normative choices are generally subjective and depend on the purpose of the LCA, it makes sense that author judgement and stakeholder consultation are used to select relevant inputs; however, quantitative approaches are available for screening parameter inputs. The general approach observed in the surveyed papers is to include parameters for which a large range of possible values has been reported in the literature or the authors know will have a significant impact on the results. While this simple approach works in most cases, especially with simpler models, it can lead to significant inputs being ignored in more complex models. Even a small change in a sensitive parameter's value can result in a significant change in the model output. In the author's experience, performing an in-depth sensitivity analysis identifies important parameters that would have otherwise gone unnoticed and helps catch errors in the LCA model. Adequate documentation on which inputs/assumptions are included in the sensitivity analysis should also be provided to meet ISO requirements and improve the quality of the surveyed work.<sup>17, 80</sup> Additionally, a model's credibility can be improved when a detailed sensitivity analysis is performed; instead of the authors stating they assumed an input is not important, they can confirm they verified that the input is insignificant.

#### *2.4.3.3 Data quality indicators and the pedigree approach for quantifying uncertainty*

When the uncertainty of an individual parameter is unknown, a pedigree approach can be used to approximate the uncertainties using DQIs. The pedigree method uses a qualitative ranking system and corresponding uncertainty factors.

Ecoinvent v3 uses an updated pedigree matrix with five indicators and five levels to determine the additional uncertainty factors.<sup>114</sup> The indicators with the top and bottom levels for each indicator are reliability (verified measurements vs. non-qualified estimates), completeness (representative data from all sites being considered vs. unknown representation), temporal correlation (data less than 3 years old vs. 15 years old), geographical correlation (data from study area vs. data from unknown or distinctly different area), and technological correlation (data from industry processes vs. data from similar process or laboratory study).<sup>114</sup> Ecoinvent has developed default uncertainty factors for each indicator and level that range from 1 to 2.8. There are an

additional 27 basic uncertainty factors for different activities or emissions, such as methane emissions from combustion, thermal energy, etc.<sup>79, 115</sup> If empirical data is available, then the basic uncertainty can be calculated using statistical analysis.

The ecoinvent v2 uncertainty factors were determined using industry experts' suggestions and are therefore subjective. In order to improve the accuracy of the uncertainty factors, Citroth et al. used several databases to empirically determine each uncertainty factor for implementation in ecoinvent v3.<sup>114</sup> Muller et al. further expanded the ecoinvent uncertainty analysis by calculating uncertainty factors for normal, triangle, PERT, and binomial distributions to overcome the restriction of requiring a lognormal distribution.<sup>79</sup>

Overall, the pedigree method is easy to use, with minimal data requirements. Although an empirical method was used to calculate the uncertainty factors, the selection of levels is subjective, and the factors are technically only valid for the databases used to determine them. Additionally, the pedigree method only assesses parameter uncertainty in inventory values. Data values entered by the practitioner will not have default uncertainty distributions assigned to them but may still be a significant source of error. For example, a user can specify that 10 kg of steel is needed for each product Y, and ecoinvent will have default uncertainty values for various steel manufacturing processes but will not include any uncertainty in the amount of steel required (that specified by the user); a distribution needs to be specified by the user. Furthermore, not all database values include default uncertainty distributions. Since uncertainty is typically dominated by a small number of critical inputs, this lack of coverage could result in underestimating the total uncertainty. 23% of the studies included in our study stated "the SimaPro/ecoinvent defaults were used" and provided no further explanation or justification.<sup>86, 87,</sup>  
<sup>92</sup> Given the severe lack of documentation in the examined literature, it is not clear if authors addressed or were aware of these gaps.

In the authors' opinion, the most significant pitfall of the ecoinvent defaults is their ease of use coupled with academic journals' willingness to accept papers without discussion or documentation on the limitations of the uncertainty results. On the other hand, when used properly, the ecoinvent defaults can drastically reduce the time it takes practitioners to perform a rigorous uncertainty analysis. Practitioners can use a screening sensitivity analysis to determine

if the inputs that do not include default uncertainty distributions will have a significant effect on the results (see 4.3.6 for further details). Ecoinvent, SimaPro, and GaBi should consider adding a warning message/note to their interface informing users of the limitations of using only the ecoinvent defaults.

#### *2.4.3.4 Modeling uncertainty as a probability distribution or scenario*

Refsgaard et al. provide a taxonomy of imperfect knowledge to determine how to represent uncertainty. Based on this taxonomy, Refsgaard et al. recommend using probability distribution when some of the outcomes and their probabilities are known and using scenarios when only the outcomes are known but no probabilities.<sup>22</sup> In the LCAs surveyed in this work, probability distributions are typically used to represent uncertainty in parameter inputs. If probabilities are not known, they are approximated using expert opinion or DQI methods.<sup>97</sup> In addition, normative choices are commonly represented as scenarios.<sup>67</sup>

It is often tempting to use probability distributions for all the uncertainties as this approach produces a single output distribution that is easy to present. However, it is not possible to identify the effect of any individual input on the results. Alternatively, a scenario approach can distinguish individual effects but requires that multiple results be displayed for each input; such a presentation can become overwhelming as the number of inputs increase. A factored design would be needed to incorporate interactions as well if multiple scenario inputs are included.

Normative inputs, also called value parameters, often represent the preference of the decision makers.<sup>46</sup> Morgan and Herion state that the value parameters tend to be values that policy makers are most unsure of and tend to be a source of debate.<sup>46</sup> They suggest that including the value parameters as possibility distributions can mask their effect and lead to confusion; instead of using a scenario (parametric) analysis, policy makers should get a clear picture of how the value parameters affect the overall policy outcome.<sup>46</sup> For this reason, Morgan and Herion suggest normative inputs should never be modeled using probability distributions. Alternatively, for discrete normative inputs in comparative LCA with dependent sampling, Huijbregts et al. suggest using a non-parametric bootstrapping method, which involves identifying two or more alternatives and assigning probabilities to each.<sup>116</sup> The probabilities must sum to one and are determined subjectively by the decision maker. Huijbregts et al. assumed equal probabilities for

all alternatives, and one of the surveyed studies by the authors used historical data to determine the share of existing mills that implemented a methane capture technology.<sup>67, 116</sup> While bootstrapping allows us to implement normative choices into Monte Carlo output results, the arbitrary application of a probability to each scenario will still mask the effect of the inputs and is not always logical. For example, assigning an equal probability to a 100-year and a 20-year time-horizon has no logical basis. However, using bootstrapping to represent scenario parameters can be useful when used in an exploratory manner. If a sensitivity screening analysis indicates the normative inputs have a negligible impact on the results, further investigation is not needed. See Chapter 2.4.3.7 for further information on dealing with normative choices.

#### *2.4.3.5 Discussion on the motivation for performing sensitivity and uncertainty analysis*

When performing LCA, the sensitivity and uncertainty analysis should not be thought of as something to add at the end of a study for the simple purpose of adding error bars to the results, which seems to be the case in the surveyed work. Sensitivity and uncertainty analyses should be integrated into the entire LCA process, with the goal of improving the quality of the analysis. The practitioner should, for example, determine what information is required, what aspects of the model need to be improved, and how policy or external factors will influence the results.

Additionally, we recommend using an exploratory mindset when performing sensitivity and uncertainty analyses. The end goal is not to determine the exact range of values the output can take with certainty, as this is likely infeasible given data limitations. Instead, the goal should be to determine what assumptions or conditions will influence the results, develop a better understanding of the limitations of the analysis, and identify opportunities to improve the robustness and understand the conclusions. Klauer and Brown suggest using a subjective interpretation of uncertainty focused on the decision makers' degree of confidence in the possible outcomes. This is similar to the Bayesian inference discussed by Ellison.<sup>117</sup> While this method is subjective, and the practitioner could be overconfident, the results are still useful if the assumptions are transparent (a requirement of ISO standards<sup>17, 80</sup>), especially for the critical assumptions.

This study found that sensitivity and uncertainty analyses provide multiple benefits to the practitioner that can offset the additional time spent performing the analysis. For example, when

the results from the Morris screening method do not align with the practitioner's expectations, the practitioner is encouraged to further examine the model to explain the disagreement. Further examination will either identify calculation errors or provide the practitioner additional insight into their model. Furthermore, the screening method can be used to guide the practitioner's time management. LCA involves collecting large amounts of data and developing various models and calculations. If the screening method suggests that a parameter such as some portion of a product shipped by rail vs. truck has a negligible effect on the outcome, then there is negligible benefit in finding the industry data. Furthermore, it may be unclear if a simple correlation will suffice or a rigorous sub-model is required. If the correlation is known to be accurate within  $\pm 25\%$ , then the correlation output can be multiplied by an "accuracy" term that can range from 0.75 to 1.25 during the sensitivity analysis. If the accuracy term is insensitive, the correlation is enough, and further work on a more rigorous model is not required. Overall, a detailed sensitivity and uncertainty analysis can save the practitioner time, while improving the quality of the analysis compared to a simpler alternative commonly seen in the surveyed works.

#### *2.4.3.6 Framework improvement*

This study found that two main approaches were used in the studied works, either sensitivity alone or an uncertainty analysis followed by a sensitivity or contribution to variance approach to identify critical inputs. That said, in another study the authors suggested using an iterative framework, which is summarized below.<sup>2</sup> The framework aims to minimize the amount of time and effort put into uncertainty analysis while maximizing the usefulness of the analysis results. Since uncertainty in the output is a product of input uncertainty and input sensitivity, an insensitive input will have a negligible effect on the output uncertainty. Therefore, input uncertainty distributions are only required for the sensitive inputs to accurately estimate output uncertainty.

In order to perform a sensitivity analysis, minimum and maximum values are required for each input. To reduce the workload, a conservatively wide estimate should be provided for each input; this also reduces the likelihood of incorrectly identifying a sensitive input as insensitive. The Morris method is then used to determine parameter sensitivities. Morris requires fewer samples than Monte Carlo and Sobol and is more effective at identifying key parameters than the OAT

method. Additional research/data collection is then performed for the sensitive inputs to refine their minimum and maximum ranges. The Morris analysis is repeated until the ranges for all the sensitive inputs have been refined. While the insensitive inputs still give conservatively wide ranges, their impact on the output uncertainty is negligible and further effort to refine the ranges is not necessary. Preliminary uncertainty distributions are then determined for the sensitive inputs identified in the final Morris iteration and a Monte Carlo uncertainty analysis is performed. Since this is a subjective approach, caution should be used to avoid prematurely eliminating sensitive inputs. If changes are made to the model, the Morris analysis should be rerun to ensure insensitive parameters have not become sensitive. When Morris screening is used, the number of inputs included in the Monte Carlo simulation can be significantly reduced and overall computing time decreased.

To identify which inputs are the largest contributors to the uncertainty distribution, a contribution of variance (COV) analysis is performed. Since COV typically requires between 2,000 to 64,000 model evaluations per input to determine accurate indices, only the sensitive inputs should be included. The practitioner should then attempt to further refine the distributions for inputs with a large COV index to improve the accuracy of the model. When this approach is used, less time is spent determining uncertainty distributions for insignificant inputs and the analysis is of a higher quality.

Common COV methods are Sobol and the Fourier amplitude sensitivity test (FAST). The Sobol method is a decomposition of the variance approximation approach, which determines inputs and input interactions contributions to the output variance.<sup>118-120</sup> The results are expressed as first order indices that represent each input's share of the total variation as a percentage. Second order interactions determine the portion of variation because of the interaction between pairs of inputs. To overcome the computational expense of performing a Sobol analysis, the FAST method was developed. FAST can calculate the Sobol indices using fewer than 1/20<sup>th</sup> as many model evaluations as the Sobol method.<sup>121, 122</sup>

The Sobol and FAST methods both assume a normal output distribution. In the case of multimodal or highly skewed distributions, the calculated indices can be misleading; therefore,

moment-independent methods such as entropy-based sensitivity and PAWN indices are needed.<sup>71, 123</sup>

#### *2.4.3.7 Discussion on framing analysis*

The goal and scope of the LCA affect how the sensitivity and uncertainty analyses are performed. The effect of the goal and scope on SUA was not discussed in the surveyed studies. As mentioned above, dependency can significantly affect the outcome of an LCA. In the surveyed study, sensitivity is performed for each pathway independently.<sup>90</sup> However, if there is dependency between the pathways' inputs, a sensitivity analysis of the differences in the pathways' results is recommended. For example, both independent pathways may be sensitive to the electricity CI, but if they use the same energy source, the difference between the two results may be insensitive to the electricity CI. It may also be useful to group similar parameters and change them simultaneously rather than individually. For example, a pipeline model may allow the user to specify pump efficiencies for each pump station. If each pump's efficiencies are changed independently, the practitioner can identify which specific stations would benefit from installing a higher efficiency pump. Alternatively, grouping the pump efficiencies would determine how the entire system's emissions would change if all the pumps were upgraded.

The audience and the goal of the LCA can affect the decision to represent uncertainty as a distribution or a pathway (see Chapter 2.4.3.4). For example, if a product is manufactured using two different technologies, pathways should be used if the goal is to compare the two technology pathways (i.e., gasoline from different sources), and if the goal is to find the average emission intensity of the product to be compared to an alternative product (gasoline vs. fuel cell vehicle), a distribution should be used.

In cases where the uncertainty is dominated by a single input, scenarios could be used to provide additional insight. For example, the CI of electric cars is dominated by the electricity CI used to charge the battery pack. Rather than presenting a single output distribution for a wide range of electricity CIs, sub-scenarios can be used with low, mid, and high electricity CIs or to represent different regions.

#### 2.4.3.8 *Data fitting methods*

When adequate data is available, parametric (fit to existing distribution) or non-parametric (fit to data without assuming distribution shape) methods can be used. The surveyed literature provided limited discussion on data fitting methods used.

Vose provides an excellent overview of several data fitting methods and suggests three key guidelines to data fitting.<sup>78</sup> First, non-symmetric biased error is difficult to identify and account for and will not be captured by data fitting methods. In the oil and gas industry, for instance, flaring events are only recorded if these last longer than an hour or release more than a specified volume of gas; reporting in this way leads to underestimation. Second, the practitioner should be aware of how different distributions handle extremes. Some distributions will not extend beyond the extreme values in the data, while others, like the normal distribution, extend to infinity. To avoid impossible scenarios, i.e., negative mass or flow rates, distributions can be truncated. However, it is generally acceptable to allow the distribution to extend beyond the sampled data, as extremes are rarely captured in the data. Third, the practitioner should always examine data for outliers or errors prior to fitting. It should be noted that in certain scenarios, removing outliers is not recommended. For example, Zimmerle et al. found that a small number of super emitters were responsible for a significant portion of natural gas fugitive emissions and ignoring them would lead to an underestimation error.<sup>124</sup>

#### 2.4.3.9 *Communicating results*

Rarely discussed in the surveyed works was the significance of overlapping uncertainty ranges for multiple pathways. It is important to account for dependency and properly communicate the level of overlap between distributions to determine if the results are conclusive. When multiple normative inputs are present, a hybrid approach can be used to present the results in an easy-to-understand manner.

##### 2.4.3.9.1 *Check statistical significance*

First, it is important to determine whether the difference in the pathway means is statistically significant. Because of the random nature of Monte Carlo simulations, the output mean (mentioned earlier as the sampling error) for each pathway will vary between runs. To test

significance, Beltran et al. suggest the null hypothesis significance testing (NHST) and modified NHST.<sup>52</sup> Henriksson et al. state that statistical significance should always be checked to confirm results, but significance should be used with caution as it does not account for dependency.<sup>125</sup> Furthermore, significance of unique means is rarely relevant in uncertain comparative LCA, as the uncertainty is not strictly a result of natural variation because of the subjective nature of the analysis. Therefore, even if the results are statistically significant, it is not practical to claim one pathway is better than another if there is significant overlap.

#### 2.4.3.9.2 *Quantifying degree of overlap*

When output distributions overlap, it is common to determine by how much. When examining histograms or a boxplot, it can be difficult to visualize how significant the overlap is. Quantitative measures can be used in these cases. Two approaches can be used to quantify the amount of overlap between two distributions. Post-hoc methods do not consider dependency between the distributions, and rigorous analytical methods can account for dependency. Post-hoc methods include assuming a normal or lognormal output distribution<sup>52</sup> and using pattern recognition methods on the empirical histograms.<sup>52, 126</sup>

Rigorous analytical methods include a basic discernability analysis that compares the results from each Monte Carlo run to determine the percentage of runs in which pathway A is greater than pathway B.<sup>52</sup> Wei et al. suggest using reliability theory in comparative LCA to expand on the discernability method to determine the confidence of the model decision.<sup>127</sup> While an Monte Carlo sample can be used for differential analysis, the coefficient of variation (CV) of the decision confidence probability  $P_D$  is  $CV = \sqrt{(1 - P_D)/(P_D * N)}$ .<sup>128</sup> Hence, thousands of samples may be required to obtain an accurate result. If computational requirements are high, first and second order reliability methods (FORM and SORM) can be used. By focusing the analysis around the design point, the number of iterations required is reduced significantly compared to the MC method.<sup>127, 129, 130</sup>

#### 2.4.3.9.3 *Classification and regression trees*

Classification and regression trees (CARTs) have two potential uses. First, if there is overlap between pathway output distributions, as discussed in Chapter 2.4.3.9.2, CART can be used to

determine whether one pathway is better. Second, when an LCA includes multiple normative inputs, CART can be used to present the normative effects in a condensed form (Chapter 2.4.3.4).

CART is used to partition the input space into sub-scenarios and can be read as a series of “if” statements. For example, in Figure 2-5, Pathway A is greater than B if  $X1 > 0.25$  and  $X2 > 0.25$ , and when  $X1 > 0.75$  and  $X2 < 0.25$ . CART can be applied using both discrete and continuous values for the model inputs and outputs.

Gonzalez et al. argued that CART is well suited for assessing Monte Carlo simulation results, as it is simple, automatically searches for non-linear effects and higher-order interactions, provides an easy-to-read output, and can identify important inputs.<sup>131</sup> Therefore, when Monte Carlo simulation output distributions overlap, the CART method can identify the sub-scenarios when  $A > B$  and  $B > A$ . The disadvantage of performing CART on a continuous Monte Carlo sample is that the generated sub-scenarios will not have as clearly defined boundaries.

As mentioned in Chapter 2.4.3.4, displaying and understanding results using scenarios with a large number of normative inputs can be difficult, while using probability distributions hides the effect of the normative inputs. Gregory et al. conducted a hybrid discernibility analysis using decision-tree partitioning to identify sub-scenarios in which each pathway dominates.<sup>132</sup> A full factorial approach was used for the normative choices and distributions for the parameter inputs. Normative inputs were either binary or had three discrete values. A Monte Carlo simulation with 1,000 samples was executed for each of the 128 normative factored designs, requiring a total of 128,000 model executions; this approach incorporated dependent sampling. For each normative factor,  $\beta$ , the percentage of runs in which  $A > B$  was calculated. The scenario was considered resolved if the value of  $\beta$  was larger than the specified cutoff value (90%). CART was then applied to the binary output (1 = resolved, 0 = unresolved) and to discrete normative inputs. The tree branches could then be used to identify critical normative choices; see Figure 2-5 for an example.

The CART method uses a pairwise approach and is therefore ideal for fully understanding a situation in which one pathway is better than another, not for providing a high-level overview of

which pathway among many is best. As the number of normative choices and the degree of overlap increases, the tree size increases, resulting in an output that is overwhelming for the reader.

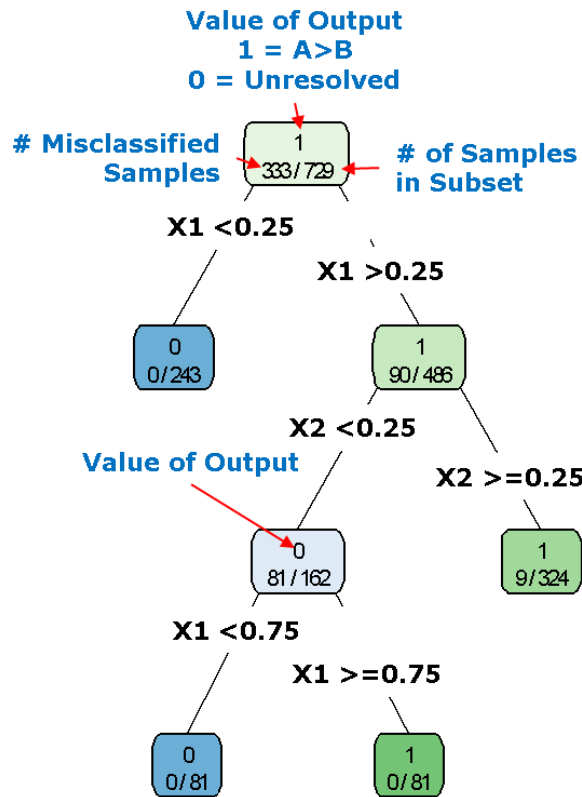


**Figure 2-5: Example of a Classification and Regression Tree (CART) generated using R<sup>133</sup>**

2.4.3.9.4 Discussion on required report information

The lack of documentation was a common issue in the surveyed work. In order to meet ISO transparency requirements, adequate documentation is required.<sup>17, 80</sup> While rigorous sensitivity and uncertainty analysis is not always possible or required, it is important to justify the method used and its limitations. Because of word limits in published papers, it may not be possible include everything in the main paper, but details can be added in an appendix. The method of selecting which inputs to include/exclude should be provided, along with any limitations of the analysis method used. A list of the inputs used in the sensitivity analysis with their value ranges should be provided. In cases where default Ecoinvent/SimaPro distributions are used, at a minimum user-specified data needs to be provided. While not required, a list of the Ecoinvent default inputs included in the analysis can be useful to the reader. If default distributions are

used, a discussion on any data gaps or limitations of the defaults should be mentioned and discussed. When Monte Carlo is used, the number of samples should be specified to provide context on the accuracy of the output distribution.

If correlations between input distributions are suspected but not included, the impact should be discussed. If correlations are included, justification and relevant data should be provided. The effect of dependency and whether it was included should be discussed. While dependency is critical for comparative LCA, it is still important for attributional LCA, as there may be dependencies in the background data.

#### *2.4.3.10 Further consideration required: modeling error*

The surveyed papers only included parameter and scenario uncertainty, not model uncertainty. Refsgaard et al. suggest that modeling error is often the largest source of uncertainty in environmental modeling because of the complex nature of environmental systems.<sup>134</sup> While LCAs of energy systems may not be as complex, structural error can still be significant. Because of the severe lack of data available to LCA practitioners, it is often not possible to validate models and quantify model uncertainty. When data is available, statistical tests of the model error or comparing the errors between training and validation data sets can be used to quantify model error.<sup>134</sup> Ramin et al. demonstrated that a Bayesian averaging technique of multiple model structures could be used to reduce model structural error.<sup>135</sup> McDonald and Urban demonstrated how increasing model complexity can decrease model accuracy because of overfitting the available data.<sup>136</sup>

When data is not available for validation, Refsgaard et al. suggest a hybrid approach using multiple model formulations, expert opinion, and pedigree analysis to produce a subjective estimate of model uncertainty.<sup>134</sup> When incorporating multiple model structures without validation data, Zelm and Huijbregts used the most complex model as a baseline to identify optimal model complexity by examining the trade-off between parameter and model uncertainty.<sup>51</sup> While the more complex models require additional uncertain parameters, increasing overall uncertainty, Zelm and Huijbregts argue that an optimal model minimizes both

parameter and model uncertainty. However, their method approximates the model uncertainty in the less complex models by assuming the most complex model as the accurate baseline, which may be untrue. However, it can be argued that the increase in overall uncertainty from the complex model is a better representation of the true uncertainty, as unacknowledged uncertainty in the simpler model is acknowledged in the complex model. Zelm and Huijbregts suggest that final model selection should strive to minimize uncertainty and incorporate all critical processes.<sup>51</sup> While the complex model increases parameter uncertainty, the additional detail can help guide future data collection to help reduce uncertainty.

Overall, as model structure error is often difficult to quantify, the existing research suggests using multiple model structures. If quantitative methods are not possible, hybrid qualitative methods such as numerical unit spread assessment pedigree (NUSAP) can be used.<sup>137</sup> Expert opinion can be used when data is scarce. However, because of the subjective nature of expert opinion, multiple frameworks have been developed for eliciting and weighting expert opinions.<sup>74-76</sup>

#### *2.4.3.11 Summary of basic and detailed analysis*

Figure 2-6 shown below provides an overview of characteristics of a basic vs. detailed SUA. In some cases a detailed SUA is not required; for example, when the LCA model uses a simple aggregated data approach. However, even when a basic analysis is acceptable, proper documentation should still be included.

<b>Basic Analysis</b>	<b>Detailed Analysis</b>
Local sensitivity	Global sensitivity
Only small # of inputs examined, limited discussion of filtering criteria	Screening method used / justification provided to identify key inputs
Includes either sensitivity or uncertainty analysis	Includes both a sensitivity and uncertainty analysis
Includes parameter uncertainty only	Includes parameter, normative, and model uncertainty
Basic description of method used, and inputs included	Detailed documentation of method used with critical parameters (ex. # of samples used in MC), documentation of input ranges used with references and justification of ranges / distributions used
Minimal interpretation of results; ex. Only error bars presented	Discussion on limitations, potential affect of correlation, dependency and statistical significance
Software defaults used as is, with no additional discussion	Potential limitations/gaps of using defaults is discussed and/or addressed
SUA added on at end to produce error bars	SUA incorporated in all stages from goal and scope development to final interpretation

**Figure 2-6: Summary characteristics of a basic vs. detailed analysis**

## 2.5 Conclusion

Current LCA practitioners are inconsistent in their implementation of sensitivity and uncertainty. Furthermore, sensitivity and uncertainty analysis should not be viewed as something that needs to be added on at the end of the project to produce error bars, but as a critical part of the analysis which is examined throughout the process.

- For mathematically simple models, using aggregated data local sensitivity can be sufficient, but for larger models using complex calculations a global sensitivity method should be used to account for interactive and non-linear effects.
  - Global sensitivity can also help the practitioner develop a deeper understanding of the problem being studied.

- For complex models, all inputs/assumptions should be included in the uncertainty analysis unless screening methods are used to identify insensitive inputs that can be ignored. Since uncertainty can be dominated by a small number of inputs, incomplete coverage can result in underestimating uncertainty.
  - Using LCA model (e.g., SimaPro/EcoInvent) defaults will not provide complete coverage; values input by the user should be screened to identify sensitive inputs which need to be included in the uncertainty analysis. For this reason, the analysis based just on the LCA model default uncertainties are not comprehensive.
  - Existing LCA software should integrate screening methods to identify critical inputs. When running an uncertainty analysis with default uncertainties software should identify which inputs are missing uncertainty distributions.
- Generic uncertainty ranges such as  $\pm 50\%$  for all inputs should not be presented as error bars on the output (uncertainty analysis) but should only be used as a basic sensitivity analysis to identify critical inputs.
- The methodology should include a discussion on the type of sensitivity/uncertainty method used, limitations in the analysis, justification on what inputs are included/excluded, and key simulation parameters such as number of samples and types of distributions used.
- Practitioners should consider how the project's goal and scope will impact their sensitivity and uncertainty analysis.
  - When performing a comparative analysis, the differential method should be used to account for dependency. Both the sensitivity and the uncertainty analysis should focus on the difference between the pathways, rather than on each individual pathway.
  - How the timeframe used will impact the assumptions and goal/scope should be considered (historical, current, future).

As a result of this work, for Excel-based LCA models, an open source template was created that uses R to generate the samples and process the results and Excel macros to generate the output file and link the Excel and R codes.<sup>2</sup> The template is called Regression, Uncertainty, and Sensitivity Tool (RUST) and has been used in several studies in the last three years.<sup>57-64</sup>

# 3 Development of the Regression, Uncertainty, and Sensitivity Tool (RUST)<sup>†</sup>

## 3.1 Introduction

Bottom-up-based life cycle assessment (LCA) approaches can be used to assess the greenhouse gas emissions of various products, including transportation fuels. Bottom-up, spreadsheet-based models involve numerous calculations and assumed values that are uncertain. Currently, most LCAs provide point estimates with a simple one-at-a-time sensitivity analysis, which provides limited insight into how the model assumptions affect the results. In order to improve the quality of LCAs, alternative sensitivity methods can be used.

Campolongo et al.<sup>111</sup> illustrated how a Morris sensitivity analysis can be used to accurately identify key parameters in a 60-parameter, non-linear model. Iooss and Lemaître,<sup>71</sup> Campolongo and Braddock,<sup>138</sup> Saltelli et al.,<sup>119</sup> and Groen et al.<sup>70</sup> examined global sensitivity, specifically for use in LCA models. Despite the numerous publications on global sensitivity analyses, simple OAT sensitivity analysis is still commonly used.

---

<sup>†</sup> This chapter is based on the following papers:

- Di Lullo, Gemechu, Oni and Kumar, "Extending sensitivity analysis using regression to effectively disseminate life cycle assessment results". *Int. J. Life Cycle Assess.* **2020**, *25*, 222-239. DOI: 10.1007/s11367-019-01674-y
- Oni, Anaya, Giwa, Di Lullo and Kumar, "Comparative assessment of blue hydrogen from steam methane reforming, autothermal reforming, and natural gas decomposition technologies for natural gas-producing regions". *Energy Conversion and Management* **2022**, *254*, 115245. DOI: <https://doi.org/10.1016/j.enconman.2022.115245>
- Di Lullo, Oni and Kumar, "Blending blue hydrogen with natural gas for direct consumption: Examining the effect of hydrogen concentration on transportation and well-to-combustion greenhouse gas emissions". *Int. J. Hydrogen Energy* **2021**, *46*, (36), 19202-19216. DOI: 10.1016/j.ijhydene.2021.03.062
- Di Lullo, Oni, Gemechu and Kumar, "Developing a greenhouse gas life cycle assessment framework for natural gas transmission pipelines". *J. Nat. Gas Sci. Eng.* **2020**, *75*, 103136. DOI: 10.1016/j.jngse.2019.103136

One of the key advantages of OAT local sensitivity analysis is its ease of implementation. Users do not require any statistics or programming background; they can simply use Excel data tables. While open source software such as SIMLAB by the Joint Research Centre (JRC) of the European Commission,<sup>94</sup> and PSUADE<sup>120</sup> simplifies global sensitivity analysis, the user still needs to automate the process of generating the output from the Excel model. R<sup>139</sup> and MATLAB<sup>140</sup> packages are available for both sensitivity and regression analyses but require programming experience and can be difficult to use. Excel add-ins such as ModelRisk by Vose Software<sup>39</sup> and CrystalBall by Oracle<sup>41</sup> are limited to performing Monte Carlo simulations. LCA software such as SimaPro,<sup>85</sup> OpenLCA,<sup>141</sup> and GaBi<sup>42</sup> are also limited to Monte Carlo simulations only.

In order to encourage the use of higher quality sensitivity analysis methods, which will improve the overall quality of the LCA, software that is easy to use is required. Hence, in this work, RStudio and Excel VBA were used to create an easy-to-use template called the Regression, Uncertainty, and Sensitivity Tool (RUST) that can be inserted into any Excel-based LCA model. We also created an iterative framework with the primary goal of producing a high-quality analysis while minimizing the data collection and computational workload. The developed framework and tool was then applied to the previously published **FUNdamental ENgineering PrinciplEs-based Model for Estimation of GreenHouse Gases in Conventional Crude Oils and Oil Sands (FUNNEL-GHG-CCO&OS)**<sup>44, 142-145</sup> and the FUNNEL-GHG natural gas transmission lines (-NGTL) models.<sup>4</sup>

## **3.2 Method**

The RUST framework for incorporating sensitivity and uncertainty analysis into LCA is illustrated in Figure 3-1. The primary goal is a high-quality analysis with minimal data collection and computational workload. Since output uncertainty is a product of input sensitivity and input uncertainty, the practitioner only needs to focus on collecting data for the sensitive inputs.

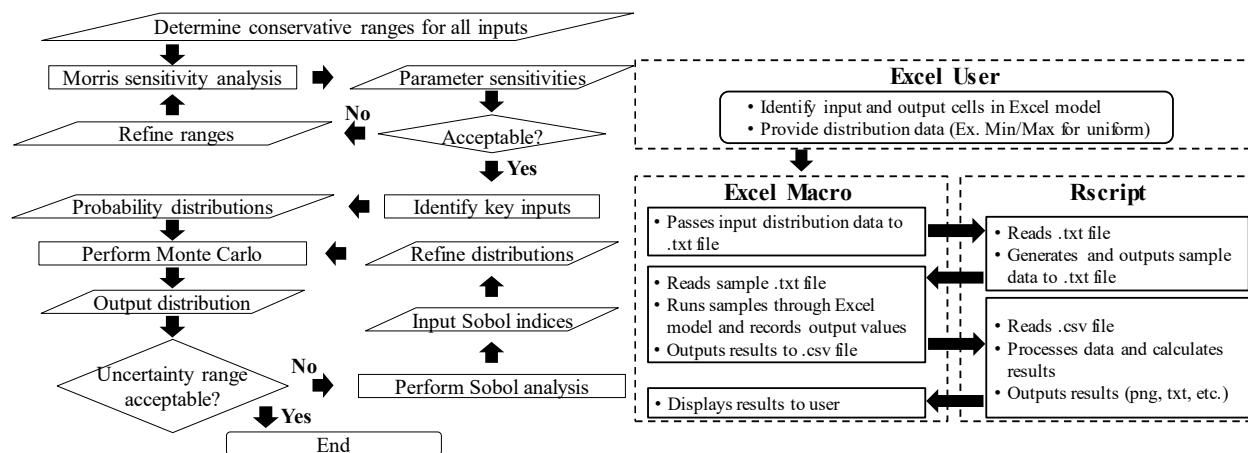


**Figure 3-1: Overview of RUST framework and process flow diagram**

RUST was created to link Excel and R in a user-friendly format. The data processing is performed in R, and Excel is used for the user interface and LCA model. Several R packages are used in the template.<sup>139, 146-154</sup> The RUST template can be used with any Excel-based LCA model and supports parallel computing to reduce computational time. The approach could also be extended to existing LCA software by creating application-specific interfaces, but that aspect is beyond the scope of this study.

It is recommended that an exploratory mindset be used when performing sensitivity and uncertainty analyses. The end goal is not to determine the exact range of values the output can take with certainty, as this is likely infeasible given data limitations, especially for future/newer technologies. Instead, the goals should be to determine what assumptions or conditions will influence the results, to develop a better understanding of the limitations of the analysis, and to identify opportunities to improve the robustness and understanding of the conclusions. Klauer and Brown suggest using a subjective interpretation of uncertainty focused on the decision makers' degree of confidence in the possible outcomes.<sup>155</sup> This is similar to the Bayesian inference discussed by Ellison.<sup>117</sup> While this method is subjective, and the practitioner could be overconfident, the results are still useful if the assumptions are transparent (a requirement of ISO standards),<sup>16, 17</sup> especially for the critical assumptions.

### 3.2.1 Sensitivity screening methods

There are numerous reviews of the many methods available for performing sensitivity and uncertainty in LCA, the most recent from Igos et al.<sup>18</sup> Existing sensitivity methods include

correlation, key issues, linear regression analysis, marginal, moment-independent modelling, Morris, OAT, scenario, and Sobol/FAST analysis.<sup>18, 26, 70</sup> This study focuses on the Morris and Sobol methods as they have an optimal balance of flexibility and ease of use. These methods can be applied to non-linear and non-monotonic problems with large input variances. The Morris method, moreover, is faster than the factored scenario method as fewer samples are required.

### 3.2.1.1 Morris method

Sensitivity is a partial derivative that can be dependent on the value of the parameter in question (non-linear) or the values of the other parameters (interactions). The Morris method uses a design of experiments approach to evaluate the partial derivative across the parameter space.<sup>113</sup> The user selects the number of levels,  $p$ , and number of OAT designs/approaches,  $r$ . The number of model evaluations required is  $N = r * (k + 1)$ , where  $k$  is the number of parameters. Values for  $p$  and  $r$  should be even and  $r$  should be larger than  $p$  to ensure uniform sampling of the space.<sup>113</sup> Typical  $r$  values are between 10 and 50.<sup>111</sup> The level specifies the number of unique values each parameter can take. In Figure 3-2,  $p = 4$ , meaning each model parameter ( $x_1, x_2, x_3$ ) can take on a value of 0, 0.33, 0.67, or 1. The values are then scaled based on the input ranges provided. Figure 3-2 shows the sample path (blue line) in which a starting point is randomly selected. One input is changed at a time, from points 1-4 and 5-8, to calculate the partial derivatives of the respective parameters. From points 4 and 5, multiple parameters are changed simultaneously, which results in a new approach. The number of approaches,  $r$ , also sets the number of derivatives calculated for each parameter. Higher  $r$  values are required to ensure that the parameter space is adequately sampled. For example, Figure 3-2 shows that no samples were taken in the bottom corner. The red line represents an example model response and illustrates the effects of the number of levels. Since only 4 levels are used, the calculated partial derivatives will always be negative. However, a positive slope between  $x_3 = 0.85$  and 1 would be detected if more levels were used. The derivative in the  $x_1$  direction would incorrectly appear to be negative over the entire domain. For non-linear equations, large  $p$  values are required to ensure that variability in the sensitivity is accurately captured. Campolongo et al. introduced an optimization approach that started with 500-1,000  $r$  approaches and then determined which 10 approaches provided the best spread of the parameter domain.<sup>111</sup> When the model's evaluation time is long, Campolongo's method can reduce the number of model evaluations; however, the brute force

approach used to select the optimal approaches can be computationally expensive. Since the FUNNEL-GHG-CCO/OS model can calculate over 100 samples/s, it is quicker to simply assess a larger number of approaches than to use Campolongo’s optimization method.

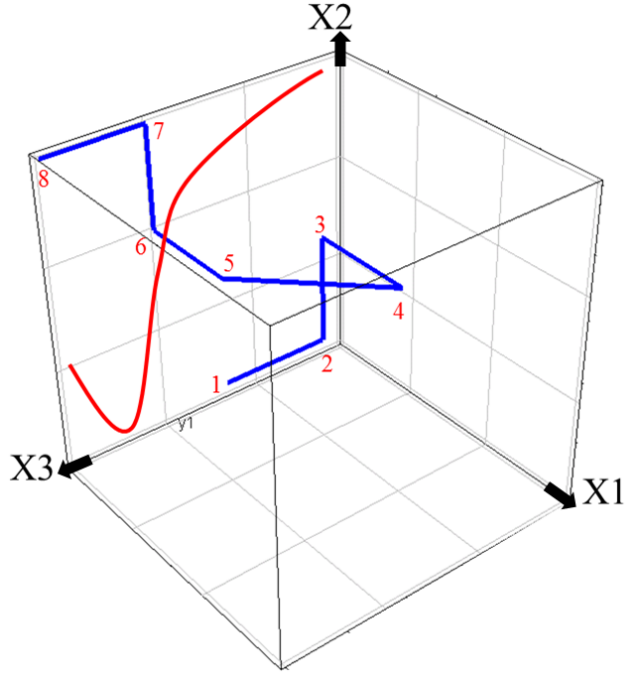


**Figure 3-2: Example of Morris sampling with three parameters ( $k$ ), two OAT designs ( $r$ ), and four levels ( $p$ )**

The partial derivative, also known as the elementary effect, for parameter  $j$  is determined for each OAT design,  $i=1$  to  $r$ , as:

$$D_j^i = \frac{f(X^i + \Delta) - f(X^i)}{\Delta} \quad (\text{Eq. 1})$$

where  $X^i$  is input ( $i=1, \dots, k$ ) and  $f(X^i)$  is the model output with the respective input. Delta is determined from the number of levels,  $p$ , as  $\Delta = s/(p - 1)$ . The step size is generally set to  $s = p/2$ ; in Figure 3-2  $s = 1$ .<sup>146</sup> To simplify the presentation of the results, the mean ( $\mu$ ) of the absolute partial derivatives and the standard deviation ( $\sigma$ ) are calculated:

$$\mu_j = \frac{1}{r} \sum_{i=1}^r |D_j^i| \quad (\text{Eq. 2})$$

$$\sigma_j = \sqrt{\frac{1}{r} \sum_{i=1}^r \left( D_j^i - \frac{1}{r} \sum_{i=1}^r D_j^i \right)^2} \quad (\text{Eq. 3})$$

The larger the  $\mu$ , the more sensitive the model output is to the input value. The standard deviation ( $\sigma$ ) shows how the sensitivity changes throughout the parameter domain. If  $\sigma$  is large, then either the partial derivative is affected by the input value as it moves across its range (non-linear) and/or the slope depends on the values of the other parameters (interactions). The absolute value of the partial derivative is taken for the mean to ensure that non-monotonic parameters are not incorrectly labeled as insignificant; the standard deviation does not use absolute values as doing so would underestimate the true variation in a non-monotonic model. The mean and standard deviation values are normalized using the parameter ranges so that they are comparable. The Morris method groups the inputs into three main categories, those with negligible effects (small  $\mu$  and  $\sigma$ ), linear effects with negligible interactions (large  $\mu$  and small  $\sigma$ ), and non-linear/large interaction effects (large  $\sigma$ ).

### 3.2.1.2 Sobol method

The Morris method identifies whether parameter sensitivities vary across the domain space; however, it cannot differentiate between non-linear and interaction effects. Nor can it identify which specific parameters are interacting. The Sobol method uses a decomposition of variance approach to identify what percentage of the overall variance can be attributed to each parameter or group of parameters.<sup>71, 118-120, 146</sup>

An ANOVA analysis is used to compare the variation between groups to the variation within the groups and to identify whether the means of the groups are significantly different. The calculated first-order Sobol indices indicate the main effect of each variable, while the Sobol total indices indicate the contribution to variance due to the main and all interaction effects. Figure 3-3 shows how two  $n \times k$  matrices can be used to generate  $k$   $AB_i$  matrices with column  $i$  from  $A$  and the remaining columns from  $B$ . The model is then run for all the samples in  $A$ ,  $B$ , and  $AB_i$  for a total

of  $N=n*(k+2)$  model evaluations, where  $n$  is the number of samples for each matrix (rows) and  $k$  is the number of inputs (columns).

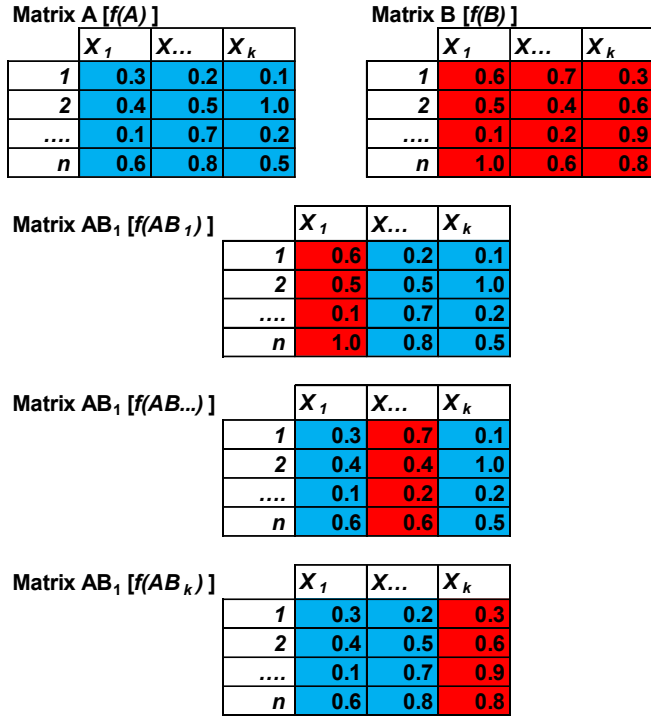


**Figure 3-3: Sobol sample generation**

The 1<sup>st</sup> and total Sobol indices for each parameter,  $i$ , are then calculated as:

$$S_i = \frac{\frac{1}{n} \sum_{j=1}^n f(B)_j * (f(AB_i)_j - f(A)_j)}{Var(Y)} \quad (\text{Eq. 4})$$

$$S_{Ti} = \frac{\frac{1}{2n} \sum_{j=1}^n (f(AB_i)_j - f(A)_j)^2}{Var(Y)} \quad (\text{Eq. 5})$$

In layman's terms, first order indices take the variation in the results that occur from changing the value of the  $i^{th}$  parameter  $(f(AB_i)_j - f(A)_j)$ , scaling the results using  $(f(B)_j * )$  and normalizing the effect against the total variance using  $/Var(Y)$ . The sum of all primary and interaction terms equals 1; hence, in a purely additive model, the sum of the first-order indices will equal 1. Parameters with low total Sobol indices can be removed, as their effect on the overall variance is insignificant and will have minimal effect on the output.

### 3.2.1.3 Morris and Sobol validation method

Because the Morris and Sobol methods use random number generators to determine the sample points, the results vary between runs. In order to confidently use these methods to quantify uncertainty, their accuracy needs to be evaluated and the minimum number of model evaluations required to obtain an accurate result needs to be determined. For the Morris method, we ran each scenario 50 times and reported the average and standard deviation of the Morris  $\mu$  and  $\sigma$ . Different  $r$  and  $p$  values were used in the scenarios to examine their effects.<sup>112</sup> For the Sobol analysis, the group sizes,  $n=2^x$  were varied from  $x = 3-15$ . To determine the standard error for each index, we used the R codes' built-in bootstrapping method.

To determine if the Morris method can accurately identify sensitive inputs, we compared the Morris and Sobol results using the parameter ranks. The Morris method used  $\mu$  and the Sobol method used the total indices instead of the 1<sup>st</sup> order indices to rank the parameters. We gave a rank of 1 to the parameter with the highest sensitivity.

### 3.2.2 Case studies

The RUST method's ability to improve the quality of LCA is showcased through two case studies conducted earlier. By identifying which inputs are most sensitive using RUST, practitioners can focus their data collection efforts more effectively and reduce the error in the model.

FUNNEL-GHG-CCO/OS is a **simple, nearly linear monotonic LCA model**. Full details of the FUNNEL-GHG-CCO/OS LCA model are available in two papers by Di Lullo et al.<sup>44, 142</sup> The bottom-up LCA model calculates the GHG intensity of gasoline produced from various crudes in gCO<sub>2</sub>eq/MJ of gasoline. that the first case study focuses on Maya, Bow River, and Athabasca mined bitumen. Maya is a heavy Mexican crude produced off the coast of Mexico using offshore drilling and nitrogen injection, Bow River is a heavy convectional crude produced using water flooding in southern Alberta, and Athabasca bitumen is produced in northern Alberta using open surface mining. Each crude has 44-65 inputs. The scope of the LCA includes the well drilling, crude production, surface processing, crude transportation, refining, transportation fuel

distribution, and combustion stages (Figure 3-4). The construction phase was not included, given its negligible contribution to total GHG emissions. The energy requirements for each piece of equipment and the associated GHG emissions were calculated using technical parameters such as unit efficiencies, production ratios, and operating temperatures and pressures (see Appendix C).

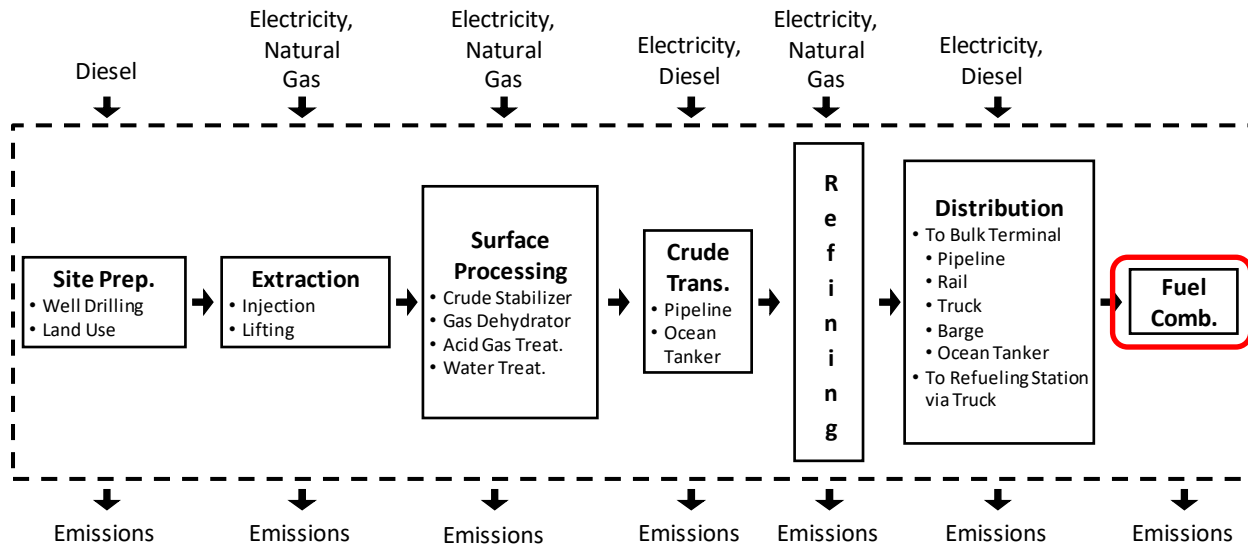


**Figure 3-4: FUNNEL-GHG-CCO/OS model boundary**

FUNNEL-GHG-NGTL is an **iterative non-linear LCA model** that calculates the GHG intensity of transporting natural gas through a high-capacity pipeline over a long distance.<sup>4</sup> The Alliance pipeline scenario had 44 inputs. The LCA scope included pipeline construction, operation, and decommissioning. Only the main transmission line and compressor stations were included; gathering pipelines and storage tanks were excluded (Figure 3-5). Technical parameters included pressure, temperature, physical properties, efficiencies, system dimensions and properties, and emission factors (see Appendix C).

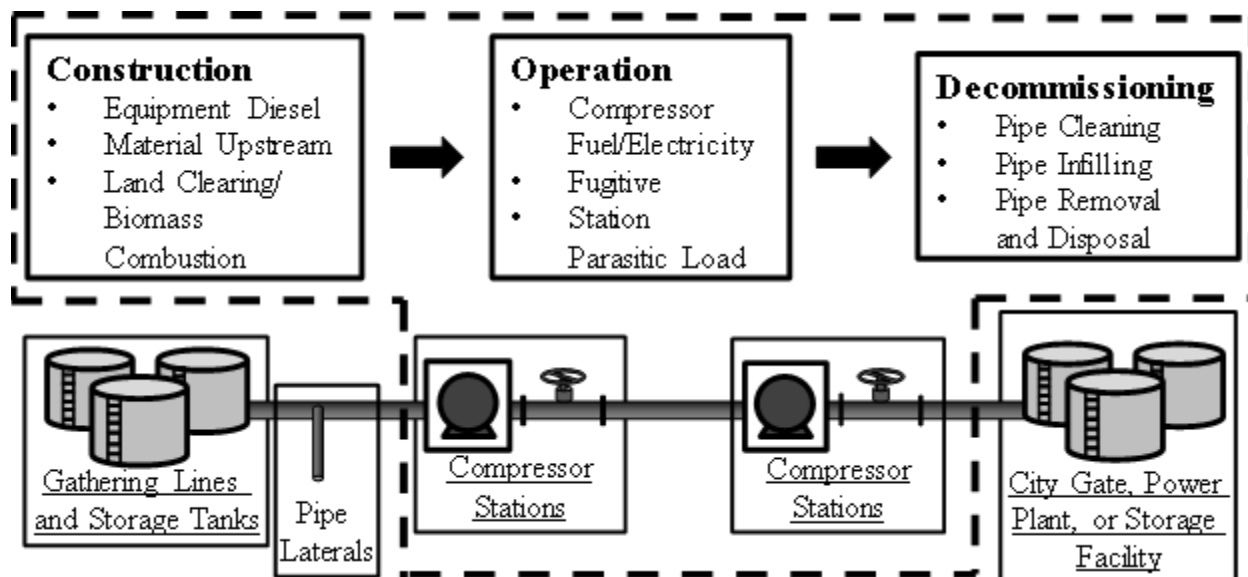


**Figure 3-5: FUNNEL-GHG-NGTL model boundary<sup>‡</sup>**

To determine the compressor energy requirements, custom Excel functions were written to calculate gas viscosity and compressibility, pipeline pressure drop, and required compressor power. The gas viscosity was calculated using a correlation by Carr et al.<sup>156</sup> that uses the gas gravity, as well as nitrogen, carbon dioxide, and hydrogen sulfide molar fractions (Eq. B1-B6).

The gas compressibility factor ( $Z$ ) is determined using the Peng-Robinson equation of state for mixtures and depends on the gas temperature, pressure, molar composition, and component acentric and binary interaction factors. The custom function determines the attraction and repulsion parameters for the gas mixture using the acentric and binary interaction parameters from Aspen Technology Inc.<sup>50</sup>

<sup>‡</sup> This model is based on work published as Di Lullo, Oni, Gemechu and Kumar, "Developing a greenhouse gas life cycle assessment framework for natural gas transmission pipelines". *J. Nat. Gas Sci. Eng.* **2020**, 75, 103136. DOI: 10.1016/j.jngse.2019.103136

**3.3 The general flow equation is used to calculate the pressure drop along the pipeline from friction and elevation losses.<sup>157, 158</sup> The flow rate split between parallel pipes uses the Newton-Raphson method; hence, the partial derivative of pressure drop with respect to the flow rate is also calculated. An iterative approach is used to calculate the average temperature, pressure, and compressibility factors. The average temperature is calculated by accounting for heat loss to the ground and the effect of expansion cooling. See Appendix B for additional details on the calculations used. The NGTL paper examined the Alliance and Prince Rupert transmission pipelines, see Chapter 3.3.5.3 for a description of the two pipeline systems.<sup>4</sup> Results and Discussion**

### **3.3.1 Application of Morris method**

To validate the Morris method, 50 runs are averaged for various  $r$  and  $p$  values. The number of runs used is arbitrary; 50 gives an adequate balance between accuracy and computing time. Two parameters were examined (shown in Figure 3-6) from the FUNNEL-GHG-CCO/OS Maya pathway, the gas-to-oil ratio (GOR) and the pipeline velocity for crude transportation to the refinery. For the Maya pathway, the GOR was the most significant parameter; it had the largest  $\mu$  and  $\sigma$  on the Morris plot. The pipeline velocity parameter was examined as it results in a non-linear response. For the NGTL model, the Alliance pipeline flow rate is examined because of the non-linear response due to iterative calculations. The coefficient of variation (CV) in the Morris  $\mu$  and  $\sigma$  values over the 50 trials was examined; only the  $\mu$  results are shown in Figure 3-6. If the CV is large, the Morris plot results will change each time the analysis is run and can lead to incorrect representations of the model sensitivity. The results of the case studies show that the CV decreases significantly as the number of approaches,  $r$ , increases; more approaches result in a better coverage of the parameter space. While increasing the number of levels,  $p$ , reduces the CV, the impact is less significant; more levels help better identify non-linear and non-monotonic behavior (see red spline in Figure 3-2). Overall, negligible benefit is seen in using  $r$  values greater than 40 in Figure 3-6, which align with Campolongo et al.'s suggestion of using 10-50 approaches.<sup>111</sup> The number of levels,  $p$ , can reduce the variance, especially when small  $r$  values

are used. However, in order to ensure uniform sampling, the number of levels,  $p$ , should be less than the number of approaches/OAT designs,  $r$ .<sup>113</sup>

The Morris  $\sigma$  CV followed a similar pattern as the  $\mu$ . The  $\mu$  and  $\sigma$  values averaged over the 50 trials were all within 5% of each other, indicating that they all converge to the same result if enough trials are used. The Morris method is meant to identify sensitive and insensitive inputs; the absolute values are not as important for initial screening purposes as the relative rank. Therefore, it is acceptable to use lower  $r$  values during initial screening.

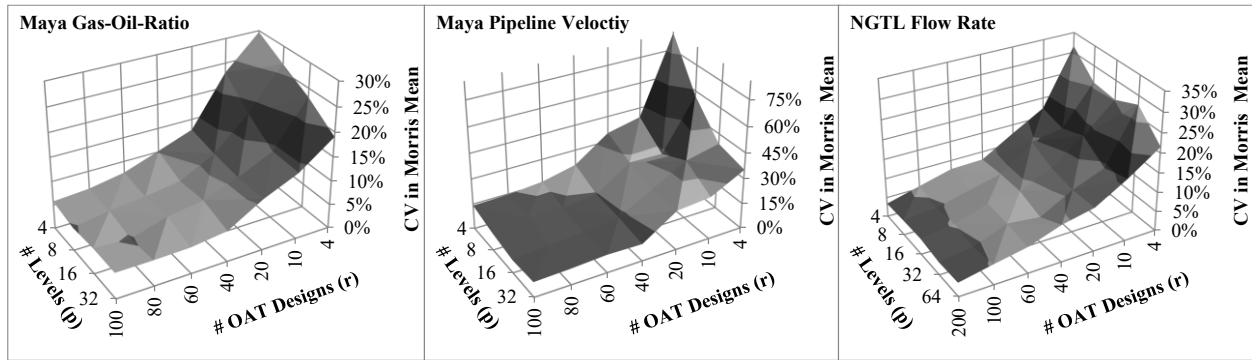


**Figure 3-6: Variation in Morris mean over 50 runs for different levels ( $p$ ) and approaches ( $r$ )**

### 3.3.2 Application of the Sobol method

Using bootstrapping, we compared the Sobol indices' accuracy for multiple sample sizes. The accuracy of the 1<sup>st</sup> order indices is approximately equal for all inputs regardless of their individual index value (Figure 3-7, left); therefore, the error is presented as a  $\pm$  that can be applied to all first-order indices, regardless of their mean value. For example, a 1<sup>st</sup> order index with a mean value of 50% and std. error of 10% would range from 40% to 60%, while a 1<sup>st</sup> order index with an average value of 4% would range from -6% and 14%.

The total order indices' accuracy varies based on the index value for each parameter, but the CVs (std. error/mean) are approximately equal for all inputs (Figure 3-7, right). The error in Sobol indices does not appear to be dependent on the number of parameters, but further testing is needed to verify this.

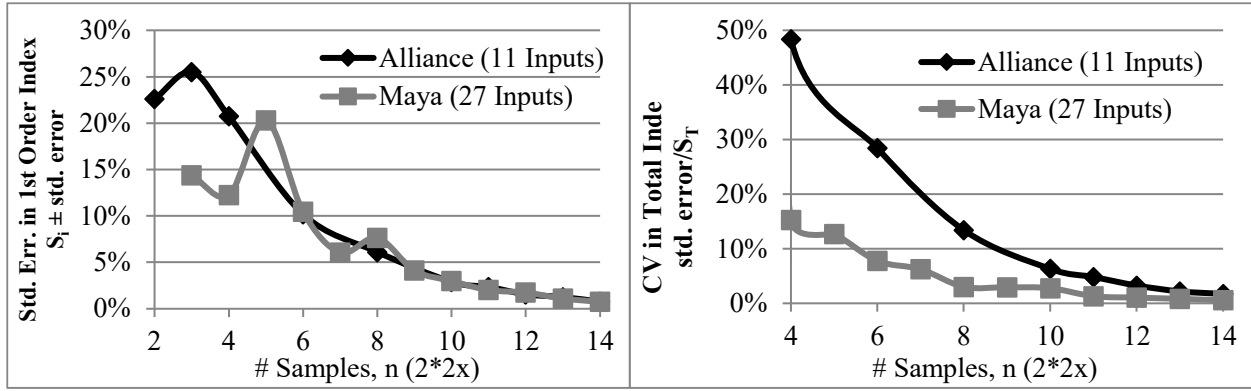


**Figure 3-7: Sobol index accuracy as a function of sample size: 1st order (left) and total (right)**

The index rankings using total indices stabilized with  $x = 4-8$ , compared to  $x = 8-10$  for the 1<sup>st</sup> order indices (Figure 3-8). Therefore, using total indices is recommended if Sobol is used for screening purposes. Preliminary results suggest the number of inputs may impact Sobol index accuracy, but further testing is needed.

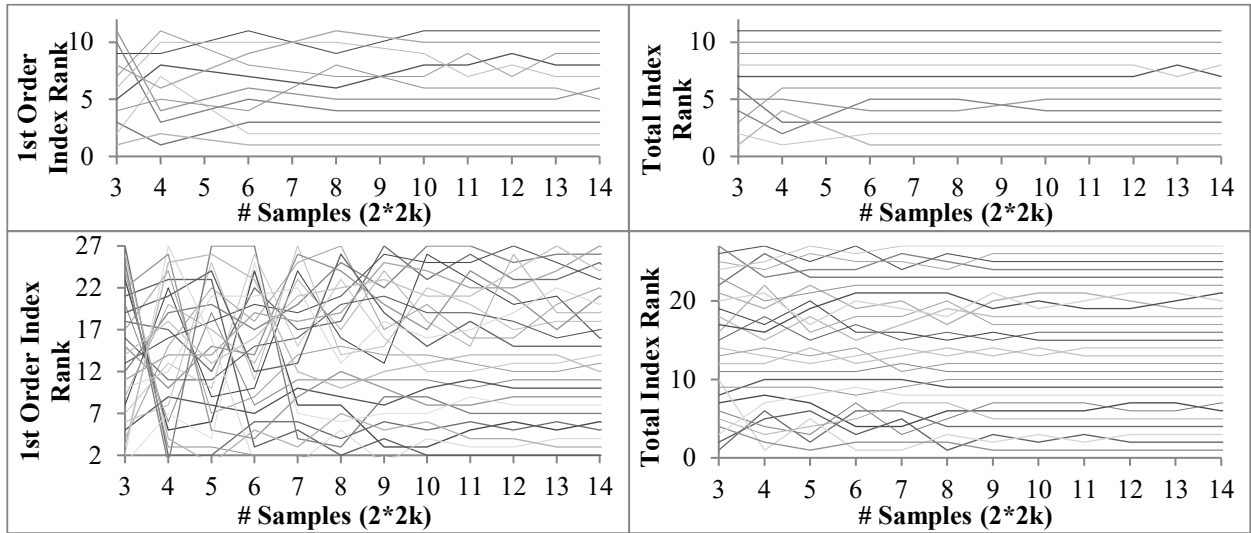


**Figure 3-8: Sobol index rank vs. sample size for Alliance (top) and Maya (bottom); each line represents an input**

### 3.3.3 Morris vs. Sobol for screening purposes

To compare the Sobol and Morris methods, we examined the ranks for the 65-parameter scenarios. The Morris method used  $r = 60$  and  $p = 32$ , the Sobol method used  $x = 13$ , and the OAT method used two samples per input plus the base case. The OAT, Morris, and Sobol methods required 131, 3,960, and 548,864 model evaluations, respectively. The parameter ranking between the OAT method and Morris can vary by up to 21 positions (Figure 3-9, left).

Unlike the Sobol methods, however, even the ranking of the most significant variables is inaccurate using the OAT method. While the ranks vary by up to seven positions for the Sobol method (see Figure 3-9, right), the ranks of the significant parameters are more stable; hence, both the Morris and Sobol methods can accurately identify the significant parameters. However, the Morris method requires fewer than 1/100th the number of model evaluations and is ideal for screening purposes. Once insensitive parameters have been removed by the Morris method, the Sobol method can be used to identify which parameters are interacting, if desired.

Results from the OAT analysis showed that ignoring interaction effects can lead to an incorrect estimation of parameter importance. The inaccuracy of the OAT method will vary between models and depends on the extent of interaction and degree of non-linearity. While the FUNNEL model is non-linear, it is also monotonic, which benefits the OAT approach. Though Groen et al.<sup>70</sup> suggest a linear regression model (without interaction terms) can be used for identifying important parameters, the model requires many samples, and the coefficients can only be used as importance measures if the model's  $R^2$  is close to one, indicating a good fit.

When using the Morris method 20-40 approaches ( $r$ ) generally provided accurate results, with minimal benefits above 40 approaches. Parameter ranks varied by an average of ten positions between runs when only 4 approaches ( $r$ ) were used. One parameter varied by 49 positions between runs; therefore, care should be taken when using a small number of runs. When 10 approaches ( $r$ ) were used, the average rank change fell to 5.5, with a maximum change in rank between runs of 14. The number of Morris samples needed will also depend on the complexity of the model; non-linear and highly interactive models require more samples, while linear additive models require fewer samples. Sobol requires  $2 \times 2^8$  for screening purposes using the total indices. If the practitioner wants to determine whether interaction effects are occurring, then  $2 \times 2^{12}$  samples are needed. Determining second-order indices to identify specific interactions requires nearly doubling the sample size.

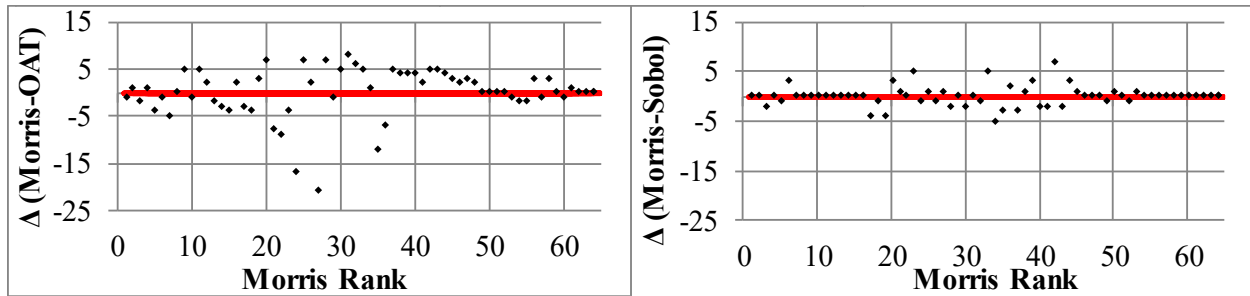


**Figure 3-9: Variations in parameter rank for Maya: OAT (left), Sobol (right) (+ means the OAT/Sobol rank's parameter is less important than the Morris method's)**

Although the Morris and Sobol methods are restricted to uncorrelated inputs, they are still useful for screening purposes. Correlated inputs can be grouped and represented as a single output. While the grouped input method cannot determine the importance of the individual inputs and requires the correlation to be approximated as a direct link, it can identify whether the grouped parameter is significant or not. Alternatively, moment-independent methods such as entropy-based sensitivity<sup>71</sup> and PAWN indices can be used<sup>123</sup>. The Sobol method can also be extended to account for correlations with two additional indices<sup>159</sup>. Since background processes are not always rigorously modeled in process based LCA, correlations between background emission factors should be investigated. For example, the background emission factors of natural gas, diesel, and fuel oil may all depend on the emission factor of the electrical grid, which is used by all three processes<sup>104</sup>. By grouping the parameters as described above, one can investigate the potential impact of dependency. Data analysis techniques such as principal component analysis (PCA) and partial least squares regression (PLS) are useful when the data set available is correlated or has a limited sample size; however, since RUST generates an uncorrelated sample to train the regression model, these methods are not needed. Furthermore, since PLS emphasises developing a predictive model, it is not useful as an alternative to the Morris methods for screening out insignificant parameters<sup>160</sup>.

### 3.3.4 RUST summary

RUST includes a mapping macro, which can be used to easily run sensitivity and uncertainty in any Excel-based LCA model. Furthermore, the Morris and Sobol analyses are performed with scripts, which can be integrated into other programs such as SimaPro and OpenLCA in future. RUST can also be used with Excel models that are linked to speciality engineering software such as Aspen HYSYS. While the case study uses a maximum of 65 parameters, RUST is capable of

assessing larger input models as the 64-bit version of Excel is no longer limited to 2GB of RAM.<sup>161</sup> Furthermore, the case study uses a single output, but multiple outputs can be specified in RUST for the Morris and Sobol analyses. Regression must be run one output at a time or with a weighted output.

Currently, RUST, Monte Carlo, and Sobol support lognormal, normal, project evaluation and review technique (PERT), modified PERT, triangle, and uniform distributions. Monte Carlo uses Latin hypercube sampling. Unlike other Excel add-ins, it does support parallel computing. Output uncertainty is a product of input uncertainty and input sensitivity; therefore, probability distributions are only required for the sensitive inputs. The Morris global sensitivity method can be used to identify sensitive inputs and a Monte Carlo simulation can then be run using probability distributions for the sensitive inputs only, reducing data collection efforts. See Chapter 2 for an in-depth review of how uncertainty is performed.

### **3.3.5 Qualitative results**

At the 2018 American Centre of Life Cycle Assessments (ACLCA) conference session on uncertainty, the question “How can consultant companies justify the additional cost of including a sensitivity and uncertainty analysis to their clients?” was asked.<sup>162</sup> This research found that sensitivity and uncertainty analyses provide many benefits to the practitioner that can offset the additional time spent performing the analysis. For example, when the results from the Morris screening method do not align with the practitioner’s expectations, it encourages further examination, which can help identify calculation errors or provide the practitioner additional insight into their model. Furthermore, the screening method can be used to guide the practitioner’s time management. LCA involves collecting large amounts of data and developing various models and calculations. This section includes qualitative examples on how RUST can help improve the quality of LCA in the energy sector.

#### *3.3.5.1 What data is important*

In this example the fossil fuel industry requested a life cycle assessment of their open pit mine reclamation plan.<sup>163</sup> The analysis required data from industry to complete, but industry had

limited resources to provide data. By using the Morris method, we were able to identify which pieces of data were critical and requested that industry provide these key data. The Morris method also identified which data was not important and allowed us to use rough estimates rather than wasting time collecting data from the industry. In this case using RUST reduced time spent on data collection, streamlining the process. The open pit modeled is used as an example, but this method can be applied to any model requiring external data.

### 3.3.5.2 Correlation or rigorous model

In the NGTL model, the Brills and Briggs correlation with an accuracy of  $\sim\pm 15\%$  was originally used to calculate the gas compressibility,  $Z$ .<sup>164</sup> In Morris, the gas compressibility,  $Z$ , was multiplied by an “accuracy” term, which can vary between 0.85 and 1.15. Since Morris identified the “accuracy” term as sensitive, the correlation was replaced with a more accurate Peng-Robinson cubic equation of state solver (Appendix B.2).<sup>165, 166</sup> Alternatively, if the correlation “accuracy” term was insensitive, then it would not be necessary to spend time developing a more rigorous model. Overall, a detailed sensitivity and uncertainty analysis can save the practitioner time while improving the quality of the analysis compared to a simpler alternative commonly seen in the surveyed works (Chapter 2).

### 3.3.5.3 Why dependency matters when comparing similar systems

As discussed in Chapter 2.4.2.3.5, dependency can have a large impact on model results. In an earlier study<sup>5</sup> I performed an LCA to compare pipeline emissions transporting pure natural gas and a natural gas hydrogen blend (hythane). Two western Canadian pipelines were examined in the study, Alliance and Prince Rupert. Alliance has three 20 MW compressors at the first station, and stations 2-7 each have a 23 MW compressor. The stations are approximately 193 km apart. Prince Rupert uses two 26.4 MW compressors at each of its eight stations. The stations are roughly 100 km apart. Table 3.1 provides a summary of each pipeline’s key characteristics. Detailed calculations are provided in Appendix B.

**Table 3.1: Overview of Alliance and Prince Rupert Pipelines<sup>4</sup>**

Specification	Alliance Pipeline (Built)	Prince Rupert Mainline (Planned)
Composition	Rich NG (89.9%)	Conventional NG (96.1%)

Specification	Alliance Pipeline (Built)	Prince Rupert Mainline (Planned)
	methane)	methane)
Route	3,000 km, BC/AB to Chicago, 1,361 km assessed	878 km, Hudson's Hope to Prince Rupert
Capacity (million m <sup>3</sup> /d)	47.2-52	56.6 (Phase 1) 101.9 (Phase 2)
Maximum allowable operating pressure (MAOP)	12 MPa	9.9 MPa
Diameter	914 mm / 36"	1219 mm / 48"
Lower heating value (LHV)	36.9 MJ/m <sup>3</sup>	33.2 MJ/m <sup>3</sup>

Differential analysis was performed for the pure natural gas pipeline and the 15% H<sub>2</sub> hythane scenarios. Dependence is important to consider when examining two similar scenarios. For example, while there may be an error in the pipeline lengths considered, it would not be appropriate to compare a longer, pure NG pipeline to a shorter, hythane pipeline. Alternatively, because of the different gas properties, the shorter length may benefit the NG pipeline more than the hythane pipeline, thereby affecting the results. In this case, the error in the length was modeled as a dependent in sensitivity and uncertainty analysis, meaning that while the length will vary, both pathways will use the same length for each sample. Some of the inputs may have weak independency. For example, the facility piping pressure drop is primarily affected by the piping layout and the number of elbows and valves, etc. (dependent), but would also be impacted by the gas properties (independent).

It is expected that the polytropic efficiency of the compressor and the turbine efficiency will be affected by the H<sub>2</sub> content of the gas (moderately independent). For pure H<sub>2</sub> compressors, faster impeller tip speeds or a large number of stages are required to achieve similar efficiencies to natural gas because of H<sub>2</sub>'s lower molecular weight.<sup>167</sup> However, there is currently insufficient data to estimate how the existing compressor efficiencies will change as H<sub>2</sub> is blended into the system. Six additional inputs – the cooler, scrubber, facility pressure drop, cooler outlet temperature, pipeline efficiency, and pipe-to-ground heat conductivity – are considered weakly independent. Since it is unclear how significant the independence is for the weak independent inputs, correlations cannot be used. Therefore, the uncertainty analysis included 3 cases to examine the effect of dependence between the inputs. In Case 1, both the moderately and weakly

independent inputs were modeled independently, and the remaining 17 inputs were dependent. In Case 2, only the two moderately independent inputs were modeled independently, and in Case 3 all of the inputs were left as dependent.

Steam methane reforming (SMR) of hydrogen with carbon capture and sequestration (CCS) was used for this work to determine hydrogen production emissions. The key outcome was to determine what CCS rate was needed to ensure that methane well-to-combustion (WTC) emissions were lower than those of pure natural gas. The breakeven percent carbon reduction required (CRR) is calculated as the  $\Delta$ WTC divided by the H<sub>2</sub> SMR emissions for each sample. The required carbon capture rate would be slightly higher to account for the additional GHG emissions generated by the carbon capture system.

Whether the inputs are modeled as dependent or independent has a negligible impact on the mean carbon reduction rate ( $\sim\Delta$ 1.5%); however, it does impact the confidence intervals (Figure 3-10). As the degree of dependence increases, the confidence intervals shrink. The uncertainty ranges for polytropic (70% to 85%) and turbine (27% to 39%) efficiency are large to account for variations in equipment size, design, and operating conditions. It is likely that the change in efficiency caused by blending H<sub>2</sub> into the gas will be significantly smaller. Therefore, the true results will lie between the Case 2 and 3 results and be closer to the Case 3 results. Figure 3-10 illustrates why it is important to use a differential analysis and consider dependency when performing an uncertainty analysis; simply assuming all inputs are independent would overestimate uncertainty, while assuming they are all dependent would underestimate uncertainty.

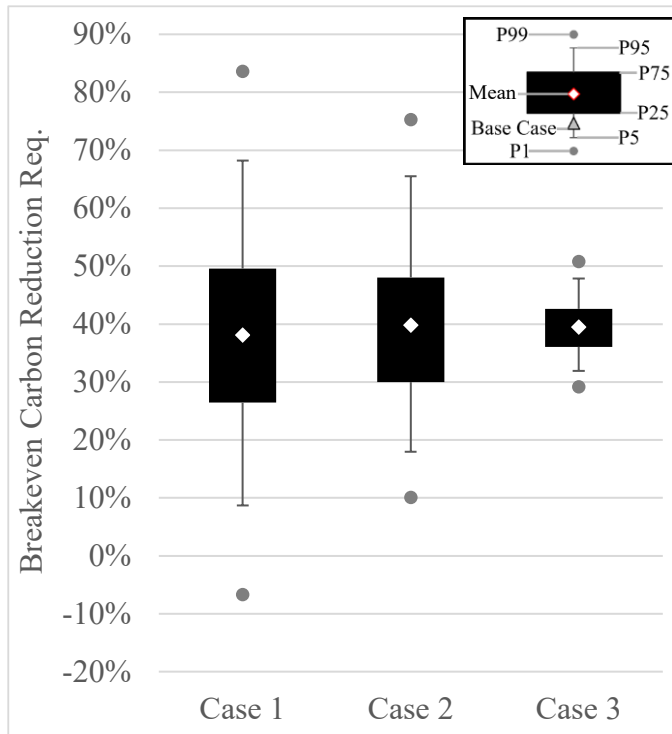


**Figure 3-10: Effect of dependency in differential analysis for 50 million m<sup>3</sup>/d Alliance**

#### 3.3.5.4 Comparing pathways with differential analysis

Oni et al.<sup>168</sup> examined four blue hydrogen production pathways for Alberta; the results are shown in Figure 3-11. The goal of the project was determine which hydrogen production method would be cheapest. The first method, steam methane reforming (SMR) uses natural gas to produce hydrogen and can be done without carbon capture and sequestration (CCS) but this results in large CO<sub>2</sub> emissions. To reduce emissions SMR can be done using mild CCS (52% reduction in CO<sub>2</sub> emissions), or moderate CCS (85% reduction in CO<sub>2</sub> emissions). The carbon capture intensity impacts the costs as additional equipment and energy is required. Autothermal reforming (ATR) also uses natural gas, but the reaction requires the use of pure oxygen instead of atmospheric air like SMR. ATR has the potential to reduce hydrogen emissions compared to SMR. ATR is examined with an aggressive 91% CCS rate as the process setup makes CCS more cost effective. Natural gas decomposition (NGD) uses natural gas to produce hydrogen and solid carbon instead of CO<sub>2</sub>. NGD still includes CCS for the natural gas consumed as fuel, the feedstock natural gas produces solid carbon.

It is unclear whether hydrogen from SMR-52% CCS is less expensive than natural gas decomposition (NGD)-CCS(Figure 3-11). However, when differential analysis is used to look at the difference between scenarios accounting for dependency in the inputs, it becomes clear that NGD-CCS costs more than SMR-CCS 52% (Figure 3-12). Differential analysis can only be done in a pairwise fashion; for four scenarios, six differential pairs are needed. If the difference is always positive for the A-B pair, then A is always larger than B. The reason for the large overlap in uncertainty ranges in Figure 3-11 is a result of all scenarios being sensitive to the hydrogen storage duration, natural gas price, and IRR, which are dependent inputs (see Figure 3-13 Morris plots). For ATR-CCS – SMR-52% CCS and SMR-85% CCS – NGD-CCS, the values are negative in approximately 5% of the scenarios. Further investigation into these scenarios using Morris/Sobol analysis on the differential results can be used to determine the conditions required for the conclusion on which is more expensive to be reversed. Figure 3-14 shows that the natural gas price and IRR are responsible for 89% of the variability in the ATR-CCS – SMR-52% CCS scenarios. For the SMR-85% CCS – NGD-CCS scenario, 90% of the variability is due to the CO<sub>2</sub> transportation costs and natural gas price. Further investigation into the model's response shows that SMR-52% is potentially cheaper than ATR-CCS when natural prices are low and IRR is high. SMR-85% CCS may outperform NGD-CCS if the CO<sub>2</sub> transportation cost and natural gas price are low.

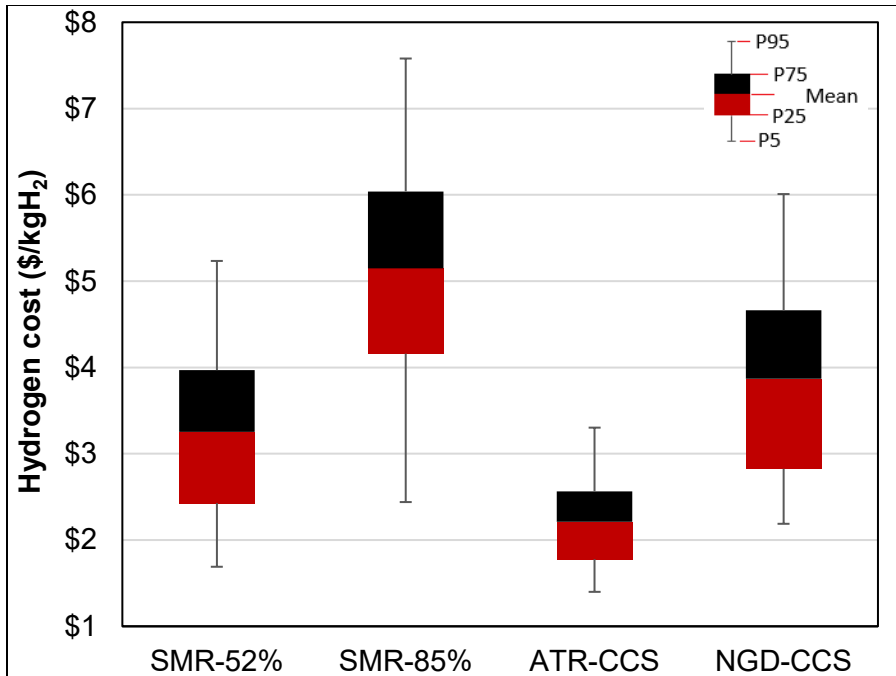


Figure 3-11: Uncertainty in cost results of blue hydrogen production technologies (from Oni et al.<sup>168</sup>)

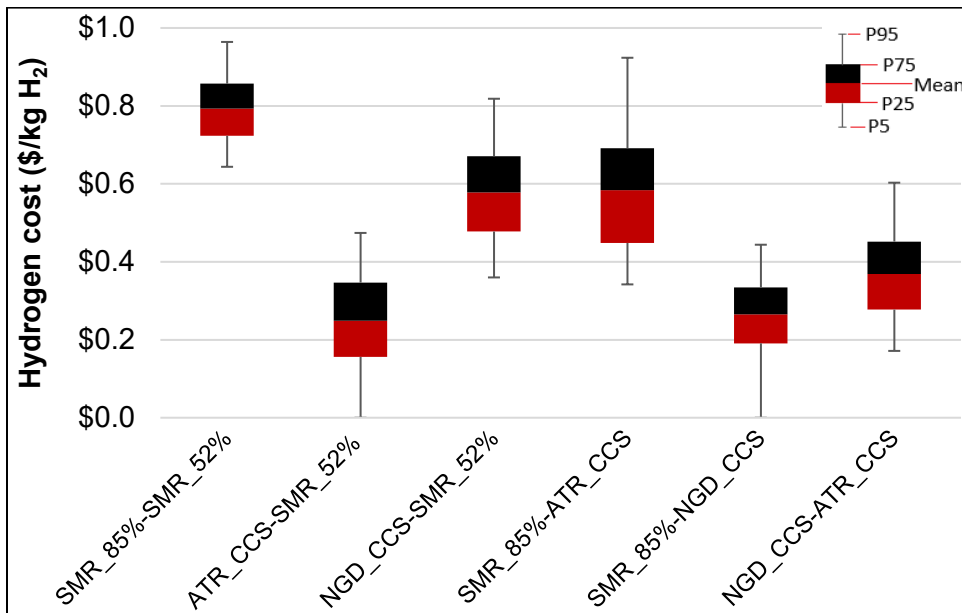
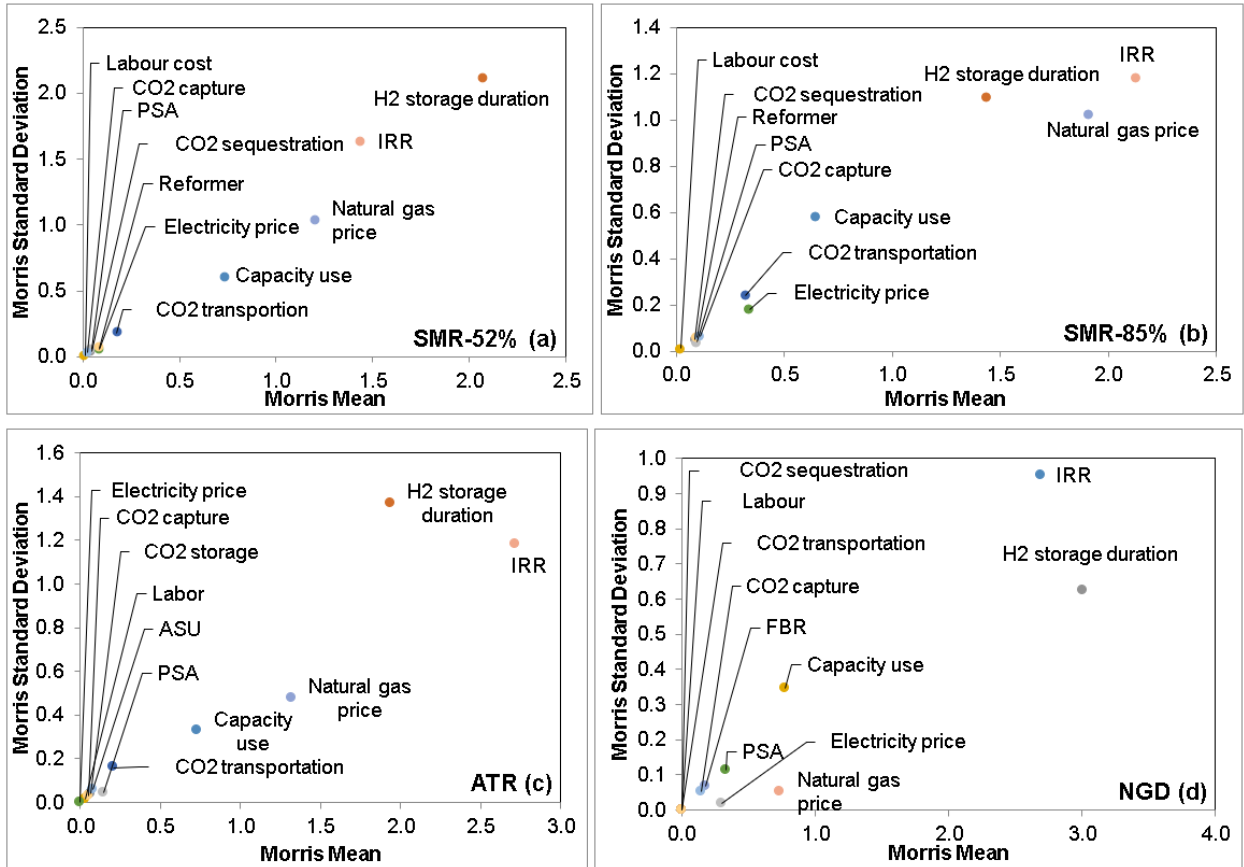
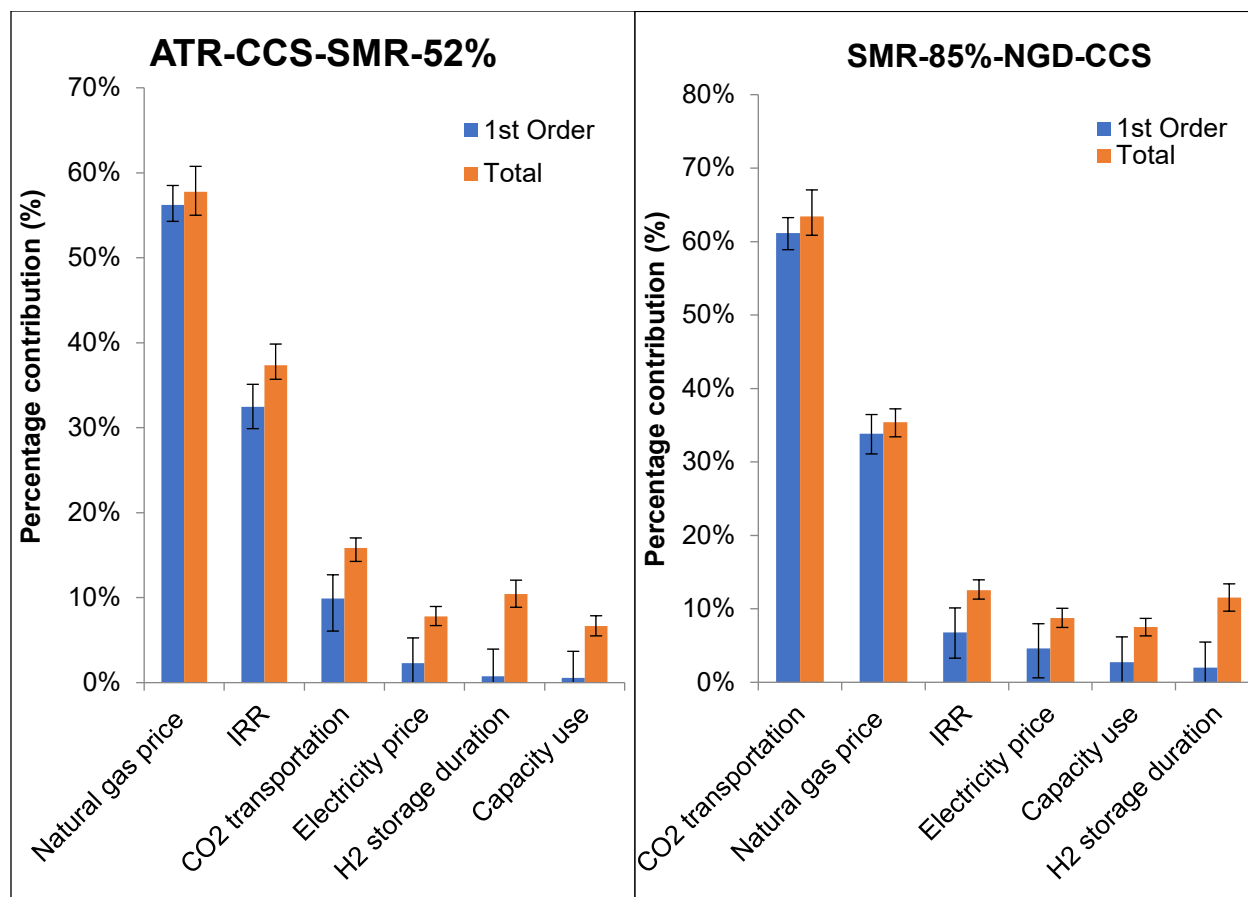


Figure 3-12: Comparative analysis of cost production for blue hydrogen technologies (from Oni et al.<sup>168</sup>)



**Figure 3-13: The influence of economic parameters on the hydrogen cost from (A) SMR-52%, (B) SMR-85% (C) ATR, and (D) NGD**



**Figure 3-14: Sobolj results for the differences between SMR-52% - ATR-CCS (left) and SMR-85% - NGD-CCS (right)**

### 3.3.5.5 Importance of linked calculations

To accurately model sensitivity and uncertainty, calculations should be properly linked. For example, instead of the temperature, pressure, density, and viscosity all being inputs, the density and viscosity should be calculated based on the temperature and pressure.

It was important that the gas properties in the study by Di Lullo et al.<sup>5</sup> on natural gas vs. methane emissions were calculated based on temperature and pressure as they varied through the system and were critical to understanding the differences between the scenarios. If calculations are not linked, the sensitivity and uncertainty may be underestimated, leading the practitioner to draw faulty conclusions.

### 3.4 Conclusion

When performing an LCA, the sensitivity and uncertainty analyses should not be thought of as something to throw on at the end for the simple purpose of adding error bars to the results, which was found in the literature review (see Chapter 2). Sensitivity and uncertainty analyses should be integrated into the entire LCA processes, with the goal of improving the quality of the analysis. For example, the user should determine what information is required, what aspects of the model need to be improved, and how policy or external factors will influence the results. When performing a comparative analysis, it is important to use a differential analysis and examine the difference between two scenarios.

This work showed how the Morris and Sobol methods can be used to identify key model parameters by accounting for interaction and non-linear effects, unlike the one-at-a-time method. The Morris method was found to require fewer than 1/100<sup>th</sup> as many model evaluations as the Sobol method, making it an effective screening method. It was determined that 20-40 samples per input (approaches) are required to accurately use the Morris method for screening purposes. Using Morris screening, we reduced the number of inputs from 60-75 to 14 for Maya, Bow, and NGTL, and 16 for Athabasca.

The developed RUST model allows practitioners to easily perform Morris and Sobol sensitivity in their Excel-based LCA models. RUST is currently being used within LCA publications<sup>57-64</sup> and industry/government projects.<sup>3, 163, 169</sup>

## 4 Development of Proxy Models with Linear Regression<sup>§</sup>

### 4.1 Introduction

We investigated proxy modeling to fulfill two purposes, to improve both usability and accuracy. Proxy models attempt to replicate results from a complex model using a simpler model structure, which is computationally cheaper to evaluate than the original complex model. Proxy modeling for usability is relevant to policy makers because using LCA for policy purposes can be a difficult and time-consuming process. Results from published studies need to be adapted to specific regions or problems of interest. *Ideally, an easy-to-use, simplified model should be made available to policy makers.* Proxy modeling for usability is also relevant to LCA practitioners since *proxy modeling can be used to streamline the publishing process for LCA models.* Currently, even when authors want to publish their models, they may be unable to because of limited resources, data confidentiality issues, or specialty software requirements, or because the model requires expert knowledge to use. Proxy modeling for improved accuracy is relevant to both LCA practitioners and policy makers since *obtaining accurate results for a complex process can be difficult. In order to reduce modeling error while keeping models simple and easy to use, proxy modeling could be used.* Additionally, rigorous models can have long computing times, making it difficult to perform alternative scenario analysis and more rigorous uncertainty analysis. Therefore, *computationally efficient proxy models can be used instead, allowing policy makers to quickly examine alternative scenarios.* For example, the regression equation can be integrated into resource planning models (Long-range Energy Alternatives Planning System [LEAP]<sup>170</sup>), extending its usability. The regression equation can be calculated at significantly higher speeds than the full model can be run, allowing more detailed assessments such as hybrid Monte Carlo methods.<sup>171</sup>

---

<sup>§</sup> This chapter is based on the paper published as Di Lullo, Gemechu, Oni and Kumar, "Extending sensitivity analysis using regression to effectively disseminate life cycle assessment results". *Int. J. Life Cycle Assess.* **2020**, *25*, 222-239. DOI: 10.1007/s11367-019-01674-y

Wang and Shan provide a detailed review of the various proxy modeling methods available.<sup>28</sup> In this research, the focus is on polynomial regression and artificial neural networks (ANN). Polynomial regression is simple to perform and works well for primarily linear models. Artificial neural networks are flexible and can be applied to a wide range of problems, and the final proxy model is simple and computationally efficient.

This chapter focusses on the application of multi-parameter least squares regression proxy modeling. The case studies from Chapter 3 are used to show how specific pathways of the FUNNEL model can be represented as a single equation rather than a large workbook with hundreds of cells. Both the crude oil to transportation fuels and the NGTL models are evaluated.<sup>4, 44, 142-145</sup> Chapter 5 investigates ANN proxy modeling.

## 4.2 Method

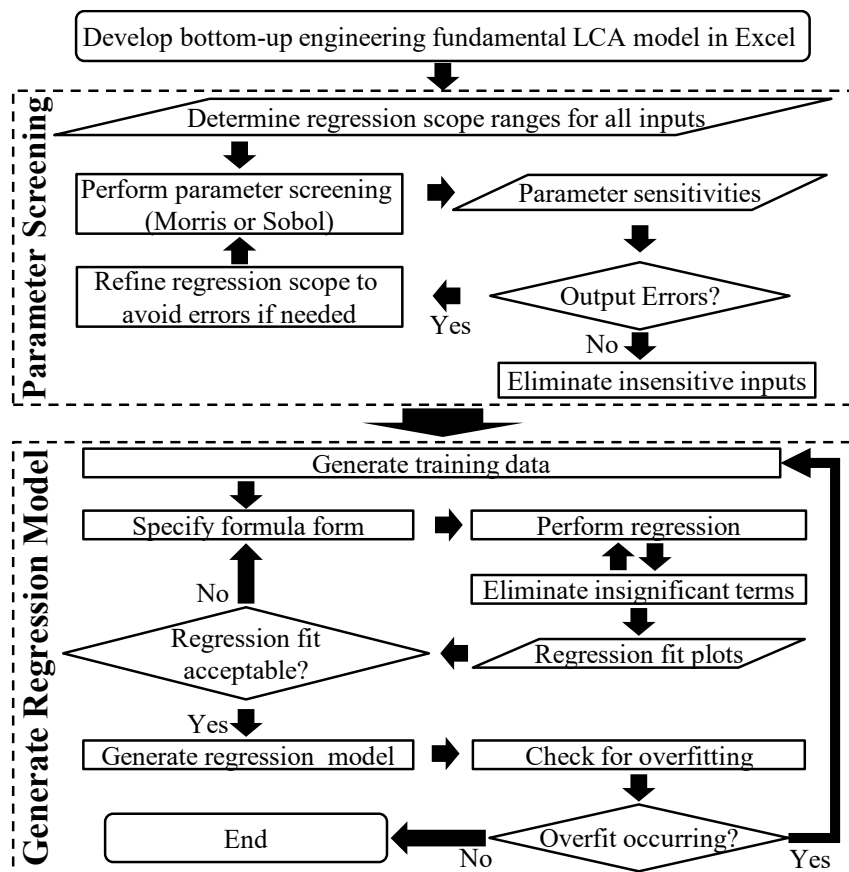


Figure 4-1: Regression framework

The goal of this work is to improve the quality of LCAs and to make them more accessible to non-experts. To improve the quality of LCA, we developed a framework for identifying critical parameters, as described in Chapter 3. This chapter focusses on using regression to create a proxy model for improved accuracy and usability by non-experts. Linear regression is then used on the critical inputs to create an approximate model. The regression equation is then validated and checked for overfitting. Figure 4-1 shows the regression framework.

#### **4.2.1 Identifying critical parameters**

LCA models can have many inputs; however, uncertainty is generally dominated by a small percentage of key inputs, which can be identified using a sensitivity analysis. Because of the size and complexity of modern models, it is not feasible to perform an in-depth sensitivity analysis on all the inputs. Screening methods are used to quickly eliminate insignificant inputs. A sensitivity analysis can also aid modelers in identifying errors within the model by identifying unexpected responses. A global sensitivity method (Chapter 3.3.3) should be used to prevent underestimating the importance of any of the inputs.

Since the regression model, described in the next Chapter, is only valid within the parameter ranges used to create the training data set, narrow ranges, which limit the regression model's scope, should be avoided. In the first stage of a conventional sensitivity analysis, conservatively large ranges are used for simplicity and to ensure that no sensitive parameters are prematurely removed. Additional time is then invested to refine the parameters' range for the sensitive parameters. In this case the ranges should not be refined and should be based on the scope of the desired regression model. Figure 4-1 provides a high-level overview of the modified sensitivity screening process.

#### **4.2.2 Developing the regression model**

The training data is generated using Latin hypercube sampling (LHS) in the open-source software R, rather than conventional Monte Carlo sampling. In Monte Carlo sampling, each point is generated independently using a random number generator. Relying on a random number generator is inefficient and can result in points being either closely clustered together or spread

far apart. LHS attempts to generate samples that are evenly spread across the entire parameter domain. Each input is split into  $N$  intervals and a sample is taken from each interval. As a result, LHS sampling error is  $O(1/N)$ , significantly lower than Monte Carlo's  $O(1/\sqrt{N})$ .<sup>99</sup> However, LHS's advantage only applies to single distributions. When multiple parameter distributions are used, the LHS method ensures the samples for each parameter are evenly distributed, but does nothing to ensure an even sampling of parameter combinations.<sup>99</sup> Therefore, LHS's advantage is reduced as the number of *significant* parameters increases. While models can have over a hundred inputs, the output uncertainty is generally dominated by only a few inputs. Therefore, LHS can still be advantageous even in large models.<sup>99</sup>

Uniform distributions should be used to ensure that the entire sample space is uniformly sampled. If triangle or normal distributions are used, there would be fewer training samples at the edge of the parameter space, which would lead to larger errors when extreme values are used. At least one sample is required for each term; however, a general rule of thumb is to use 10-15 samples per term to avoid overfitting.<sup>172</sup> More samples may be needed if there is a high degree of collinearity.

Quadratic regression takes on the following form:

$$y = c_{n1}x_1 + \dots + c_{n2}x_1x_2 + \dots + c_{n3}x_1x_2x_3 \dots + c_{n4}x_1^2 \dots + c_{n4}x_1^2x_2 \quad \text{(Eq. 6)}$$

where the terms 1 to 3 represent 1<sup>st</sup>, 2<sup>nd</sup>, and 3<sup>rd</sup> order interactions, and the terms 4 to 5 refer to 1<sup>st</sup> and 2<sup>nd</sup> order non-linear terms, respectively. The starting quadratic model will contain all combinations of the various interaction and non-linear terms. The highest level of interaction is specified and includes all the lower interaction levels as well. For example, third-level interactions include every possible two- and three-term combination of the parameters. The total number of coefficients in the first iteration is calculated as:

$$N_c = \sum_{L=1}^L \frac{k_p!}{(k_p - L)!} + 1 \quad \text{(Eq. 7)}$$

where  $L$  is the order of interactions and  $k_p$  is the number of proxy inputs. The number of proxy inputs is equal to the number of actual model inputs plus the number of non-linear inputs ( $k_p = k_a + k_{nl}$ ). For example, a model with two inputs,  $x_1$  and  $x_2$ , with squared and cubed terms for  $x_1$  would have four proxy inputs ( $x_1, x_2, x_1^2, x_1^3$ ).

The goal in using a regression model is to find which combination of parameters and interaction terms best replicates the underlying model. There are multiple approaches to model selection, but none is perfect, and expert judgment is required.<sup>173-175</sup> Models with a large number of parameters and levels of interaction can contain thousands of terms, resulting in billions of possible regression model combinations. Since it is not possible to evaluate every combination, a stepwise approach is used instead of a best subset approach.<sup>174, 175</sup> The process starts by including every term and iteratively eliminating the terms with the highest  $p$  values. When a term's  $p$  value is less than 0.05, there is less than a 5% chance that this term is irrelevant and that the coefficient is zero; hence, terms with larger  $p$  values are eliminated, as their coefficients are most likely zero. The two-sided  $p$  values are calculated within R using the t-statistic, which is calculated from the standard errors of the coefficients. Multicollinearity between terms leads to significant instability in the  $p$  values, which makes it difficult to determine which terms to eliminate.<sup>176</sup> Since the interaction terms will be correlated with the individual parameter terms, multicollinearity will occur even if the parameters in the original model are not correlated ( $x_1$  correlated with  $x_1 * x_2$  terms). By centering the data before running the regression analysis, we significantly reduce the multicollinearity of the inputs.<sup>176</sup> Once a term is eliminated and the regression analysis is updated, the  $p$  values for the remaining terms will be updated, and, if there is multicollinearity within the data, a term that appears to be insignificant may become significant. As a result, terms are removed in an iterative fashion, rather than simultaneously, until only terms with  $p$  values less than  $2 * 10^6$  remain.

To increase the accuracy of the regression model, non-linear squared and cubed terms may be required. In order to avoid multicollinearity between the primary ( $x_1$ ), squared ( $x_1^2$ ), and cubed ( $x_1^3$ ) terms, an orthogonal polynomial is required. An orthogonal polynomial uses a weighting function to ensure the dot product over a specified interval is equal to zero. This transformation is accomplished using the `polynom` library in R.<sup>153</sup> Adding non-linear terms to the regression model can help improve accuracy; however, when the number of coefficients is increased, the

sample size and computing time increase. Therefore, non-linear terms should only be included for inputs that are suspected to have non-linear effects. Morris cannot be used to identify non-linear inputs as it cannot differentiate between non-linear and interaction effects. To identify which inputs may have non-linear effects, an OAT approach is used. For each input, 5 samples are generated between the minimum and maximum values. Excel's built-in trendline function is then used to fit 1<sup>st</sup>, 2<sup>nd</sup>, and 3<sup>rd</sup> order polynomial trendlines to the 5 samples. The R<sup>2</sup> value is then calculated for each trendline. If the R<sup>2</sup> value is equal to one for the 1<sup>st</sup> order trendline, then the input exhibits a linear trend. Alternatively, if the R<sup>2</sup> value is less than one for the 1<sup>st</sup> order trendline, then either a squared or cubed term should be added to the regression model based on the trendline's R<sup>2</sup> value.

#### **4.2.3 Validating the regression model**

A valid regression model should have a high adjusted R<sup>2</sup> value and a normally distributed residual error across the entire output domain. Low R<sup>2</sup> values suggest a non-linear model may be needed. Alternatively, a higher level of interaction can improve the R<sup>2</sup> value. To ensure that the errors are normally distributed, residual vs. fitted plots, normal Q-Q plots, and residual histograms are used. The residuals vs. fitted plots can be used to determine if the residuals are uniformly distributed along the output domain.<sup>177</sup> The red line in Figure 4-2a&b (residuals vs. fitted) is a smoothed average of the residuals; ideally, it should be flat and equal to zero. In Figure 4-2a, the curved residuals indicate a common issue wherein the regression model is attempting a linear fit to a non-linear model. However, the conning effect (residual increases as fitted value increases) can indicate multiple non-linear effects are not being accounted for (Figure 4-2b). If the residuals are normally distributed, then the normal Q-Q plots should produce a straight diagonal line (Figure 4-2c&d).<sup>178</sup> An upward curve on the right or a downward curve on the left of the residual normal Q-Q plots indicates a heavier than normal tail. A downward curve on the right or an upward curve on the left of the residual normal Q-Q plots indicates a lighter than normal tail.

The histograms can be used to illustrate the Q-Q plots; the red line is an ideal normal distribution for comparison (Figure 4-2e&f). Ideally, the model residuals should match the red line, with the median at zero. A nonzero median suggests a bias in the model. Skewed distributions with a long

tail suggest the regression model is inaccurate within a portion of the parameter domain and may indicate insufficient coverage of the parameter domain within the training sample.

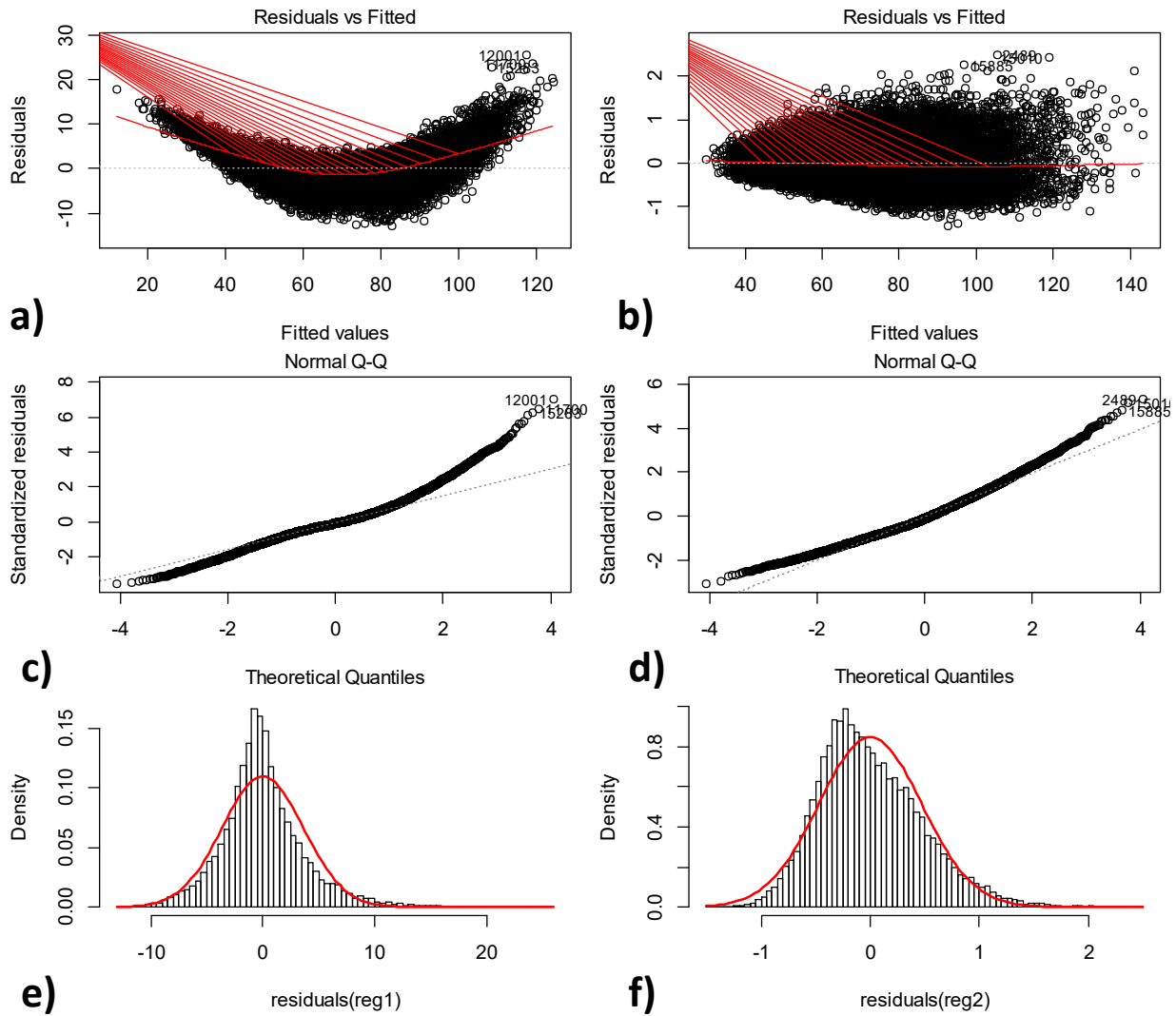


**Figure 4-2: Regression verification example with a poor fit (left) and a better fit (right)**

#### 4.2.4 Developing and validating the regression model process

The regression model is developed using the method shown in Figure 4-1. To avoid errors in the  $p$  values, the data is centered to reduce multicollinearity and a stepwise approach is used to determine the final regression model form. To avoid removing a large number of parameters at once, the  $p$  value cut-off point starts at 0.9 and progressively decreases to  $2.5e-16$ .

Once the iterative calculation is completed, a text file is loaded into Excel with a summary of the output. The output includes the minimum, 5<sup>th</sup>, 25<sup>th</sup>, 75<sup>th</sup>, and 95<sup>th</sup> percentile, and maximum residual values; the number of terms in the regression model; the Akaike information criterion (AIC); and the mean squared error (MSE) for each iteration. The Akaike information criterion balances the goodness of fit and the number of terms in the regression model. The lower the AIC value, the more efficient the regression model. The user can select which model form to use by balancing trade-offs in accuracy and number of terms. Residual vs. actual plots, normal Q-Q plots, and residual histograms are then generated for the optimal model to verify that the residuals are normally distributed.

Once the regression coefficients have been determined, it is important to check for overfitting. The regression model should replicate the true model; however, when overfitting occurs, the regression model begins to fit random patterns within the training data and falsely suggests an accurate regression model has been determined. If overfitting occurs, using new samples could result in significantly larger residuals. A general rule of thumb is to use 10-15 samples per term to avoid overfitting<sup>172, 175</sup>; however, more samples may be needed if there is a high degree of collinearity. The overfitting macro generates multiple samples using unique seeds and compares the average and standard deviation of the residual minimum, 5<sup>th</sup> percentile, 95<sup>th</sup> percentile, and maximum values. Large standard deviations indicate overfitting is most likely occurring. To prevent overfitting, the number of samples used to train the regression model should be increased.

#### **4.2.5 Model template**

RStudio is used to perform both the sensitivity and regression analyses. While RStudio can be used directly to perform the analyses, a template was created to make it user friendly. The users simply need to insert their existing Excel models into the RUST files and fill in the specified inputs. Excel macros programmed in VBA will prepare the data and execute Rscripts to perform the analysis. The main inputs are folder locations for saving .txt and .csv files, high-level inputs for the various functions, and the parameter table. The parameter table specifies the value ranges and provides the input cell address for each parameter. The Excel macros will then generate the

required sample file, run the samples through the user’s model, generate an output file, perform the desired analysis, and put out the results (Figure 4-3). A “mapping inputs” macro is provided to streamline the process. A demonstration of the process is provided in Appendix C. The Morris and Sobol analyses were run using Pujol et al.<sup>146</sup> R library.<sup>145</sup>

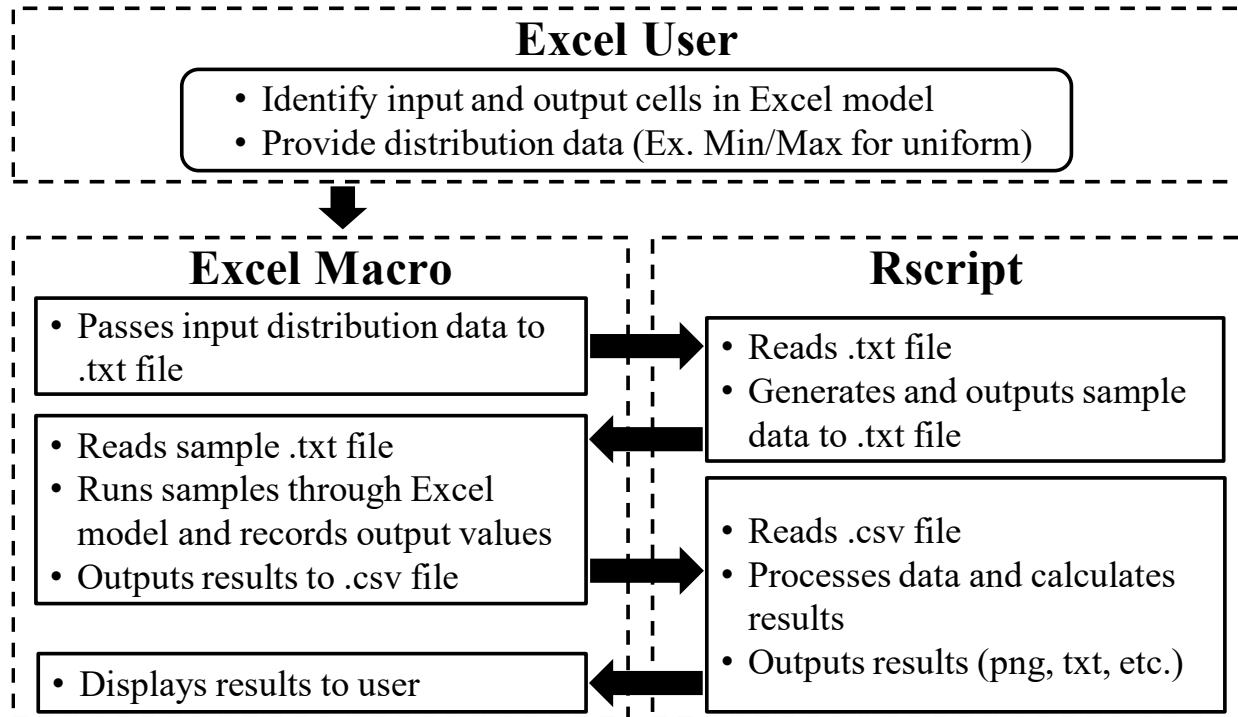


**Figure 4-3: RUST background process flow diagram**

#### 4.2.6 Case study

The same case studies described in Chapter 3.2.2 are used here. The Maya, Bow River, and Mined Bitumen (MB) models are simple, nearly linear, monotonic LCA models, while the Alliance NGTL pipeline model is an iterative and non-linear LCA model. A list of inputs used is provided in Appendix C. These case studies are described in greater detail in Chapter 3.2.2

### 4.3 Results and Discussion

The Morris method was used with 60 OAT designs ( $r$ ) and 32 levels ( $p$ ), and the results were used to produce Figure 4-4. Each data point represents a parameter. The Excel template generates the Morris plot and adds data labels, so it is easy to identify each parameter. The data

labels were removed in Figure 4-4 to reduce the image size. The parameters in red box A were eliminated, as they were insensitive and did not have significant non-linear or interaction effects. It is important to look at the actual value of the Morris  $\mu$  and  $\sigma$  when deciding when to eliminate parameters rather than just the relative position, as an excessively large parameter can skew the axis scale. Selecting the cut-off point between sensitive and insensitive is subjective. The axis scale should be considered, as well as the clustering of parameters. For example, a parameter can be deemed insensitive if the Morris mean is less than 1% of the base case value and has a low Morris standard deviation. For the Figure 4-4 Morris plot, the inputs in box B have similar sensitivities, hence they should all be either included or excluded as a group. The parameters in the top right with  $\mu \approx 6-8$  and  $\sigma \approx 4-5$  gCO<sub>2</sub>eq/MJ illustrate the advantage of the Morris method. Depending on the base case used in an OAT local sensitivity analysis, these parameters could have sensitivities of 1-2 gCO<sub>2</sub>eq/MJ and be grouped with the insensitive parameters. The Sobol method was not required in this scenario as the Morris method sufficiently reduced the number of parameters.

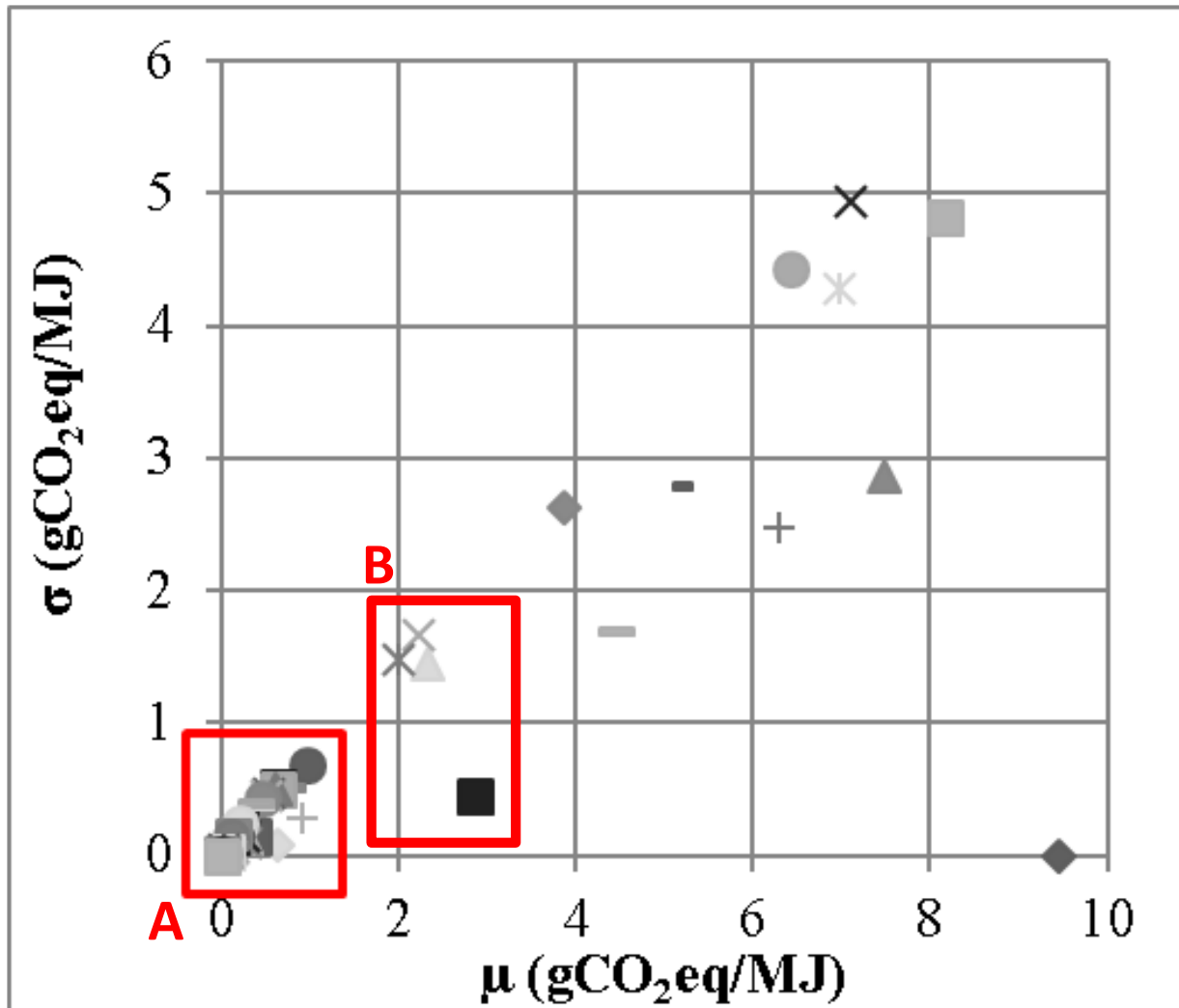
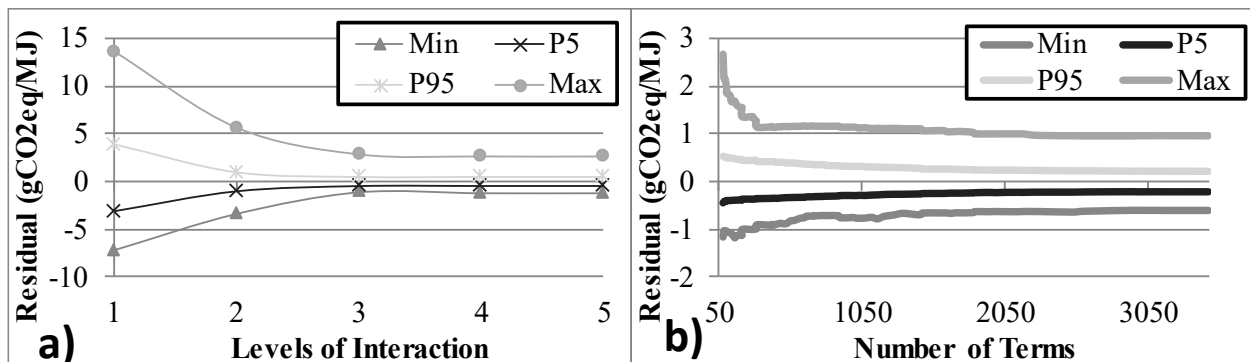


Figure 4-4: Morris screening of the FUNNEL-GHG-CCO/OS Maya pathway

#### 4.3.1 Validating the regression model form

The regression analysis was performed for the Maya pathway using the 14 critical parameters with 1<sup>st</sup>, 2<sup>nd</sup>, 3<sup>rd</sup>, 4<sup>th</sup>, and 5<sup>th</sup> level interactions. Three scenarios with training sample sizes of 3,000, 5,000, and 10,000 samples were used for comparison. For 5 levels of interaction, a minimum of 3,472 samples is required; hence, 5<sup>th</sup> level interactions are not included in the 3,000-sample scenario. Since an iterative method is used to narrow down which terms are included in the final regression model, the number of samples per term will increase as terms are eliminated, thereby reducing the chance of overfitting in the final model. Theoretically, if the number of samples is too small, then potentially significant terms could be eliminated during the initial

iterations. However, the results show that the number of samples used does not have a detectable effect on the accuracy of the final form of the regression model. The accuracy was strongly related to the level of interaction and the number of terms included (see Figure 4-5); this relationship will be model-specific. Caution should be used when assessing the accuracy of the regression model versus the number of terms included, as overfitting can occur. As shown in Figure 4-5, moving from 320 to 316 terms causes a jump from 2.05 to 2.27 gCO<sub>2</sub>eq/MJ in the residual variance (max residual – min residual). An overfit check with 100 runs of 1,000 samples each on both the 320 and the 316 term models found that the residual variance ranges were 1.8-3.2 and 3.0-3.2 gCO<sub>2</sub>/MJ, respectively, indicating they both have the same level of accuracy when tested against new samples. The residual variance uses the maximum and minimum residuals to ensure there are no outliers. While it may be tempting to use a regression model with more terms to improve accuracy, the model should be verified with a new sample to ensure the improved accuracy is not due to overfitting.



**Figure 4-5: The effect of levels of interaction used (left) and number of terms included in the final regression model (right) on the residual (both use 5,000 samples in training data; right plot uses 5th level interactions)**

### 4.3.2 High-level checks

For the Maya pathway, the 5,000-sample, 4<sup>th</sup>-level interaction regression model was used. The predicted vs. actual, residual vs. actual, normal Q-Q, and residual histogram plots were generated for the final regression model with 84 terms (Figure 4-6). The actual vs. predicted plot shows no large deviations/outliers; however, there is an indication that the regression model will underpredict emissions when actual emissions are large (Figure 4-6a). The residual vs. predicted plot confirms that the regression model underpredicts emissions for the extreme scenarios, and that there is a slight bias in the residuals (Figure 4-6b). The normal Q-Q (Figure 4-6c) plots'

upward curve on the right indicates that the right tail is slightly longer than for a normal distribution, which is illustrated by the histogram (Figure 4-6d). Overall, the plots indicate that the residual is approximately normally distributed with no major problems, but it should be noted that the residual error will increase as the predicted value increases. This conning effect may indicate non-linear effects are not being accounted for.

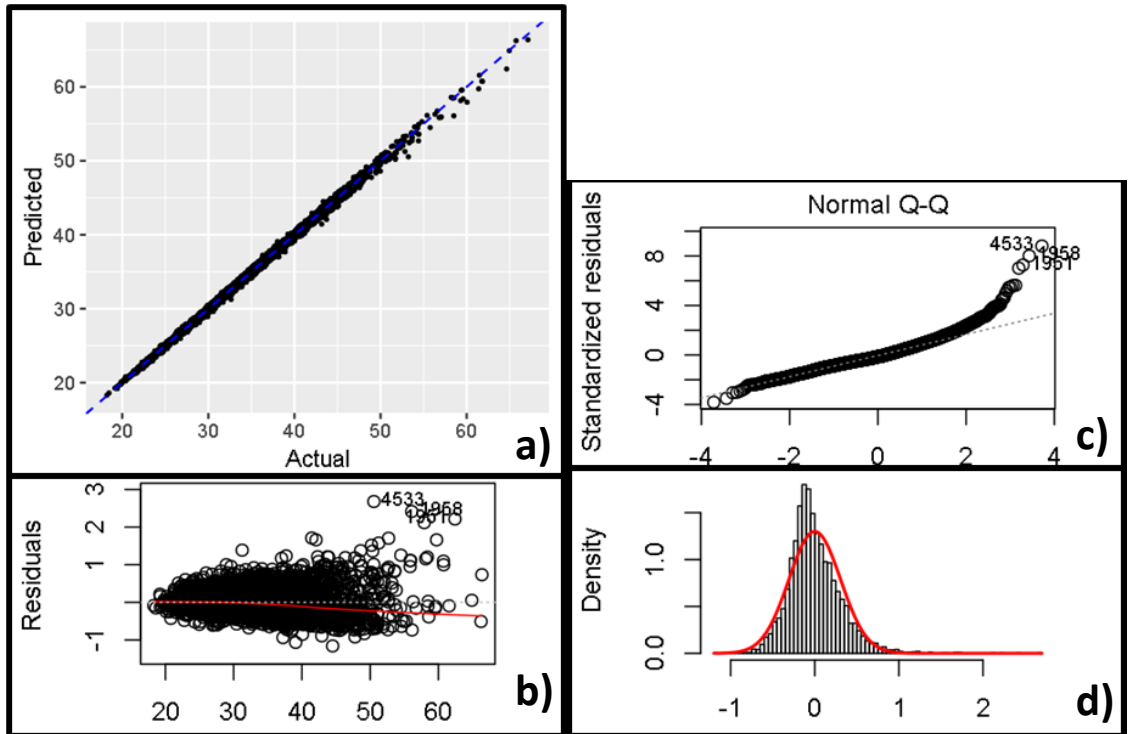


**Figure 4-6: Regression residual verification for FUNNEL-GHG-CCO/OS Maya pathway**

### 4.3.3 Overfitting checks

To check for overfitting, the range of residual variance (max residual – min residual) across 100 runs, each with 1,000 samples, was compared to the training set residual variance (Table 4.1). When 4<sup>th</sup> level interactions are used with 14 parameters, the total number of terms is 1470; when all terms are included in the regression model, the number of samples per term is 2, 3.4, and 6.8 for the 3,000, 5,000, and 10,000 sample scenarios, respectively, all of which are lower than the suggested 10-15 samples per term. As a result, the residual variances from the overfit check are significantly larger than the training set variances. The final form of the regression model includes only 46, 43, and 39 coefficients, which result in 77, 116, and 217 samples per term for

the 3,000-, 5,000-, and 10,000-sample scenarios, respectively; hence, their residual variance is similar to the training set and indicates that overfitting has not occurred (Table 4.1).

**Table 4.1: Maya range of residual variance (max – min) with 4th level interactions, ranges from 100 runs with 1,000 samples each (the same overfit check samples were used in every scenario)**

Scenario	All Terms		Final Form	
	Overfit check	Training set	Overfit check	Training set
3,000	36,590-114,890	1.72	2.41-4.86	4.07
5,000	13,670-53,290	1.95	1.94-4.08	3.84
10,000	13,18-38,250	2.49	1.91-3.58	3.09

#### 4.3.4 Checking model response

A well-fitted model should be able to accurately predict both the output values and sensitivities (partial derivative). The accuracy of the output values has already been addressed. To determine the accuracy of the partial derivative, the Morris method is used. If the regression model perfectly predicts the emission intensity, the  $\mu$  and  $\sigma$  values of the partial derivative should be the same, providing the same sample is used. Overall, the regression model accurately captures the model response. The average and standard deviation values of the derivative are accurate to within 4% and 15%, respectively (Table 4.2). The large error in the Morris  $\sigma$  for the refinery emissions is acceptable since the value is approximately zero. The regression model underpredicts the  $\sigma$  in the crude low heating value (LHV) correction factor while maintaining accuracy in the  $\mu$ , suggesting that there may be errors in the regression model’s predictions for the extreme scenarios.

**Table 4.2: Verifying the regression model response using Morris**

Parameter	Morris $\mu$			Morris $\sigma$		
	Orig.	Regr.	%Error	Orig.	Regr.	%Error
Crude LHV correction	5.72	5.61	-1.8%	2.96	2.53	-14.5%
Land-use emissions	2.99	3.01	0.4%	0.48	0.50	3.3%
Inj. GOR	7.14	7.09	-0.7%	4.65	4.59	-1.4%
Prod. GOR	7.15	7.06	-1.2%	5.89	5.75	-2.3%
Compressor energy	3.58	3.52	-1.7%	3.70	3.51	-5.0%
Compressor driver eff.	2.23	2.14	-4.0%	2.14	1.94	-9.4%
Electricity emission factor	5.07	5.06	-0.3%	3.29	3.25	-1.2%
Fugitive gas volume	6.44	6.42	-0.3%	4.80	4.79	-0.3%

Flared gas	4.56	4.54	-0.4%	1.61	1.60	-0.2%
Flaring efficiency	1.97	1.93	-2.0%	1.63	1.57	-3.9%
Refinery Emissions	9.45	9.47	0.2%	0.00	0.00	14.9%
Refinery Yield Factor	6.40	6.37	-0.5%	2.71	2.66	-2.1%
CH4 GWP	5.00	5.01	0.1%	3.03	2.96	-2.1%
NG Emission Factor	1.84	1.89	3.0%	1.42	1.46	2.1%

#### 4.3.5 Final regression models

Once the regression formula has been determined, an Excel macro generates the final formula from the text file. Excel formulas are limited to 8192 characters; hence, long formulas may need to be split between two or more cells. Overall, the original FUNNEL-GHG-CCO/OS model, which includes hundreds of calculations and multiple Excel worksheets, can be simplified down to the 14-parameter regression model. The same approach was applied to the Bow River water flood crude and Athabasca mined bitumen crudes from Alberta, Canada; the regression accuracies are shown in Table 4.3. Each model contains between 58 and 96 terms and 1393 and 2989 characters, well within Excel’s 8192-character limit. The regression model inputs include technology flows, emission flows, and characterization factors, as shown in Appendix C.

The maximum and minimum residuals are less than 10% of the base case for the FUNNEL-GHG-CCO/OS scenarios, while 90% of the residuals are within  $\pm 2\%$  of the base case. The FUNNEL-GHG-NGTL regression models are less accurate with residuals up to  $\pm 30\%$  of the base case; however, the residuals are within  $\pm 5\%$  of the base case 90% of the time.

**Table 4.3: Regression summary for Maya nitrogen injection, Bow River water flood and Athabasca mined bitumen**

Residual (gCO <sub>2</sub> eq/MJ)	Base Case	Min	5 <sup>th</sup> Percentile	95 <sup>th</sup> Percentile	Max	# of terms
Maya	26.5	-1.16	-0.44	0.53	2.68	58
Maya (squared)	26.5	-0.63	-0.08	0.07	0.44	164
Bow River	33.2	-1.17	-0.54	0.7	2.46	72
Bow River (squared)	33.2	-0.38	-0.10	0.10	0.55	135
Athabasca	36.4	-0.19	-0.12	0.17	0.34	96
NGTL	1.28	-0.38	-0.04	0.06	0.27	54
NGTL (squared)	1.28	-0.26	-0.04	0.05	0.27	80
NGTL (cubed)	1.28	-0.25	-0.04	0.05	0.27	79

The original Maya and Bow River regression model exhibited conning of the residuals which may indicate non-linear effects that are not accurately accounted for. When we tested the models for non-linear inputs using the trendline approach described in Chapter 4.2.2, we found multiple non-linear inputs. However, none of the  $R^2$  values equaled one, indicating a more complex response was occurring (see Appendix C.3). To determine whether adding non-linear terms to the regression model would improve the fit, the Bow River and Maya crudes were rerun, since their residuals were larger than the Athabasca pathway. Maya included a squared term for the crude LHV and compressor driver efficiency, and Bow included crude LHV, pipeline capacity, and pipeline velocity. The results in Table 4.3 indicate that adding the non-linear terms reduced the residuals by 40-80% but increased the size of the formula by 65-90%. The non-linear models did not exhibit any signs of overfitting. Therefore, including non-linear terms can improve the regression model's accuracy, at the expense of requiring longer computing times and producing a larger regression model. For the NGTL model, adding either squared or both squared and cubed terms did not significantly improve the accuracy but did increase the number of terms by 48%.

#### **4.4 Conclusion**

Unlike earlier studies, which simply examined the sensitivity methods available,<sup>18, 70</sup> this work goes one step further by adding a multi-parameter regression model. While publishing the full LCA model is often preferable, it is not always possible because of difficulties making the model user friendly, non-disclosure agreements, or other confidentiality concerns. Furthermore, in some cases a simplified version of the LCA model is preferable. For example, non-technical policy makers may want to examine how the LCA results change when key inputs are adjusted without having to learn a complex model. Since journal papers need to be concise, researchers are often limited in how many scenarios/alternatives they can present. By including a regression model, the usefulness of an LCA to fellow researchers and policy makers is increased as they can examine scenarios specific to their needs. The regression model can also improve the life of a paper by allowing users to update key values such as methane's GWP, which is updated each time a new assessment report is released by the IPCC.<sup>179</sup>

The levels of interaction and number of terms need to be varied until a model with the desired accuracy is obtained. The FUNNEL-GHG-CCO/OS regression models have accuracies of:

Maya $_{-1.2}^{+2.7}$ , Bow $_{-1.2}^{+2.5}$ , and Athabasca $_{-0.2}^{+0.3}$ gCO<sub>2</sub>eq/MJ. To improve the fit for the Maya and Bow River pathways, non-linear terms were added, resulting in new accuracies: Maya $_{-0.6}^{+0.4}$  and Bow $_{-0.4}^{+0.6}$ . For the FUNNEL-GHG-NGTL model, the accuracies were NGTL $_{-0.38}^{+0.27}$ ,  $_{-0.26}^{+0.27}$ ,  $_{-0.25}^{+0.27}$  for the linear, squared, and cubed regression models, respectively. The NGTL model uses an iterative solver and is highly non-linear. In order to further improve its accuracy, we considered ANN modeling (discussed in Chapter 5). The regression formulas are small enough to fit into a single Excel cell, making it easy to publish the model.

The uncertainty simulation can also be run using the regression model rather than the full model to reduce computational times for complex models. However, running uncertainty in the regression model introduces additional model uncertainty depending on the accuracy of the regression model. In the cases of the Maya, Bow, and Athabasca crude pathways evaluated in this work, the parameter uncertainty will be an order of magnitude larger than the regression model uncertainty, which would make the modeling error negligible. Given its low regression accuracy, the NGTL model should not be used for a sensitivity analysis. Since the regression model can be evaluated quickly, increasingly complex analysis such as hybrid and nested Monte Carlo methods, which attempt to separate aleatory (random) and epistemic (known with poor precision) uncertainty and require a large number of model evaluations, can now be performed in less time.<sup>171</sup>

Alternative data analysis techniques such as principal component analysis (PCA) and partial least squares regression (PLS) are useful when the data set available is correlated or has a limited sample size; however, since RUST generates an uncorrelated sample to train the regression model, these methods are not needed. Furthermore, since PLS emphasises developing a predictive model, it is not useful as an alternative to the Morris methods for screening out insignificant parameters.<sup>160</sup> Additionally, correlations are not required in training the regression model. If the model is accurate when trained with uncorrelated data, it will also be accurate when correlated inputs are used.

# 5 Development of Artificial Neural Network-based Proxy Models for Life Cycle Assessment of Energy Pathways\*\*

## 5.1 Introduction

The motivation to create proxy models was discussed in Chapter 4. *This chapter focuses on proxy modeling for complex non-linear models that multi-parameter linear regression is unable to accurately map.* ANNs allow us to create easy-to-use, accurate models for complex processes in LCA, thus increasing their usefulness.

Process models such as the NGTL model present unique challenges that multi-parameter proxy modeling cannot overcome. First, process models can have piece-wise characteristics; for example, friction loss of fluid flowing through a pipe experiences laminar, transitional, and turbulent flow regimes. Generating a proxy model that can correctly estimate friction loss across all three flow regimes requires more flexibility than multi-parameter regression can provide. In a large process model of an oil refinery, different units, physical laws, and chemical processes will dominate the results in different regions of the parameter space, leading to piece-wise responses. Second, the process models may not be valid at every point in the parameter space, and the boundary of the valid solution space may be unknown. For example, in the NGTL model a combination of high flow rate and high losses would result in a negative pressure in the pipeline, causing the model to fail. Third, the number of inputs may be large, leading to infeasible design of experiment (DOE) sample sizes (curse of dimensionality).

ANNs were chosen because they have been demonstrated to be “general universal approximators.”<sup>181</sup> Unlike in conventional regression, the user is not required to specify the functional form (linear, quadratic, etc.), thus removing a significant source of error.<sup>182</sup> Furthermore, the flexibility of ANNs can be used to address piece-wise, valid-solution space, and

---

\*\* This chapter is based on work published as: Di Lullo, Oni and Kumar, "Using proxy models and adaptive sampling to integrate complex engineering models into life cycle assessments of energy systems". *To be submitted to Energy Convers. Manage.* 2022.

curse of dimensionality limitations of multi-parameter regression. Overall, ANNs generally have higher accuracy than alternative meta-modeling methods and are easy to use.<sup>183, 184</sup> However, ANNs still suffer from the curse of dimensionality. In order to reduce the number of model evaluations required to generate training data for the ANN, an intelligent sampling strategy is required.

In order to train a proxy model, samples need to be taken over the parameter space. Sampling strategies include design of experiments (DOE), one-shot space-filling, sequential space-filling, and adaptive designs.<sup>185</sup> DOE uses a structured sampling approach designed for simple linear and quadratic regression models and was originally developed to perform physical experiments with a small number of inputs. DOE focuses on reducing random errors from physical experiments, with samples focused on the edge of the boundary space. Sacks et al.<sup>186</sup> and Simpson et al.<sup>187</sup> state that as computer simulations suffer from systematic, not random error, space-filling designs are more appropriate than classical DOE methods. Through Monte Carlo sampling can be used for proxy modeling, it is inefficient.<sup>28</sup> While one-shot space-filling may result in a better spread between samples, it is often not possible to know how many samples are needed to train a proxy model with adequate accuracy; therefore, sequential methods are needed. Sequential methods do not use any information related to the current proxy model accuracy; they simply attempt to supplement the current sample while maintaining optimal sample spacing or selecting new points that maximize information gain. However, maximizing information gain is only related to the model structure (linear, quadratic, etc.) but does not reflect whether the model structure accurately fits the underlying data. Improvements from sequential sampling decrease as the sample size increases. Further improvements may require sampling specific regions of space where complex behavior occurs. Adaptive sampling attempts to identify areas where additional samples would improve model accuracy. Adaptive methods include looking for areas with large residual errors and identifying areas of complex behavior (gradient methods).<sup>185</sup> While the areas of classical and space-filling sampling have been thoroughly researched, the area of high dimensional, adaptive sampling requires further research.<sup>28, 185</sup> *This chapter describes the development of an adaptive method for high dimensionality problems.*

The objectives of this chapter are to:

1. Compare the accuracy of quadratic and ANN regression for proxy modeling of LCA models.
2. Develop a new adaptive sampling method to minimize extreme error rather than mean squared error.
3. Identify optimal sampling methods for reducing maximum error, while minimizing the number of model evaluations needed.

## 5.2 Methods

Proxy modeling involves three main time-consuming processes: generating samples, calculating target values for samples, and training the proxy model (Figure 5-1). The sample generation step involves selecting multiple test points (input value combinations). Sample generation is relatively quick when random sampling is used, but increases in time if space-filling or adaptive methods are used. Following sample generation, the samples are fed into the true model to calculate target values (output values). In this work, the true model is the complex engineering model that we are trying to replicate. The time required to generate the target values is dependent on the true computer model. For the natural gas transmission line (NGTL) model, generating target values takes <1s per sample; however, for complex engineering models, each sample can take minutes to hours. The time required for model training depends on the method (quadratic regression vs. ANN), structure (linear vs. non-linear, network size), the number of samples used, and the training algorithm selected. This work assumes target value generation is the most time-consuming process. Therefore, this work examines methods to reduce the number of true model evaluations required, at the expense of increased sample generation and model training times. The model's accuracy will be evaluated and if it is inadequate, additional samples will be generated.

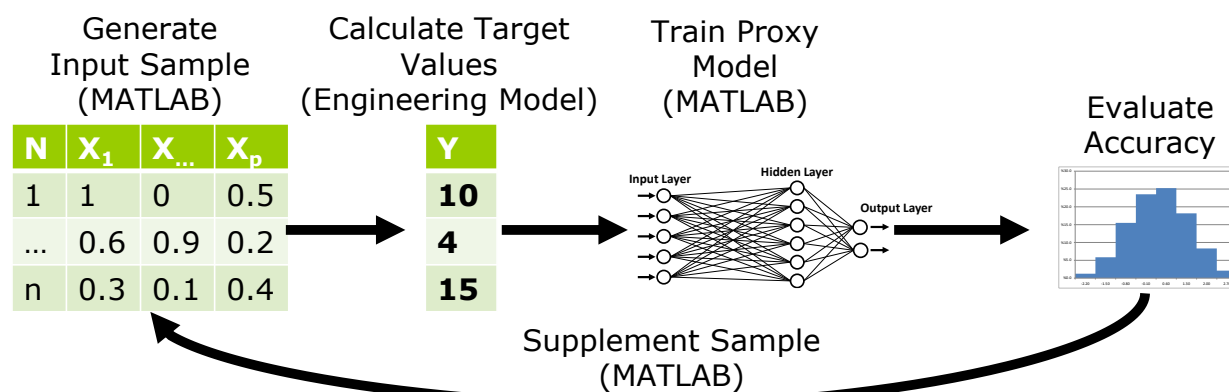


**Figure 5-1: High level proxy modeling method**

### 5.2.1 Case studies

The same case studies used in Chapter 3.2.2 are used here. The scenarios have different numbers of inputs and mathematical complexity. The CCO/OS model for the Maya, Bow River, and Mined Bitumen (MB) scenarios are all deterministic, with no iterative calculations. The NGTL model includes multiple iterative solvers, resulting in a complex non-linear relationship between the inputs and outputs. The model inputs are provided in Appendix C. Bow and Maya have 14 inputs, MB has 16, and NGTL has 10. The models used in this work are Excel-based models that have relatively short computing times (less than 1 s/sample), allowing rapid testing of different proxy modeling methods. Once a framework is established, this method will be applied to more computationally expensive Aspen HYSYS models.

### 5.2.2 Standardized validation set

In MATLAB, the ANN training algorithm splits the data set into training, validation, and testing data sets. The validation set is used to determine when to stop the solver and therefore indirectly affects the accuracy of the proxy model. To compare the accuracy of various experiments using different proxy model forms and sample generation strategies, an external data set is needed. The external validation data set contains 500,000 samples and is used only to determine the proxy model's final accuracy and has no influence on model training. The external validation set is not the same as the MATLAB internal validation set.

### 5.2.3 Defining model accuracy

Typically, the mean squared error (MSE) is used to quantify model accuracy; however, it is not always sufficient. Since LCAs contain significant uncertainties in their input values, small errors in the proxy model will be negligible in comparison. Therefore, reducing the error below a certain minimum will provide no additional value. However, an ideal proxy model should be reliable and able to produce accurate results over the entire input parameter domain. In this case, it would be acceptable for the average error to increase if the extreme error decreases.

The acceptable level of error is subjective and depends on how the model is used. In this work, any error above 5% indicates an unreliable model with poor accuracy (unacceptable level of error). Ideally, we would like the error to be below 1% to provide reliable and relevant results (ideal level of error). A low error is required so that end-users can be confident that as they vary each input, the change in the output is due to the true model's response, not modeling error. Because of the level of uncertainty in the model input values (from an LCA perspective), reducing the error below 0.1% provides no additional benefit (optimal level of error).

### 5.2.4 Regression methods

Two proxy methods were examined in this work: quadratic and ANN regression. Details on quadratic regression were provided in Chapter 4.2.2.

Unlike in conventional regression, the user is not required to specify the functional form (linear, quadratic, etc.) for ANN models, thus removing a significant source of error.<sup>182</sup> Rather than adding more orders of interaction or higher power polynomials to increase the model form's complexity, ANN simply increases the number of nodes in the hidden layer. For complex abstract processes such as image recognition, multiple hidden layers can be used; however, a single layer is sufficient for mapping a continuous function.<sup>188</sup> For a feed-forward ANN with a single hidden layer, the number of coefficients is calculated as:

$$N_c = (k_a + 1) * HN + (HN + 1) \quad \text{(Eq. 8)}$$

where  $HN$  is the number of hidden nodes.

In this work, the common *tanh* transfer function is used for the hidden nodes and a linear transfer function is used for the output node. ANN training is performed in MATLAB.

### 5.2.5 Evaluation methods

Because of the random nature of numerical methods, results can vary between runs; the variation may be due to the solver converging to different solutions or using a different training sample set. As a result, in order to confirm that the difference between two proxy models is due to either the proxy model form or the sampling strategy used, multiple repetitions are required so that statistical significance can be checked. For quadratic regression, a deterministic solver is used, resulting in minimal variation in the results when the solver is rerun on the same sample. Therefore, only 5 repetitions using different sample seeds are used for verifying statistical significance and determining error bars of quadratic regression results. For ANN regression, large variations are observed in the proxy model's accuracy due to both using different samples and running the solver multiple times on the same sample. Therefore, the ANN models are trained 10 times on each of the 5 samples, resulting in 50 repetitions. Because of the time required to generate the target values, only 5 seeds are used, while 10 repetitions are used to improve accuracy without drastically increasing the computing time. In order to determine if the results are statistically significant, a two-tailed t-test assuming unequal variance (heteroscedastic) is used.<sup>189</sup>

To improve the stability in the results when using an automated process, the MATLAB (`trainlm` and `trainNetwork`) code was modified to save the weights and biases from the best epoch, rather than using the last epoch (see Appendix D.7). The maximum number of validation failure's stopping criteria can significantly affect model accuracy: too low, and the solver will terminate prematurely; too high, and the final epoch can overfit the data. By specifying a higher number of max failures (20 instead of the default 6), premature termination is prevented; by using weights from the best epoch, the overfitting that occurs in the final epoch is avoided. This work found that using the best epoch weights and biases results in less variability when a model is repeatedly trained on the same data set, especially for models with small samples that were prone to overfitting the data. The max number of epochs was set to 10,000 to prevent premature

termination of the solver. The ANN training algorithm randomly splits the samples into train (70%), validation (15%), and test (15%) subsets.

Table 5.1 provides an overview of the type of data recorded and what purpose that data serves. Data was recorded for each iteration to ensure results are statistically significant.

**Table 5.1: Experimental data recorded**

<b>Sample Data</b>	<b>Purpose</b>
Sample histogram bin frequency data (10 bins used)	Used to examine differences in sample coverage of the various sampling algorithms (Appendix D.6).
<b>Proxy Model Data</b>	<b>Purpose</b>
# of coefficients in final model	Indicates model complexity and can be used to indicate if overfitting will occur.
# of solver iterations/epochs	Used to monitor stability and ensure solver is not terminating early.
<b>Proxy Model Performance</b>	<b>Purpose</b>
For training data & external validation set residuals: min, max, 1, 5, 25, 75, 95, and 99 percentile values	Used to ensure symmetrical error distribution, determine if overfitting is occurring.
For external validation set absolute residual: 1, 5, 25, 50, 75, 95, and 99 percentiles, max and avg. values	Used to determine if extreme errors occur due to lack of coverage/overfitting by examining tails of error distribution.
Time required for input sample generation, target value generation, and proxy model training	Used to examine trade-offs between longer sample generation and proxy modeling time vs. shorter target training times.

The typical residual values include both positive and negative errors, which makes accuracy comparisons more difficult, as the results are not always symmetrical. Therefore, percentile values are calculated based on the absolute value of the residuals as it does not matter if the model over- or underestimates the output value.

In some instances, the models may fail to converge and terminate prematurely. If the ANN training was done manually, the user would ignore this result and try again. Since we used an automated process, it was not possible to identify the failed scenarios. We compared the results from using all runs to the results using 50% of the best performing runs. The filtered results using the best runs reduced the upper error limit in the results caused by the skewed failed runs.

50% was selected as it insured poorly performing runs were ignored. Although the unfiltered results provide stronger support for our findings and conclusions, they are more prone to include scenarios where accuracy is extremely low, skewing the results.

## **5.2.6 Experimental methods**

Key experiment parameters include sample size and model structure parameters. For quadratic regression, the starting sample size must be larger than the number of coefficients. For ANN, small starting sizes result in overfitting, so a starting size of 1,000 samples was selected based on preliminary experiments. The step size used has no effect when a random sample is used; however, it will affect the results when adaptive sampling methods are used. A preliminary step size of 500 and 1,000 samples was selected for the quadratic and ANN methods, respectively. Based on preliminary investigation, ANN networks will use 5, 15, 25, and 50 hidden nodes. The addition of squared terms for quadratic regression is based on previous work with the FUNNEL models.<sup>2</sup>

## **5.2.7 Sampling methods**

There are many means of determining a sample with optimal spread between the points. Sampling-based methods include regular grid, random sequence, quasi-random (Halton, Sobol, Hammersley), stratified sampling, Latin hypercube designs (LHD), and randomized orthogonal arrays. Criterion-based methods include uniform design, max-min distance, tessellation, and statistical/entropy. However, all of these methods are limited to a small number of inputs because of long computing times. Additionally, sequential space-filling samples further increase computing times.<sup>185</sup> The goal of maximizing the sample spread is to ensure the domain is adequately searched and no major features are missed. Iterative space-filling algorithms is an active area of research.<sup>190</sup>

### *5.2.7.1 Spread method*

We required a simple method that would work in a high-dimensionality parameter space; therefore, a modified max-min method was developed for MATLAB. The Manhattan distance is used instead of the Euclidian distance, as it provides better representation in high dimensional space.<sup>191</sup> A small seed sample ( $n$  samples) is generated using a Monte Carlo simulation with uniform distributions for each input. The minimum distance between each point and its nearest

neighbor is calculated. Since it is difficult to calculate the optimal spacing distance in high dimensional space,<sup>192</sup> the 95<sup>th</sup> percentile is used as an approximate measure for the cut-off criteria (dCut). A new point will only be accepted if the distance to its nearest neighbor (dNN) is larger than a dNN of 95% of the existing samples. While dCut does not represent the optimal spacing, it does result in a better spaced sample than the conventional random approach (see Appendix D.6).

The spread method begins by generating a random candidate point and calculating its dNN using the existing sample. Since calculating the dNN is time-consuming, a guess and check method was found to be inefficient; instead, an optimization method was introduced to move the original candidate point away from its close neighbors (CNs) (Figure 5-2:). Rather than using all previous  $n$  samples, a subset of  $N_{CN}$  samples is used to determine what direction and how far to move the candidate sample. Using only  $N_{CN}$  samples reduces the computational burden while still improving the sample spacing. In the original code, the inputs excessively took on values of 0 or 1; therefore, Criterion 1 in Figure 5-2: was modified to evaluate the current sample spread and modify the starting area. To further decrease the number of samples taken at the parameter space surface, the original candidate starting point was also restricted. Further details are provided in Appendix D.6.

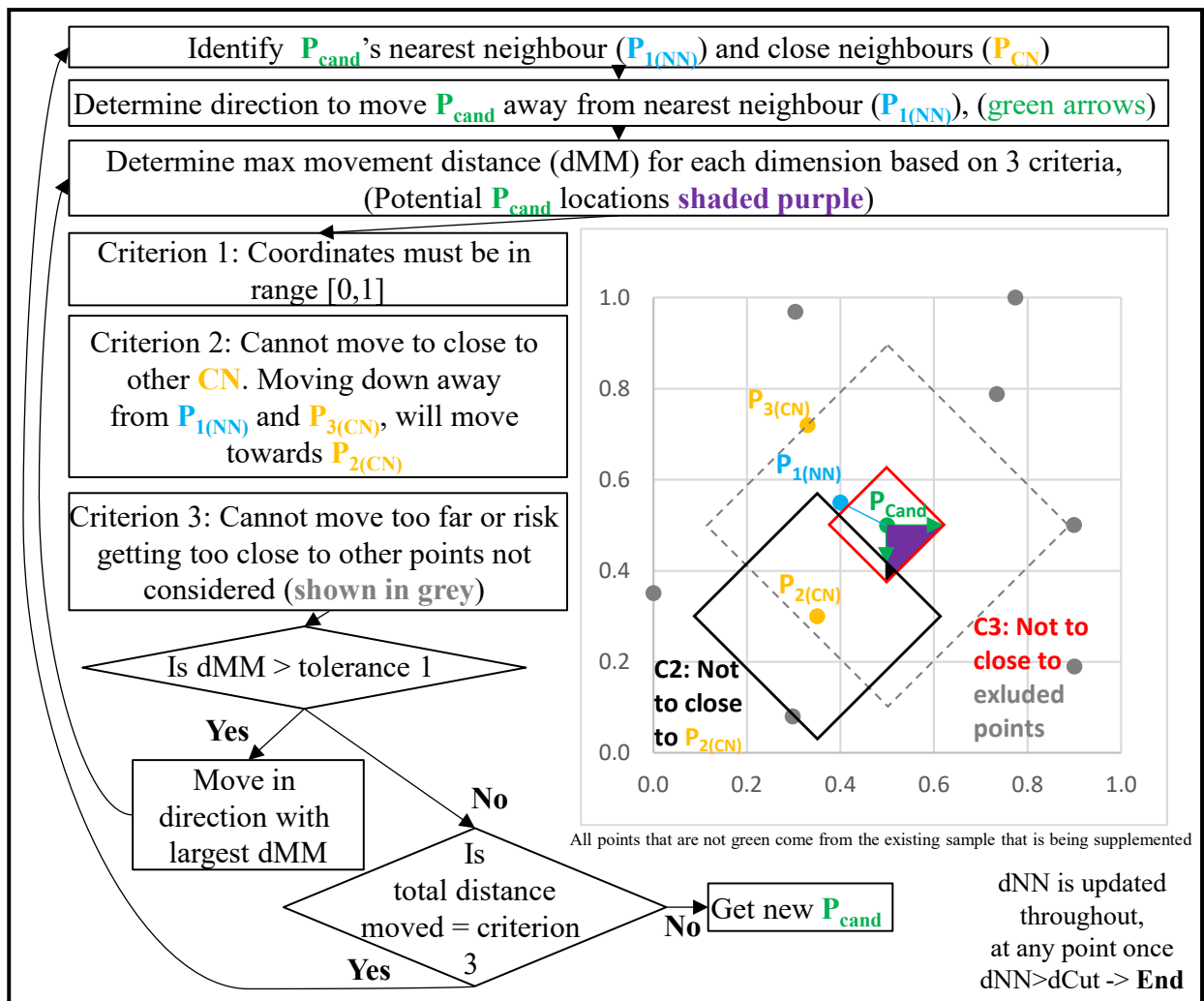


**Figure 5-2: Optimized method to increase distance to nearest neighbour (dNN) by moving the candidate point (CN: closest neighbour, NN: nearest neighbour, Cand: candidate point, dMM: max movement distance, dCut: cut-off distance required)**

### 5.2.7.2 High error method

An alternative method is to focus samples in areas where the model is currently producing poor estimates. Adaptive sampling needs to balance two objectives, local vs. global exploration. Global exploration is important to ensure all areas of the domain have been adequately investigated and to fill any gaps in the data. Local exploration aims to improve accuracy by adding samples in areas with complex behavior. Adaptive methods must attempt to balance the

two. Global exploration uses a distance criterion to ensure adequate sampling; however, in local regions of high complexity, clustered samples are needed to improve accuracy.

In this work, we developed the high error adaptive sampling algorithm. We based this method on the principle of improving ANN performance through bagging and boosting.<sup>193</sup> However, instead of trying to improve model accuracy by averaging the results of multiple models, we focused on using the disagreement between models to identify optimal new samples. ANN training requires splitting the samples into training, validation, and testing samples. Validation is used to determine when training should stop to avoid overfitting but is not used to identify node weights and biases. The testing sample is not involved in training and is used to evaluate overall performance. Training begins by randomly splitting the initial sample into five baskets; each basket is used by three ANNs, one as the training sample, one as the validation sample, and one as the testing sample. In this work, all five ANNs have identical configurations and numbers of nodes. Since the trained ANNs are computationally efficient, 1 million samples can be run through each of the 5 ANN models in under one second. For each sample, the maximum disagreement (MD) is calculated as the difference between the highest and lowest values from the five different ANNs. The  $N_{MD}$  samples with the largest MD are then selected as potential candidates (PC) where  $N_{MD} = 10 * N_{NS}$  and  $N_{NS}$  is the number of new samples needed.

To prevent clustering, when many points are selected in a small region of subspace, a modified version of the spread algorithm is used. The cut-off criteria selection needs to balance local vs. global exploration. Too large, and it will not be possible to generate points close to areas of complex behavior. Too small, and multiple points may be selected too close to existing points limiting global exploration. In the original spread algorithm, dCut was based on the 95<sup>th</sup> percentile of the original sample. In the high error method, dCut will use the 50<sup>th</sup> percentile. Future work will examine how the value of dCut impacts the results.

A candidate point is selected from the potential candidate set and the dNNs are calculated to the original sample. The candidate point is then moved away from its nearest neighbor (NN) until  $dNN > dCut$ . Since dCut is smaller for the high error method, this process has a low computational cost and Criterion 2 is not as restrictive. The algorithm then uses the same 3 criteria as the spread algorithm to limit movement. However, instead of moving in the direction

that will maximize the dNN, the algorithm aims to maximize the MDs calculated from the 5 ANN models. In this case, 100 test points are taken along each dimension between the current candidate position and the maximum movement distance (along the green arrows in Figure 5-2:). In MATLAB, it takes approximately the same amount of time to run a single point through all 5 ANNs as it does to run thousands of points, so there is no benefit to minimizing the number of points used in a single run. The candidate is then moved to the location with the maximum MD and the process is repeated until improvements in MD fall below a minimum threshold. The candidate point is added to the sample and the next point in the potential candidate set is examined.

Once all the samples and their target values are determined, a single ANN is trained on the new data set to produce the final proxy model.

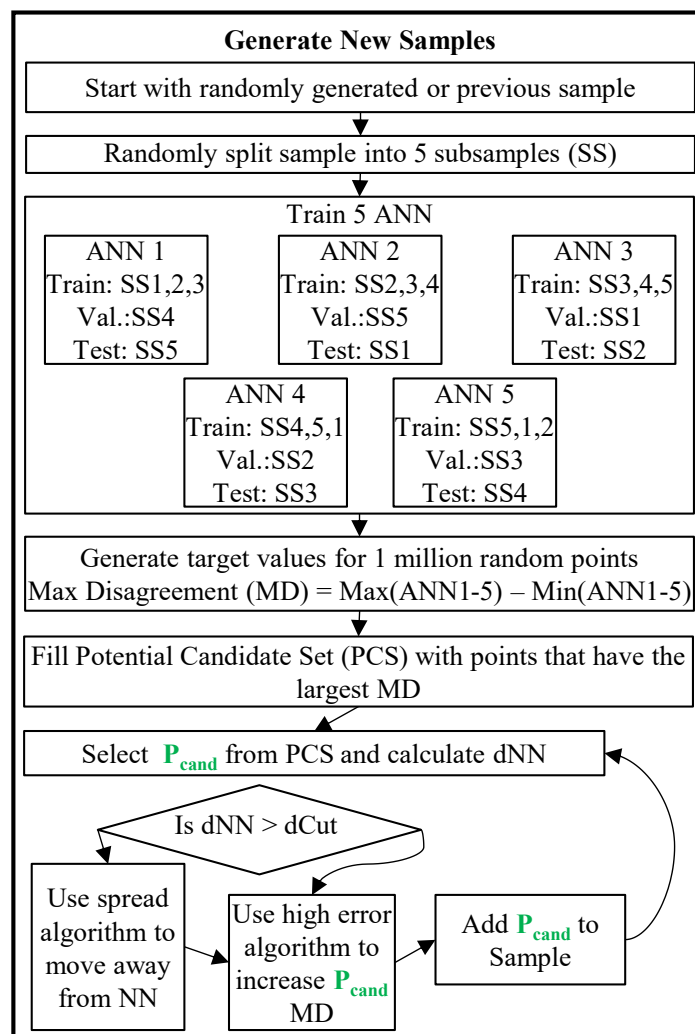


**Figure 5-3: High error sampling method (SS: subsample, MD: max disagreement, PCS: potential candidate set, dCut: cut-off distance required, dNN: distance to nearest neighbour, Pcand: candidate point)**

### 5.2.7.3 *Combination and random methods*

In the combination sampling method, half the points were generated using the spread method and half using the high error methods. This was done to try to better balance local and global exploration. The random method uses Monte Carlo sampling with uniform distributions and was used as the baseline scenario. The non-random sampling methods were only applied to the ANN models as they are more flexible than the quadratic models. The quadratic models are limited by their functional form, rather than sample quality based on preliminary work.

## 5.3 Results and Discussion

The ability of various quadratic and ANN proxy models to replicate the underlying complex models was evaluated for various proxy model configurations and sampling methods. Additional results are provided in Appendix D for the four case studies and four network sizes.

### 5.3.1 Quadratic regression

While quadratic models are easy to understand, they have limitations in terms of accuracy. The accuracy of the linear and nonlinear quadratic regression models was assessed for various sample sizes and orders of interactions. The green, orange, and red lines in Figure 5-4: represent 0.1% (optimal), 1% (ideal), and 5% (unacceptable) levels of error (Chapter 5.2.3). Increasing the order of interactions above two does not improve performance for the linear models. For non-linear models, accuracy improves by increasing orders of interaction up to 4. Overall, increasing the sample size had a negligible impact on accuracy directly; indirectly, larger samples allowed fitting more complex regression models to the data, which improved accuracy. Results for Bow and MB are similar and are provided in Appendix D.1. For the NGTL model, switching from linear to non-linear and increasing the levels of interaction above 3 had a negligible effect on accuracy (Figure 5-4: and 1-3). The lack of improvement results from the limited flexibility of quadratic proxy models. If the underlying complex model does not follow a quadratic form, then

adding additional samples or interaction terms will not improve accuracy without the risk of overfitting the data.

For Maya, Bow, and MB, the error is below the optimal error level 99% of the time for the NLO3&4 models; however, their maximum error is between the unacceptable and optimal levels and could still be improved. For the NGTL case study, the proxy model is less accurate, with maximum errors above the unacceptable level and 75% to 95% of errors above the optimal level (Appendix D.1).

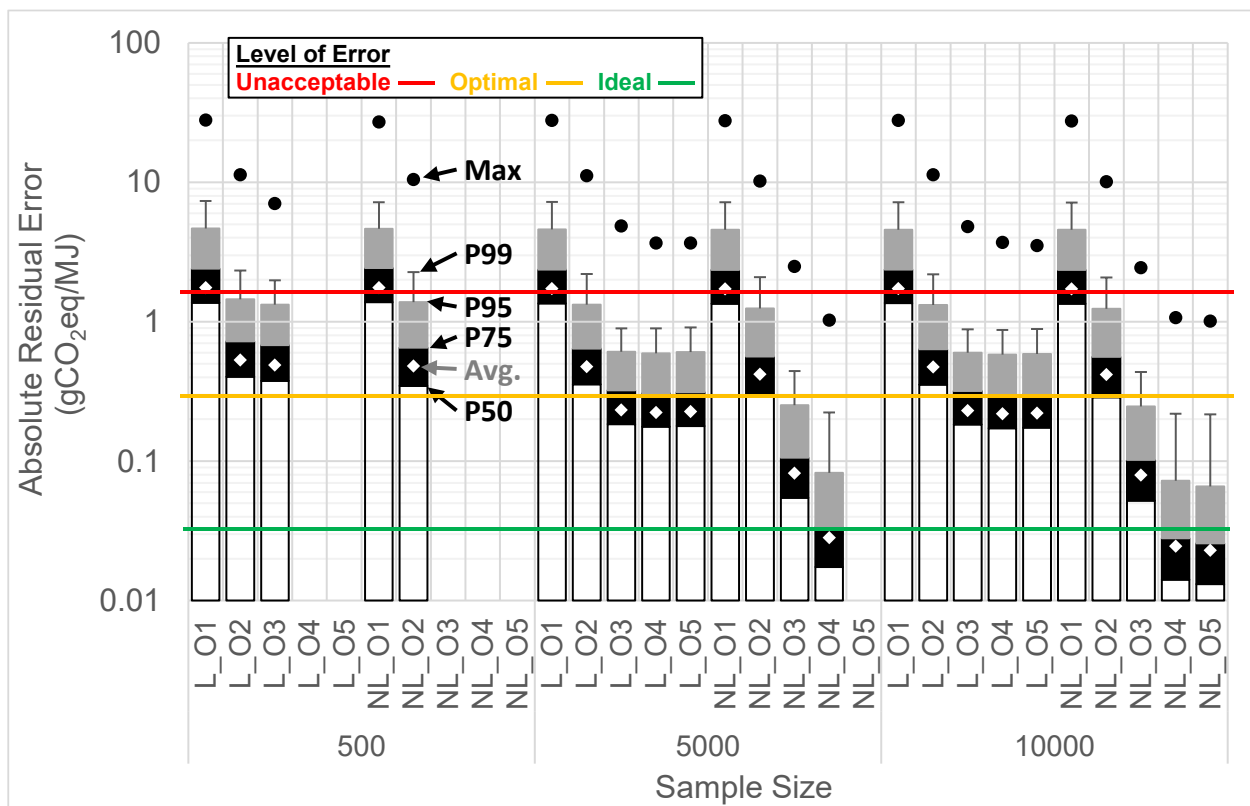


**Figure 5-4: Maya quadratic regression absolute residual results: L=Linear, NL=Non-linear, O#=Order of interactions**

### 5.3.2 ANN regression

If the regression model's accuracy is inadequate using quadratic regression, then ANN regression can be used to improve performance. As universal approximators, ANN's functional forms are not limited to quadratic equations. Complex non-linear iterative models with long computing times should use ANN from the beginning.

Of the four sampling methods examined, only two, random and high error, are presented here. The differences between the spread and the random, and between the high error and the combo method, are not statistically significant. The spread and combo results are presented in Appendix D.

Figure 5-5: shows how the ANN accuracy is affected by the number of nodes in the hidden layer. When only 1,000 samples are used, the 50-node proxy model is less accurate than the smaller networks. The 50-node network includes 801 coefficients and likely overfits the data as there are only 1.25 samples per coefficient. The larger the relative difference between the MSE from the MATLAB internal testing set over the training set, the higher the likelihood of overfitting.

Figure 5-6: shows how the overfitting is related to the number of samples per coefficient for different sized networks. Error bars that extend below 1% indicate that in some instances the training MSE was less than the testing MSE. If fewer than ten samples are used per coefficient, the probability of overfitting is high, with the testing MSE being 100-10,000% larger than the training MSE. Figure 5-6's results line up with linear regression's rule-of-thumb to use at least 10 samples per coefficient.<sup>172</sup> While smaller networks are less likely to overfit (in Figure 5-6:), this does not mean they are more accurate overall. For Maya's using 5,000 samples, the training MSE was on average 146% and 5% larger than the testing MSE for the 50 and 5 node networks, respectively (Figure 5-5:); however, in Figure 5-5:, the 50-node network's absolute residual error is lower than the 5-node network's. Trends for Bow and MB were like Maya's. The NGTL model, which is non-linear and includes an iterative solver, is more prone to overfitting.

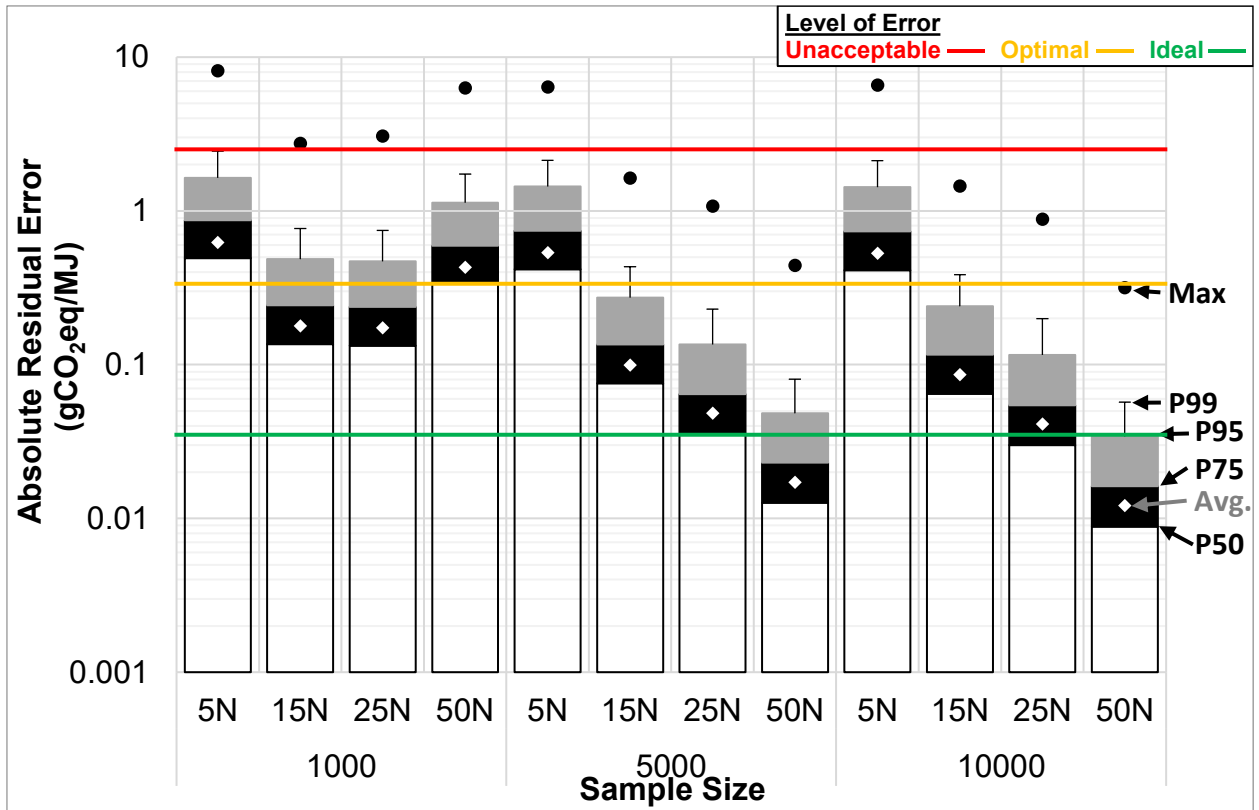
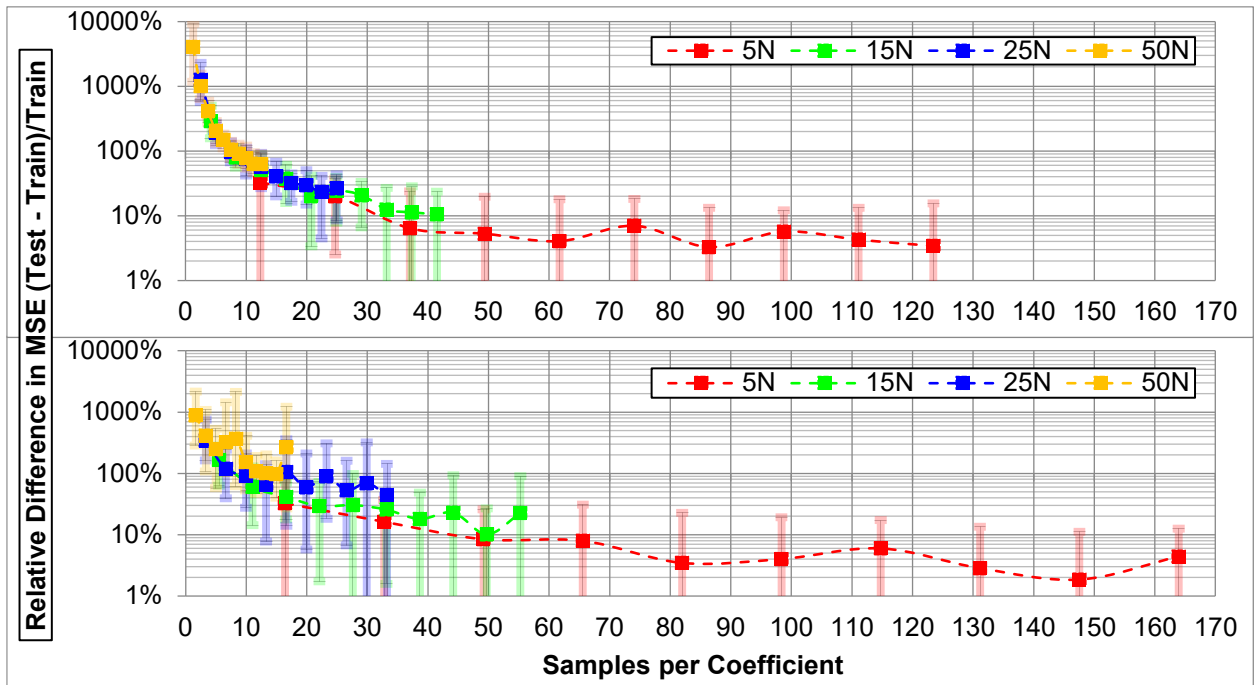


Figure 5-5: Maya ANN regression absolute residual results: N=Nodes in hidden layer of ANN



**Figure 5-6: Overfit check for Maya (top) and NGTL (bottom) using random sampling (test MSE >> train MSE indicates overfitting); error bars represent 90% CI**

5.3.2.1 Random ANN vs. quadratic

In the NGTL scenario, the quadratic model performed poorly with a maximum error equal to approximately 8% of the model’s average output value (Figure 6). However, the large 50N Rand ANN model significantly improved the model’s accuracy; the average and maximum absolute residual were reduced by 89% and 70%, respectively. The Bow, Maya and MB results are similar and are provided in Table 5.2.

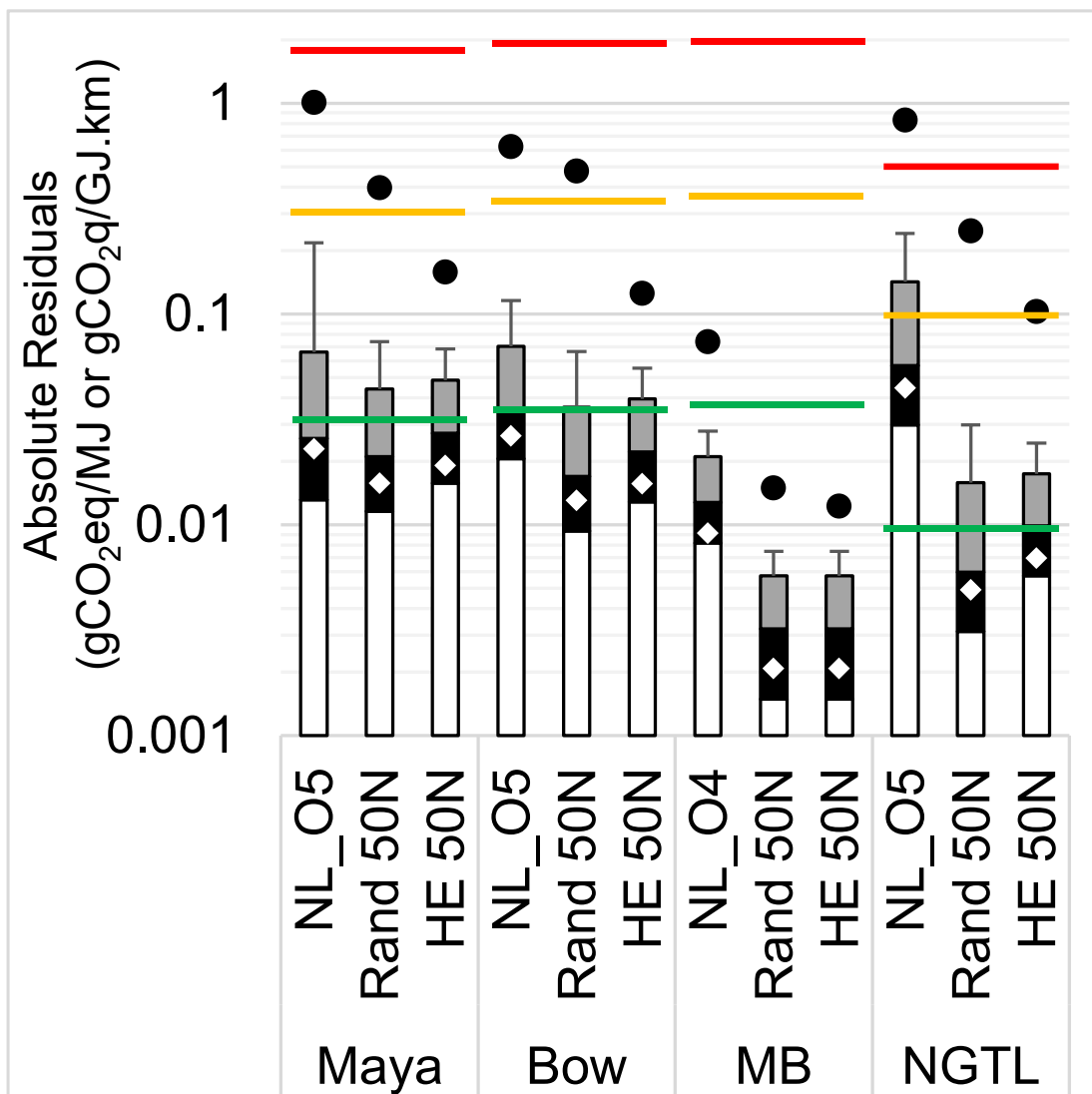


**Figure 5-7: Absolute residual results (Maya, Bow, NGTL use 10,000 samples; MB uses 7,000 samples) NL\_O5 =nonlinear quadratic with 5<sup>th</sup> order interactions, Rand 50N= 50 node ANN with random sampling, HE 50N = 50 node ANN with high error sampling**

To determine why the quadratic models perform better than the smaller ANN models, we compared the change in the average and max absolute residuals to the change in the number of coefficients used by each proxy model (Table 5.2). When an ANN model uses more coefficients than a quadratic model, the ANN average and max absolute residual values decrease. That said, some smaller ANN models outperformed the quadratic models. The NGTL 15-node ANN model used 35% fewer coefficients and still reduced the average and max absolute residuals by 67% and 68%, respectively. Similarly, the MB ANNs used fewer coefficients and still outperformed the quadratic model, except for the 5N scenario. Overall, the ANNs outperformed the quadratic models when the same sample size and a similar number of coefficients were used.

**Table 5.2: Change in the number of coefficients, average absolute error, and maximum absolute error from using ANN (random sampling) compared to the best performing quadratic regression proxy model**

# Hidden Nodes	Maya			Bow			MB			NGTL		
	Coeff	Avg.	Max	Coeff	Avg	Max	Coeff	Avg	Max	Coeff	Avg	Max
5N	-84%	2505%	686%	-85%	2448%	1113%	-91%	1007%	1042%	-78%	143%	2%
15N	-53%	356%	69%	-55%	296%	185%	-74%	-33%	-3%	-35%	-67%	-68%
25N	-22%	103%	1%	-26%	47%	25%	-57%	-70%	-53%	8%	-81%	-75%
50N	55%	-31%	-61%	48%	-51%	-23%	-13%	-77%	-80%	115%	-89%	-70%

### 5.3.2.2 Random vs. high error

While the average error of the FUNNEL and NGTL ANN models is below the acceptable error, the models still have the occasional high error (max absolute residual). Preliminary investigations into ANN configurations determined that adding more nodes continued to reduce the MSE but failed to reduce the maximum error. Figure 5-8 was generated using the NGTL model with 26 inputs and 50 k random Monte Carlo samples. Similar results were observed by Li and Marfatia.<sup>194</sup>

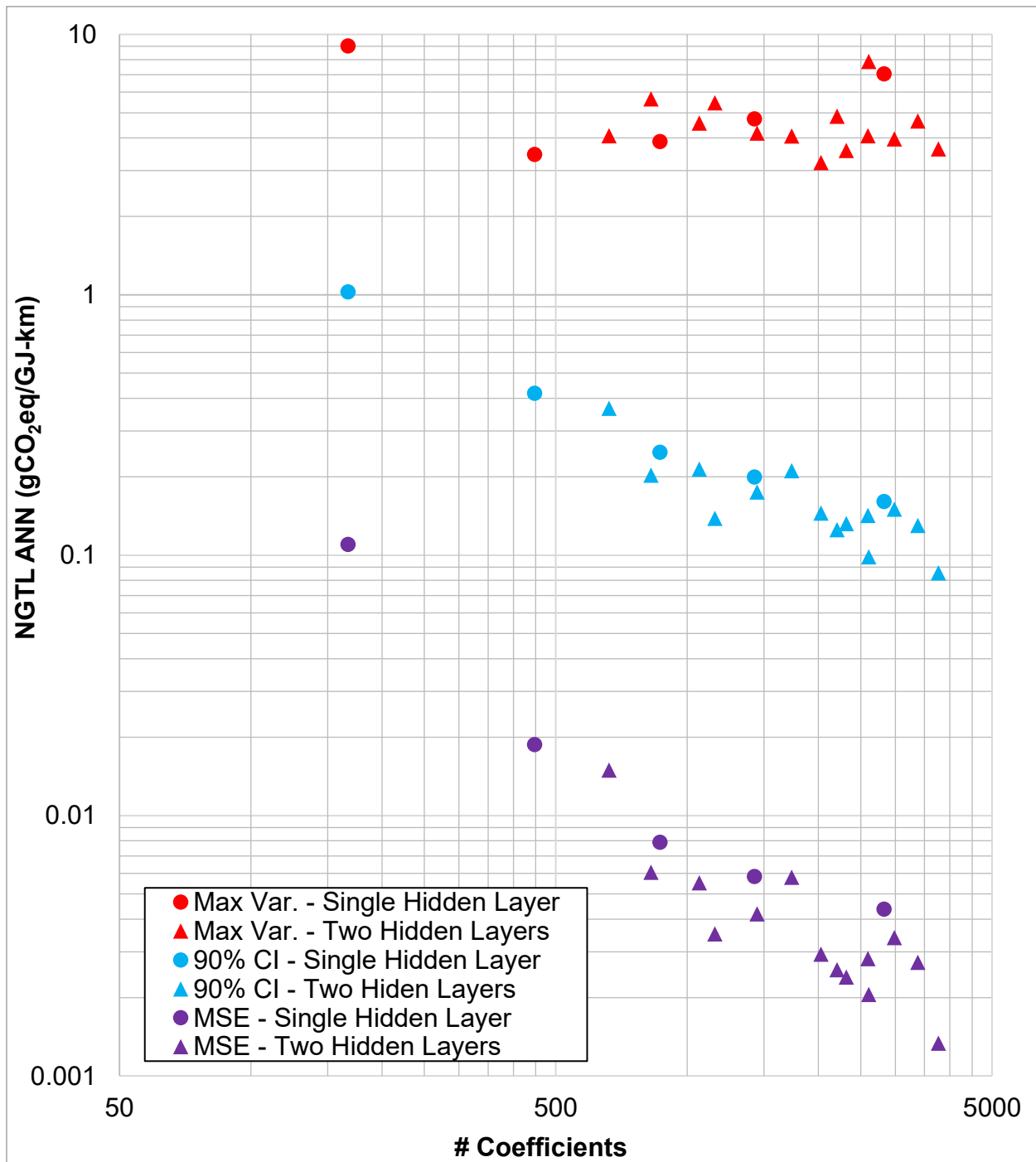


Figure 5-8: NGTL accuracy vs. # of coefficients (50,000 random samples, 26 inputs)

The random error ANN method results show that adding additional samples will continue to reduce both the MSE and maximum error; however, the rate of reduction in the maximum error will slow significantly after a certain point (see Figure D7 in the Appendix). Overall, simply

adding more data points or increasing the number of nodes in the ANN model will not significantly reduce maximum error; therefore, to reduce the maximum error, we used the high error adaptive sampling method.

The results for the NGTL ANN proxy model with 50 nodes are shown below (Figure 5-9:). The MSE is larger for the high error method for most sample sizes; however, the maximum error was reduced by between 33% and 66%. The reduction in the max error is statistically significant for the larger sample sizes. The variability in the max error is also smaller using the high error method than with the random approach, even though both methods use a similar number of epochs during training; if one method were causing the solver to terminate early, it would reduce the number of epochs.

Outliers appear in the max absolute residuals using the random method and a sample size of 8,000. Using internal data, these model runs appear acceptable, as the large error only occurs in the external data set. Since a typical practitioner who does not have the large external validation set used in this work would be unaware of the potential for large errors, these outliers are left in the data, rather than being removed.

Compared to the random sampling method, the high error method increases the mean absolute residual error (Figure 6, above). For the NGTL scenario, the increase in the mean absolute residual (overall accuracy) needs to be balanced against the reduction in maximum error (overall stability). In this case, the mean, P75, P95, and P99 absolute errors are still below the acceptable error limit (orange bar), so the slight increase compared to the random method is acceptable. Both the random and high error ANN methods outperform the quadratic model for a given sample size for the NGTL scenario.

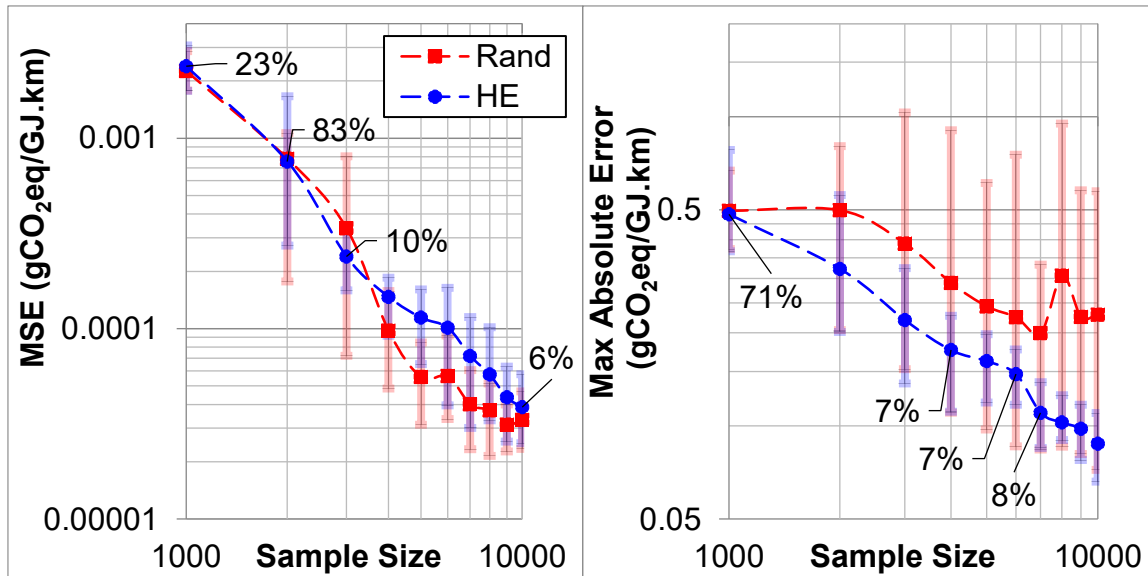


Figure 5-9: NGTL 50N ANN MSE and max absolute error using external validation set ( $p$ -value  $>5\%$  implies the difference in means is not statistically significant;  $p$  values  $<5\%$  are not shown); error bars represent 90%CI (Rand: random sample, HE: high error sample)

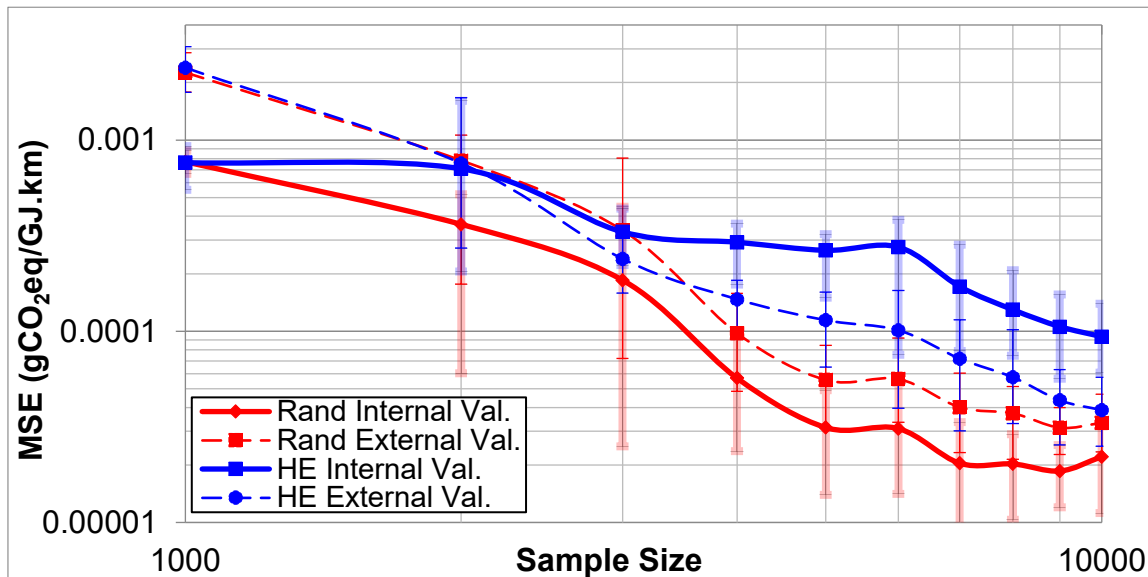


Figure 5-10: NGTL 50N ANN MSE using internal and external validation samples (Rand: random sample, HE: high error sample)

Figure 5-10: shows the MSEs for the internal and external data sets. The internal set includes all the samples used in MATLAB to train the ANN (train, test, and validation samples). The external set is the standardized validation set containing 500,000 samples. Normally, a modeler

would not have a large external validation set available and would have to rely on the internal set only.

The high error method has a negative effect on the MSE when the internal data set is used, especially during the first iteration, increasing the sample size from 1,000 to 2,000 samples. This is likely due to the addition of samples in areas of complex model behavior. The ANN struggles with these areas, increasing the MSE. However, when we used the larger external set, the overall MSE decreases. To confidently use the high error method, an initial randomly generated validation set should be created and set aside to ensure the high error sampling method does not affect it. The creation of an external validation set may require generating more samples, offsetting some of the high error methods benefits. Future work would need to examine how large the external set needs to be. The external validation set may need to be iteratively increased along with the training set.

#### *5.3.2.2.1 Impact of the number of ANN nodes and sample size on HE benefit over Rand*

For the NGTL scenario, the improvement from using the high error method increases with sample size and number of nodes in the ANN (Figure D9 in the Appendix). The high error method reduces the absolute maximum error on average when 15 or more nodes are used in the hidden layer (Figure D10, Appendix). The MB and NGTL scenarios are the only ones to see an increase in the absolute maximum error for the smallest 5-node network. The MB scenario results are unique, as this is the simplest model and already has errors below the ideal criteria when random sampling is used (Figure 5-7:). Therefore, the benefit of using the high error method is reduced for the MB scenarios (Figure D10). For the NGTL scenario, using the high error sampling method with a small 5-node network will increase the maximum error by up to 20% (Figure D10).

### 5.3.2.3 Combo sampling method

160 scenarios were run: ten sample sizes from 1,000 to 10,000, 4 network configurations (5, 15, 25, 50 nodes), and 4 models (Maya, Bow, MB, NGTL). In 83% of the scenarios, the difference between the high error and the combo sampling method average absolute maximum error is not statistically significant. Overall, the combo results were similar to the high error results and had less variability between runs than the random method. Therefore, only a portion of the new generated samples needs to use the high error method to improve results. In this work, combo assumes 50% of the samples are generated randomly and 50% using the high error method. Future work should investigate how to identify the optimal ratio that will reduce extreme errors while maintaining or reducing the MSE.

### 5.3.3 Time required

The iterative method has three time-consuming steps: sample generation, target value generation, and proxy model training. The target generation time is not significantly affected by the sampling strategy used or the final sample size (Appendix D.4). Small deviations between target generation times may occur if the underlying model relies on an iterative solver; high error points may be in regions where the true model has difficulty converging.

The random method sample generation time is less than 0.001s/1,000 samples for all scenarios. Using the spread method increases sampling time to between 4 and 5s/1,000 samples. For the high error and combo methods, sampling time takes up to 6,000s/1,000 samples for MB and 800s/1,000 samples for NGTL (Figure D12). Since the HE/combo sampling methods involve training 5 ANNs on the existing sample to identify new points, it is a time-consuming process. The more hidden nodes there are in the ANN, the longer sampling takes. Depending on the model, training time may not change based on the sampling strategy (see Figures D11 & D12). Figure 5-11: shows the cumulative time to generate samples, generate target values, and train the ANN using a step size of 1,000 samples. In this scenario, generating target values from the true model is the longest step for smaller sample sizes. However, as the sample size increases, the sample generation and ANN training take more time (Figure 5-11: & D11-13).

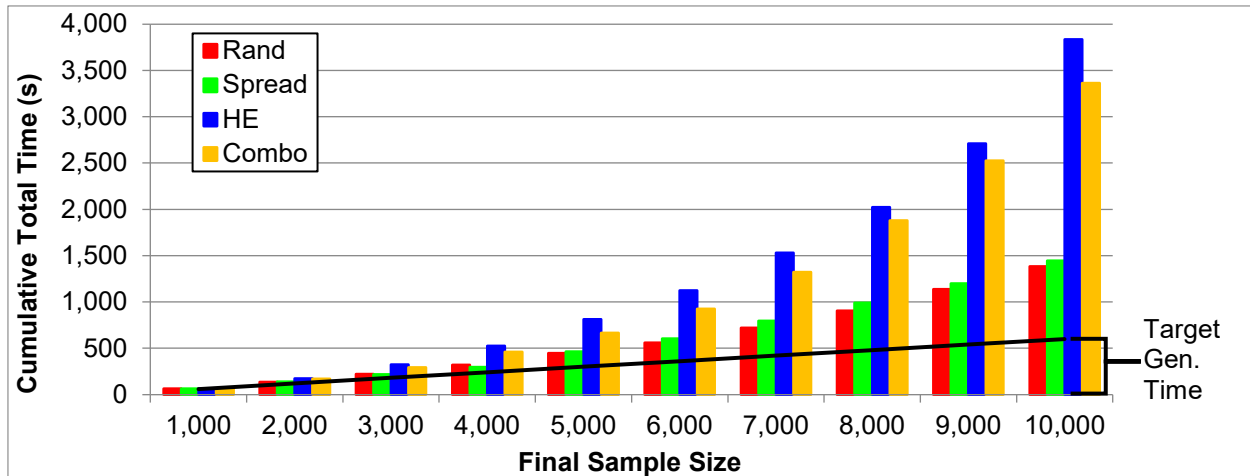


**Figure 5-11: Cumulative time to produce proxy models for NGTL 50-node ANN (Rand: random sample, HE: high error sample)**

Ideally, the HE method’s longer sampling and training time will be offset by requiring fewer samples. For the NGTL scenario, Figure 5-12: shows the residual distributions for the one-shot random method with 10,000 samples compared to the cumulative HE method with multiple sample sizes.

While the average MSE is always lowest for the random method, the HE max error is lower than the random methods when more than 3,000 samples are used (Figure 5-12:). Therefore, we could generate fewer target values and get an acceptable model using the HE method. The times shown in Figure 5-12: assume that the random method generates 10,000 samples in a single cycle and is not iterative. The HE method starts with 1,000 samples and iteratively adds 1,000 samples at a time. Figure 5-12: shows the cumulative time required to reach each sample size. In the NGTL scenario, the time required to train a 5,000-sample model using the cumulative HE method is comparable to training a one-shot 10,000 sample model using the random approach.

When more computationally intensive models are used in the future, the benefit of the HE method will be further improved. The NGTL model currently takes  $\sim 0.06s/\text{target value}$ ; if the target value generation took  $\sim 120s/\text{target value}$  then the HE method using 9,000 or fewer samples would take less time than the one-shot random method using 10,000 samples.

The combo method achieves similar reductions in the maximum error as the high error method but takes between 2% and 18% less time and also reduces the average absolute error (Tables D2-4 in the Appendix). Similar to the random method, the combo method is less stable than the high error method (Figure 5-9:). Using the high error or combo method can decrease maximum error and reduce time required, but it will increase the average absolute error. The practitioner would need to decide if the trade-off is justified.

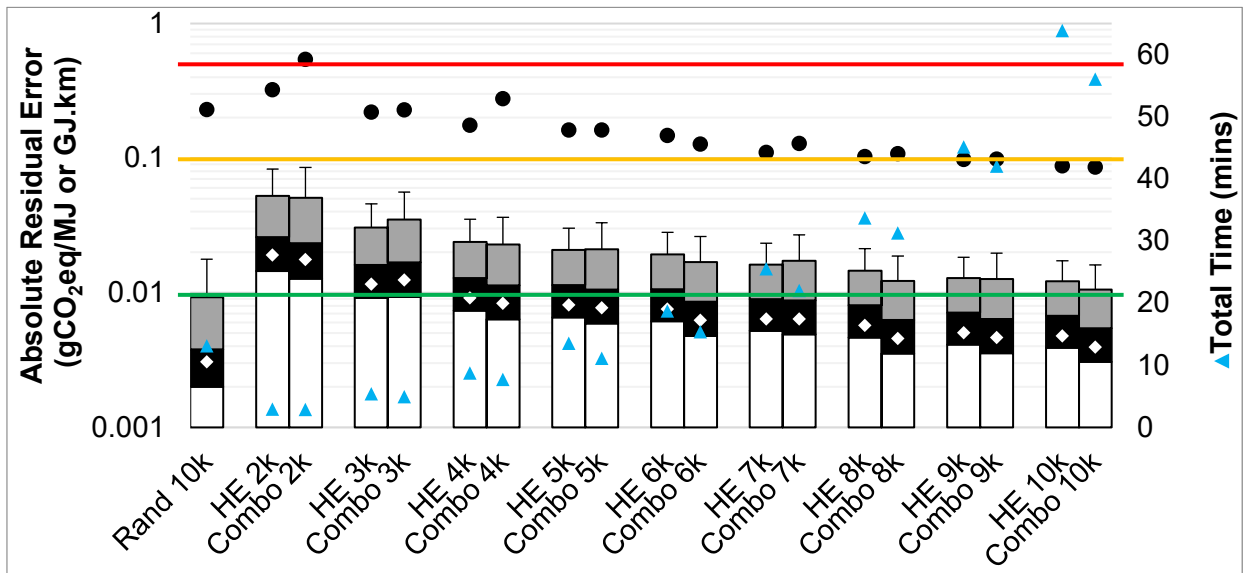


**Figure 5-12: One-shot random sampling vs. cumulative high error (HE) and combo sampling (k: thousand samples)**

### 5.3.4 Future improvements

The high error method uses dCut to limit how close the new samples are to existing samples when searching for areas of disagreement. This work assumed dCut would be equal to the 50<sup>th</sup> percentile distance between existing samples. Future work should investigate adjusting the value of dCut to further improve performance.

The combo method assumes a 50/50 split between random and high error samples. Reducing the number of high error samples selected would decrease sample generation time but may reduce the reduction in the maximum error. It may be possible to adjust the sampling ratio based on the ratio of the maximum and mode absolute error.

In this research, an external data set with 500,000 samples was used to compare the high error and random sampling results, which is not practical. Further investigation into an appropriate external sample size is needed. The external data set may need to be supplemented along with the training data.

The adaptive method used here added 1,000 samples for each iteration. Using fewer samples per iteration could improve accuracy while reducing the number of samples needed to obtain an acceptable accuracy. However, it would increase sample generation and training time, as these would occur more frequently.

Currently, the number of nodes in the ANN hidden layer is held constant as more samples are added. Future research should examine how adding additional nodes as the sample size increases impacts the sampling strategies.

## **5.4 Conclusion**

This work found that easy-to-use proxy models could be created for various LCA models. While quadratic regression can work for simpler models, ANN performed better for the complex iterative NGTL model.

At a certain point, adding additional samples no longer improves the accuracy of a quadratic model, as the proxy model structure limits it. Adding additional interaction coefficients or non-linear terms will also fail to improve accuracy if the models do not follow a polynomial response. For the FUNNEL models, adding non-linear terms improved performance more than it increased the level of interaction; however, this is model-specific.

For ANN models, if there was overfitting, increasing the number of nodes increased accuracy compared to adding more samples. Overfitting is significantly reduced if at least 10 samples are used per coefficient. For the complex NGTL model, the ANN proxy model outperformed the quadratic regression model using fewer coefficients when the sample sizes were equal; for the simpler models, ANN would outperform quadratic when it used more coefficients since it does not stall like quadratic models do.

While multiple spread sample approaches were examined in this work, none showed a statistically significant improvement on par with random sampling. The high error method reduced the maximum error and the variation in the maximum error across multiple samples and training sessions. However, the high error method increased the average and mode absolute error. While the random sampling method overestimated accuracy using the testing and validation sampling, the high error method underestimated accuracy when compared to the external data set. Therefore, the high error method is less likely to give a false sense of accuracy. Using the high error method, it is possible to reduce the maximum error while using fewer samples than the random method, which reduces overall computing time compared to the random method when the complex engineering model target value generation times are long. While the high error method can decrease the maximum error by up to 80%, it will increase the MSE and average absolute error. The high error method is therefore beneficial when the practitioner is willing to accept an increase in average error for a decrease in the maximum error, providing the end user with a more stable proxy model. The combo method found that only 50% of the samples need to be determined using the high error method to obtain similar results, which will decrease overall computing time.

Future work will apply methods developed here to rigorous Aspen models of upgraders and refineries. This work found that proxy models can be used to accurately replicate complex engineering models while also providing an easy-to-use interface that conceals confidential data.

## **6 Conclusions and Recommendations for Future Work**

Overall, this research aimed at further improving the quality of LCA results so they can be used as reliable information to support decision-making in environmental protection and GHG emission reductions strategies in the energy sector. This was done by developing RUST and the corresponding framework. The work on proxy models will make LCA more flexible and allow practitioners to share models without having to worry about confidential data.

The survey of how existing LCA practitioners implement sensitivity and uncertainty (Chapter 2) found that current methods are inconsistent and of low quality. It is recommended that sensitivity and uncertainty analysis should not be viewed as something that needs to be added on at the end of the project to produce error bars but as a critical part of the analysis included throughout the process. Key recommendations are: using global instead of local sensitivity, ensuring all inputs/assumptions are included in the screening analysis, avoiding the use of EcoInvent defaults without understanding their limitations, requiring acceptable levels of detail from journals, integrating screening software into existing LCA software, avoiding the use of generic uncertainty ranges, including appropriate justification for methods used/inputs included, considering the impact of goal and scope on sensitivity and uncertainty analysis, and using differential analysis for comparative LCA. Figure 6-1 provides an overview of what separates a simple and detailed sensitivity and uncertainty analysis based on findings from the literature survey.

<b>Basic Analysis</b>	<b>Detailed Analysis</b>
Local sensitivity	Global sensitivity
Only small # of inputs examined, limited discussion of filtering criteria	Screening method used / justification provided to identify key inputs
Includes either sensitivity or uncertainty analysis	Includes both a sensitivity and uncertainty analysis
Includes parameter uncertainty only	Includes parameter, normative, and model uncertainty
Basic description of method used, and inputs included	Detailed documentation of method used with critical parameters (ex. # of samples used in MC), documentation of input ranges used with references and justification of ranges / distributions used
Minimal interpretation of results; ex. Only error bars presented	Discussion on limitations, potential affect of correlation, dependency and statistical significance
Software defaults used as is, with no additional discussion	Potential limitations/gaps of using defaults is discussed and/or addressed
SUA added on at end to produce error bars	SUA incorporated in all stages from goal and scope development to final interpretation

**Figure 6-1: Summary characteristics of a basic vs. detailed analysis**

Based on the survey findings, the Regression, Uncertainty, and Sensitivity Tool (RUST) was developed and validated in Chapter 3. This work showed how the Morris and Sobol methods can be used to identify key model parameters by accounting for interaction and non-linear effects, unlike the one-at-a-time method. The Morris method was found to require fewer than 1/100<sup>th</sup> as many model evaluations as the Sobol method, making it an effective screening method. Using Morris screening, we reduced the number of inputs needed for the Monte Carlo simulation from between 60 and 75 to 14 for Maya, Bow, and NGTL, and 16 for Athabasca. Figure 6-2 provides a overview of the RUST methodology.

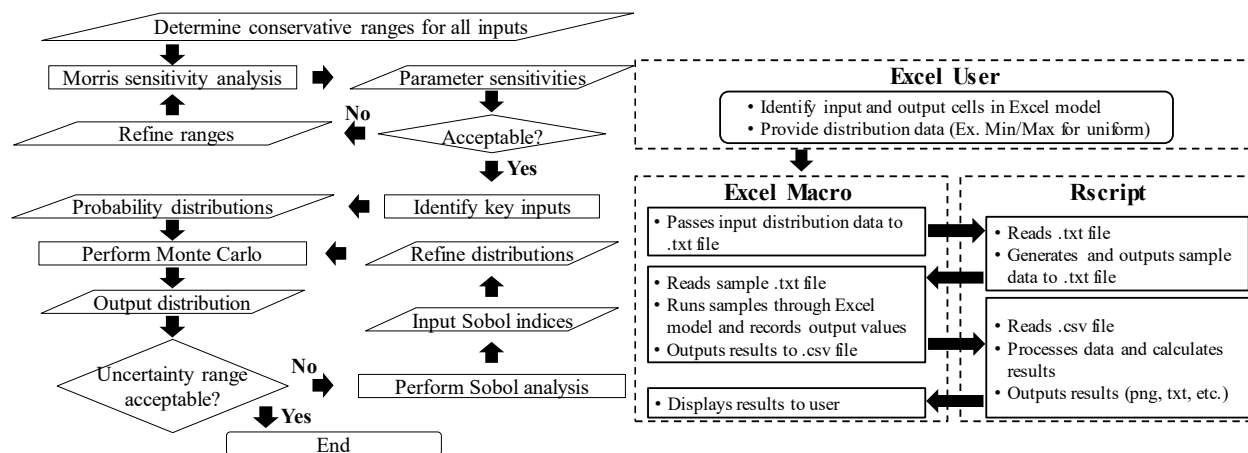


**Figure 6-2: Overview of RUST framework and process flow diagram**

While publishing the full LCA model is often preferable, it is not always possible because of difficulties making the model user friendly as well as non-disclosure agreements or other confidentiality concerns. In Chapter 4, it was showed that quadratic linear proxy models could be used to represent some LCA models, Figure 6-3 provides an overview of the methodology used. A stepwise approach was used to identify the optimal proxy model configuration. The process starts by including every term and iteratively eliminating the terms with the highest  $p$  values. Multicollinearity between terms leads to significant instability in the  $p$  values, or a term that appears to be insignificant may become significant once others are removed; hence, an iterative approach is used to avoid prematurely removing important inputs. The levels of interaction and number of terms were be varied until a model with the desired accuracy was obtained. The FUNNEL-GHG-CCO/OS regression models were found to have accuracies of  $\text{Maya}_{-1.2}^{+2.7}$ ,  $\text{Bow}_{-1.2}^{+2.5}$ , and  $\text{Athabasca}_{-0.2}^{+0.3} \text{gCO}_2\text{eq/MJ}$ . By adding non-linear terms, the accuracies were improved to  $\text{Maya}_{-0.6}^{+0.4}$ , and  $\text{Bow}_{-0.4}^{+0.6}$ . For the FUNNEL-GHG-NGTL model, the accuracies were  $\text{NGTL}_{-0.38}^{+0.27}$ ,  $\text{NGTL}_{-0.26}^{+0.27}$ ,  $\text{NGTL}_{-0.25}^{+0.27}$  for the linear, squared, and cubed regression models, respectively. Running uncertainty on the regression model introduces additional model uncertainty based on the accuracy of the regression model. In the case of the Maya, Bow, and Athabasca crude pathways evaluated in this work, the parameter uncertainty will be an order of magnitude larger than the regression model uncertainty, which would make the modeling error negligible. The NGTL model should not be used for a sensitivity analysis because of the low regression accuracy; a more accurate model is needed.

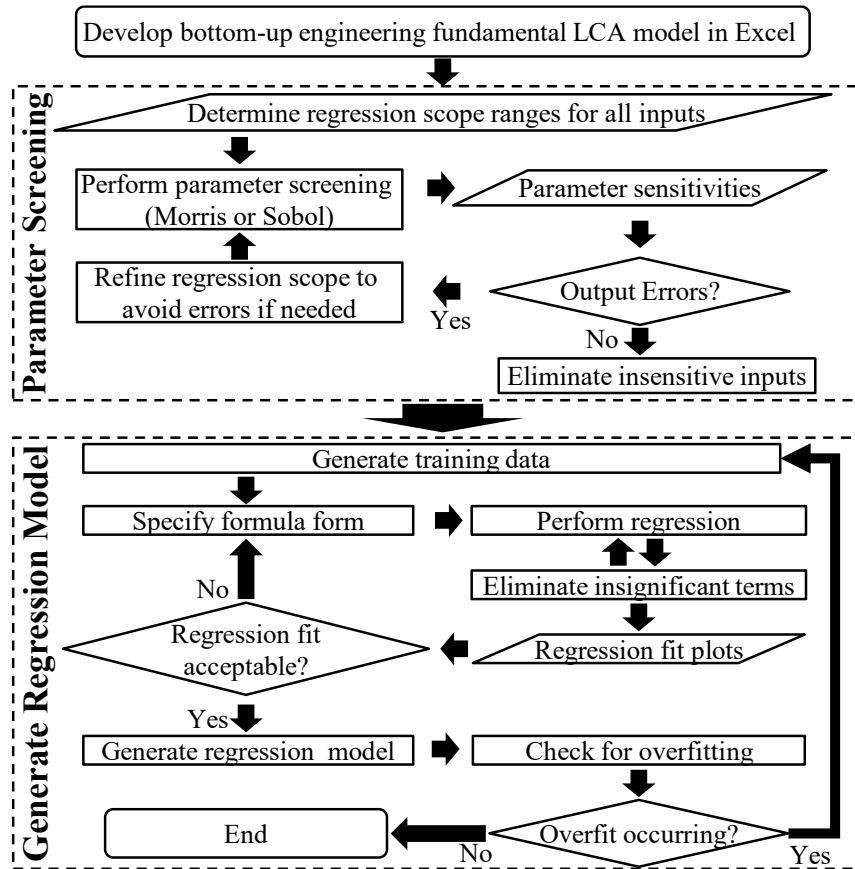


**Figure 6-3: Quadratic Regression framework**

At a certain point, adding additional samples no longer improves the accuracy of a quadratic model, as the proxy model structure limits it. In Chapter 5, ANN proxy models are discussed as a means of improving the accuracy of the NGTL proxy model. An iterative approach was used as shown in Figure 6-4. Unlike quadratic regression, ANN models do not experience a stalling effect as the sample size increases. For ANN models, if overfitting does not occur, increasing the number of nodes increases the accuracy more readily than adding more samples. Overfitting is significantly reduced if at least 10 samples are used per coefficient. For the complex NGTL model, the ANN proxy model outperforms the quadratic regression model using fewer coefficients when the sample sizes are equal; for the simpler models, ANN outperforms quadratic when it uses more coefficients since it does not stall like quadratic models.

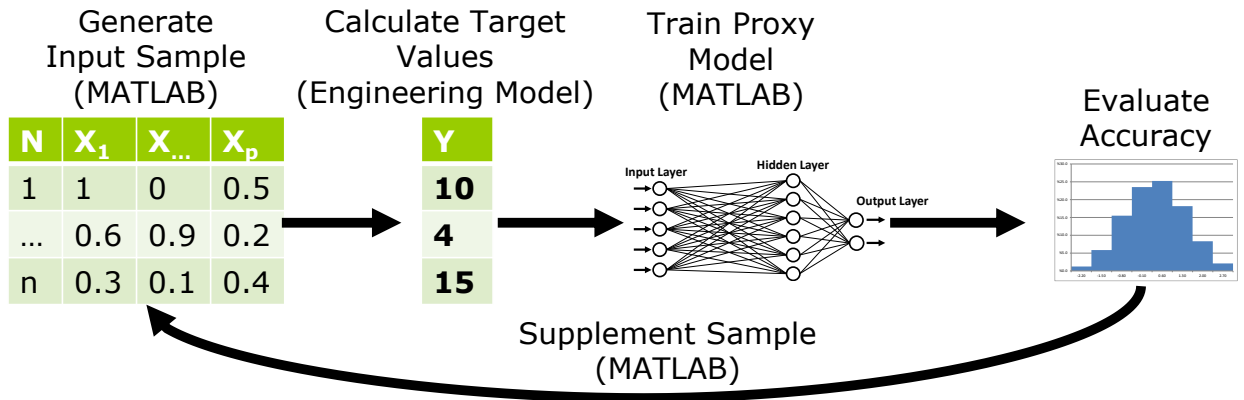


**Figure 6-4: High level ANN proxy modeling method**

Multiple spread sample approaches were examined in this work, and none showed a statistically significant improvement over random sampling. Using the high error method, it is possible to reduce the maximum error while using fewer samples than the random method, which reduces overall computing time compared to the random method when the complex engineering model target value generation times are long (see Figure 6-5). While the high error method can decrease the maximum error by up to 80%, it will increase the MSE and average absolute error (see Figure 6-6). The high error method is therefore beneficial when the practitioner is willing to accept an increase in average error for a decrease in the maximum error, providing the end user with a more stable proxy model. The combo method found that only 50% of the samples need to be determined using the high error method to obtain similar results, which will decrease overall computing time.

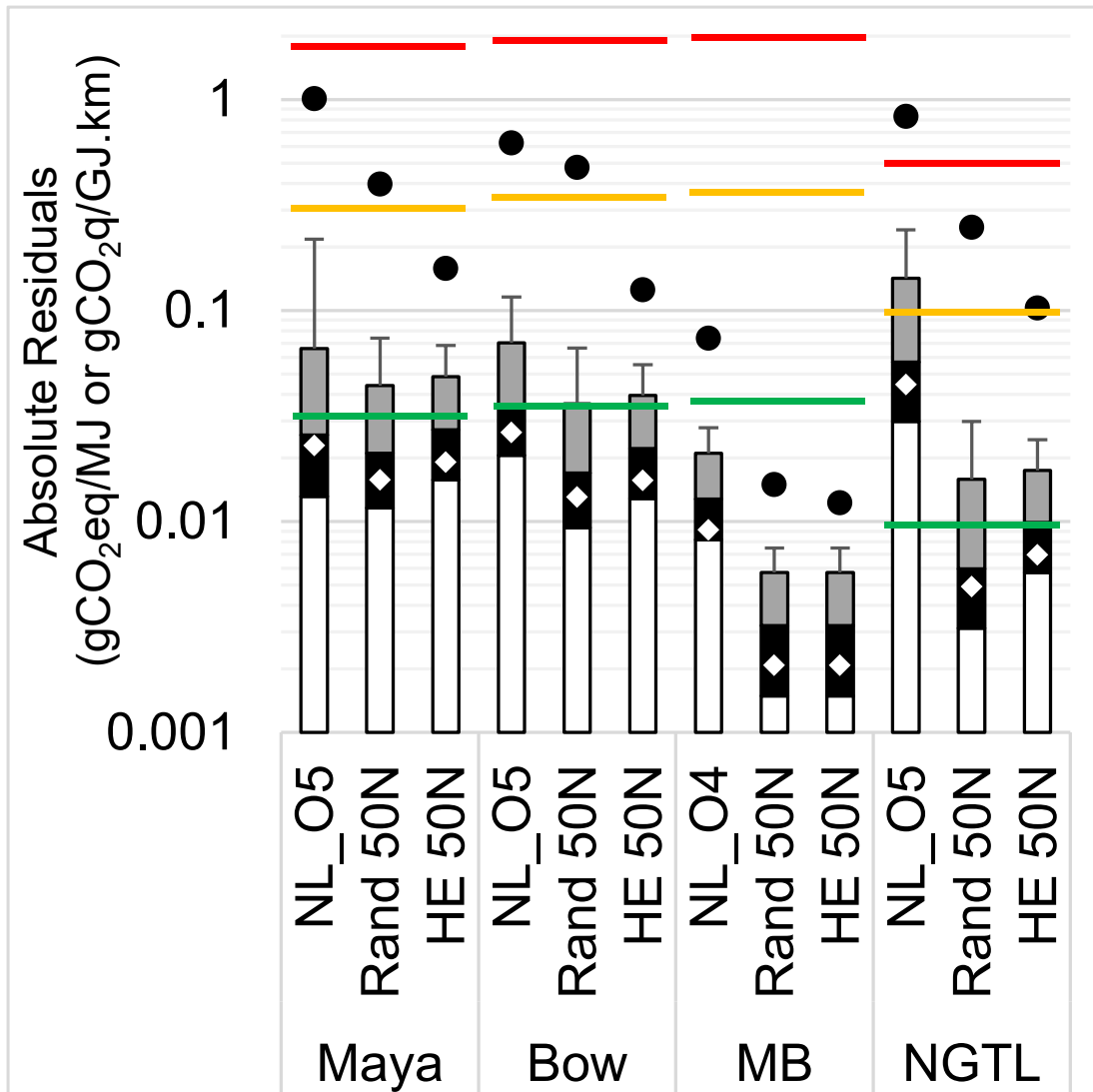


**Figure 6-5: Absolute residual results: Maya, Bow, NGTL use 10,000 samples; MB uses 7,000 samples (NL\_O5 =nonlinear quadratic with 5<sup>th</sup> order interactions, Rand 50N= 50 node ANN with random sampling, HE 50N = 50 node ANN with high error sampling)**

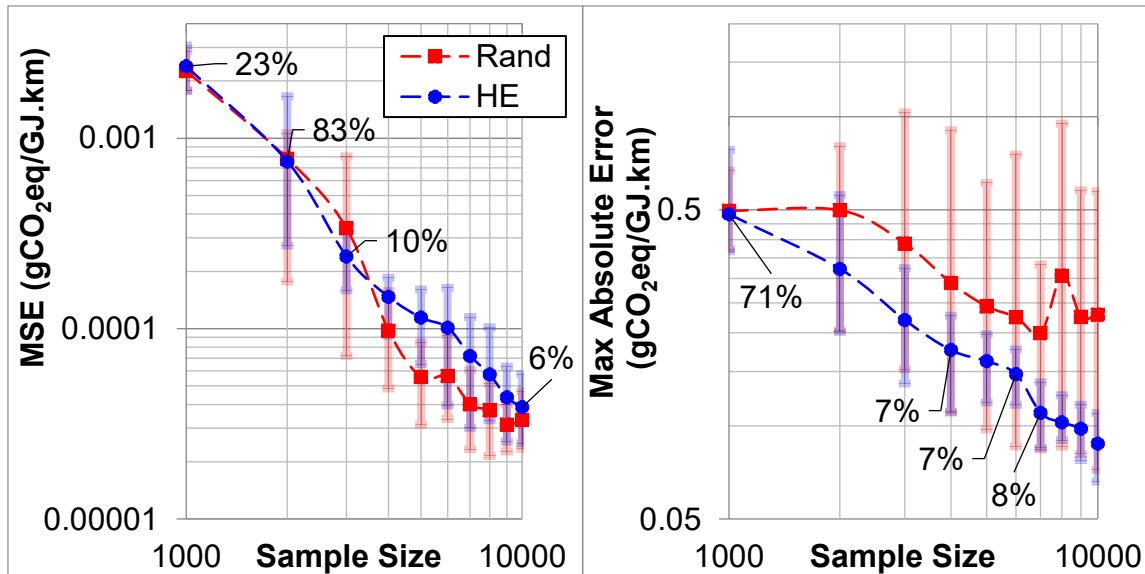


**Figure 6-6: NGTL 50N ANN MSE and max absolute error using external validation set (p-value >5% implies the difference in means is not statistically significant; p values <5% are not shown); error bars represent 90%CI**

## 6.1 Novelty

This work produced a standardized approach to performing sensitivity and uncertainty analysis in LCA which was currently missing. The sensitivity and uncertainty framework lead to the development of the Regression, Uncertainty, and Sensitivity Tool (RUST).

While the use of ANN for proxy modeling is not new, this work investigated new sampling strategies. The spread and high error sampling methods were developed for this work to reduce the number of samples needed for training a proxy model.

The natural gas transmission (NGTL) model is the first LCA to examine gas pipeline emission intensities using a bottom-up approach. Our work on hythane pipelines is also new and was used to examine both the engineering and environmental performance of natural gas-hydrogen pipelines in Canada.

## 6.2 Recommendations for Future Work

The surveyed papers only included parameter and scenario uncertainty, not model uncertainty. Structural error can be significant, because of the severe lack of data available to LCA

practitioners, it is often not possible to validate models and quantify model uncertainty. While methods for validating models exist, the field requires further research.

Current sensitivity and uncertainty analysis articles use a basic approach and often provide insufficient information for the reader to verify the methodology used. A guide of key requirements for sensitivity and uncertainty analysis in LCA should be developed and distributed to journal editors and reviewers.

While the high error adaptive sampling method was shown to reduce the maximum absolute error in ANN proxy models the algorithm can be improved. This work showed that the high error and combo method produced similar results; further investigation should look into determining what share of new data points should use the high error method versus the random method to both minimize error and computing time.

RUST model developed in this research and its corresponding framework are used by in several LCA publications<sup>57-64</sup> and industry/government projects.<sup>3, 163, 169</sup> There is a large number of research studies focused on developing Aspen models of various industrial process. In future, the proxy modeling framework developed here can be applied to these models to create simplified versions that can be integrated into existing LCAs. Work using the Long-range Energy Alternatives Planning (LEAP) software, an integrated resource planning model, can also use the framework to integrate accurate submodels into their Canada-wide analysis to further improve accuracy. LEAP models depend on interactions between energy systems; proxy models can help accurately model such interactions.

## Bibliography

1. Di Lullo, G.; Gemechu, E.; Oni, A. O.; Kumar, A., Investigation and discussion of how practitioners currently implement sensitivity and uncertainty analysis in estimation of GHG in life cycle assessments of energy systems and improvements needed. *Submitted to Int. J. Life Cycle Assess. Oct 25, 2021.*
2. Di Lullo, G.; Gemechu, E.; Oni, A. O.; Kumar, A., Extending sensitivity analysis using regression to effectively disseminate life cycle assessment results. *Int. J. Life Cycle Assess.* **2020**, *25*, 222-239. DOI: 10.1007/s11367-019-01674-y
3. Oni, A. O.; Anaya, K.; Giwa, T.; Di Lullo, G.; Kumar, A., Comparative assessment of blue hydrogen from steam methane reforming, autothermal reforming, and natural gas decomposition technologies for natural gas-producing regions. *Energy Conversion and Management* **2022**, *254*, 115245. DOI: <https://doi.org/10.1016/j.enconman.2022.115245>
4. Di Lullo, G.; Oni, A. O.; Gemechu, E.; Kumar, A., Developing a greenhouse gas life cycle assessment framework for natural gas transmission pipelines. *J. Nat. Gas Sci. Eng.* **2020**, *75*, 103136. DOI: 10.1016/j.jngse.2019.103136
5. Di Lullo, G.; Oni, A. O.; Kumar, A., Blending blue hydrogen with natural gas for direct consumption: Examining the effect of hydrogen concentration on transportation and well-to-combustion greenhouse gas emissions. *Int. J. Hydrogen Energy* **2021**, *46*, (36), 19202-19216. DOI: 10.1016/j.ijhydene.2021.03.062
6. McManus, M. C.; Taylor, C. M., The changing nature of life cycle assessment. *Biomass Bioenergy* **2015**, *82*, 13-26. DOI: 10.1016/j.biombioe.2015.04.024
7. Environment and Climate Change Canada. *Clean fuel standard: Proposed regulatory approach*; Ottawa, 2019.
8. California Air and Resources Board. *Unofficial electronic version of the low carbon fuel standard regulation*; 2019.
9. Bowyer, C.; Skinner, I.; Malins, C.; Nanni, S.; Baldock, D. *Low carbon transport fuel policy for Europe post 2020*; Transport and Environment: 2015.
10. ICF International. *Independent assessment of the European commission's fuel quality directive's "conventional" default value*; Natural Resources Canada: Ottawa, 2013.
11. Michalski, W. *Critiques of Life Cycle Assessment*; Worcester Polytechnic Institute: Worcester Polytechnic Institute, Apr. 5, 2015, 2015.
12. Keesom, W.; Unnasch, S.; Moretta, J. *Life Cycle Assessment Comparison of North American and Imported Crudes prepared for Alberta Energy Research Institute*; AERI 1747; Jacobs Consultancy: Chicago, IL, 2009.

13. Rosenfeld, J.; Pont, J.; Law, K.; Hirshfeld, D.; Kolb, J. *Comparison of North American and Imported Crude Oil Lifecycle GHG Emissions - Final Report Prepared for Alberta Energy Research Institute*; TIAX Case No. D5595; TIAX LLC: Cupertino, CA, 2009.
14. Gordon, D.; Brandt, A.; Bergerson, J.; Jonathan, K. *Know Your Oil: Creating a Global oil-climate index*; Carnegie Endowment for International Peace: Washington, 2015.
15. Zampori, L.; Saouter, E.; Schau, E.; Cristobal, J.; Castellani, V.; Sala, S. *Guide for interpreting life cycle assessment result*; Joint Research Centre Technical Reports: 2016.
16. International Organization for Standardization (ISO). ISO 14040:2006: Environmental management - Life cycle assessment - Principles and framework. 2006.
17. International Organization for Standardization (ISO), ISO 14044:2006: Environmental management - Life cycle assessment - Requirements and guidelines. 2006.
18. Igos, E.; Benetto, E.; Meyer, R.; Baustert, P.; Othoniel, B., How to treat uncertainties in life cycle assessment studies? *Int. J. Life Cycle Assess.* **2018**. DOI: 10.1007/s11367-018-1477-1
19. Heijungs, R.; Huijbregts, M. A. J. In *A review of approaches to treat uncertainty in LCA*, Presented at Proceedings of the biennial meeting of iEMSs, Complexity and integrated resources management, 2004.
20. Lloyd, S. M.; Ries, R., Characterizing, propagating, and analyzing uncertainty in life-cycle assessment: A survey of quantitative approaches. *J. Ind. Ecol.* **2007**, *11*, (1), 161-179. DOI: 10.1162/jiec.2007.1136
21. Uusitalo, L.; Lehikoinen, A.; Helle, I.; Myrberg, K., An overview of methods to evaluate uncertainty of deterministic models in decision support. *Environ. Modell. Software* **2015**, *63*, 24-31. DOI: 10.1016/j.envsoft.2014.09.017
22. Refsgaard, J. C.; van der Sluijs, J. P.; Højberg, A. L.; Vanrolleghem, P. A., Uncertainty in the environmental modelling process – A framework and guidance. *Environ. Modell. Software* **2007**, *22*, (11), 1543-1556. DOI: 10.1016/j.envsoft.2007.02.004
23. Ross, S.; Evans, D.; Webber, M., How LCA studies deal with uncertainty. *Int. J. Life Cycle Assess.* **2002**, *7*, (1), 47. DOI: 10.1007/bf02978909
24. Tu, Q.; Eckelman, M.; Zimmerman, J., Meta-analysis and harmonization of life cycle assessment studies for algae biofuels. *Environ. Sci. Technol.* **2017**, *51*, (17), 9419-9432. DOI: 10.1021/acs.est.7b01049
25. Byrne, D. M.; Lohman, H. A. C.; Cook, S. M.; Peters, G. M.; Guest, J. S., Life cycle assessment (LCA) of urban water infrastructure: emerging approaches to balance objectives and inform comprehensive decision-making. *Environ. Sci. Water Res. Technol.* **2017**, *3*, (6), 1002-1014. DOI: 10.1039/C7EW00175D

26. Ferretti, F.; Saltelli, A.; Tarantola, S., Trends in sensitivity analysis practice in the last decade. *Sci. Total Environ.* **2016**, *568*, 666-670. DOI: 10.1016/j.scitotenv.2016.02.133
27. Budzinski, M. The differentiation between variability uncertainty and knowledge uncertainty in life cycle assessment: A product carbon footprint of bath powder "Blue Grape". Diploma thesis, Technical University Dresden, Dresden, 2012.
28. Wang, G. G.; Shan, S., Review of metamodeling techniques in support of engineering design optimization. *J. Mech. Des.* **2006**, *129*, (4), 370-380. DOI: 10.1115/1.2429697
29. Taheri-Rad, A.; Khojastehpour, M.; Rohani, A.; Khoramdel, S.; Nikkhah, A., Energy flow modeling and predicting the yield of Iranian paddy cultivars using artificial neural networks. *Energy* **2017**, *135*, 405-412. DOI: 10.1016/j.energy.2017.06.089
30. Nabavi-Pelesaraei, A.; Rafiee, S.; Mohtasebi, S. S.; Hosseinzadeh-Bandbafha, H.; Chau, K.-w., Integration of artificial intelligence methods and life cycle assessment to predict energy output and environmental impacts of paddy production. *Sci. Total Environ.* **2018**, *631-632*, 1279-1294. DOI: 10.1016/j.scitotenv.2018.03.088
31. Safa, M.; Samarasinghe, S., Determination and modelling of energy consumption in wheat production using neural networks: "A case study in Canterbury province, New Zealand". *Energy* **2011**, *36*, (8), 5140-5147. DOI: 10.1016/j.energy.2011.06.016
32. Chen, P.; Jing, Q., A comparison of two adaptive multivariate analysis methods (PLSR and ANN) for winter wheat yield forecasting using Landsat-8 OLI images. *Adv. Space Res.* **2017**, *59*, (4), 987-995. DOI: 10.1016/j.asr.2016.11.029
33. Kaab, A.; Sharifi, M.; Mobli, H.; Nabavi-Pelesaraei, A.; Chau, K.-w., Combined life cycle assessment and artificial intelligence for prediction of output energy and environmental impacts of sugarcane production. *Sci. Total Environ.* **2019**, *664*, 1005-1019. DOI: 10.1016/j.scitotenv.2019.02.004
34. Kalogirou, S. A.; Bojic, M., Artificial neural networks for the prediction of the energy consumption of a passive solar building. *Energy* **2000**, *25*, (5), 479-491. DOI: 10.1016/S0360-5442(99)00086-9
35. Sharif, S. A.; Hammad, A., Developing surrogate ANN for selecting near-optimal building energy renovation methods considering energy consumption, LCC and LCA. *J. Build. Eng.* **2019**, *25*, 100790. DOI: 10.1016/j.jobbe.2019.100790
36. Duprez, S.; Fouquet, M.; Herreros, Q.; Jusselme, T., Improving life cycle-based exploration methods by coupling sensitivity analysis and metamodels. *Sustain. Cities Soc.* **2019**, *44*, 70-84. DOI: 10.1016/j.scs.2018.09.032
37. Sasena, M.; Parkinson, M.; Goovaerts, P.; Papalambros, P.; Reed, M., Adaptive experimental design applied to ergonomics testing procedure. **2002**, (36223), 529-537. DOI: 10.1115/DETC2002/DAC-34091

38. Liu, H. Taylor Kriging Metamodeling For Simulation Interpolation, Sensitivity Analysis And Optimization. Auburn University, Auburn, Alabama, 2009.
39. Vose Software. *ModelRisk*, 2019.
40. Palisade. *@RISK*, 2019.
41. Oracle. *Crystal Ball*, 2019.
42. thinkstep. *GaBi Product Sustainability Software*, 2019.
43. Green Design Institute Economic Input-Output Life Cycle Assessment. <http://www.eiolca.net/Method/LCAApproaches.html> (Aug 7, 2019),
44. Di Lullo, G.; Zhang, H.; Kumar, A., Uncertainty in well-to-tank with combustion greenhouse gas emissions of transportation fuels derived from North American crudes. *Energy* **2017**, *128*, 475-486. DOI: 10.1016/j.energy.2017.04.040
45. Soiket, M. I. H.; Oni, A. O.; Kumar, A., The development of a process simulation model for energy consumption and greenhouse gas emissions of a vapor solvent-based oil sands extraction and recovery process. *Energy* **2019**, *173*, 799-808. DOI: 10.1016/j.energy.2019.02.109
46. Morgan, M. G.; Herion, M., *Uncertainty: A guide to dealing with uncertainty in quantitative risk and policy analysis*. Cambridge University Press: Cambridge, 1990.
47. Williams, E. D.; Weber, C. L.; Hawkins, T. R., Hybrid framework for managing uncertainty in life cycle inventories. *J. Ind. Ecol.* **2009**, *13*, (6), 928-944. DOI: 10.1111/j.1530-9290.2009.00170.x
48. Ascough, J. C.; Maier, H. R.; Ravalico, J. K.; Strudley, M. W., Future research challenges for incorporation of uncertainty in environmental and ecological decision-making. *Ecol. Modell.* **2008**, *219*, (3), 383-399. DOI: 10.1016/j.ecolmodel.2008.07.015
49. Huijbregts, M. A. J.; Norris, G.; Bretz, R.; Citroth, A.; Maurice, B.; von Bahr, B.; Weidema, B.; de Beaufort, A. S. H., Framework for modelling data uncertainty in life cycle inventories. *Int. J. Life Cycle Assess.* **2001**, *6*, (3), 127. DOI: 10.1007/bf02978728
50. Aspen Technology Inc., Aspen HYSYS. 8.4 ed.; 2016.
51. van Zelm, R.; Huijbregts, M. A. J., Quantifying the trade-off between parameter and model structure uncertainty in life cycle impact assessment. *Environ. Sci. Technol.* **2013**, *47*, (16), 9274-9280. DOI: 10.1021/es305107s
52. Mendoza Beltran, A.; Prado, V.; Font Vivanco, D.; Henriksson, P. J. G.; Guinée, J. B.; Heijungs, R., Quantified uncertainties in comparative life cycle assessment: what can be concluded? *Environ. Sci. Technol.* **2018**, *52*, (4), 2152-2161. DOI: 10.1021/acs.est.7b06365

53. ecoinvent. *ecoinvent 3.5 database*, Switzerland, 2019.
54. Environment and Climate Change Canada *Clean Fuel Standard: Proposed Regulatory Approach*; Ottawa, 2019.
55. Argonne National Laboratory Energy Systems Division: Life-Cycle Analysis. <https://www.anl.gov/es/lifecycle-analysis> (Aug. 7, 2019),
56. Agrawal, N.; Ahiduzzaman, M.; Kumar, A., The development of an integrated model for the assessment of water and GHG footprints for the power generation sector. *Appl. Energy* **2018**, *216*, 558-575. DOI: <https://doi.org/10.1016/j.apenergy.2018.02.116>
57. Safaei, M.; Oni, A. O.; Gemechu, E. D.; Kumar, A., Evaluation of energy and GHG emissions' footprints of bitumen extraction using Enhanced Solvent Extraction Incorporating Electromagnetic Heating technology. *Energy* **2019**, *186*, 115854. DOI: 10.1016/j.energy.2019.115854
58. Safaei, M.; Oni, A. O.; Gemechu, E. D.; Kumar, A., Evaluation of energy and greenhouse gas emissions of bitumen-derived transportation fuels from toe-to-heel air injection extraction technology. *Fuel* **2019**, *256*, 115930. DOI: 10.1016/j.fuel.2019.115930
59. A.O. Oni, E. D. G., Y. K. A. Jaimes, I. Toro, Amit Kumar *The life cycle greenhouse gas emissions and energy footprints of Pttep Canada Limited's oil sands extraction pathways*; University of Alberta: PTTEP Canada Limited (PTTEPCA), Nov., 2019.
60. Rahman, M. M.; Gemechu, E.; Oni, A. O.; Kumar, A., The greenhouse gas emissions' footprint and net energy ratio of utility-scale electro-chemical energy storage systems. *Energy Convers. Manage.* **2021**, *244*, 114497. DOI: 10.1016/j.enconman.2021.114497
61. Rahman, M. M.; Gemechu, E.; Oni, A. O.; Kumar, A., The development of a techno-economic model for the assessment of the cost of flywheel energy storage systems for utility-scale stationary applications. *Sustainable Energy Technol. Assess.* **2021**, *47*, 101382. DOI: 10.1016/j.seta.2021.101382
62. Rahman, M. M.; Oni, A. O.; Gemechu, E.; Kumar, A., The development of techno-economic models for the assessment of utility-scale electro-chemical battery storage systems. *Appl. Energy* **2021**, *283*, 116343. DOI: 10.1016/j.apenergy.2020.116343
63. Kukkikatte Ramamurthy Rao, H.; Gemechu, E.; Thakur, U.; Shankar, K.; Kumar, A., Techno-economic assessment of titanium dioxide nanorod-based perovskite solar cells: From lab-scale to large-scale manufacturing. *Appl. Energy* **2021**, *298*, 117251. DOI: 10.1016/j.apenergy.2021.117251
64. Ramamurthy Rao, H. K.; Gemechu, E.; Thakur, U.; Shankar, K.; Kumar, A., Life cycle assessment of high-performance monocrystalline titanium dioxide nanorod-based perovskite solar cells. *Sol. Energy Mater. Sol. Cells* **2021**, *230*, 111288. DOI: 10.1016/j.solmat.2021.111288

65. Loucks, D. P.; Beek, E. v., Chapter 9: Model Sensitivity and Uncertainty Analysis. In *Water Resource Systems Planning and Management: An Introduction to Methods, Models, and Applications*, Springer: 2005.
66. Kleijnen, J. P. C., Sensitivity Analysis Versus Uncertainty Analysis: When to Use What? In *Predictability and Nonlinear Modelling in Natural Sciences and Economics*, Grasman, J.; van Straten, G., Eds. Springer Netherlands: Dordrecht, 1994; pp 322-333.
67. Abdul-Manan, A. F. N., Lifecycle GHG emissions of palm biodiesel: Unintended market effects negate direct benefits of the Malaysian economic transformation plan (ETP). *Energy Policy* **2017**, *104*, 56-65. DOI: 10.1016/j.enpol.2017.01.041
68. Norton, J., An introduction to sensitivity assessment of simulation models. *Environ. Modell. Software* **2015**, *69*, (Supplement C), 166-174. DOI: 10.1016/j.envsoft.2015.03.020
69. Montgomery, D. C., *Design and Analysis of Experiments, 8th Edition*. John Wiley & Sons, Incorporated: 2012.
70. Groen, E. A.; Bokkers, E. A. M.; Heijungs, R.; de Boer, I. J. M., Methods for global sensitivity analysis in life cycle assessment. *Int. J. Life Cycle Assess.* **2017**, *22*, (7), 1125-1137. DOI: 10.1007/s11367-016-1217-3
71. Iooss, B.; Lemaître, P., A review on global sensitivity analysis methods. In *Uncertainty Management in Simulation-Optimization of Complex Systems*, Dellino, G.; Meloni, C., Eds. Springer US: Boston, MA, 2015; Vol. 59, pp 101-122.
72. Ravalico, J. K.; Maier, H. R.; Dandy, G. C.; Norton, J.; Croke, B. In *A comparison of sensitivity analysis techniques for complex models for environmental management*, Presented at MODSIM05: International Congress on Modelling and Simulation Advances and Applications for Management and Decision Making Proceedings, 2005.
73. United States Environmental Protection Agency. *Exposure factors handbook: Report EPA/600/8-89/043*; US EPA: Washington, DC, USA, 1989.
74. Martin, T. G.; Burgman, M. A.; Fidler, F.; Kuhnert, P. M.; Low-Choy, S.; McBride, M.; Mengersen, K., Eliciting expert knowledge in conservation science Obtención de conocimiento de expertos en ciencia de la conservación. *Conserv. Biol.* **2012**, *26*, (1), 29-38. DOI: 10.1111/j.1523-1739.2011.01806.x
75. O'Hagan, A., Probabilistic uncertainty specification: Overview, elaboration techniques and their application to a mechanistic model of carbon flux. *Environ. Modell. Software* **2012**, *36*, 35-48. DOI: 10.1016/j.envsoft.2011.03.003
76. Krueger, T.; Page, T.; Hubacek, K.; Smith, L.; Hiscock, K., The role of expert opinion in environmental modelling. *Environ. Modell. Software* **2012**, *36*, 4-18. DOI: 10.1016/j.envsoft.2012.01.011

77. Heijungs, R.; Frischknecht, R., Representing statistical distributions for uncertain parameters in LCA. Relationships between mathematical forms, their representation in EcoSpold, and their representation in CMLCA. *Int. J. Life Cycle Assess.* **2005**, *10*, (4), 248-254. DOI: 10.1065/lca2004.09.177
78. Vose, D., *Risk Analysis: A quantitative guide*. 2nd ed.; John Wiley & Sons, LTD: Chichester, England, 2000; p 418.
79. Muller, S.; Lesage, P.; Ciroth, A.; Mutel, C.; Weidema, B. P.; Samson, R., The application of the pedigree approach to the distributions foreseen in ecoinvent v3. *Int. J. Life Cycle Assess.* **2014**, *21*, (9), 1327-1337. DOI: 10.1007/s11367-014-0759-5
80. International Organization for Standardization (ISO), ISO 14040:2006: Environmental management - Life cycle assessment - Principles and framework. 2006.
81. Lansche, J.; Müller, J., Life cycle assessment (LCA) of biogas versus dung combustion household cooking systems in developing countries – A case study in Ethiopia. *J. Cleaner Prod.* **2017**, *165*, 828-835. DOI: 10.1016/j.jclepro.2017.07.116
82. Welfle, A.; Gilbert, P.; Thornley, P.; Stephenson, A., Generating low-carbon heat from biomass: Life cycle assessment of bioenergy scenarios. *J. Cleaner Prod.* **2017**, *149*, 448-460. DOI: 10.1016/j.jclepro.2017.02.035
83. Czyrnek-Delêtre, M. M.; Rocca, S.; Agostini, A.; Giuntoli, J.; Murphy, J. D., Life cycle assessment of seaweed biomethane, generated from seaweed sourced from integrated multi-trophic aquaculture in temperate oceanic climates. *Appl. Energy* **2017**, *196*, 34-50. DOI: 10.1016/j.apenergy.2017.03.129
84. Zhang, X.; Bauer, C.; Mutel, C. L.; Volkart, K., Life cycle assessment of power-to-gas: Approaches, system variations and their environmental implications. *Appl. Energy* **2017**, *190*, 326-338. DOI: 10.1016/j.apenergy.2016.12.098
85. Pré Consultants B.V. *SimaPro*, 2019.
86. Bicer, Y.; Dincer, I., Comparative life cycle assessment of hydrogen, methanol and electric vehicles from well to wheel. *Int. J. Hydrogen Energy* **2017**, *42*, (6), 3767-3777. DOI: 10.1016/j.ijhydene.2016.07.252
87. Briones Hidrovo, A.; Uche, J.; Martínez-Gracia, A., Accounting for GHG net reservoir emissions of hydropower in Ecuador. *Renewable Energy* **2017**, *112*, 209-221. DOI: 10.1016/j.renene.2017.05.047
88. Crossin, E., Life cycle assessment of a mallee eucalypt jet fuel. *Biomass Bioenergy* **2017**, *96*, 162-171. DOI: 10.1016/j.biombioe.2016.11.014
89. Vandepaer, L.; Cloutier, J.; Amor, B., Environmental impacts of lithium metal polymer and lithium-ion stationary batteries. *Renewable Sustainable Energy Rev.* **2017**, *78*, 46-60. DOI: 10.1016/j.rser.2017.04.057

90. Nimana, B.; Verma, A.; Di Lullo, G.; Rahman, M. M.; Canter, C. E.; Olateju, B.; Zhang, H.; Kumar, A., Life cycle analysis of bitumen transportation to refineries by rail and pipeline. *Environ. Sci. Technol.* **2017**, *51*, (1), 680-691. DOI: 10.1021/acs.est.6b02889
91. Liu, X. V.; Hoekman, S. K.; Farthing, W.; Felix, L., TC2015: Life cycle analysis of co-formed coal fines and hydrochar produced in twin-screw extruder (TSE). *Environ. Prog. Sustainable Energy* **2017**, *36*, (3), 668-676. DOI: 10.1002/ep.12552
92. Benveniste, G.; Pucciarelli, M.; Torrell, M.; Kendall, M.; Tarancón, A., Life cycle assessment of microtubular solid oxide fuel cell based auxiliary power unit systems for recreational vehicles. *J. Cleaner Prod.* **2017**, *165*, 312-322. DOI: 10.1016/j.jclepro.2017.07.130
93. Jung, K. A.; Lim, S. R.; Kim, Y.; Park, J. M., Opportunity and challenge of seaweed bioethanol based on life cycle CO<sub>2</sub> assessment. *Environ. Prog. Sustainable Energy* **2017**, *36*, (1), 200-207. DOI: 10.1002/ep.12446
94. Joint Research Centre (JRC) of the European Commission. *SIMLAB*, 2.2; European Union Science HUB: 2016.
95. Sigman, K. *Introduction to reducing variance in Monte Carlo simulations*; Department of Industrial Engineering and Operations Research: New York, March 29, 2016, 2007.
96. Amarakoon, S.; Vallet, C.; Curran, M. A.; Haldar, P.; Metacarpa, D.; Fobare, D.; Bell, J., Life cycle assessment of photovoltaic manufacturing consortium (PVMC) copper indium gallium (di)selenide (CIGS) modules. *Int. J. Life Cycle Assess.* **2018**, *23*, (4), 851-866. DOI: 10.1007/s11367-017-1345-4
97. Li, Z.; Du, H.; Xiao, Y.; Guo, J., Carbon footprints of two large hydro-projects in China: Life-cycle assessment according to ISO/TS 14067. *Renewable Energy* **2017**, *114*, 534-546. DOI: 10.1016/j.renene.2017.07.073
98. Manandhar, A.; Shah, A., Life cycle assessment of feedstock supply systems for cellulosic biorefineries using corn stover transported in conventional bale and densified pellet formats. *J. Cleaner Prod.* **2017**, *166*, 601-614. DOI: 10.1016/j.jclepro.2017.08.083
99. Chrisman, L. Latin Hypercube vs. Monte Carlo Sampling. <http://www.lumina.com/blog/latin-hypercube-vs.-monte-carlo-sampling> (July 13, 2017),
100. Henriksson, P. J. G.; Heijungs, R.; Dao, H. M.; Phan, L. T.; de Snoo, G. R.; Guinée, J. B., Product carbon footprints and their uncertainties in comparative decision contexts. *PLoS One* **2015**, *10*, (3), e0121221. DOI: 10.1371/journal.pone.0121221
101. Qin, Y.; Suh, S., What distribution function do life cycle inventories follow? *Int. J. Life Cycle Assess.* **2017**, *22*, (7), 1138-1145. DOI: 10.1007/s11367-016-1224-4

102. Heijungs, R.; Henriksson, P. J. G.; Guinée, J. B., Pre-calculated LCI systems with uncertainties cannot be used in comparative LCA. *Int. J. Life Cycle Assess.* **2017**, *22*, (3), 461-461. DOI: 10.1007/s11367-017-1265-3
103. Qin, Y.; Suh, S., Does the use of pre-calculated uncertainty values change the conclusions of comparative life cycle assessments? – An empirical analysis. *PLoS One* **2018**, *13*, (12), e0209474. DOI: 10.1371/journal.pone.0209474
104. Suh, S.; Qin, Y., Pre-calculated LCIs with uncertainties revisited. *Int. J. Life Cycle Assess.* **2017**, *22*, (5), 827-831. DOI: 10.1007/s11367-017-1287-x
105. Uusitalo, V.; Leino, M.; Kasurinen, H.; Linnanen, L., Transportation biofuel efficiencies from cultivated feedstock in the boreal climate zone: Case Finland. *Biomass Bioenergy* **2017**, *99*, 79-89. DOI: 10.1016/j.biombioe.2017.02.017
106. Neupane, B.; Konda, N. V. S. N. M.; Singh, S.; Simmons, B. A.; Scown, C. D., Life-cycle greenhouse gas and water intensity of cellulosic biofuel production using cholinium lysinate ionic liquid pretreatment. *ACS Sustainable Chem. Eng.* **2017**, *5*, (11), 10176-10185. DOI: 10.1021/acssuschemeng.7b02116
107. Röder, M.; Thornley, P., Waste wood as bioenergy feedstock. Climate change impacts and related emission uncertainties from waste wood based energy systems in the UK. *Waste Manage.* **2018**, *74*, 241-252. DOI: 10.1016/j.wasman.2017.11.042
108. Zhang, Y.; Kendall, A., Life cycle performance of cellulosic ethanol and corn ethanol from a retrofitted dry mill corn ethanol plant. *Bioenergy Res.* **2017**, *10*, (1), 183-198. DOI: 10.1007/s12155-016-9776-5
109. Li, S.; Gao, L.; Jin, H., Realizing low life cycle energy use and GHG emissions in coal based polygeneration with CO<sub>2</sub> capture. *Appl. Energy* **2017**, *194*, 161-171. DOI: 10.1016/j.apenergy.2017.03.021
110. Saltelli, A.; Annoni, P., How to avoid a perfunctory sensitivity analysis. *Environ. Modell. Software* **2010**, *25*, (12), 1508-1517. DOI: 10.1016/j.envsoft.2010.04.012
111. Campolongo, F.; Cariboni, J.; Saltelli, A., An effective screening design for sensitivity analysis of large models. *Environ. Modell. Software* **2007**, *22*, (10), 1509-1518. DOI: 10.1016/j.envsoft.2006.10.004
112. Campolongo, F.; Cariboni, J., Sensitivity analysis: how to detect important factors in large models. Institute for the Protection and Security of the Citizen, Ed. Office for Official Publications of the European Communities: Luxembourg, 2007.
113. Morris, M. D., Factorial sampling plans for preliminary computational experiments. *Technometrics* **1991**, *33*, (2), 161-174. DOI: 10.2307/1269043

114. Ciroth, A.; Muller, S.; Weidema, B.; Lesage, P., Empirically based uncertainty factors for the pedigree matrix inecoinvent. *Int. J. Life Cycle Assess.* **2013**, *21*, (9), 1338-1348. DOI: 10.1007/s11367-013-0670-5
115. Greenhouse Gas Protocol *Quantitative Inventory Uncertainty*; ghgprotocol.org, p 10.
116. Huijbregts, M. A. J.; Gilijamse, W.; Ragas, A. M. J.; Reijnders, L., Evaluating uncertainty in environmental life-cycle assessment. A case study comparing two insulation options for a Dutch one-family dwelling. *Environ. Sci. Technol.* **2003**, *37*, (11), 2600-2608. DOI: 10.1021/es020971+
117. Ellison, A. M., Bayesian inference in ecology. *Ecol. Lett.* **2004**, *7*, (6), 509-520. DOI: 10.1111/j.1461-0248.2004.00603.x
118. Sobol, I. M., Sensitivity estimates for nonlinear mathematical models. *Math. Model. Comput. Exp.* **1993**, *1*, (4), 407-414.
119. Saltelli, A.; Tarantola, S.; Campolongo, F.; Ratto, M., *Sensitivity analysis in practice: A guide to assessing scientific models*. John Wiley & Sons Ltd.: West Sussex, England, 2004; p 219.
120. Gan, Y.; Duan, Q.; Gong, W.; Tong, C.; Sun, Y.; Chu, W.; Ye, A.; Miao, C.; Di, Z., A comprehensive evaluation of various sensitivity analysis methods: A case study with a hydrological model. *Environ. Modell. Software* **2014**, *51*, 269-285. DOI: 10.1016/j.envsoft.2013.09.031
121. Saltelli, A.; Tarantola, S.; Chan, K. P. S., A quantitative model-independent method for global sensitivity analysis of model output. *Technometrics* **1999**, *41*, (1), 39-56. DOI: 10.1080/00401706.1999.10485594
122. Saltelli, A.; Bolado, R., An alternative way to compute Fourier amplitude sensitivity test (FAST). *Comput. Stat. Data Anal.* **1998**, *26*, (4), 445-460. DOI: 10.1016/S0167-9473(97)00043-1
123. Pianosi, F.; Wagener, T., A simple and efficient method for global sensitivity analysis based on cumulative distribution functions. *Environ. Modell. Software* **2015**, *67*, 1-11. DOI: 10.1016/j.envsoft.2015.01.004
124. Zimmerle, D. J.; Williams, L. L.; Vaughn, T. L.; Quinn, C.; Subramanian, R.; Duggan, G. P.; Willson, B.; Opsomer, J. D.; Marchese, A. J.; Martinez, D. M.; Robinson, A. L., Methane emissions from the natural gas transmission and storage system in the United States. *Environ. Sci. Technol.* **2015**, *49*, (15), 9374-9383. DOI: 10.1021/acs.est.5b01669
125. Henriksson, P. J. G.; Rico, A.; Zhang, W.; Ahmad-Al-Nahid, S.; Newton, R.; Phan, L. T.; Zhang, Z.; Jaithiang, J.; Dao, H. M.; Phu, T. M.; Little, D. C.; Murray, F. J.; Satapornvanit, K.; Liu, L.; Liu, Q.; Haque, M. M.; Kruijssen, F.; de Snoo, G. R.; Heijungs, R.; van Bodegom, P. M.; Guinée, J. B., Comparison of asian aquaculture

- products by use of statistically supported life cycle assessment. *Environ. Sci. Technol.* **2015**, *49*, (24), 14176-14183. DOI: 10.1021/acs.est.5b04634
126. Cha, S.-H., *Comprehensive Survey on Distance/Similarity Measures Between Probability Density Functions*. 2007; Vol. 1.
  127. Wei, W.; Larrey-Lassalle, P.; Faure, T.; Dumoulin, N.; Roux, P.; Mathias, J.-D., Using the reliability theory for assessing the decision confidence probability for comparative life cycle assessments. *Environ. Sci. Technol.* **2016**, *50*, (5), 2272-2280. DOI: 10.1021/acs.est.5b03683
  128. Hurtado, J. E.; Alvarez, D. A., The encounter of interval and probabilistic approaches to structural reliability at the design point. *Comput. Methods Appl. Mech. Eng.* **2012**, *225-228*, 74-94. DOI: 10.1016/j.cma.2012.03.020
  129. Zhao, Y.-G.; Ono, T., A general procedure for first/second-order reliability method (FORM/SORM). *Struct. Saf.* **1999**, *21*, (2), 95-112. DOI: 10.1016/S0167-4730(99)00008-9
  130. Larsson, O., Reliability analysis. Lund University.
  131. Gonzalez, O.; O'Rourke, H. P.; Wurpts, I. C.; Grimm, K. J., Analyzing Monte Carlo simulation studies with classification and regression trees. *Struct. Equ. Modeling* **2018**, *25*, (3), 403-413. DOI: 10.1080/10705511.2017.1369353
  132. Gregory, J. R.; Noshadravan, A.; Olivetti, E. A.; Kirchain, R. E., A methodology for robust comparative life cycle assessments incorporating uncertainty. *Environ. Sci. Technol.* **2016**, *50*, (12), 6397-6405. DOI: 10.1021/acs.est.5b04969
  133. Therneau, T.; Atkinson, B. *rpart: Recursive Partitioning and Regression Trees*, R package version 4.1-13; 2018.
  134. Refsgaard, J. C.; van der Sluijs, J. P.; Brown, J.; van der Keur, P., A framework for dealing with uncertainty due to model structure error. *Adv. Water Resour.* **2006**, *29*, (11), 1586-1597. DOI: 10.1016/j.advwatres.2005.11.013
  135. Ramin, M.; Labencki, T.; Boyd, D.; Trolle, D.; Arhonditsis, G. B., A Bayesian synthesis of predictions from different models for setting water quality criteria. *Ecol. Modell.* **2012**, *242*, 127-145. DOI: 10.1016/j.ecolmodel.2012.05.023
  136. McDonald, C. P.; Urban, N. R., Using a model selection criterion to identify appropriate complexity in aquatic biogeochemical models. *Ecol. Modell.* **2010**, *221*, (3), 428-432. DOI: 10.1016/j.ecolmodel.2009.10.021
  137. Van Der Sluijs, J. P.; Craye, M.; Funtowicz, S.; Kloprogge, P.; Ravetz, J.; Risbey, J., Combining quantitative and qualitative measures of uncertainty in model-based environmental assessment: The NUSAP system. *Risk Anal.* **2005**, *25*, (2), 481-492. DOI: 10.1111/j.1539-6924.2005.00604.x

138. Campolongo, F.; Braddock, R., Sensitivity analysis of the IMAGE greenhouse model. *Environ. Modell. Software* **1999**, *14*, (4), 275-282. DOI: 10.1016/S1364-8152(98)00079-6
139. R Core Team and contributors worldwide. The R Stats Package. <https://stat.ethz.ch/R-manual/R-devel/library/stats/html/00Index.html> (Dec. 14, 2017),
140. Mathworks. MATLAB. <https://www.mathworks.com/products/matlab.html> (Feb. 14, 2019),
141. GreenDelta. *OpenLCA*, 2018.
142. Di Lullo, G.; Zhang, H.; Kumar, A., Evaluation of uncertainty in the well-to-tank and combustion greenhouse gas emissions of various transportation fuels. *Appl. Energy* **2016**, *184*, 413-426. DOI: 10.1016/j.apenergy.2016.10.027
143. Nimana, B.; Canter, C.; Kumar, A., Energy consumption and greenhouse gas emissions in upgrading and refining of Canada's oil sands products. *Energy* **2015**, *83*, 65-79. DOI: <http://dx.doi.org/10.1016/j.energy.2015.01.085>
144. Rahman, M. M.; Canter, C.; Kumar, A., Well-to-wheel life cycle assessment of transportation fuels derived from different North American conventional crudes. *Appl. Energy* **2015**, *156*, 159-173. DOI: <http://dx.doi.org/10.1016/j.apenergy.2015.07.004>
145. Rahman, M. M.; Canter, C.; Kumar, A., Greenhouse gas emissions from recovery of various North American conventional crudes. *Energy* **2014**, *74*, 607-617. DOI: <http://dx.doi.org/10.1016/j.energy.2014.07.026>
146. Pujol, G.; Iooss, B.; Janon, A.; Boumhaout, K.; Veiga, S. D.; Delage, T.; Fruth, J.; Gilquin, L.; Guillaume, J.; Gratiot, L. L.; Lemaitre, P.; Nelson, B. L.; Monari, F.; Oomen, R.; Ramos, B.; Roustant, O.; Song, E.; Staum, J.; Touati, T.; Weber, F. sensitivity: Global Sensitivity Analysis of Model Outputs. <https://cran.r-project.org/package=sensitivity> (Dec. 14, 2017),
147. Wickham, H.; Hester, J.; Francois, R.; Jylänki, J.; Jørgensen, M. readr: Read Rectangular Text Data. <https://cran.r-project.org/package=readr> (Dec. 14, 2017),
148. Regis Pouillot, M.-L. D.-M., Jean-Baptiste Denis mc2d: Tools for Two-Dimensional Monte-Carlo Simulations. <https://cran.r-project.org/package=mc2d> (Dec. 14, 2017),
149. Carnell, R. triangle: Provides the standard distribution functions for the triangle distribution. <https://cran.r-project.org/package=triangle> (Dec. 14, 2017),
150. Koenker, R.; Portnoy, S.; Ng, P. T.; Zeileis, A.; Grosjean, P.; Ripley, B. D. quantreg: Quantile Regression. <https://cran.r-project.org/package=quantreg> (Dec. 14, 2017),
151. Carnell, R. lhs: Latin hypercube samples. <https://cran.r-project.org/package=lhs> (Dec. 14, 2017),

152. Wickham, H.; Chang, W. ggplot2: Create Elegant Data Visualisations Using the Grammar of Graphics. <https://cran.r-project.org/package=ggplot2> (Dec. 14, 2017),
153. Venables, B.; Hornik, K.; Maechler, M. polynom: A Collection of Functions to Implement a Class for Univariate polynomial Manipulations. <https://CRAN.R-project.org/package=polynom> (Feb. 14, 2019),
154. Grothendieck, G. nls2: Non-linear regression with brute force. <https://cran.r-project.org/package=nls2> (Dec. 14, 2017),
155. Klauer, B.; Brown, J. D., Conceptualising imperfect knowledge in public decision-making: ignorance, uncertainty, error and risk situations. *Environ. Res. Eng. Manag.* **2004**, *1*, (27), 124-128.
156. Carr, N. L.; Kobayashi, R.; Burrows, D. B., Viscosity of hydrocarbon gases under pressure. *J. Pet. Technol.* **1954**. DOI: 10.2118/297-G
157. Carroll, L.; Hudkins, R. W., Advanced Pipeline Design.
158. Coelho, P. M.; Pinho, C., Considerations about equations for steady state flow in natural gas pipelines. *J. Braz. Soc. Mech. Sci. Eng.* **2007**, *29*, 262-273. DOI: 10.1590/S1678-58782007000300005
159. Rabitz, H., Global sensitivity analysis for systems with independent and/or correlated inputs. *Procedia - Social and Behavioral Sciences* **2010**, *2*, (6), 7587-7589. DOI: 10.1016/j.sbspro.2010.05.131
160. Minitab Inc. What is partial least squares regression? <https://support.minitab.com/en-us/minitab/18/help-and-how-to/modeling-statistics/regression/supporting-topics/partial-least-squares-regression/what-is-partial-least-squares-regression/> (Feb. 14, 2019),
161. Microsoft Support Memory usage in the 32-bit edition of Excel 2013 and 2016. <https://support.microsoft.com/en-ca/help/3066990/memory-usage-in-the-32-bit-edition-of-excel-2013-and-2016> (Feb. 2, 2019),
162. Di Lullo, G.; Gemechu, E.; Oni, A.; Kumar, A. In *Developing a practical framework to meet ISO requirements on sensitivity and uncertainty*, Presented at LCA XVIII, Fort Collins, Colorado, 2018.
163. Di Lullo, G.; Hoffman, D.; Zhang, H.; Gemechu, E.; Shaw, C.; Daly, C.; Kumar, A., Personal communication oil and gas industry interested in LCA of their operations. 2018.
164. Fattah, K. A. A.-e., Analysis shows magnitude of Z-factor error. *Oil Gas J.* **1995**.
165. Peng, C.; Xu, C.; Liu, Q.; Sun, L.; Luo, Y.; Shi, J., Fate and transformation of CuO nanoparticles in the soil-rice system during the life cycle of rice plants. *Environ. Sci. Technol.* **2017**, *51*, (9), 4907-4917. DOI: 10.1021/acs.est.6b05882

166. Ren, H. Y.; Li, C. J.; Xie, G., Evaluation of state equations of natural gas in pipeline transportation. *Adv. Mater. Res.* **2012**, 463-464, 936-939. DOI: 10.4028/[www.scientific.net/AMR.463-464.936](http://www.scientific.net/AMR.463-464.936)
167. Di Bella, F. A. *Development of a centrifugal hydrogen pipeline gas compressor*; 2015.
168. Oni, A. O.; Anaya, K.; Giwa, T.; Lullo, G. D.; Kumar, A., Comparative assessment of blue hydrogen from steam methane reforming, autothermal reforming, and natural gas decomposition technologies for natural gas-producing regions. *Submitted to Energy Convers. Manage. Oct. 20, 2021* **2021**.
169. Di Lullo, G.; Hoffman, D.; Zhang, H.; Gemechu, E.; Shaw, C.; Metsaranta, J.; Daly, C.; Kumar, A. In *Carbon life cycle assessment of a Suncor Energy Inc. oil sands reclamation project*, Presented at 2019 Oil Sands Innovation Summit, Calgary, AB, 2019.
170. Heaps, C. G. Long-range Energy Alternatives Planning (LEAP) system. <https://www.energycommunity.org> (June 14, 2018),
171. Pedroni, N.; Zio, E., Empirical comparison of methods for the hierarchical propagation of hybrid uncertainty in risk assessment, in presence of dependences. *Int. J. Uncertainty Fuzziness Knowledge Based Syst.* **2012**, 20, (04), 509-557. DOI: 10.1142/S0218488512500250
172. Frost, J. Overfitting Regression Models: Problems, Detection, and Avoidance. <http://statisticsbyjim.com/regression/overfitting-regression-models/> (May 26, 2017),
173. Olejnik, S.; Mills, J.; Keselman, H., Using Wherry's adjusted R<sup>2</sup> and Mallow's Cp for model selection from all possible regressions. *J. Exp. Educ.* **2000**, 68, (4), 365-380. DOI: 10.1080/00220970009600643
174. Frost, J. Regression Smackdown: Stepwise versus Best Subsets! <http://blog.minitab.com/blog/adventures-in-statistics-2/regression-smackdown-stepwise-versus-best-subsets> (Sept. 13, 2017),
175. Frost, J. The Danger of Overfitting Regression Models. <http://blog.minitab.com/blog/adventures-in-statistics-2/the-danger-of-overfitting-regression-models> (Sept. 3, 2015),
176. Frost, J. What Are the Effects of Multicollinearity and When Can I Ignore Them? <http://blog.minitab.com/blog/adventures-in-statistics-2/what-are-the-effects-of-multicollinearity-and-when-can-i-ignore-them> (May 2, 2013),
177. Chouldechova, A. Regression diagnostic plots. [https://www.andrew.cmu.edu/user/achoulde/94842/homework/regression\\_diagnostics.html](https://www.andrew.cmu.edu/user/achoulde/94842/homework/regression_diagnostics.html) (Sept. 13, 2017),
178. Ihaka, R. Quantiles and Quantile Based Plots. <https://www.stat.auckland.ac.nz/~ihaka/787/lectures-quantiles.pdf> (Sept. 13, 2017),

179. Myhre, G.; Shindell, D.; Bréon, F.-M.; Collins, W.; Fuglestedt, J.; Huang, J.; Koch, D.; Lamarque, J.-F.; Lee, D.; Mendoza, B.; Nakajima, T.; Robock, A.; Stephens, G.; T., T.; Zhang, H., Anthropogenic and Natural Radiative Forcing. *Climate Change 2013: The Physical Science Basis. Contribution of Working Group to the Fifth Assessment Report of the Intergovernmental Panel on Climate Change*, Stocker, T. F.; Qin, D.; Plattner, G.-K.; Tignor, M.; Allen, S. K.; Boschung, J.; Nauels, A.; Xia, Y.; V., B.; Midgley, P. M., Eds. Cambridge University Press: Cambridge and New York, 2013.
180. Di Lullo, G.; Oni, A. O.; Kumar, A., Using proxy models and adaptive sampling to integrate complex engineering models into life cycle assessments of energy systems. *To be submitted to Energy Convers. Manage.* **2022**.
181. Hornik, K.; Stinchcombe, M.; White, H., Multilayer feedforward networks are universal approximators. *Neural Networks* **1989**, 2, (5), 359-366. DOI: 10.1016/0893-6080(89)90020-8
182. Fonseca, D. J.; Navarrese, D. O.; Moynihan, G. P., Simulation metamodeling through artificial neural networks. *Eng. Appl. Artif. Intell.* **2003**, 16, (3), 177-183. DOI: 10.1016/S0952-1976(03)00043-5
183. Hachicha, W., A simulation metamodeling based neural networks for lot-sizing problem in MTO sector. *Int. J. Simul. Model* **2011**, 10, 191-203. DOI: 10.2507/IJSIMM10(4)3.188
184. Kilmer, R. A. Artificial neural network metamodels of stochastic computer simulations. Doctoral thesis, University of Pittsburgh, 1994.
185. Liu, H.; Ong, Y.-S.; Cai, J., A survey of adaptive sampling for global metamodeling in support of simulation-based complex engineering design. *Struct. Multidiscip. Optim.* **2018**, 57, (1), 393-416. DOI: 10.1007/s00158-017-1739-8
186. Sacks, J.; Welch, W. J.; Mitchell, T. J.; Wynn, H. P., Design and analysis of computer experiments. *Statist. Sci.* **1989**, 4, (4), 409-423. DOI: 10.1214/ss/1177012413
187. Jin, R.; Chen, W.; Simpson, T. W., Comparative studies of metamodeling techniques under multiple modelling criteria. *Struct. Multidiscip. Optim.* **2001**, 23, (1), 1-13. DOI: 10.1007/s00158-001-0160-4
188. Heaton, J., *Introduction to Neural Networks for Java, 2nd Edition*. Heaton Research, Inc.: 2008.
189. Microsoft Support T.TEST function. <https://support.microsoft.com/en-us/office/t-test-function-d4e08ec3-c545-485f-962e-276f7cbcd055?ns=excel&version=90&syslcid=1033&uilcid=1033&appver=zx1900&heloid=xlmain11.chm60589&ui=en-us&rs=en-us&ad=us> (Sept. 24, 2021),

190. Loyola R, D. G.; Pedernana, M.; Gimeno García, S., Smart sampling and incremental function learning for very large high dimensional data. *Neural Networks* **2016**, *78*, 75-87. DOI: 10.1016/j.neunet.2015.09.001
191. Aggarwal, C. C.; Hinneburg, A.; Keim, D. A. In *On the surprising behavior of distance metrics in high dimensional space*, Presented at Database Theory, Berlin, Heidelberg, 2001.
192. Pronzato, L., Minimax and maximin space-filling designs: some properties and methods for construction (hal-01496712). *Journal de la Societe Francaise de Statistique* **2017**, *158*, (1), 7-36.
193. Schwenk, H.; Bengio, Y., Boosting neural networks. *Neural Comput.* **2000**, *12*, 1869-1887. DOI: 10.1162/089976600300015178
194. Li, X.; Marfatia, Z. In *High fidelity surrogate models for steady-state simulation and optimization of natural gas transmission networks*, Presented at CCEC 2020 Virtual Conference, 2020.
195. Telsnig, T.; Weinrebe, G.; Finkbeiner, J.; Eltrop, L., Life cycle assessment of a future central receiver solar power plant and autonomous operated heliostat concepts. *Sol. Energy* **2017**, *157*, 187-200. DOI: 10.1016/j.solener.2017.08.018
196. Parajuli, R.; Knudsen, M. T.; Birkved, M.; Djomo, S. N.; Corona, A.; Dalgaard, T., Environmental impacts of producing bioethanol and biobased lactic acid from standalone and integrated biorefineries using a consequential and an attributional life cycle assessment approach. *Sci. Total Environ.* **2017**, *598*, 497-512. DOI: 10.1016/j.scitotenv.2017.04.087
197. Guo, F.; Wang, X.; Yang, X., Potential pyrolysis pathway assessment for microalgae-based aviation fuel based on energy conversion efficiency and life cycle. *Energy Convers. Manage.* **2017**, *132*, 272-280. DOI: 10.1016/j.enconman.2016.11.020
198. Ayodele, T. R.; Ogunjuyigbe, A. S. O.; Alao, M. A., Life cycle assessment of waste-to-energy (WtE) technologies for electricity generation using municipal solid waste in Nigeria. *Appl. Energy* **2017**, *201*, 200-218. DOI: 10.1016/j.apenergy.2017.05.097
199. Dias, G. M.; Ayer, N. W.; Kariyapperuma, K.; Thevathasan, N.; Gordon, A.; Sidders, D.; Johannesson, G. H., Life cycle assessment of thermal energy production from short-rotation willow biomass in Southern Ontario, Canada. *Appl. Energy* **2017**, *204*, 343-352. DOI: 10.1016/j.apenergy.2017.07.051
200. Bicer, Y.; Dincer, I., Life cycle assessment of nuclear-based hydrogen and ammonia production options: A comparative evaluation. *Int. J. Hydrogen Energy* **2017**, *42*, (33), 21559-21570. DOI: 10.1016/j.ijhydene.2017.02.002

201. Akinyele, D. O., Environmental performance evaluation of a grid-independent solar photovoltaic power generation (SPPG) plant. *Energy* **2017**, *130*, 515-529. DOI: 10.1016/j.energy.2017.04.126
202. Peters, J. F.; Weil, M., Aqueous hybrid ion batteries – An environmentally friendly alternative for stationary energy storage? *J. Power Sources* **2017**, *364*, 258-265. DOI: 10.1016/j.jpowsour.2017.08.041
203. Zhang, T.; Xie, X.; Huang, Z., The policy recommendations on cassava ethanol in China: Analyzed from the perspective of life cycle “E & W”. *Resour. Conserv. Recycl.* **2017**, *126*, 12-24. DOI: 10.1016/j.resconrec.2017.07.008
204. Boonrod, B.; Prapainainar, C.; Narataruksa, P.; Kantama, A.; Saibautrong, W.; Sudsakorn, K.; Mungcharoen, T.; Prapainainar, P., Evaluating the environmental impacts of bio-hydrogenated diesel production from palm oil and fatty acid methyl ester through life cycle assessment. *J. Cleaner Prod.* **2017**, *142*, 1210-1221. DOI: 10.1016/j.jclepro.2016.07.128
205. Ertem, F. C.; Neubauer, P.; Junne, S., Environmental life cycle assessment of biogas production from marine macroalgal feedstock for the substitution of energy crops. *J. Cleaner Prod.* **2017**, *140*, 977-985. DOI: 10.1016/j.jclepro.2016.08.041
206. Handler, R. M.; Shi, R.; Shonnard, D. R., Land use change implications for large-scale cultivation of algae feedstocks in the United States Gulf Coast. *J. Cleaner Prod.* **2017**, *153*, 15-25. DOI: 10.1016/j.jclepro.2017.03.149
207. Serra, P.; Giuntoli, J.; Agostini, A.; Colauzzi, M.; Amaducci, S., Coupling sorghum biomass and wheat straw to minimise the environmental impact of bioenergy production. *J. Cleaner Prod.* **2017**, *154*, 242-254. DOI: 10.1016/j.jclepro.2017.03.208
208. Siddiqui, O.; Dincer, I., Comparative assessment of the environmental impacts of nuclear, wind and hydro-electric power plants in Ontario: A life cycle assessment. *J. Cleaner Prod.* **2017**, *164*, 848-860. DOI: 10.1016/j.jclepro.2017.06.237
209. De Falco, M.; Capocelli, M.; Losito, G.; Piemonte, V., LCA perspective to assess the environmental impact of a novel PCM-based cold storage unit for the civil air conditioning. *J. Cleaner Prod.* **2017**, *165*, 697-704. DOI: 10.1016/j.jclepro.2017.07.153
210. Mahbub, N.; Oyedun, A. O.; Kumar, A.; Oestreich, D.; Arnold, U.; Sauer, J., A life cycle assessment of oxymethylene ether synthesis from biomass-derived syngas as a diesel additive. *J. Cleaner Prod.* **2017**, *165*, 1249-1262. DOI: 10.1016/j.jclepro.2017.07.178
211. Rodríguez, R.; Espada, J. J.; Moreno, J.; Vicente, G.; Bautista, L. F.; Morales, V.; Sánchez-Bayo, A.; Dufour, J., Environmental analysis of Spirulina cultivation and biogas production using experimental and simulation approach. *Renewable Energy* **2018**, *129*, 724-732. DOI: 10.1016/j.renene.2017.05.076

212. Brancoli, P.; Ferreira, J. A.; Bolton, K.; Taherzadeh, M. J., Changes in carbon footprint when integrating production of filamentous fungi in 1st generation ethanol plants. *Bioresour. Technol.* **2018**, *249*, 1069-1073. DOI: 10.1016/j.biortech.2017.10.085
213. Hua, J.; Wu, Y.; Chen, H., Alternative fuel for sustainable shipping across the Taiwan Strait. *Transp. Res. Part D Transp. Environ.* **2017**, *52*, 254-276. DOI: 10.1016/j.trd.2017.03.015
214. Chang, W. R.; Hwang, J. J.; Wu, W., Environmental impact and sustainability study on biofuels for transportation applications. *Renewable Sustainable Energy Rev.* **2017**, *67*, 277-288. DOI: 10.1016/j.rser.2016.09.020
215. Abuşoğlu, A.; Özahi, E.; İhsan Kutlar, A.; Al-jaf, H., Life cycle assessment (LCA) of digested sewage sludge incineration for heat and power production. *J. Cleaner Prod.* **2017**, *142*, 1684-1692. DOI: 10.1016/j.jclepro.2016.11.121
216. Ankathi, S. K.; Potter, J. S.; Shonnard, D. R., Carbon footprint and energy analysis of bio-CH<sub>4</sub> from a mixture of food waste and dairy manure in Denver, Colorado. *Environ. Prog. Sustainable Energy* **2018**, *37*, (3), 1101-1111. DOI: 10.1002/ep.12762
217. Bartolozzi, I.; Rizzi, F.; Frey, M., Are district heating systems and renewable energy sources always an environmental win-win solution? A life cycle assessment case study in Tuscany, Italy. *Renewable Sustainable Energy Rev.* **2017**, *80*, 408-420. DOI: 10.1016/j.rser.2017.05.231
218. Cronin, K. R.; Runge, T. M.; Zhang, X.; Izaurralde, R. C.; Reinemann, D. J.; Sinistore, J. C., Spatially explicit life cycle analysis of cellulosic ethanol production scenarios in southwestern Michigan. *Bioenergy Res.* **2017**, *10*, (1), 13-25. DOI: 10.1007/s12155-016-9774-7
219. Ding, N.; Yang, Y.; Cai, H.; Liu, J.; Ren, L.; Yang, J.; Xie, G. H., Life cycle assessment of fuel ethanol produced from soluble sugar in sweet sorghum stalks in North China. *J. Cleaner Prod.* **2017**, *161*, 335-344. DOI: 10.1016/j.jclepro.2017.05.078
220. Escamilla-Alvarado, C.; Poggi-Varaldo, H. M.; Ponce-Noyola, M. T., Bioenergy and bioproducts from municipal organic waste as alternative to landfilling: a comparative life cycle assessment with prospective application to Mexico. *Environ. Sci. Pollut. Res.* **2017**, *24*, (33), 25602-25617. DOI: 10.1007/s11356-016-6939-z
221. Friesenhan, C.; Agirre, I.; Eltrop, L.; Arias, P. L., Streamlined life cycle analysis for assessing energy and exergy performance as well as impact on the climate for landfill gas utilization technologies. *Appl. Energy* **2017**, *185*, 805-813. DOI: 10.1016/j.apenergy.2016.10.097
222. Gao, D.; Qiu, X.; Zheng, X.; Zhang, Y., Life cycle analysis of coal-based synthetic natural gas for heat supply and electricity generation in China. *Chem. Eng. Res. Des.* **2018**, *131*, 709-722. DOI: 10.1016/j.cherd.2017.10.036

223. Hackl, R.; Hansson, J.; Norén, F.; Stenberg, O.; Olshammar, M., Cultivating *Clostridium* intestinalis to counteract marine eutrophication: Environmental assessment of a marine biomass based bioenergy and biofertilizer production system. *Renewable Energy* **2018**, *124*, 103-113. DOI: 10.1016/j.renene.2017.07.053
224. Hu, A. H.; Huang, L. H.; Lou, S.; Kuo, C. H.; Huang, C. Y.; Chian, K. J.; Chien, H. T.; Hong, H. F., Assessment of the carbon footprint, social benefit of carbon reduction, and energy payback time of a high-concentration photovoltaic system. *Sustainability (Switzerland)* **2017**, *9*, (1). DOI: 10.3390/su9010027
225. Kommalapati, R.; Kadiyala, A.; Shahriar, M. T.; Huque, Z., Review of the life cycle greenhouse gas emissions from different photovoltaic and concentrating solar power electricity generation systems. *Energies* **2017**, *10*, (3). DOI: 10.3390/en10030350
226. Lee, U.; Han, J.; Wang, M., Evaluation of landfill gas emissions from municipal solid waste landfills for the life-cycle analysis of waste-to-energy pathways. *J. Cleaner Prod.* **2017**, *166*, 335-342. DOI: 10.1016/j.jclepro.2017.08.016
227. Lombardi, L.; Mendecka, B.; Carnevale, E.; Stanek, W., Environmental impacts of electricity production of micro wind turbines with vertical axis. *Renewable Energy* **2018**, *128*, 553-564. DOI: 10.1016/j.renene.2017.07.010
228. Maharjan, S.; Wang, W. C.; Teah, H. Y., Life cycle assessment of palm-derived biodiesel in Taiwan. *Clean Technol. Environ. Policy* **2017**, *19*, (4), 959-969. DOI: 10.1007/s10098-016-1290-0
229. Monteiro Lunardi, M.; Wing Yi Ho-Baillie, A.; Alvarez-Gaitan, J. P.; Moore, S.; Corkish, R., A life cycle assessment of perovskite/silicon tandem solar cells. *Prog. Photovoltaics Res. Appl.* **2017**, *25*, (8), 679-695. DOI: 10.1002/pip.2877
230. Morrison, B.; Golden, J. S., Life cycle assessment of co-firing coal and wood pellets in the Southeastern United States. *J. Cleaner Prod.* **2017**, *150*, 188-196. DOI: 10.1016/j.jclepro.2017.03.026
231. Parajuli, R.; Knudsen, M. T.; Djomo, S. N.; Corona, A.; Birkved, M.; Dalgaard, T., Environmental life cycle assessment of producing willow, alfalfa and straw from spring barley as feedstocks for bioenergy or biorefinery systems. *Sci. Total Environ.* **2017**, *586*, 226-240. DOI: 10.1016/j.scitotenv.2017.01.207
232. Pehme, S.; Veromann, E.; Hamelin, L., Environmental performance of manure co-digestion with natural and cultivated grass – A consequential life cycle assessment. *J. Cleaner Prod.* **2017**, *162*, 1135-1143. DOI: 10.1016/j.jclepro.2017.06.067
233. Petrescu, L.; Cormos, C. C., Environmental assessment of IGCC power plants with pre-combustion CO<sub>2</sub> capture by chemical & calcium looping methods. *J. Cleaner Prod.* **2017**, *158*, 233-244. DOI: 10.1016/j.jclepro.2017.05.011

234. Petrescu, L.; Bonalumi, D.; Valenti, G.; Cormos, A. M.; Cormos, C. C., Life cycle assessment for supercritical pulverized coal power plants with post-combustion carbon capture and storage. *J. Cleaner Prod.* **2017**, *157*, 10-21. DOI: 10.1016/j.jclepro.2017.03.225
235. Rahman, K. M.; Melville, L.; Fulford, D.; Huq, S. M. I., Green-house gas mitigation capacity of a small scale rural biogas plant calculations for Bangladesh through a general life cycle assessment. *Waste Manage. Res.* **2017**, *35*, (10), 1023-1033. DOI: 10.1177/0734242X17721341
236. Ramachandran, S.; Yao, Z.; You, S.; Massier, T.; Stimming, U.; Wang, C. H., Life cycle assessment of a sewage sludge and woody biomass co-gasification system. *Energy* **2017**, *137*, 369-376. DOI: 10.1016/j.energy.2017.04.139
237. Stougie, L.; Tsalidis, G. A.; van der Kooi, H. J.; Korevaar, G., Environmental and exergetic sustainability assessment of power generation from biomass. *Renewable Energy* **2018**, *128*, 520-528. DOI: 10.1016/j.renene.2017.06.046
238. Sundaram, S.; Kolb, G.; Hessel, V.; Wang, Q., Energy-efficient routes for the production of gasoline from biogas and pyrolysis oil - process design and life-cycle assessment. *Ind. Eng. Chem. Res.* **2017**, *56*, (12), 3373-3387. DOI: 10.1021/acs.iecr.6b04611
239. Uusitalo, V.; Väisänen, S.; Inkeri, E.; Soukka, R., Potential for greenhouse gas emission reductions using surplus electricity in hydrogen, methane and methanol production via electrolysis. *Energy Convers. Manage.* **2017**, *134*, 125-134. DOI: 10.1016/j.enconman.2016.12.031
240. Valli, L.; Rossi, L.; Fabbri, C.; Sibilla, F.; Gattoni, P.; Dale, B. E.; Kim, S.; Ong, R. G.; Bozzetto, S., Greenhouse gas emissions of electricity and biomethane produced using the Biogasdoneright™ system: four case studies from Italy. *Biofuels, Bioprod. Biorefin.* **2017**, *11*, (5), 847-860. DOI: 10.1002/bbb.1789
241. Wagner, M.; Lewandowski, I., Relevance of environmental impact categories for perennial biomass production. *GCB Bioenergy* **2017**, *9*, (1), 215-228. DOI: 10.1111/gcbb.12372
242. Wang, W. C.; Teah, H. Y., Life cycle assessment of small-scale horizontal axis wind turbines in Taiwan. *J. Cleaner Prod.* **2017**, *141*, 492-501. DOI: 10.1016/j.jclepro.2016.09.128
243. Wang, X.; Guo, F.; Li, Y.; Yang, X., Effect of pretreatment on microalgae pyrolysis: Kinetics, biocrude yield and quality, and life cycle assessment. *Energy Convers. Manage.* **2017**, *132*, 161-171. DOI: 10.1016/j.enconman.2016.11.006
244. Winjobi, O.; Zhou, W.; Kulas, D.; Nowicki, J.; Shonnard, D. R., Production of hydrocarbon fuel using two-step torrefaction and fast pyrolysis of pine. Part 2: Life-cycle

- carbon footprint. *ACS Sustainable Chemistry and Engineering* **2017**, *5*, (6), 4541-4551. DOI: 10.1021/acssuschemeng.7b00373
245. Woytiuk, K.; Sanscartier, D.; Amichev, B. Y.; Campbell, W.; Van Rees, K., Life-cycle assessment of torrefied coppice willow co-firing with lignite coal in an existing pulverized coal boiler. *Biofuels, Bioprod. Biorefin.* **2017**, *11*, (5), 830-846. DOI: 10.1002/bbb.1788
246. Monroy-Loperena, R., A note on the analytical solution of cubic equations of state in process simulation. *Ind. Eng. Chem. Res.* **2012**, *51*, (19), 6972-6976. DOI: 10.1021/ie2023004
247. Mohitpour, M.; Golshan, H.; Murry, A., *Pipeline Design & Construction: A Practical Approach*. 3rd ed.; American Society of Mechanical Engineers: New York, NY, 2007.
248. Haddad, J.; Behbahani, R. M., Optimization of a natural gas transmission system. *Int. J. Comput. Appl. Technol.* **2013**, *66*, (11), 35-42.
249. Alliance Pipeline Ltd. *Comprehensive study report*; National Energy Board: Ottawa, July 3, 1997, 1998.
250. Moshfeghian, D. M. *Compressor Calculations: Rigorous Using Equation of State vs Shortcut Method*; PetroSkills: jcambell.com, 2011.
251. NOVA Gas Transmission Ltd. *B03 - NOVA Gas Transmission Ltd. - Northwest Mainline Expansion Application (A29090)*; National Energy Board: Ottawa, 2011.
252. Zéberg-Mikkelsen, C. K.; Quiñones-Cisneros, S. E.; Stenby, E. H., Viscosity prediction of hydrogen + natural gas mixtures (hythane). *Ind. Eng. Chem. Res.* **2001**, *40*, (13), 2966-2970. DOI: 10.1021/ie0010464
253. Chung, T. H.; Ajlan, M.; Lee, L. L.; Starling, K. E., Generalized multiparameter correlation for nonpolar and polar fluid transport properties. *Ind. Eng. Chem. Res.* **1988**, *27*, (4), 671-679. DOI: 10.1021/ie00076a024
254. Zéberg-Mikkelsen, C. K.; Quiñones-Cisneros, S. E.; Stenby, E. H., Viscosity modeling of light gases at supercritical conditions using the friction theory. *Ind. Eng. Chem. Res.* **2001**, *40*, (17), 3848-3854. DOI: 10.1021/ie000987d
255. Wilke, C. R., A viscosity equation for gas mixtures. *J Chem Phys* **1950**, *18*, (4), 517-519. DOI: 10.1063/1.1747673
256. Quiñones-Cisneros, S. E.; Zéberg-Mikkelsen, C. K.; Stenby, E. H., One parameter friction theory models for viscosity. *Fluid Phase Equilib.* **2001**, *178*, (1), 1-16. DOI: 10.1016/S0378-3812(00)00474-X

257. Schmidt, K. A. G.; Quiñones-Cisneros, S. E.; Carroll, J. J.; Kvamme, B., Hydrogen sulfide viscosity modeling. *Energy Fuels* **2008**, *22*, (5), 3424-3434. DOI: 10.1021/ef700701h
258. Ahmed, T., Chapter 15 - Vapor-Liquid Phase Equilibria. In *Reservoir Engineering Handbook (Fifth Edition)*, Ahmed, T., Ed. Gulf Professional Publishing: 2019; pp 1109-1225.

## Appendix A: Surveyed Papers

### A.1. Scopus Survey Filter

The following search string was used in Scopus on February 18, 2018:

```
( TITLE-ABS-KEY ( [Life Cycle Assessment] ) OR TITLE-ABS-KEY ( [Life Cycle Analysis] ) OR TITLE-ABS-KEY ( [LCA] ) )  
AND ( TITLE-ABS-KEY ( energy ) OR TITLE-ABS-KEY ( fuel ) ) AND ( LIMIT-TO ( SRCTYPE , "j" ) ) AND ( EXCLUDE ( SUBJAREA , "MEDI" ) OR EXCLUDE ( SUBJAREA , "BIOC" ) OR EXCLUDE ( SUBJAREA , "IMMU" ) OR EXCLUDE ( SUBJAREA , "PHAR" ) OR EXCLUDE ( SUBJAREA , "VETE" ) ) AND ( LIMIT-TO ( PUBYEAR , 2017 ) ) AND ( LIMIT-TO ( LANGUAGE , "English" ) ) AND ( LIMIT-TO ( EXACTKEYWORD , "Greenhouse Gases" ) OR LIMIT-TO ( EXACTKEYWORD , "Global Warming" ) ) AND ( EXCLUDE ( EXACTKEYWORD , "Costs" ) OR EXCLUDE ( EXACTKEYWORD , "Economics" ) OR EXCLUDE ( EXACTKEYWORD , "Economic Analysis" ) OR EXCLUDE ( EXACTKEYWORD , "Cost Benefit Analysis" ) OR EXCLUDE ( EXACTKEYWORD , "Recycling" ) OR EXCLUDE ( EXACTKEYWORD , "Economic And Social Effects" ) OR EXCLUDE ( EXACTKEYWORD , "Investments" ) OR EXCLUDE ( EXACTKEYWORD , "Environmental Economics" ) OR EXCLUDE ( EXACTKEYWORD , "Cost Analysis" ) OR EXCLUDE ( EXACTKEYWORD , "Commerce" ) )
```

## A.2. Surveyed Work

The surveyed work is listed below; a value of 1 in the adjacent columns indicates the study included the specified analysis. The column headers are sensitivity, one-at-a-time (OAT), factored design of experiments (Factored), uncertainty, Monte Carlo (MC), best worst case scenarios (BWCS), and contribution of variance (COV) analysis.

**Table A1: Overview of surveyed papers**

<b>Paper Name</b>	<b>Author</b>	<b>Sensitivity</b>	<b>OAT</b>	<b>Factored</b>	<b>Uncertainty</b>	<b>MC</b>	<b>BWCS</b>	<b>COV</b>
<b>Life cycle assessment of a future central receiver solar power plant and autonomous operated heliostat concepts</b>	Telsnig et al. <sup>195</sup>	1	1	0	0	0	0	0
<b>Environmental impacts of producing bioethanol and biobased lactic acid from standalone and integrated biorefineries using a consequential and an attributional life cycle assessment approach</b>	Parajuli et al. <sup>196</sup>	1	1	0	0	0	0	0
<b>Potential pyrolysis pathway assessment for microalgae-based aviation fuel based on energy conversion efficiency and life cycle</b>	Guo et al. <sup>197</sup>	1	1	0	0	0	0	0
<b>Lifecycle GHG emissions of palm biodiesel: Unintended market effects negate direct benefits of the Malaysian Economic Transformation Plan (ETP)</b>	Abdul-Manan <sup>67</sup>	1	0	1	1	1	0	0
<b>Life Cycle Assessment of Power-to-Gas: Approaches, system variations and their environmental implications</b>	Zhang et al. <sup>84</sup>	1	1	1	0	0	0	0
<b>Life cycle assessment of seaweed biomethane, generated from seaweed sourced from integrated multi-trophic aquaculture in temperate oceanic climates</b>	Czyrnek-Delêtre et al. <sup>83</sup>	1	1	1	0	0	0	0
<b>Life cycle assessment of waste-to-energy (WtE) technologies for electricity generation using municipal solid waste in Nigeria</b>	Ayodele et al. <sup>198</sup>	0	0	0	0	0	0	0

<b>Paper Name</b>	<b>Author</b>	<b>Sensitivity</b>	<b>OAT</b>	<b>Factored</b>	<b>Uncertainty</b>	<b>MC</b>	<b>BWCS</b>	<b>COV</b>
<b>Life cycle assessment of thermal energy production from short-rotation willow biomass in Southern Ontario, Canada</b>	Dias et al. <sup>199</sup>	1	1	0	0	0	0	0
<b>Comparative life cycle assessment of hydrogen, methanol and electric vehicles from well to wheel</b>	Bicer et al. <sup>86</sup>	0	0	0	1	1	0	0
<b>Life cycle assessment of nuclear-based hydrogen and ammonia production options: A comparative evaluation</b>	Bicer et al. <sup>200</sup>	1	1	0	0	0	0	0
<b>Uncertainty in well-to-tank with combustion greenhouse gas emissions of transportation fuels derived from North American crudes</b>	Di Lullo et al. <sup>44</sup>	1	1	0	1	1	0	1
<b>Environmental performance evaluation of a grid-independent solar photovoltaic power generation (SPPG) plant</b>	Akinyele <sup>201</sup>	1	0	1	0	0	0	0
<b>Aqueous hybrid ion batteries – An environmentally friendly alternative for stationary energy storage?</b>	Peters et al. <sup>202</sup>	1	1	0	0	0	0	0
<b>The policy recommendations on cassava ethanol in China: Analyzed from the perspective of life cycle “2E &amp; W”</b>	Zhang et al. <sup>203</sup>	1	1	0	0	0	0	0
<b>Evaluating the environmental impacts of bio-hydrogenated diesel production from palm oil and fatty acid methyl ester through life cycle assessment</b>	Boonrod et al. <sup>204</sup>	0	0	0	0	0	0	0
<b>Environmental life cycle assessment of biogas production from marine macroalgal feedstock for the substitution of energy crops</b>	Ertem et al. <sup>205</sup>	0	0	0	0	0	0	0
<b>Generating low-carbon heat from biomass: Life cycle assessment of bioenergy scenarios</b>	Welfle et al. <sup>82</sup>	1	0	1	0	0	0	0
<b>Land use change implications for large-scale cultivation of algae feedstocks in the United States Gulf Coast</b>	Handler et al. <sup>206</sup>	1	1	1	0	0	0	0
<b>Coupling sorghum biomass and wheat straw to minimise the environmental impact of bioenergy production</b>	Serra et al. <sup>207</sup>	1	1	0	0	0	0	0
<b>Comparative assessment of the environmental impacts of nuclear, wind and hydro-electric power plants in Ontario: A life cycle</b>	Siddiqui et al. <sup>208</sup>	1	1	0	0	0	0	0

<b>Paper Name</b>	<b>Author</b>	<b>Sensitivity</b>	<b>OAT</b>	<b>Factored</b>	<b>Uncertainty</b>	<b>MC</b>	<b>BWCS</b>	<b>COV</b>
<b>assessment</b>								
<b>Life Cycle Assessment of microtubular solid oxide fuel cell based auxiliary power unit systems for recreational vehicles</b>	Benveniste et al. <sup>92</sup>	1	1	0	1	1	0	0
<b>LCA perspective to assess the environmental impact of a novel PCM-based cold storage unit for the civil air conditioning</b>	De Falco et al. <sup>209</sup>	1	1	0	0	0	0	0
<b>A life cycle assessment of oxymethylene ether synthesis from biomass-derived syngas as a diesel additive</b>	Mahbub et al. <sup>210</sup>	1	1	0	0	0	0	0
<b>Environmental analysis of Spirulina cultivation and biogas production using experimental and simulation approach</b>	Rodríguez et al. <sup>211</sup>	0	0	0	0	0	0	0
<b>Carbon footprints of two large hydro-projects in China: Life-cycle assessment according to ISO/TS 14067</b>	Li et al. <sup>97</sup>	1	1	0	1	1	0	1
<b>Changes in carbon footprint when integrating production of filamentous fungi in 1st generation ethanol plants</b>	Brancoli et al. <sup>212</sup>	1	0	1	0	0	0	0
<b>Transportation biofuel efficiencies from cultivated feedstock in the boreal climate zone: Case Finland</b>	Uusitalo et al. <sup>105</sup>	0	0	0	1	0	1	0
<b>Alternative fuel for sustainable shipping across the Taiwan Strait</b>	Hua et al. <sup>213</sup>	1	1	0	0	0	0	0
<b>Environmental impact and sustainability study on biofuels for transportation applications</b>	Chang et al. <sup>214</sup>	1	0	1	0	0	0	0
<b>Life cycle assessment (LCA) of digested sewage sludge incineration for heat and power production</b>	Abuşoğlu et al. <sup>215</sup>	0	0	0	0	0	0	0
<b>Life cycle assessment of photovoltaic manufacturing consortium (PVMC) copper indium gallium (di)selenide (CIGS) modules</b>	Amarakoon et al. <sup>96</sup>	1	1	0	1	0	1	0
<b>Carbon Footprint and Energy Analysis of Bio-CH<sub>4</sub> from a Mixture of Food Waste and Dairy Manure in Denver, Colorado</b>	Ankathi et al. <sup>216</sup>	0	0	0	0	0	0	0
<b>Are district heating systems and renewable energy sources always an environmental win-win solution? A life cycle assessment case study in Tuscany, Italy</b>	Bartolozzi et al. <sup>217</sup>	0	0	0	0	0	0	0
<b>Accounting for GHG net reservoir emissions of hydropower in</b>	Briones Hidrovo et al. <sup>87</sup>	1	1	0	1	1	0	0

<b>Paper Name</b>	<b>Author</b>	<b>Sensitivity</b>	<b>OAT</b>	<b>Factored</b>	<b>Uncertainty</b>	<b>MC</b>	<b>BWCS</b>	<b>COV</b>
<b>Ecuador</b>								
<b>Spatially Explicit Life Cycle Analysis of Cellulosic Ethanol Production Scenarios in Southwestern Michigan</b>	Cronin et al. <sup>218</sup>	1	0	1	1	0	0	0
<b>Life cycle assessment of a mallee eucalypt jet fuel</b>	Crossin <sup>88</sup>	1	1	0	1	1	0	0
<b>Life cycle assessment of fuel ethanol produced from soluble sugar in sweet sorghum stalks in North China</b>	Ding et al. <sup>219</sup>	1	1	0	0	0	0	0
<b>Bioenergy and bioproducts from municipal organic waste as alternative to landfilling: a comparative life cycle assessment with prospective application to Mexico</b>	Escamilla-Alvarado et al. <sup>220</sup>	1	1	0	0	0	0	0
<b>Streamlined life cycle analysis for assessing energy and exergy performance as well as impact on the climate for landfill gas utilization technologies</b>	Friesenhan et al. <sup>221</sup>	1	1	0	0	0	0	0
<b>Life cycle analysis of coal-based synthetic natural gas for heat supply and electricity generation in China</b>	Gao et al. <sup>222</sup>	0	0	0	0	0	0	0
<b>Cultivating <i>Ciona intestinalis</i> to counteract marine eutrophication: Environmental assessment of a marine biomass based bioenergy and biofertilizer production system</b>	Hackl et al. <sup>223</sup>	1	1	0	0	0	0	0
<b>Assessment of the carbon footprint, social benefit of carbon reduction, and energy payback time of a high-concentration photovoltaic system</b>	Hu et al. <sup>224</sup>	1	0	1	0	0	0	0
<b>Opportunity and challenge of seaweed bioethanol based on life cycle CO<sub>2</sub> assessment</b>	Jung et al. <sup>93</sup>	0	0	0	1	1	0	1
<b>Review of the life cycle greenhouse gas emissions from different photovoltaic and concentrating solar power electricity generation systems</b>	Kommalapati et al. <sup>225</sup>	0	0	0	0	0	0	0
<b>Life cycle assessment (LCA) of biogas versus dung combustion household cooking systems in developing countries – A case study in Ethiopia</b>	Lansche et al. <sup>81</sup>	1	1	0	1	0	1	0

<b>Paper Name</b>	<b>Author</b>	<b>Sensitivity</b>	<b>OAT</b>	<b>Factored</b>	<b>Uncertainty</b>	<b>MC</b>	<b>BWCS</b>	<b>COV</b>
<b>Evaluation of landfill gas emissions from municipal solid waste landfills for the life-cycle analysis of waste-to-energy pathways</b>	Lee et al. <sup>226</sup>	1	1	0	0	0	0	0
<b>Realizing low life cycle energy use and GHG emissions in coal based polygeneration with CO<sub>2</sub> capture</b>	Li et al. <sup>109</sup>	0	0	0	1	0	1	0
<b>TC2015: Life cycle analysis of co-formed coal fines and hydrochar produced in twin-screw extruder (TSE)</b>	Liu et al. <sup>91</sup>	1	1	0	1	1	0	0
<b>Environmental impacts of electricity production of micro wind turbines with vertical axis</b>	Lombardi et al. <sup>227</sup>	1	0	1	0	0	0	0
<b>Life cycle assessment of palm-derived biodiesel in Taiwan</b>	Maharjan et al. <sup>228</sup>	0	0	0	0	0	0	0
<b>Life cycle assessment of feedstock supply systems for cellulosic biorefineries using corn stover transported in conventional bale and densified pellet formats</b>	Manandhar et al. <sup>98</sup>	1	1	0	1	1	0	0
<b>A life cycle assessment of perovskite/silicon tandem solar cells</b>	Monteiro Lunardi et al. <sup>229</sup>	1	1	0	0	0	0	0
<b>Life cycle assessment of co-firing coal and wood pellets in the Southeastern United States</b>	Morrison et al. <sup>230</sup>	1	0	1	0	0	0	0
<b>Life-cycle greenhouse gas and water intensity of cellulosic biofuel production using cholinium lysinate ionic liquid pretreatment</b>	Neupane et al. <sup>106</sup>	1	1	0	1	0	1	0
<b>Life cycle analysis of bitumen transportation to refineries by rail and pipeline</b>	Nimana et al. <sup>90</sup>	1	1	0	1	1	0	1
<b>Environmental life cycle assessment of producing willow, alfalfa and straw from spring barley as feedstocks for bioenergy or biorefinery systems</b>	Parajuli et al. <sup>231</sup>	1	1	0	0	0	0	0
<b>Environmental performance of manure co-digestion with natural and cultivated grass – A consequential life cycle assessment</b>	Pehme et al. <sup>232</sup>	1	1	0	0	0	0	0
<b>Environmental assessment of IGCC power plants with pre-combustion CO<sub>2</sub> capture by chemical &amp; calcium looping methods</b>	Petrescu et al. <sup>233</sup>	0	0	0	0	0	0	0
<b>Life Cycle Assessment for supercritical pulverized coal power plants with post-combustion carbon capture and storage</b>	Petrescu et al. <sup>234</sup>	0	0	0	0	0	0	0

<b>Paper Name</b>	<b>Author</b>	<b>Sensitivity</b>	<b>OAT</b>	<b>Factored</b>	<b>Uncertainty</b>	<b>MC</b>	<b>BWCS</b>	<b>COV</b>
<b>Green-house gas mitigation capacity of a small scale rural biogas plant calculations for Bangladesh through a general life cycle assessment</b>	Rahman et al. <sup>235</sup>	0	0	0	0	0	0	0
<b>Life cycle assessment of a sewage sludge and woody biomass co-gasification system</b>	Ramachandran et al. <sup>236</sup>	1	1	0	0	0	0	0
<b>Waste wood as bioenergy feedstock. Climate change impacts and related emission uncertainties from waste wood based energy systems in the UK</b>	Röder et al. <sup>107</sup>	1	1	1	1	0	1	0
<b>Environmental and exergetic sustainability assessment of power generation from biomass</b>	Stougie et al. <sup>237</sup>	1	0	1	0	0	0	0
<b>Energy-efficient routes for the production of gasoline from biogas and pyrolysis oil - process design and life-cycle assessment</b>	Sundaram et al. <sup>238</sup>	0	0	0	0	0	0	0
<b>Meta-analysis and harmonization of life cycle assessment studies for algae biofuels</b>	Tu et al. <sup>24</sup>	0	0	0	1	1	0	0
<b>Potential for greenhouse gas emission reductions using surplus electricity in hydrogen, methane and methanol production via electrolysis</b>	Uusitalo et al. <sup>239</sup>	1	1	0	0	0	0	0
<b>Greenhouse gas emissions of electricity and biomethane produced using the Biogasdoneright™ system: four case studies from Italy</b>	Valli et al. <sup>240</sup>	0	0	0	0	0	0	0
<b>Environmental impacts of lithium metal polymer and lithium-ion stationary batteries</b>	Vandepaer et al. <sup>89</sup>	1	1	0	1	1	0	0
<b>Relevance of environmental impact categories for perennial biomass production</b>	Wagner et al. <sup>241</sup>	0	0	0	0	0	0	0
<b>Life cycle assessment of small-scale horizontal axis wind turbines in Taiwan</b>	Wang et al. <sup>242</sup>	0	0	0	0	0	0	0
<b>Effect of pretreatment on microalgae pyrolysis: Kinetics, biocrude yield and quality, and life cycle assessment</b>	Wang et al. <sup>243</sup>	0	0	0	0	0	0	0
<b>Production of hydrocarbon fuel using two-step torrefaction and fast</b>	Winjobi et al. <sup>244</sup>	1	1	1	0	0	0	0

<b>Paper Name</b>	<b>Author</b>	<b>Sensitivity</b>	<b>OAT</b>	<b>Factored</b>	<b>Uncertainty</b>	<b>MC</b>	<b>BWCS</b>	<b>COV</b>
<b>pyrolysis of pine. Part 2: life-cycle carbon footprint</b>								
<b>Life-cycle assessment of torrefied coppice willow co-firing with lignite coal in an existing pulverized coal boiler</b>	Woytiuk et al. <sup>245</sup>	1	0	1	0	0	0	0
<b>Life cycle performance of cellulosic ethanol and corn ethanol from a retrofitted dry mill corn ethanol plant</b>	Zhang et al. <sup>108</sup>	1	1	1	0	0	1	0

## Appendix B: NGTL Functions

To determine the compressor energy requirements, custom Excel functions were written to calculate the gas viscosity and compressibility, pipeline pressure drop, and compressor power required. Additional calculations for determining emissions associated with end-of-life nitrogen purging are also included.

### B.1. Natural Gas Viscosity<sup>4</sup>

The gas viscosity is calculated using a correlation by Carr et al.<sup>156</sup> that uses the gas gravity as well as nitrogen, carbon dioxide, and hydrogen sulfide molar fractions (Eq. B1-B6).

The gas viscosity at atmospheric pressure is given by:

$$\mu = \mu_{HC} + \mu_{N_2} + \mu_{CO_2} + \mu_{H_2S} \quad (\text{Eq. B1})$$

$$\mu_{HC} = 8.188 * 10^{-3} - 6.15 * 10^{-3} \log(\gamma) + (1.709 * 10^{-5} - 2.062 * 10^{-6} \gamma) * T \quad (\text{Eq. B2})$$

$$\mu_{N_2} = [9.59 * 10^{-3} + 8.48 * 10^{-3} \log(\gamma)] * y_{N_2} \quad (\text{Eq. B3})$$

$$\mu_{CO_2} = [6.24 * 10^{-3} + 9.08 * 10^{-3} \log(\gamma)] * y_{CO_2} \quad (\text{Eq. B4})$$

$$\mu_{H_2S} = [3.73 * 10^{-3} + 8.49 * 10^{-3} \log(\gamma)] * y_{H_2S} \quad (\text{Eq. B5})$$

where  $\gamma$  is the gas gravity and  $y$  is the molar fraction.

The custom Excel function is defined as:

$$\text{GasViscositySTD}(\gamma, y_{N_2}, y_{CO_2}, y_{H_2S}) \quad (\text{Eq. B6})$$

## B.2. Peng-Robinson

The gas compressibility factor,  $Z$ , is determined using the Peng-Robinson equation of state for mixtures and depends on the gas temperature, pressure, molar composition, and component acentric factors. The cubic root of the Peng-Robinson equation is approximated using Cardano's method. The largest root is the compressibility factor for the gas,  $Z$ . Once  $Z$  is determined, it is plugged back into the Peng-Robinson equation to check its accuracy. If the absolute is greater than  $10e-6$ , the Newton-Raphson method is used to calculate the root. To ensure the solver does not overshoot the correct root and converge to one of the smaller roots, an initial guess of  $Z = +0.05$  is used and the maximum step size is set to 10% of the current  $Z$  estimate. The solver terminates when the change in the  $Z$  value is less than 0.001.

The general cubic equation of state is:

$$p = \frac{RT}{v - b_m} - \frac{a_m}{(v^2 + 2vb_m - b_m^2)} \quad (\text{Eq. B7})$$

where  $P$  is pressure in MPa,  $T$  is temperature in K,  $R$  is the gas constant in  $\text{m}^3\text{MPa/mol.K}$ , and  $v$  is the volume in  $\text{m}^3/\text{mol}$ . When  $Z$  is defined as:

$$Z = \frac{pv}{RT} \quad (\text{Eq. B8})$$

the cubic equation can be rewritten as:

$$Z^3 + C_1 * Z^2 + C_2 * Z + C_3 = 0 \quad (\text{Eq. B9})$$

where the coefficients are defined as:

$$C_1 = \frac{-1}{B} \quad (\text{Eq. B10})$$

$$C_2 = A - 3 * B^2 - 2 * B \quad (\text{Eq. B11})$$

$$C_3 = -(A * B - B^2 - B^3) \quad (\text{Eq. B12})$$

where  $A$  and  $B$  are dimensionless parameters:

$$A = \frac{a_m * P}{(R * T)^2} \quad (\text{Eq. B13})$$

$$B = \frac{b_m * P}{R * T} \quad (\text{Eq. B14})$$

and  $a_m$  and  $b_m$  are the attraction and repulsion parameters of the gas mixture:

$$a_m = \sum_{i=1}^n \sum_{j=1}^n m_i * m_j (1 - k_{ij}) \sqrt{a_i * a_j} \quad (\text{Eq. B15})$$

$$b_m = \sum_{i=1}^n m_i * b_i \quad (\text{Eq. B16})$$

The binary interaction parameters,  $k_{ij}$ , are taken from Aspen HYSYS.<sup>50</sup> The attraction and repulsion parameters of the pure components are calculated as:

$$a = 0.457 * \frac{R^2 * T_c^2}{P_c} \left[ 1 + \kappa \left( 1 - \sqrt{\frac{T}{T_c}} \right) \right]^2 \quad (\text{Eq. B17})$$

$$b = 0.0778 * \frac{R * T_c}{P_c} \quad (\text{Eq. B18})$$

where  $T_c$  and  $P_c$  are the critical temperature and pressure in K and MPa, respectively. The parameter  $\kappa$  is a function of the acentric factor,  $\omega$ :

$$\kappa = 0.37464 + 1.54226\omega - 0.26992\omega^2 \quad (\text{Eq. B19})$$

Once the coefficients  $C_1$ ,  $C_2$ , and  $C_3$  are calculated, the cubic roots can be approximated using Cardano's method.<sup>246</sup>

$$Q = \frac{C_1^2 - 3C_2}{9} \quad (\text{Eq. B20})$$

$$r = \frac{2C_1^3 - 9C_1C_2 + 27C_3}{54} \quad (\text{Eq. B21})$$

If  $r^2 \leq Q^3$ , then three real roots exist and are calculated as:

$$\theta = \cos^{-1} \frac{r}{Q^{3/2}} \quad (\text{Eq. B22})$$

$$Z_1 = -2Q^{0.5} \cos\left(\frac{\theta}{3}\right) - \frac{C_1}{3} \quad (\text{Eq. B23})$$

$$Z_2 = -2Q^{0.5} \cos\left(\frac{\theta + 2\pi}{3}\right) - \frac{C_1}{3} \quad (\text{Eq. B24})$$

$$Z_3 = -2Q^{0.5} \cos\left(\frac{\theta - 2\pi}{3}\right) - \frac{C_1}{3} \quad (\text{Eq. B25})$$

If  $r^2 > Q^3$ , then we assume a positive square root and calculate:

$$D = -1 * \text{Sgn}(r) \left( |r| + \sqrt{r^2 - Q^3} \right)^{\frac{1}{3}} \quad (\text{Eq. B26})$$

If  $D = 0$ , then  $E = 0$ , otherwise:

$$E = \frac{Q}{D} \quad (\text{Eq. B27})$$

The 1<sup>st</sup> root is:

$$Z_1 = D + E - \frac{C_1}{3} \quad (\text{Eq. B28})$$

If  $D \neq E$ , then the remaining roots are zero; otherwise:

$$Z_2 = Z_3 = -\frac{(D + E)}{2} - \frac{C_1}{3} \quad (\text{Eq. B29})$$

The largest root is the compressibility factor for the gas,  $Z$ . Once  $Z$  is determined, it is plugged back into Eq. B9 to check its accuracy. If the absolute value of Eq. B9 is greater than  $10\text{e-}6$ , the Newton-Raphson method is used to calculate the root. To ensure the solver does not overshoot the correct root and converge to one of the smaller roots, an initial guess of  $Z + 0.05$  is used and the maximum step size is set to 10% of the current  $Z$  estimate. The solver terminates when the change in the  $Z$  value is less than 0.001.

The custom Excel formula is:

$$\text{PengRob}(T, P, \text{molfrac}) \quad (\text{Eq. B30})$$

The user highlights the molar composition as a range ordered methane, ethane, propane, butane, pentane, carbon dioxide, hydrogen sulfide, and nitrogen.

### **B.3. Compressor Power**

The compressor inlet and outlet pressure are calculated as:

$$P_{\text{Comp.In}} = P_{\text{Pipe.Out}} - 0.5\Delta P_{\text{Facility}} - \Delta P_{\text{Scrubber}} \quad (\text{Eq. B31})$$

$$P_{\text{Comp.Out}} = P_{\text{Pipe.In}} + 0.5\Delta P_{\text{Facility}} \quad (\text{Eq. B32})$$

where  $\Delta P_{\text{Scrubber}}$  and  $\Delta P_{\text{Facility}}$  are the scrubber and facility piping pressure drops, respectively, in MPa. The compression ratio, CR, is dependent on the compressor pressures and the interstage cooler pressure drop. First, the number of stages are calculated as:

$$N_{Stages} = \ln \frac{\frac{P_{Comp.Out}}{P_{Comp.In}}}{1 + \Delta P_{Cooler}} \bigg/ \ln \frac{CR_{max}}{1 + \Delta P_{Cooler}} \quad (\text{Eq. B33})$$

where all pressures are in MPa, except  $\Delta P_{Cooler}$ , which is a percentage. The actual CR is calculated from either the calculated or user-specified number of stages as:

$$CR = \left[ \frac{P_{Comp.Out}}{P_{Comp.In}} * (1 + \Delta P_{Cooler})^{N_{Stages}-1} \right]^{1/N_{Stages}} \quad (\text{Eq. B34})$$

The compressor power is then calculated using a custom Excel function. Internally, the outlet temperature and compressibility factor are iteratively calculated for each stage. The heat capacity ratio is determined using the gas composition. An iterative approach is used were  $Z_{out}$  is assumed to be 1 for the first iteration and then calculated using the PengRob function, which is dependent on the outlet temperature. The iteration terminates either after 20 iterations or when the relative error in  $Z_{out}$  is less than 0.1%. The inlet temperature is taken as the pipeline outlet temperature for the 1<sup>st</sup> stage and as the cooler outlet temperature for the remaining stages. The interstage and outlet coolers drop the natural gas temperature down to 25-50°C; the base case assumes 40°C<sup>247-249</sup>.

The outlet temperature is calculated using equations from Mohitpour et al.<sup>247</sup> and Moshfeghian<sup>250</sup>:

$$T_{out} = T_{in} * CR^{\frac{k-1}{k*\eta_p}} \quad (\text{Eq. B35})$$

where  $T_{out}$  and  $T_{in}$  are the compressor temperatures in K,  $k$  is the heat capacity ratio, and  $\eta_p$  is the polytrophic efficiency.

The compressor power for each stage is then calculated using equations from Mohitpour et al.<sup>247</sup> as:

$$\frac{HP}{MMSCFD} = 0.15426 * \frac{k}{k-1} \frac{T_{in}}{\eta_M} * \frac{Z_{in} + Z_{out}}{2} * \left( CR^{\frac{k-1}{k*\eta_A}} - 1 \right) \quad (\text{Eq. B36})$$

where  $\eta_M$  and  $\eta_p$  are the mechanical and polytropic efficiencies. The total compressor power in kW is:

$$Power = \sum_{i=1}^{N_{Stages}} HP_i * \frac{0.7457}{1177.17} * Q \quad (\text{Eq. B37})$$

where  $Q$  is the flow rate in m<sup>3</sup>/hr. The custom 2 x 1 array Excel function for the compressor power is defined as:

$$CompressorPower(T_{In}, T_{Cooler}, N_{Stages}, CR, P_{Comp.In}, \gamma, \eta_p, \eta_M, molfrac, P_{Pipe.Out}, \Delta P_{Facility}, \Delta P_{Cooler}, PowerLimit, Q) \quad (\text{Eq. B38})$$

with the compressor power in kW and the outlet pressure in MPa as outputs.

If the power required is larger than the station power limit, the outlet pressure is iteratively reduced. A simple step algorithm is used with the error equal to the power required minus the power limit. Pressure step sizes of -0.5, +0.05, and -0.01 MPa are used. The step size changes when the error value switches from positive to negative or vice versa. The function outputs both the compressor power requirement and pipeline inlet pressure. If the power is limited by the station limit, a cascade effect will occur wherein the pressure drops as the gas travels down the pipeline.

The compressor power calculation accuracy is verified using Aspen HYSYS and is accurate within  $\pm 2\%$ .<sup>50</sup>

### B.3.1. Compressor power calculation updates

The following modifications were made to the compressor power macro in Di Lullo et al.<sup>5</sup>:

1. Density is calculated using the GERG model instead of Equation B43

2. Compressibility is now calculated using the GERG model instead of the Peng-Robinson macro
3. The gas-specific heat ratio ( $k$ ) is calculated using GERG rather than being supplied by the user with  $k_{avg} = (k_{inlet} + k_{outlet})/2$
4. The molecular weight is calculated using GERG rather than assuming a typical value
5. Equation B36 is updated to account for the mixture's specific molecular weight

$$Intensity = \frac{k}{k-1} \frac{T_{in} * R}{MW} * \frac{Z_{in} + Z_{out}}{2} * \left( CR^{\frac{k-1}{k*\eta_p}} - 1 \right) \quad \text{Eq. B36}$$

where *Intensity* is in MPa-m<sup>3</sup>/g,  $\eta_p$  is the polytrophic efficiency,  $T_{in}$  is the compressor inlet temperature in K,  $Z_{in}$  and  $Z_{out}$  are the inlet and outlet compressibility factors,  $k$  is the heat capacity ratio,  $CR$  is the compression ratio,  $MW$  is the molecular weight in g/mol, and  $R$  is the ideal gas constant in MPa-m<sup>3</sup>/K-mol.

The old Equation B37 for the total compressor power in kW is now:

$$Power = \sum_{i=1}^{N_{Stages}} Intensity_i * \frac{\rho_s}{\eta_M * \eta_p} * Q * \frac{1000 \text{ g}}{1 \text{ kg}} * \frac{1000 \text{ kW}}{1 \text{ MW}} * \frac{1 \text{ hr}}{3600 \text{ s}} \quad \text{Eq. B37}$$

where  $\eta_M$  is the mechanical efficiency and  $\rho_s$  is the density at standard conditions in m<sup>3</sup>/hr. The unit conversions are used to cancel out the MPa unit, which is equal to 1,000,000 kg-J/m<sup>3</sup>.

#### **B.4. Pipeline Pressure Drop**

The user must specify either the inlet or outlet pressure and the function will calculate the other pressure. This is useful as it allows the user to specify a delivery pressure and then calculate the required compressor pressure. If a parallel is used, an iterative approach is used to determine the flow rate for both pipelines; the user must supply an initial guess for the flow rate split between the two Chapters.

The Reynold number is calculated as:

$$Re = \frac{1.5616 * Q * G}{\mu * D} \quad (\text{Eq. B39})$$

where  $Q$  is the flow rate in  $\text{m}^3/\text{s}$ ,  $G$  is the gas gravity,  $\mu$  is the gas viscosity in  $P$ , and  $D$  is the diameter in  $\text{m}$ .

An initial friction factor/transmission factor estimate is determined from the White equation:<sup>158</sup>

$$tr = \sqrt{\frac{1}{f}} = \frac{1}{\sqrt{1.02}} (\log Re)^{1.25} \quad (\text{Eq. B40})$$

An iterative application of the Colebrook equation is then used until the relative error is less than 0.001%:<sup>157, 158</sup>

$$tr = -2 \log \left( \frac{e}{3.7D} + \frac{2.51tr}{Re} \right) \quad (\text{Eq. B41})$$

where  $e$  is the absolute roughness in  $\text{m}$ .

The average pressure is calculated as:

$$P_{avg} = \frac{2}{3} \left( P_A + P_B - \frac{P_A * P_B}{P_A + P_B} \right) \quad (\text{Eq. B42})$$

where  $P_A$  and  $P_B$  are pressures in  $\text{MPa}$ . If the user specifies the inlet pressure, then  $P_A = P_{in}$ ,  $solvesgn = 1$ , and  $P_B$  is the solved outlet pressure. If the user specifies the outlet pressure, then  $P_A = P_{out}$ ,  $solvesgn = -1$ , and  $P_B$  is the solved inlet pressure.

The density in  $\text{kg}/\text{m}^3$  is calculated as:

$$\rho = [M_g * P * 10 / (Z * R * T)] / 1000 \quad (\text{Eq. B43})$$

where  $M_g$  is the gas molar mass in  $\text{g}/\text{mol}$  and  $R$  is the ideal gas constant in  $\text{bar} \cdot \text{m}^3/\text{K} \cdot \text{mol}$ .

The general flow equation is used and is broken down for simplicity as:<sup>157, 158</sup>

$$C = \frac{\pi}{4\rho_s} * \sqrt{\frac{M_g}{R * 1e6}} \quad (\text{Eq. B44})$$

$$PE = 2P_{avg} * 1e6 * \rho_{avg} * g * H \quad (\text{Eq. B45})$$

$$k = \left( \frac{Q}{C * \eta_{pipe} * tr * D^{2.5}} \right)^2 * L * T_{avg} * Z_{avg} \quad (\text{Eq. B46})$$

$$\frac{dk}{dQ} = \frac{2 * Q * L * T_{avg} * Z_{avg}}{C * \eta_{pipe} * tr * D^{2.5}} \quad (\text{Eq. B47})$$

$$P_B = \left[ \sqrt{(P_A * 1e6)^2 + solvesgn * (-k - PE)} \right] / 1e6 \quad (\text{Eq. B48})$$

$$\frac{dP_B}{dQ} = \left[ -0.5 * solvesgn * \frac{dk}{dQ} * (P_A * 1e6)^2 + \frac{solvesgn}{\sqrt{-k - PE}} \right] / 1e6 \quad (\text{Eq. B49})$$

where  $\rho_s$  and  $\rho_{avg}$  are the gas density at standard and average conditions in kg/m<sup>3</sup>,  $g$  is the acceleration due to gravity in m<sup>2</sup>/s,  $H$  is the elevation change in m,  $\eta_{pipe}$  is the pipeline efficiency,  $L$  is the pipeline length in m,  $T_{avg}$  is the average temperature in K, and  $Z_{avg}$  is the average compressibility.

If required, the flow adjustments for the parallel Chapters are:

$$Q_{adj} = \frac{P_{B_i} - P_{B_{i-1}}}{\frac{dP_{B_i}}{dQ} - \frac{dP_{B_{i-1}}}{dQ}} \quad (\text{Eq. B50})$$

$$Q_{//} = Q_{//} + Q_{adj} \quad (\text{Eq. B51})$$

$$Q_m = Q_m - Q_{adj} \quad (\text{Eq. B52})$$

The average temperature is calculated by accounting for heat loss to the ground and the effect of expansion cooling.<sup>251</sup> The average Joules-Thompson expansion coefficient in K/m is:<sup>247</sup>

$$JL = \frac{JT * |\Delta P|}{L} \quad (\text{Eq. B53})$$

where  $JT$  is the Joules-Thompson coefficient in K/MPa and  $\Delta P$  is the pressure drop across the pipeline length. This analysis assumes the pressure drops linearly along the pipeline, which does not occur. The average temperature is then approximated as:

$$A = \frac{\pi D * U}{Q * \rho_s * Cp} \quad (\text{Eq. B54})$$

$$T_{avg} = \left( \frac{1}{L} T_{in} - T_s + \frac{JL}{A} \right) * \frac{-1}{A} (e^{-A*L} - 1) + T_s - \frac{JL}{A} \quad (\text{Eq. B55})$$

where  $U$  is the overall ground-to-pipe heat conductivity in W/m<sup>2</sup>K,  $Cp$  is the gas-specific heat capacity in J/kgK,  $T_{in}$  is the gas temperature at the pipe inlet/compressor after cooler outlet, and  $T_s$  is the soil temperature.

The custom 4 x 1 array Excel function is defined as:

$$\begin{aligned} &ParrallelPipePressureDrop(D, \mu, \gamma, T_{in}, T_s, \eta_{pipe}, P_{Pipe.In}, P_{Pipe.Out}, Q, L, H, e, \\ &molfrac, U, Cp, JT, Parallel, D//, Q_g) \end{aligned} \quad (\text{Eq. B56})$$

with the inlet and outlet pressure in Pa, mainline flow rate in m<sup>3</sup>/hr, and fluid outlet temperature in K as outputs.

#### **B.4.1. Pipe pressure drop calculation update**

The following modifications were made to the pipeline pressure drop macro from Di Lullo et al.<sup>5</sup>:

1. Density is calculated using the GERG model instead of Equation B43
2. Compressibility is now calculated using the GERG model instead of the Peng-Robinson macro

3. The viscosity macro from Appendix B.3.1 is replaced with the new macro found in Appendix B.5 at average pipeline conditions; the new viscosity still uses the Peng-Robinson instead of GERG (Appendix B.5.)
4. JT in Equation B53 and Cp in Equation B54 are calculated using the GERG model at the average pressure and temperature

## B.5. Updated Natural Gas and Hythane Viscosity

The following updates are from Di Lullo et al.<sup>5</sup>.

Using Zéberg-Mikkelsen et al.'s equations the total gas viscosity is:<sup>252</sup>

$$\eta = \eta_0 + \eta_f \quad \text{Eq. B57}$$

where  $\eta_0$  is the dilute gas viscosity and  $\eta_f$  is the residual friction term.

The dilute gas viscosity in  $\mu\text{P}$  is calculated using Chung et al.'s equation:<sup>253</sup>

$$\eta_0 = 40.785 * F_c * \frac{\sqrt{MW * T}}{v_c^{2/3} * \Omega} \quad \text{Eq. B58}$$

where  $T$  is the temperature in K.

The reduced collision integral is then calculated as:

$$\Omega = \frac{1.16145}{T^*} + \frac{0.52487}{\exp(0.773207 * T^*)} + \frac{2.16178}{\exp(2.437877 * T^*)} - 6.435 * 10^{-4} * T^{*0.14874} * \sin(18.0323 * T^{*-0.76830} - 7.27371) \quad \text{Eq. B59}$$

with

$$T^* = 1.2593 * T/T_c \quad \text{Eq. B60}$$

where  $T_c$  is the critical temperature in K.

The  $F_c$  factor is calculated as:

$$F_c = 1 - 0.2756 * \omega \quad \text{Eq. B61}$$

where  $\omega$  is acentric factor used in the Peng-Robinson EOS (Appendix B.2).

For hydrogen and methane, the dilute gas viscosity in  $\mu\text{P}$  is calculated using equations from Zéberg-Mikkelsen et al.<sup>254</sup>

$$\eta_{0_{H2}} = -1.55199 * T^{0.5} + 2.92788 * T^{0.645731} \quad \text{Eq. B62}$$

$$\eta_{0_{CH4}} = 13.3919 * T^{0.5} - 479429 * T^{0.160913} \quad \text{Eq. B63}$$

The mixture's critical viscosity is then calculated using the Wilke mixing rule:<sup>255</sup>

$$\eta_{0_{mx}} = \sum_{i=1}^n \frac{x_i * \eta_{0,i}}{\sum_{j=1}^n x_j * \phi_{i,j}} \quad \text{Eq. B64}$$

with

$$\phi_{i,j} = \frac{\left[ 1 + \left( \frac{\eta_{0,i}}{\eta_{0,j}} \right)^{0.5} * \left( \frac{MW_i}{MW_j} \right)^{0.25} \right]^2}{\frac{4}{\sqrt{2}} \left[ 1 + \frac{MW_i}{MW_j} \right]^2} \quad \text{Eq. B65}$$

where  $x_i$  is the mole fraction.

The residual friction term can be further broken down as:

$$\eta_f = \kappa_a * P_a + \kappa_r * P_r + \kappa_{rr} * P_r^2 \quad \text{Eq. B66}$$

where  $P_a$  is the attractive pressure and  $P_r$  is the repulsive pressure taken from the PR EOS.

For the n-alkanes, N<sub>2</sub>, CO<sub>2</sub>, and H<sub>2</sub>S, the pure component friction coefficients are calculated using the one-parameter f-theory used by Zéberg-Mikkelsen et al. for hythane mixtures:<sup>252</sup>

$$\kappa_a = \hat{\kappa}_a * \frac{\eta_c}{P_c} \quad \text{Eq. B67}$$

$$\kappa_r = \hat{\kappa}_r * \frac{\eta_c}{P_c} \quad \text{Eq. B68}$$

$$\kappa_{rr} = \hat{\kappa}_{rr} * \frac{\eta_c}{P_c^2} \quad \text{Eq. B69}$$

and the friction coefficients  $\hat{\kappa}_a$ ,  $\hat{\kappa}_r$ , and  $\hat{\kappa}_{rr}$  are then broken down into their temperature independent and dependent terms using Quiñones-Cisneros et al.'s method:<sup>256</sup>

$$\hat{\kappa}_a = \hat{\kappa}_a^c + \Delta\hat{\kappa}_a \quad \text{Eq. B70}$$

$$\hat{\kappa}_r = \hat{\kappa}_r^c + \Delta\hat{\kappa}_r \quad \text{Eq. B71}$$

$$\hat{\kappa}_{rr} = \hat{\kappa}_{rr}^c + \Delta\hat{\kappa}_{rr} \quad \text{Eq. B72}$$

The temperature-dependent terms are then calculated for each component of the mixture as:

$$\begin{aligned} \Delta\hat{\kappa}_a = & \kappa_{a,0,0}(\Gamma - 1) + (\kappa_{a,1,0} + \kappa_{a,1,1} * \psi) * (\exp(\Gamma - 1) - 1) \\ & + (\kappa_{a,2,0} + \kappa_{a,2,1} * \psi + \kappa_{a,2,2} * \psi^2) * (\exp(2\Gamma - 2) - 1) \end{aligned} \quad \text{Eq. B73}$$

$$\begin{aligned} \Delta\hat{\kappa}_r = & \kappa_{r,0,0}(\Gamma - 1) + (\kappa_{r,1,0} + \kappa_{r,1,1} * \psi) * (\exp(\Gamma - 1) - 1) \\ & + (\kappa_{r,2,0} + \kappa_{r,2,1} * \psi + \kappa_{r,2,2} * \psi^2) * (\exp(2\Gamma - 2) - 1) \end{aligned} \quad \text{Eq. B74}$$

$$\Delta\hat{\kappa}_{rr} = \kappa_{rr,2,1} * \psi * (\exp(2\Gamma) - 1) * (\Gamma - 1)^2 \quad \text{Eq. B75}$$

with

$$\Gamma = \frac{T_c}{T} \quad \text{Eq. B76}$$

and

$$\psi = \frac{R * T_c}{P_c} \quad \text{Eq. B77}$$

where  $R$  is the ideal gas constant in  $\text{cm}^3\text{-bar/mol-K}$  and  $P_c$  is the critical pressure in bar.

The residual friction parameters are taken from Quiñones-Cisneros et al.<sup>256</sup> and are only applicable to the Peng-Robinson EOS (Table B1).

**Table B1: Residual friction parameters from Quiñones-Cisneros et al.<sup>256</sup>**

$\hat{\kappa}_a^c$	-0.140464
$\hat{\kappa}_r^c$	0.0119902
$\hat{\kappa}_{rr}^c$	0.000855115
$\kappa_{a,0,0}$	-0.0489197
$\kappa_{a,1,0}$	0.270572
$\kappa_{a,1,1}$	$-1.10473 * 10^{-4}$
$\kappa_{a,2,0}$	-0.0448111
$\kappa_{a,2,1}$	$4.08972 * 10^{-5}$
$\kappa_{a,2,2}$	$-5.79765 * 10^{-9}$
$\kappa_{r,0,0}$	-0.357875
$\kappa_{r,1,0}$	0.637572
$\kappa_{r,1,1}$	$-6.02128 * 10^{-5}$
$\kappa_{r,2,0}$	-0.079024
$\kappa_{r,2,1}$	$3.72408 * 10^{-5}$
$\kappa_{r,2,2}$	$-5.6561 * 10^{-9}$
$\kappa_{rr,2,1}$	$1.3729 * 10^{-8}$

Quiñones-Cisneros et al.'s method is also used to calculate the critical viscosity for C2 to C5 n-alkanes as:<sup>256</sup>

$$\eta_c = 0.597556 * P_c * MW^{0.601652} \quad \text{Eq. B78}$$

where  $P_c$  is the critical pressure in Bar, and  $MW$  is the molecular weight in g/mol.

The constant values of 376.872<sup>256</sup>, 317.985<sup>257</sup>, and 174.179<sup>256</sup> are used for the critical viscosities for CO<sub>2</sub>, H<sub>2</sub>S, and N<sub>2</sub> in  $\mu\text{P}$ .

For hydrogen and methane, the friction coefficients  $\kappa_a$ ,  $\kappa_r$ , and  $\kappa_{rr}$  are determined as:

$$\kappa_a = k_a \quad \text{Eq. B79}$$

$$\kappa_r = k_r \quad \text{Eq. B80}$$

$$\kappa_{rr} = k_{rr} * \Gamma^2 \quad \text{Eq. B81}$$

**Table B2: Friction coefficients for hydrogen and methane<sup>254</sup>**

$\mu\text{P}/\text{bar}$	Hydrogen	Methane
$k_r$	-0.00185308	0.0731796
$k_a$	-0.332575	-0.382909
$k_{rr}$	0.000135146	0.0000663615

To calculate properties of the mixture, mass fractions are needed. We used Quiñones-Cisneros et al.'s method<sup>256</sup> to approximate mass fractions from molar fractions and MW:

$$z_i = \frac{x_i}{MW_i^{0.3} * MM} \quad \text{Eq. B82}$$

with

$$MM = \sum_{i=1}^n \frac{x_i}{MW_i^{0.3}} \quad \text{Eq. B83}$$

The 0.3 power was taken from Quiñones-Cisneros et al.<sup>256</sup> for PR EOS. The friction coefficients for the mixtures were then calculated as:

$$\kappa_{a\_mx} = \sum_{i=1}^n z_i * \kappa_{a,i} \quad \text{Eq. B84}$$

$$\kappa_{r\_mx} = \sum_{i=1}^n z_i * \kappa_{r,i} \quad \text{Eq. B85}$$

$$\kappa_{rr\_mx} = \sum_{i=1}^n z_i * \kappa_{rr,i} \quad \text{Eq. B86}$$

The PR EOS was used to determine the attractive pressure  $P_a$  and the repulsive pressure  $P_r$ <sup>258</sup> as follows:

$$P_a = \frac{-a_m * T}{V * (V + b_m) + b_m * (V - b_m)} \quad \text{Eq. B87}$$

and

$$P_r = \frac{R * T}{V - b_m} \quad \text{Eq. B88}$$

where  $a_m$  and  $b_m$  are calculated using the PR macro, Eqs. B15 and B16 from Appendix B.2.

The volume was then calculated as:

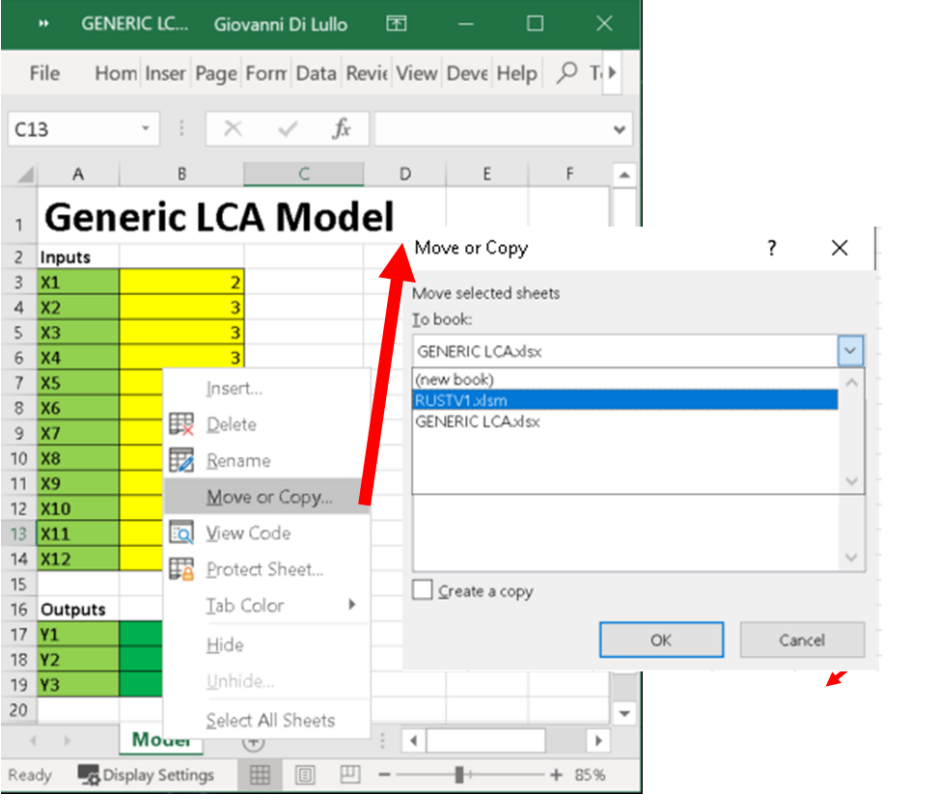
$$V = Z * R * \frac{T}{P} \quad \text{Eq. B89}$$

where the compressibility  $Z$  is calculated using the PR macro. Since the various constants used in the viscosity model were developed using the PR, they must be used with the PR and not the GERG model.

# Appendix C: RUST Demonstration and Input Ranges

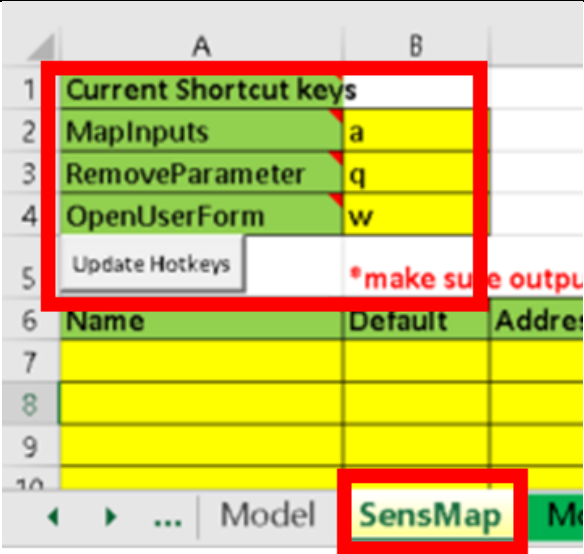
## C.1. Rust Demonstration

This Chapter provides an overview of RUST to illustrate how the research framework can be applied to any Excel-based LCA model. The underlying Rscripts that are used to generate the samples and process the results can be applied to other LCA software but require a new interface program and are outside the scope of this study.

<b>Step 1</b>	
First the user must move their Excel model into the RUST template file.	

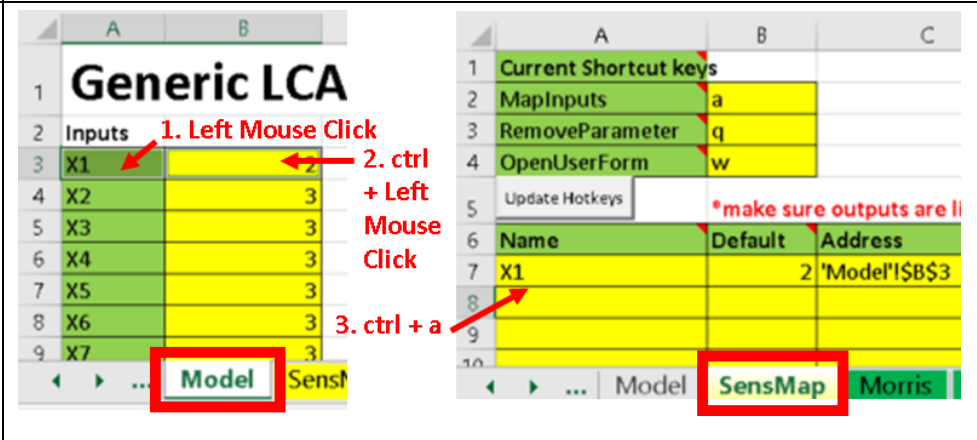
**Step 2**

The next step is to map the inputs and outputs. This can be done quickly by using the MapInputs macro, which is assigned to the Ctrl+a shortcut/hotkey. The user can alter the shortcut keys used by changing cells B2:B4 on the SensMap sheet and clicking the Update Hotkeys button.



**Step 3**

In the LCA model sheets the user can then select the inputs/outputs and run the MapInputs macro, which fill in the SensMap sheet. Outputs should be listed last in the SensMap table. Inputs and outputs can also be specified manually, if desired.



**Step 4**

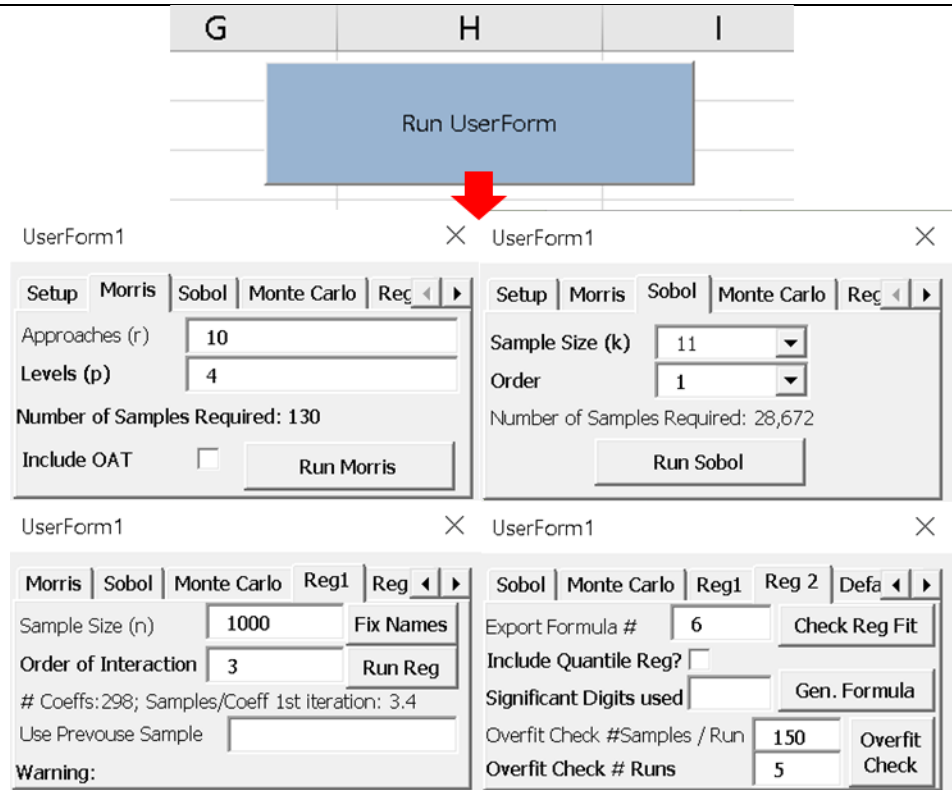
Distributions can then be specified for each input. The uniform, triangle, PERT, normal, and lognormal distributions are available. In this study, uniform distributions are used. For the outputs, the user should specify the “Output” distribution. RUST can support multiple outputs.

**Step 5**

Next, the user should specify the distribution parameters (min, most likely, and max or mean and standard deviation) for each input’s distribution.

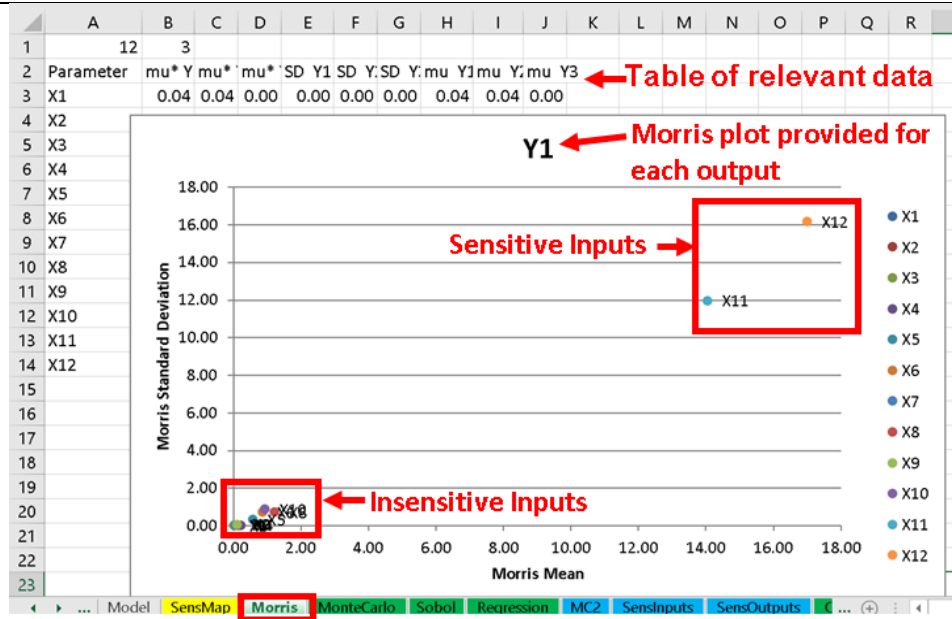
**Step 6**

Clicking the Run UserForm button will activate the user interface. The user should elect the relevant tab and specify the required information. The number of cores to use can be specified on the Setup tab.



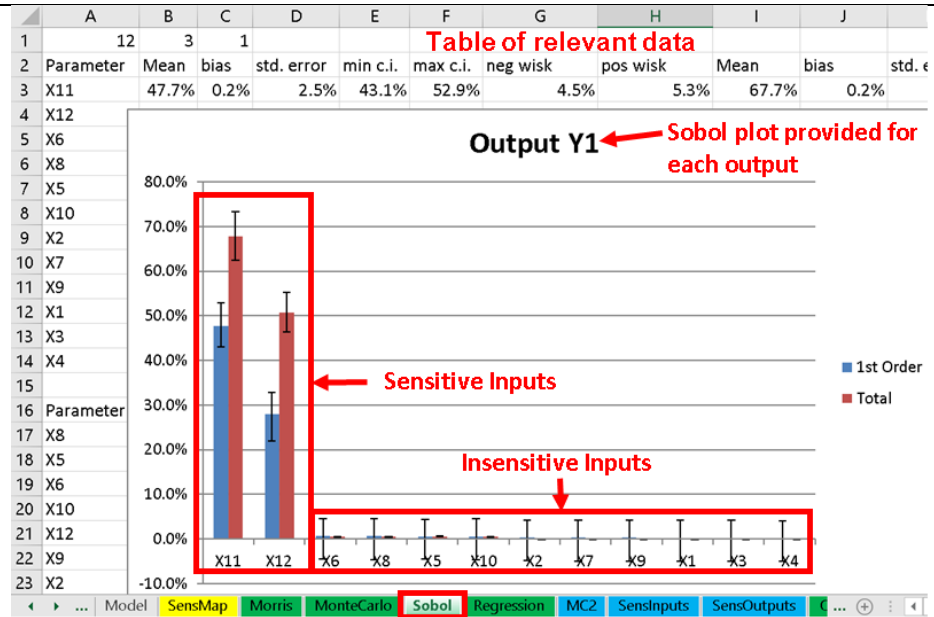
**Step 7**

Once the Morris analysis is complete the Morris sheet will be activated.



**Step 8**

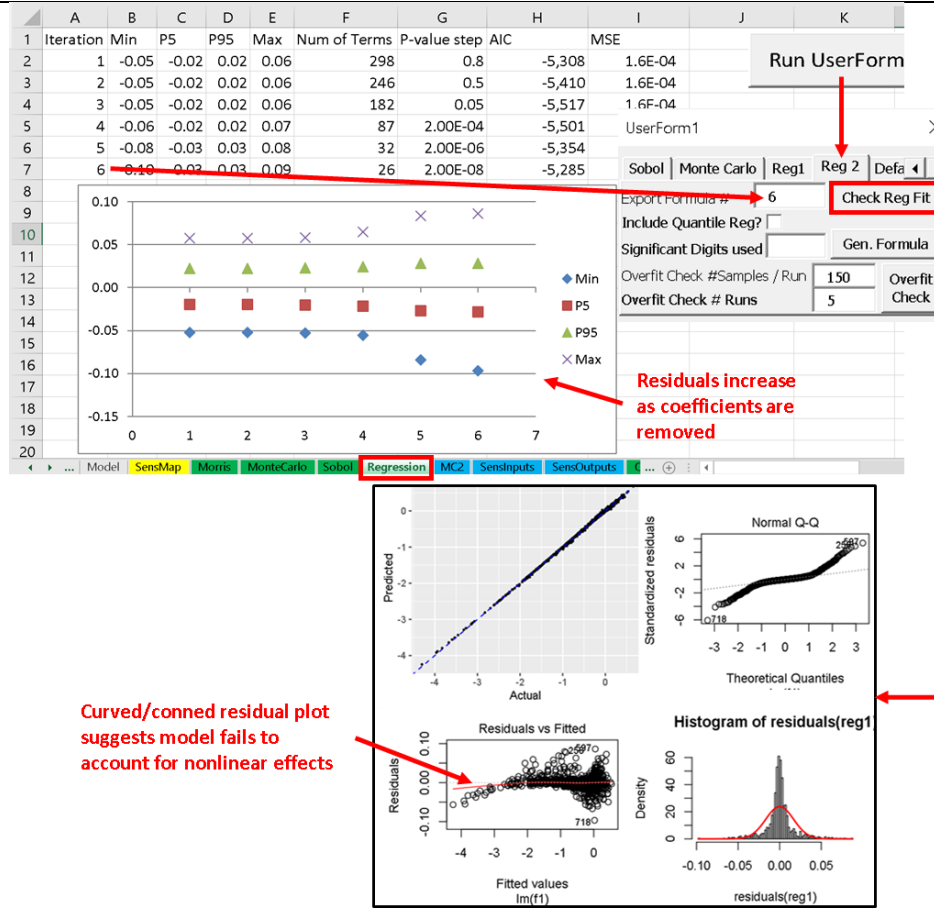
Similarly, once the Sobol analysis is complete the Sobol sheet will be activated.



**Step 9**

After the sensitivity analysis is completed, the regression analysis can be run using only the key inputs. The regression analysis must be done for one output at a time.

After the Run Regression button is selected, the regression sheet will open and display the residuals for each iteration of the stepwise regression processes. Residual plots are then generated using the Check Reg Fit button for the specified regression model.



**Step 10**

Once a satisfactory model is selected, the regression formula can be generated. For regression models with many terms the formula may need to be split into multiple cells as Excel limits a formula to 8,192 characters.

**Inputs for regression model formula**

**Regression model coefficients used to generate formula**

**3<sup>rd</sup> order interaction**

**2<sup>nd</sup> order interaction**

**Individual effect**

	U	V
X1	Intercept	7.63E-01
X2	X2	9.53E-03
X3	X5	-2.64E-01
X4	X6	-2.65E-01
X5	X8	-2.62E-01
X6	X10	-2.65E-01
X7	X11	-1.57E-03
X8	X12	-2.79E-03
X9	X5 * X6	8.95E-02
X10	X5 * X8	8.95E-02
X11	X5 * X10	8.93E-02
X12	X6 * X8	8.99E-02
	X6 * X10	9.00E-02
	X8 * X10	8.81E-02
	X5 * X6 * X8	-3.01E-02
	X5 * X6 * X10	-3.02E-02
	X5 * X8 * X10	-2.97E-02
	X6 * X8 * X10	-3.01E-02
	X7	4.67E-04
	X9	-4.37E-04
	X11 * X12	1.36E-02
	X7 * X10	1.01E-02
	X2 * X12	1.00E-02
	X9 * X10	-9.54E-03
	X3	1.04E-02
	X1	1.08E-02

### Step 11

The final regression model can then be used instead of the original model. In this example, the original model was relatively simple; however, the process works for complex models as well. The regression model helps simplify the model and hide any confidential data.

The screenshot displays an Excel spreadsheet titled "Generic LCA Model" with columns A through D and rows 1 through 19. The spreadsheet is divided into "Inputs" (rows 3-14) and "Outputs" (rows 17-19). The "Inputs" section contains variables X1 through X12, with values 2, 3, 3, 3, 3, 3, 3, 3, 3, 3, 3, and 3 respectively. The "Outputs" section contains Y1 (1.88), Y2 (-0.50), and Y3 (6). Two red arrows point from the regression model formula in cell C18 to the original model formula in cell C3. The original model formula is: 
$$=(\text{SUM}(\text{B3:B5})+(\text{B6})-\{(\text{B7}*\text{B8}*\text{B10})-\text{B9}+\text{B11}\}*\text{B12}+(\text{B13}^{\wedge}1.1)*(\text{B14}^{\wedge}1.05)+(\text{B4}*\text{B14}))/100$$
 The regression model formula is: 
$$=0.00952669798067955*\text{B4}-0.26378247182725*\text{B7}-0.265065916094415*\text{B8}-0.262144127746683*\text{B10}-0.264829720614757*\text{B12}$$
 The spreadsheet also shows a status bar at the bottom with "UserForm Defaults" and "Model S".

## C.2. Original Input Ranges

Table C1: Maya original input values (61 inputs total)<sup>††</sup>

Maya	Units	Min	Max
Crude API	° API	18	26
Crude LHV err.	N/A	0.75	1.25
Average field production rate	bbbl/d	605,833	1,817,500
Well depth	ft	4,583	13,749
Well lifetime productivity	bbbl/well	23,725,000	71,175,000
Land use emissions	gCO <sub>2</sub> eq/MJ	0.00	2.00
Gas injected ratio	scf/bbl	200	5,000
Water production ratio	m <sup>3</sup> /m <sup>3</sup>	0	10
Gas production ratio	scf/bbl	0	2,000
Gas lift ratio	scf/bbl	0	2,000
Compressor energy	kWh-d/scf	0.004	0.012
Compressor driver efficiency	%	60%	100%
Suction pressure	psi	100	500
Discharge pressure	psi	1,500	3,000
Atmospheric temperature	degrees R	450	600
Suction temperature	degrees R	550	700
Compressibility factor	N/A	0.8	1.2
Specific heat ratio	N/A	1.20	1.35
Polytropic index	N/A	1.0	1.5
Interstage cooling efficiency	%	60%	100%
Crude oil specific heat adjustment	N/A	0.75	1.00
Feed temperature	°F	80	160
Process temperature	°F	250	450
Heat loss	%	0%	10%
Pump efficiency	%	40%	90%
Amount of water in inlet gas	lb of H <sub>2</sub> O/MMScf	30	70
TEG to water ratio	gal TEG/lb H <sub>2</sub> O	1	3
Glycol pump discharge pressure	psi	600	1,000
Amine solution K value	d-gal/min-MMscf	1.1	1.9
Operating pressure	psig	200	500
Electricity intensity for produced water	kWh/bbl	0.2	1
Electricity intensity for imported water	kWh/bbl	0.2	1
Extraction electricity EF	gCO <sub>2</sub> eq/MJ	200	1,000
Surface processing elec. EF	gCO <sub>2</sub> eq/MJ	200	1,000
NG boiler eff.	%	60%	100%

<sup>††</sup> Maya originally had 65 inputs when the OAT vs. Morris analysis was run (discussed in Chapter 3) but was later simplified to 61 to remove unnecessary inputs.

<b>Maya</b>	<b>Units</b>	<b>Min</b>	<b>Max</b>
<b>Fugitive gas volume</b>	%	2.1%	7.0%
<b>Flared gas volume</b>	scf/bbl	0	150
<b>Flaring efficiency</b>	%	80%	100%
<b>Pipeline capacity</b>	bpd	100,000	800,000
<b>Pipeline velocity</b>	m/s	1.3	3.1
<b>Pipe length</b>	km	100	400
<b>Kinematic viscosity</b>	CST	10	350
<b>Absolute roughness</b>	m	0.0000046	0.00046
<b>Pipeline elec. EF</b>	gCO <sub>2</sub> eq/kWh	200	1,000
<b>Pipeline pump efficiency</b>	%	60%	100%
<b>Tanker distance</b>	km	600	2,000
<b>Ocean tanker weight</b>	DWT	160,000	320,000
<b>Average speed of tanker</b>	km/h	20	40
<b>Origin-to-destination load factor</b>	N/A	0.6	1.0
<b>Destination-to-origin load factor</b>	N/A	0.6	1.0
<b>Refinery emissions</b>	gCO <sub>2</sub> eq/MJ	14.2	23.6
<b>Ref. conversion factor</b>	MJ crude/MJ prod.	1.12	1.86
<b>Barge share gasoline transport</b>	%	0%	100%
<b>CH4</b>	GWP	20.4	47.6
<b>N<sub>2</sub>O</b>	GWP	200	400
<b>Diesel EF err.</b>	N/A	0.75	1.25
<b>NG EF err.</b>	N/A	0.75	1.25
<b>Marine vessel combustion EF err.</b>	N/A	0.75	1.25
<b>LHV of residual oil err.</b>	N/A	0.75	1.25
<b>Barge EF err.</b>	N/A	0.75	1.25
<b>Rail EF err.</b>	N/A	0.75	1.25

**Table C2: Bow River original input values (54 inputs total)**

<b>Bow River</b>	<b>Units</b>	<b>Min</b>	<b>Max</b>
<b>Crude API</b>	°API	22	27
<b>Crude LHV err.</b>	N/A	0.75	1.25
<b>Average field production rate</b>	bbl/d	267,041	801,123
<b>Well depth</b>	ft	1,640	4,920
<b>Well lifetime productivity</b>	bbl/well	160,088	480,264
<b>Land use emissions</b>	gCO <sub>2</sub> eq/MJ	0	2.5
<b>Water injection ratio</b>	m <sup>3</sup> /m <sup>3</sup>	0.5	8
<b>Water production ratio</b>	m <sup>3</sup> /m <sup>3</sup>	2	50
<b>Gas Production Ratio</b>	scf/bbl	100	4,000
<b>Discharge pressure</b>	psi	600	1,000
<b>Pump efficiency inj.</b>	%	40%	90%
<b>Pump efficiency lift</b>	%	40%	90%

<b>Bow River</b>	<b>Units</b>	<b>Min</b>	<b>Max</b>
<b>Average pipe diameter</b>	in	1.75	3.75
<b>Well oil production</b>	bbl/d	8	16
<b>Dynamic viscosity of water</b>	cP	0.1	0.3
<b>Dynamic viscosity of crude</b>	cP	0.5	10
<b>Absolute roughness</b>	m	0.0000046	0.00046
<b>Average reservoir pressure</b>	psi	400	3,000
<b>Crude oil specific heat err.</b>	N/A	0.75	1.00
<b>Feed temperature</b>	°F	80	160
<b>Process temperature</b>	°F	250	450
<b>Heat loss</b>	%	0%	10%
<b>Heater efficiency</b>	%	60%	80%
<b>Pump efficiency stabilizer</b>	%	60%	100%
<b>Amount of water in inlet gas</b>	lb of H <sub>2</sub> O/MMScf	30	70
<b>TEG to water ratio</b>	gal TEG/lb H <sub>2</sub> O	1	3
<b>Glycol pump discharge pressure</b>	psi	600	1,000
<b>Amine solution K value</b>	d-gal/min-MMscf	1.1	1.9
<b>Operating pressure</b>	psig	200	500
<b>Electricity intensity for produced water</b>	kWh/bbl	0.2	1
<b>Electricity intensity for imported water</b>	kWh/bbl	0.2	1
<b>Extraction electricity EF</b>	gCO <sub>2</sub> eq/kWh	200	1,000
<b>NG boiler eff.</b>	%	60%	100%
<b>Fugitive gas volume</b>	%	2.1%	7.0%
<b>Flared gas volume</b>	scf/bbl	0	200
<b>Flaring efficiency</b>	%	80%	100%
<b>Pipeline capacity</b>	bpd	100,000	800,000
<b>Pipeline velocity</b>	m/s	0.8	3.8
<b>Pipe length</b>	km	2,000	3,200
<b>Kinematic viscosity</b>	CST	5	350
<b>Absolute roughness</b>	m	0.0000046	0.00046
<b>Pipeline elec. EF</b>	gCO <sub>2</sub> eq/kWh	200	1,000
<b>Pipeline pump efficiency</b>	%	60%	100%
<b>Gasoline refinery emissions</b>	gCO <sub>2</sub> eq/MJ	13.2	22.0
<b>Ref. conversion factor</b>	MJ crude/MJ prod.	1.07	1.79
<b>Barge share gasoline transport</b>	%	0%	100%
<b>CH<sub>4</sub></b>	GWP	20.4	47.6
<b>N<sub>2</sub>O</b>	GWP	200	400
<b>Diesel EF err.</b>	N/A	0.75	1.25
<b>NG EF err.</b>	N/A	0.75	1.25
<b>Marine vessel combustion EF err.</b>	N/A	0.75	1.25
<b>LHV of residual oil err.</b>	N/A	0.75	1.25
<b>Barge EF err.</b>	N/A	0.75	1.25
<b>Rail EF err.</b>	N/A	0.75	1.25

**Table C3: Mined Bitumen (MB) original input values (40 inputs total)**

<b>Mined Bitumen</b>	<b>Units</b>	<b>Min</b>	<b>Max</b>
<b>Crude LHV err.</b>	N/A	0.95	1.05
<b>Land use emissions</b>	gCO <sub>2</sub> eq/MJ	0.83	2.33
<b>Electricity consumption</b>	kWh/m <sup>3</sup> bitumen	94.8	162.0
<b>Bitumen saturation</b>	%	10.61%	12.12%
<b>Shovel fuel consumption</b>	L/h	375	740
<b>Shovel rated payload</b>	t	218	363
<b>Shovel cycle times</b>	s	20	36
<b>Shovel fill factor</b>	%	85%	95%
<b>Shovel availability</b>	%	75%	95%
<b>Truck fuel consp.</b>	L/h	406	580
<b>Truck rated payload</b>	t	218	363
<b>Truck cycle times</b>	min	15.8	44.0
<b>Hot water consp. for sepr.</b>	m <sup>3</sup> /m <sup>3</sup>	6	9
<b>Hot water temp.</b>	°C	50	75
<b>Inlet water temp.</b>	°C	2	25
<b>NG boiler eff.</b>	%	60%	100%
<b>Electricity credit</b>	g/kWh	50	990
<b>Cogeneration steam capacity</b>	%	0%	100%
<b>Extraction electricity EF</b>	gCO <sub>2</sub> eq/kWh	200	1,000
<b>Cogen modifier</b>	N/A	1	4
<b>Oil sands fugitive emissions</b>	gCO <sub>2</sub> eq/m <sup>3</sup> bit	3,604	96,220
<b>Pipeline capacity</b>	bpd	100,000	800,000
<b>Pipeline velocity</b>	m/s	0.8	3.8
<b>Pipe length</b>	km	2,000	3,200
<b>Kinematic viscosity</b>	CST	5	350
<b>Absolute roughness</b>	m	0.0000046	0.00046
<b>Pipeline elec. EF</b>	gCO <sub>2</sub> eq/kWh	200	1,000
<b>Pipeline pump efficiency</b>	%	60%	100%
<b>Diluent ratio</b>	%	0%	30%
<b>Refinery emissions</b>	gCO <sub>2</sub> eq/MJ	18	24
<b>Ref. conversion factor</b>	MJ crude/MJ prod.	1.41	1.73
<b>Barge share gasoline transport</b>	%	0%	100%
<b>CH<sub>4</sub></b>	GWP	20.4	47.6
<b>N<sub>2</sub>O</b>	GWP	200	400
<b>Diesel EF err.</b>	N/A	0.75	1.25
<b>NG EF err.</b>	N/A	0.75	1.25
<b>Marine vessel combustion EF err.</b>	N/A	0.75	1.25
<b>LHV of residual oil err.</b>	N/A	0.75	1.25
<b>Barge EF err.</b>	N/A	0.75	1.25
<b>Rail EF err.</b>	N/A	0.75	1.25

**Table C4: NGTL original input values (44 inputs total)**

<b>NGTL</b>	<b>Units</b>	<b>Min</b>	<b>Max</b>
Cooler pressure drop	%	0	2%
Scrubber pressure drop	MPa	0	0.4
Facility piping pressure drop	MPa	0	0.2
Interstage cooler outlet temperature	C	25	55
Polytropic efficiency	%	70%	85%
Compressor mechanical efficiency	%	9%	100%
Turbine efficiency	%	27%	39%
Absolute roughness	m	5e-6	1.5e-5
Pipeline efficiency	%	90%	100%
Ground temperature	C	4	17
Pipe thickness	mm	10	25
Length adjustment	N/A	0.95	1.05
Elevation adjustment	N/A	0	1
Fugitive adjustment	N/A	0.1	3
Joule-Thomson coefficient	K/MPa	3.8	6.2
Natural gas specific heat	J/kg.K	2100	3200
Pipe to ground heat conductivity U	W/m2.K	0	3
Pipeline average right-of-way width	M	15	45
% of right-of-way cleared	%	50%	100%
Pipeline steel density	kg/m <sup>3</sup>	7470	8050
Recycled steel mix	%	0%	100%
Pipeline lifespan	yrs.	35	65
Concrete density	kg/m <sup>3</sup>	1740	2400
Station parasitic electricity consumption	kW	500	2000
Station parasitic heat consumption	kW	400	1600
CH <sub>4</sub> GWP	N/A	20.4	47.6
N <sub>2</sub> O GWP	N/A	200	400
NG turbine combustion EF adjs.	N/A	0.75	1.25
Virgin steel EF adjs.	N/A	0.75	1.25
Recycled steel EF adjs.	N/A	0.75	1.25
Concrete EF adjs.	N/A	0.75	1.25
Pipeline construction diesel EF adjs.	N/A	0.5	1.5
Biomass combustion	kgCO <sub>2</sub> eq/m2	0.006	0.05
Pig leakage rate	%	0	50%
Number of pig passes	N/A	2	10
N <sub>2</sub> generation electricity consumption	kWh/tonne N <sup>2</sup>	100	500
N <sub>2</sub> generation electricity EF	gCO <sub>2</sub> eq/kWh	300	1100
% pipeline filled with concrete	%	0%	50%
% pipeline removed	%	0%	50%
Utilization rate	%	80%	100%
Max allowable operating pressure (MAOP)	MPa	10	12.2
Pipe inner diameter	mm	910	920
Flow rate	m <sup>3</sup> /hr	1,554,792	1,945,833
Inlet pressure to first compressor	MPa	5	7

### C.3. Refined Input Ranges

The trendline R<sup>2</sup> values are provided for a linear, 2<sup>nd</sup> order polynomial, and 3<sup>rd</sup> order polynomial fit for each input.

**Table C5: Maya refined input values (14 inputs total)**

Maya	Units	Min	Max	Trendlines R <sup>2</sup>
Crude LHV err.	N/A	0.8	1.25	0.98, 0.82, 0.70
Land use emissions	gCO <sub>2</sub> eq/MJ	0.00	2.00	1
Gas injected ratio	scf/bbl	200	5,000	1
Gas production ratio	scf/bbl	0	2,000	1.00, 0.91, 0.80
Compressor energy	kWh-d/scf	0.004	0.012	1
Compressor driver eff.	%	60%	100%	0.98, 0.82, 0.70
Extraction electricity EF	gCO <sub>2</sub> eq/kWh	200	1,000	1
Fugitive gas vol.	% prod. gas	2%	7%	1
Flared gas vol.	scf/bbl	0	150	1
Flaring eff.	%	80%	100%	1
Refinery emissions	gCO <sub>2</sub> eq/MJ	14.2	23.6	1
Ref. conversion factor	MJ crude/MJ prod.	1.12	1.86	1
CH <sub>4</sub> GWP	N/A	20.4	47.6	1
NG EF err.	N/A	0.75	1.25	1

**Table C6: Bow River refined input values (14 inputs total)**

Bow River	Units	Min	Max	Trendlines R <sup>2</sup>
Crude LHV err.	N/A	0.75	1.25	0.98, 0.82, 0.70
Land use emissions	gCO <sub>2</sub> eq/MJ	0	2.5	1
Water production ratio	m <sup>3</sup> /m <sup>3</sup>	2	50	1.00, 0.93, 0.84
Gas production ratio	scf/bbl	100	4,000	1.00, 0.92, 0.82
Elec. produce water	kWh/bbl	0.2	1	1
Extraction electricity EF	gCO <sub>2</sub> eq/kWh	200	1,000	1
Fugitive gas vol.	% prod. gas	0.021	0.07	1
Flared gas vol.	scf/bbl	0	200	1
Pipeline capacity	bpd	200,000	600,000	0.93, 0.73, 0.60
Pipeline velocity	m/s	1.4	2.8	0.98, 0.98, 0.91
Pipeline elec. EF	gCO <sub>2</sub> eq/kWh	200	1,000	1
Refinery emissions	gCO <sub>2</sub> eq/MJ	13.2	22.0	1
Ref. conversion factor	MJ crude/MJ prod.	1.1	1.79	1
CH <sub>4</sub> GWP	N/A	20.4	47.6	1

**Table C7: Mined Bitumen (MB) refined input values (16 inputs total)**

<b>Mined Bitumen</b>	<b>Units</b>	<b>Min</b>	<b>Max</b>
<b>Crude LHV err.</b>	N/A	0.95	1.05
<b>Land use emissions</b>	gCO <sub>2</sub> eq/MJ	0.83	2.33
<b>Bitumen saturation</b>	%	10.6%	12.1%
<b>Truck fuel consumption</b>	L/h	406	580
<b>Truck rated payload</b>	t	218	363
<b>Truck cycle times</b>	min	15.8	44
<b>Hot water consumption for sepr.</b>	m <sup>3</sup> /m <sup>3</sup>	6	9
<b>Hot water temp.</b>	°C	50	75
<b>Inlet water temp.</b>	°C	2	25
<b>Extraction electricity EF</b>	gCO <sub>2</sub> eq/kWh	200	1,119
<b>Oil sands fugitive emissions</b>	gCO <sub>2</sub> eq/m <sup>3</sup> bit	3,604	96,220
<b>Pipeline velocity</b>	m/s	0.8	2.0
<b>Refinery emissions</b>	gCO <sub>2</sub> eq/MJ	18	24
<b>Ref. conversion factor</b>	MJ crude/MJ prod.	1.41	1.73
<b>CH<sub>4</sub> GWP</b>	N/A	20.4	47.6
<b>NG EF err.</b>	N/A	0.75	1.25

**Table C8: NGTL refined input values (10 inputs total)\*\***

<b>NGTL</b>	<b>Units</b>	<b>Min</b>	<b>Max</b>	<b>Trendlines R<sup>2</sup></b>
<b>Pipeline pressure</b>	MPa	11.0	12.5	0.95, 0.77, 0.64
<b>Interstage cooler outlet temp.</b>	C	10	35	1.00, 0.93, 0.83
<b>Polytropic eff.</b>	%	70%	95%	0.97, 0.80, 0.67
<b>Turbine eff.</b>	%	20%	50%	0.99, 0.86, 0.74
<b>Absolute roughness</b>	m	5.00E-06	5.00E-05	1.00, 0.88, 0.77
<b>Length err.</b>	%	95%	105%	0.94, 0.74, 0.60
<b>Flow rate</b>	m <sup>3</sup> /hr	1,554,792	1,906,375	0.97, 0.99, 0.93
<b>Fugitive adjustment</b>	%	10%	300%	1.00, 0.92, 0.82
<b>CH<sub>4</sub> GWP</b>	N/A	10	90	1.00, 0.92, 0.82
<b>NG EF err.</b>	%	50%	150%	1.00, 0.92, 0.82

\*\* As discussed in Chapters 3 & 4, Alliance used 11 inputs; this was reduced to 10 in Chapter 5.

# Appendix D: Proxy Modeling Supplementary Results and Algorithms

## D.1. Quadratic Regression Results

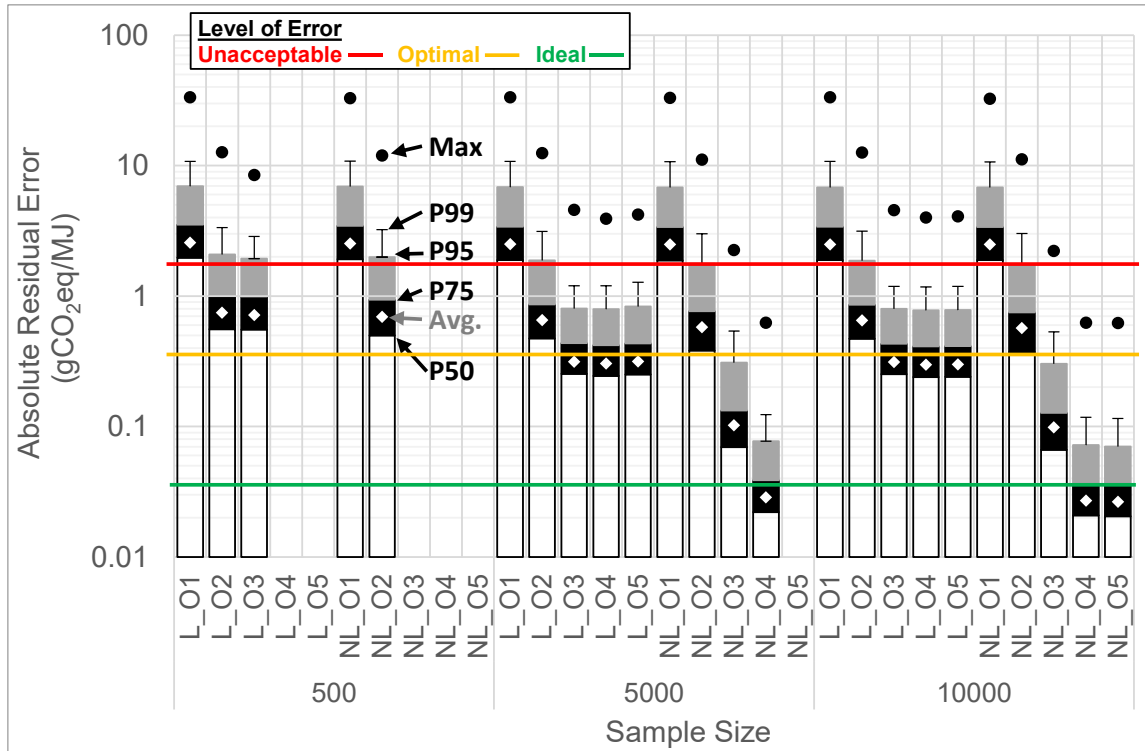


Figure D1: Bow quadratic regression absolute residual results: L=Linear, NL=Non-linear, O#=Order of interactions

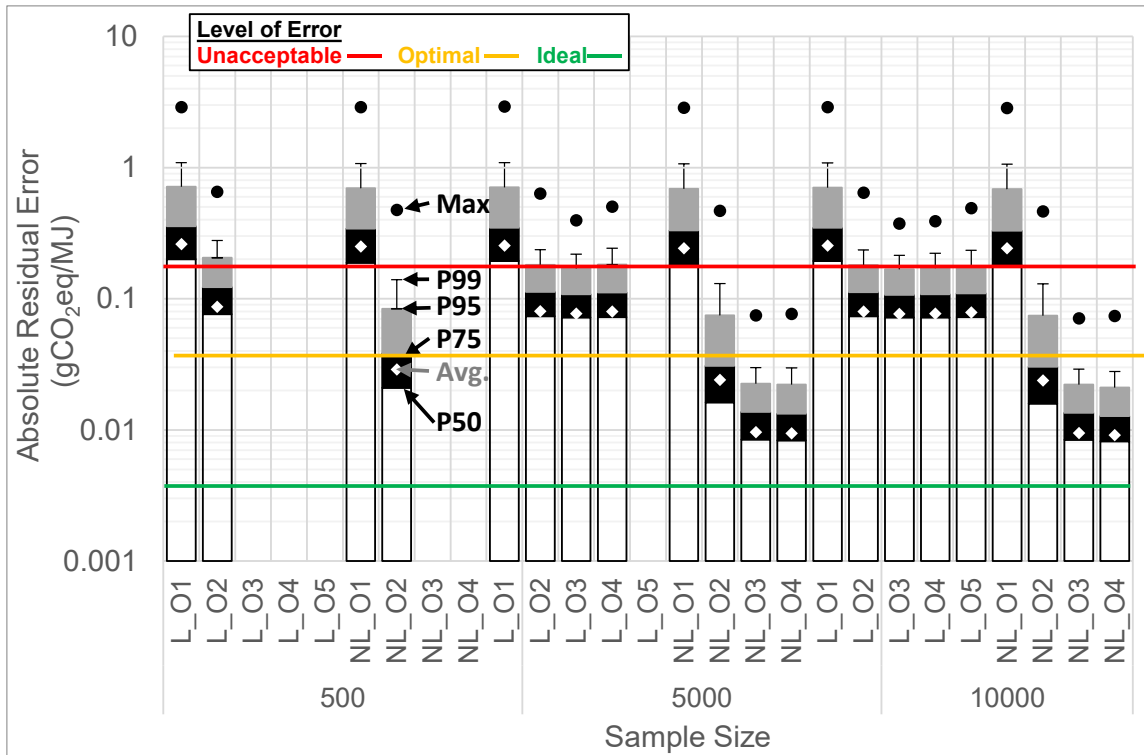


Figure D2: MB quadratic regression absolute residual results: L=Linear, NL=Non-linear, O#=Order of interactions

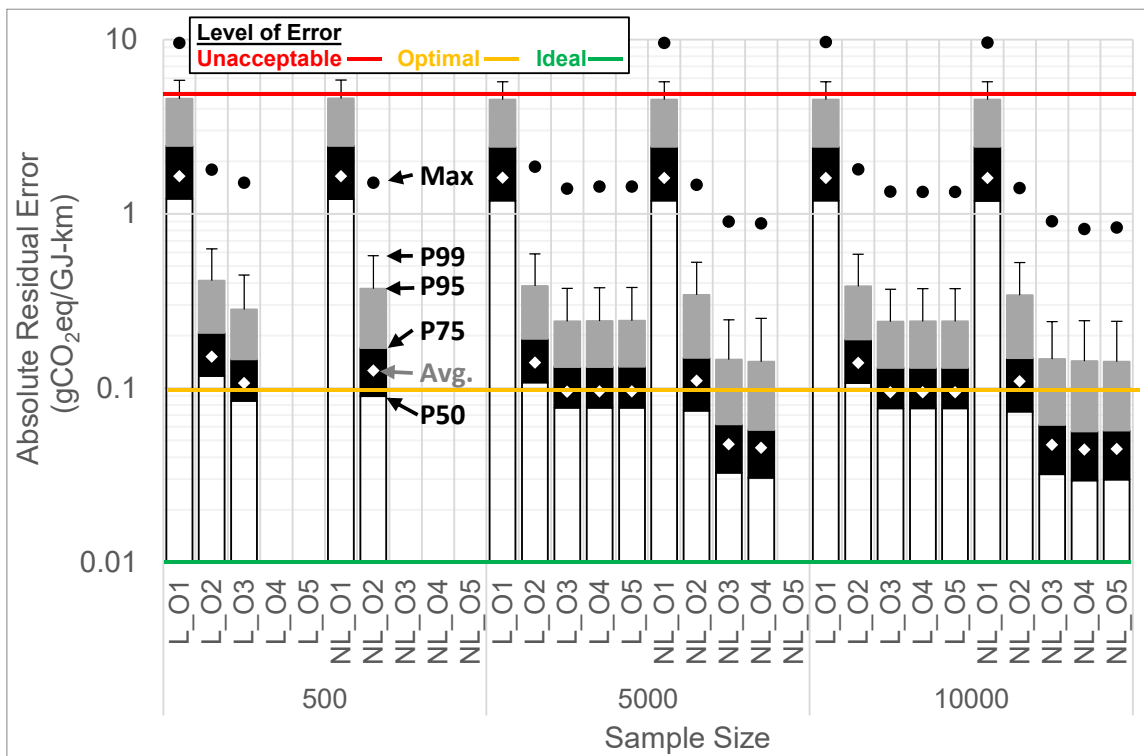


Figure D3: NGTL quadratic regression absolute residual results: L=Linear, NL=Non-linear, O#=Order of interactions

## D.2. ANN Regression Results

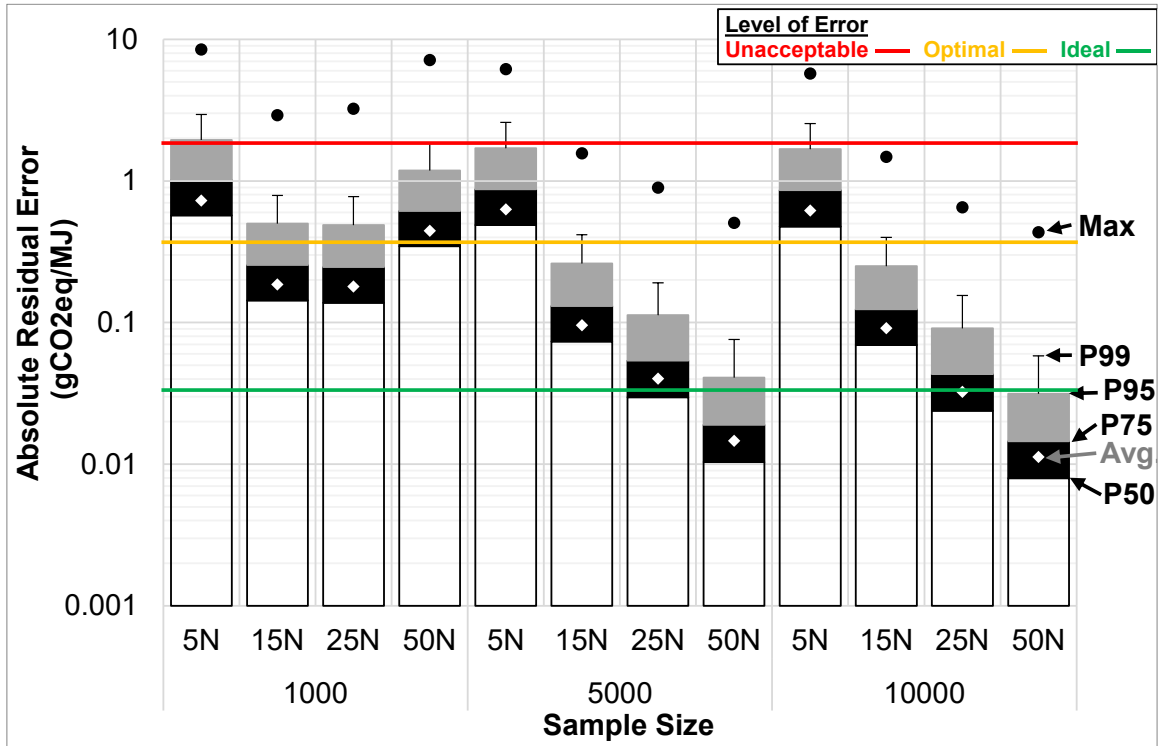


Figure D4: Bow ANN regression absolute residual results: N=Nodes in hidden

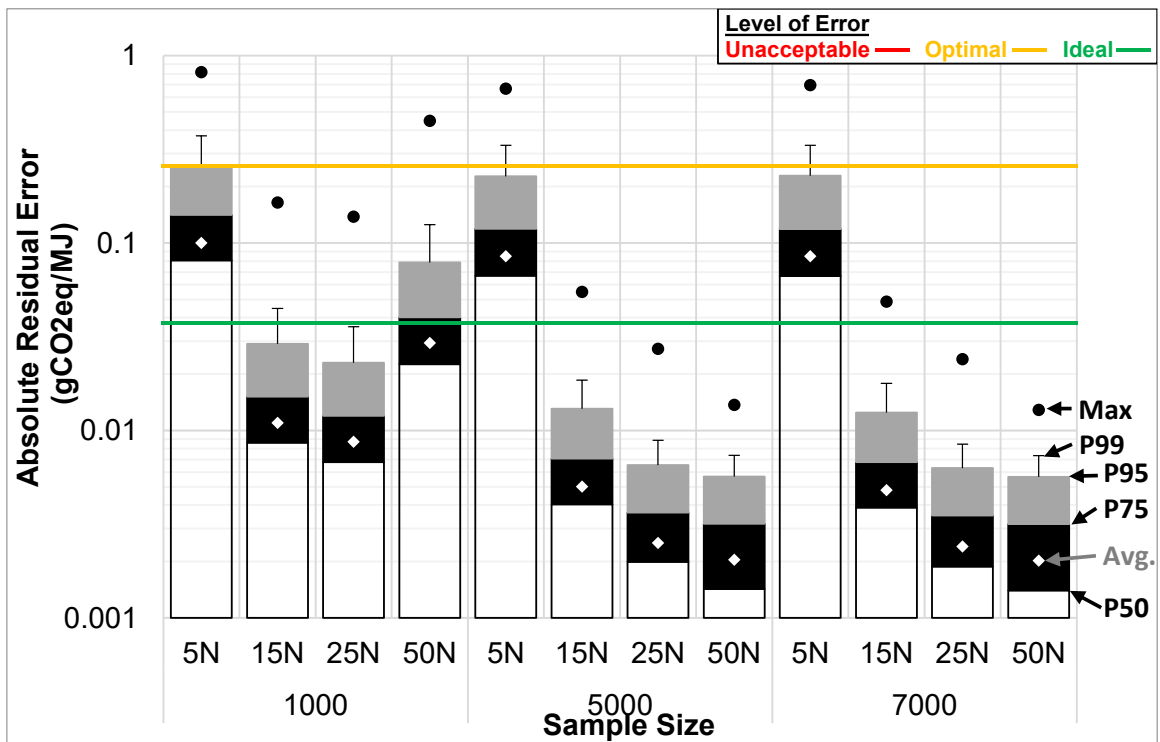


Figure D5: MB ANN regression absolute residual results: N=Nodes in hidden

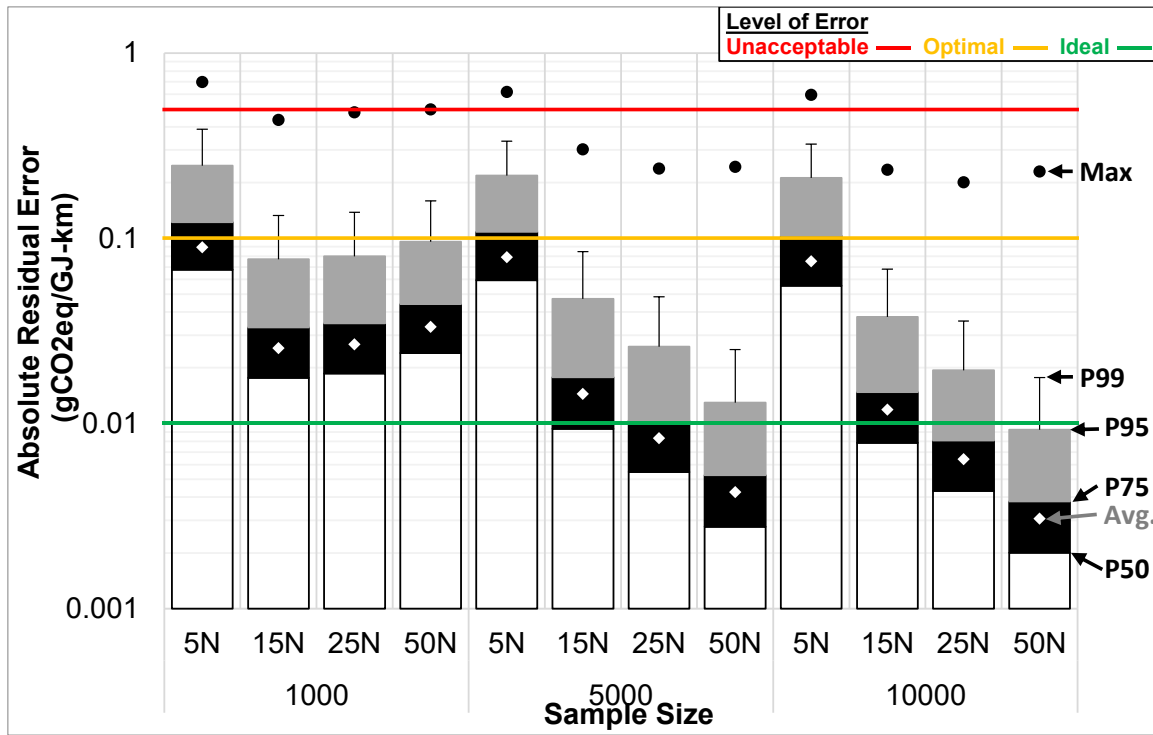


Figure D6: NGTL ANN regression absolute residual results: N=Nodes in hidden

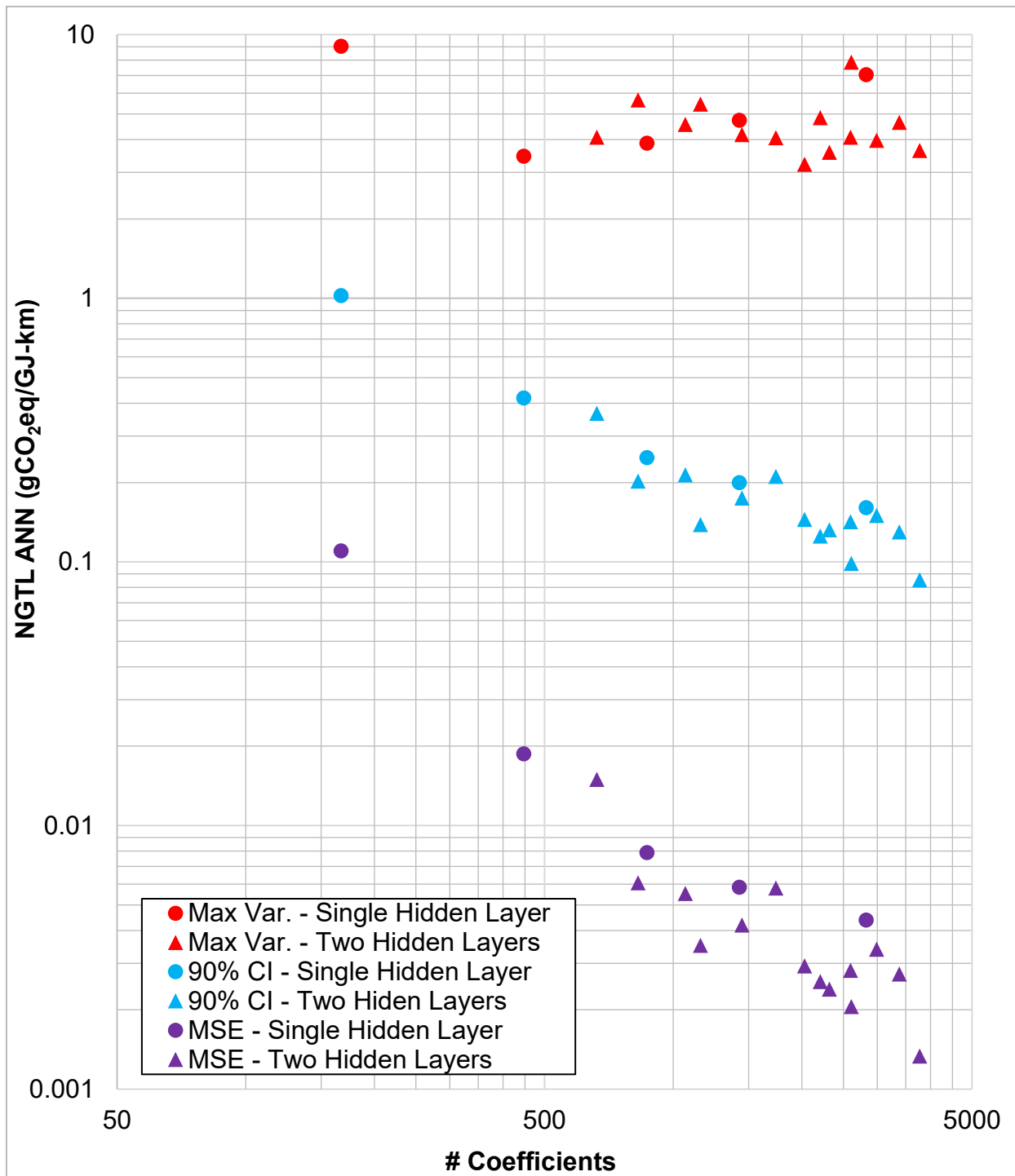


Figure D7: NGTL accuracy vs. # of coefficients (50,000 random samples, 26 inputs)

### D.3. ANN Results vs. Sample Size and Method

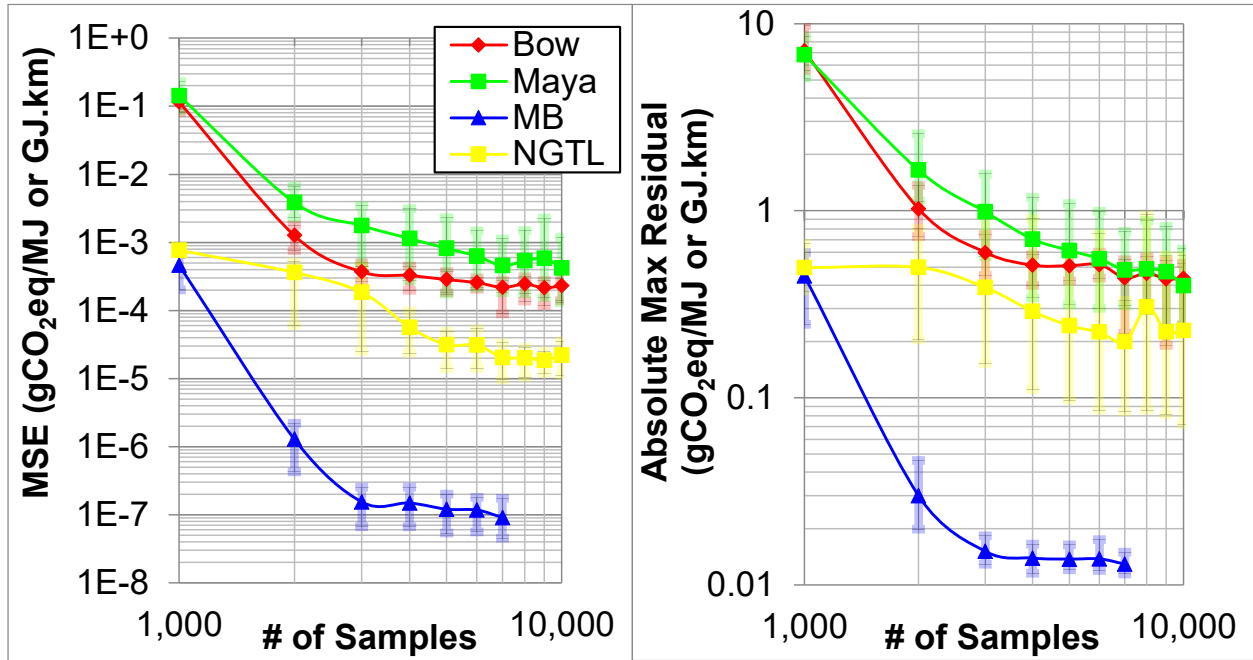


Figure D8: MSE and absolute max residual for 50N ANN proxy models (log-log scale)

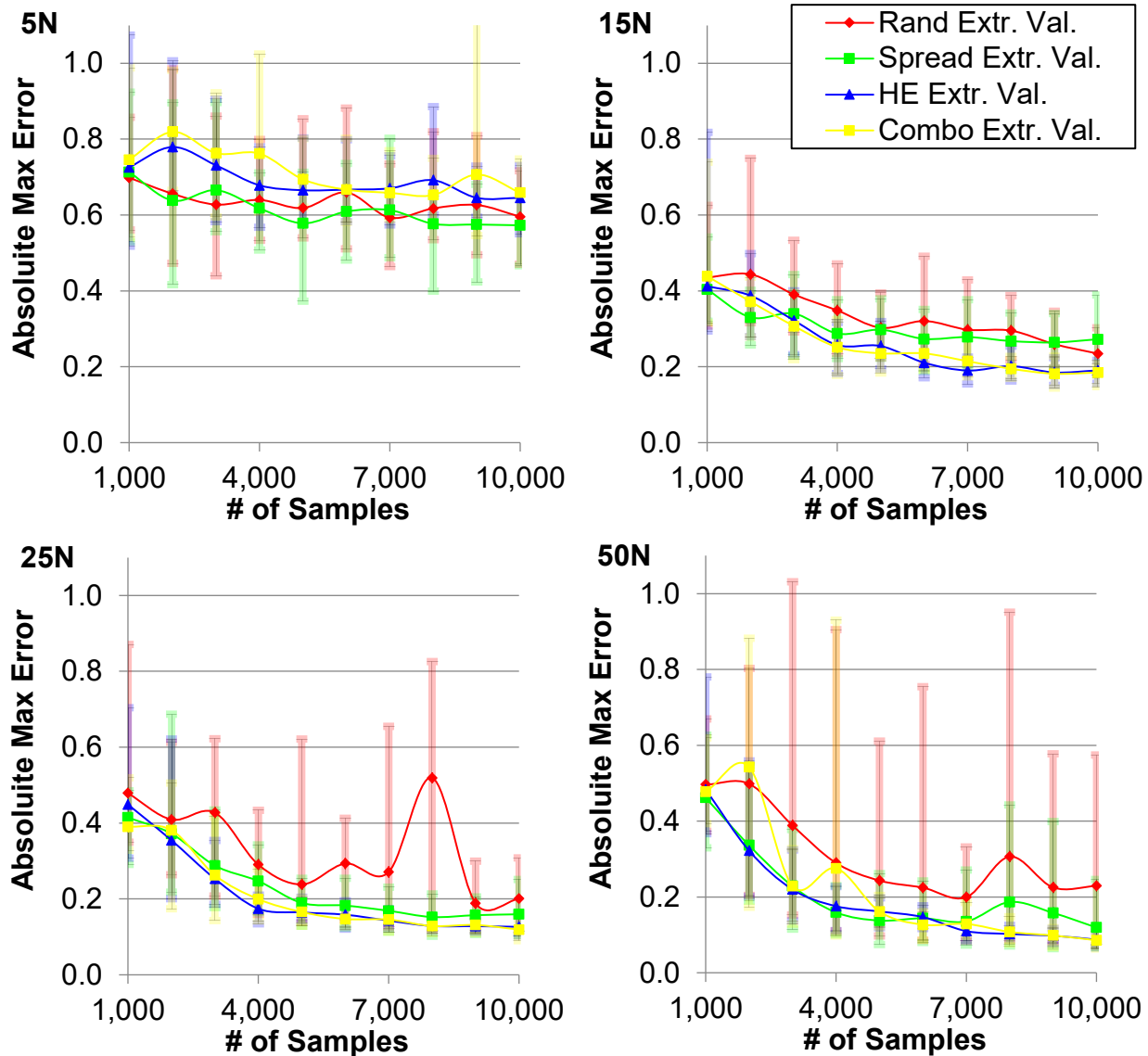


Figure D9: Absolute max error for NGTL proxy model using 5, 15, 25, and 50 nodes in hidden layers

Table D1: Figure D9 random and high error statistical significance ( $p$  value  $< 5\%$  indicates the difference in means is statistically significant)

# of Samples	5N	15N	25N	50N
1,000	55%	57%	50%	71%
2,000	1%	14%	21%	1%
3,000	0%	0%	1%	1%
4,000	16%	0%	0%	7%
5,000	7%	0%	2%	3%

6,000	81%	0%	7%	7%
7,000	0%	0%	0%	8%
8,000	1%	0%	17%	1%
9,000	40%	0%	0%	3%
10,000	2%	0%	2%	3%

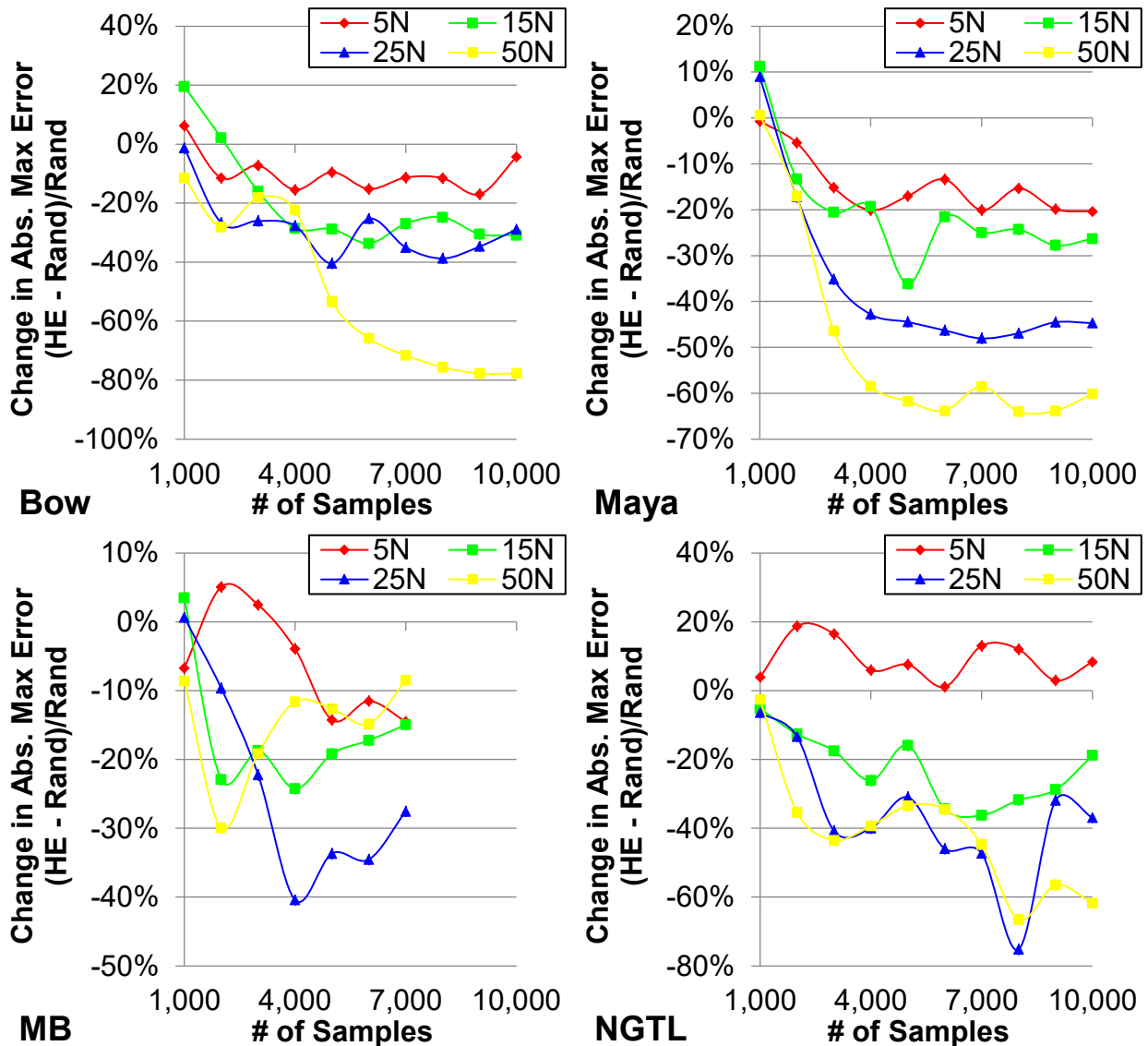


Figure D10: Change in absolute max error using random and high error sampling for proxy model using 5, 15, 25, and 50 nodes in hidden layers (uses external validation sample)

## D.4. Computing Time Required

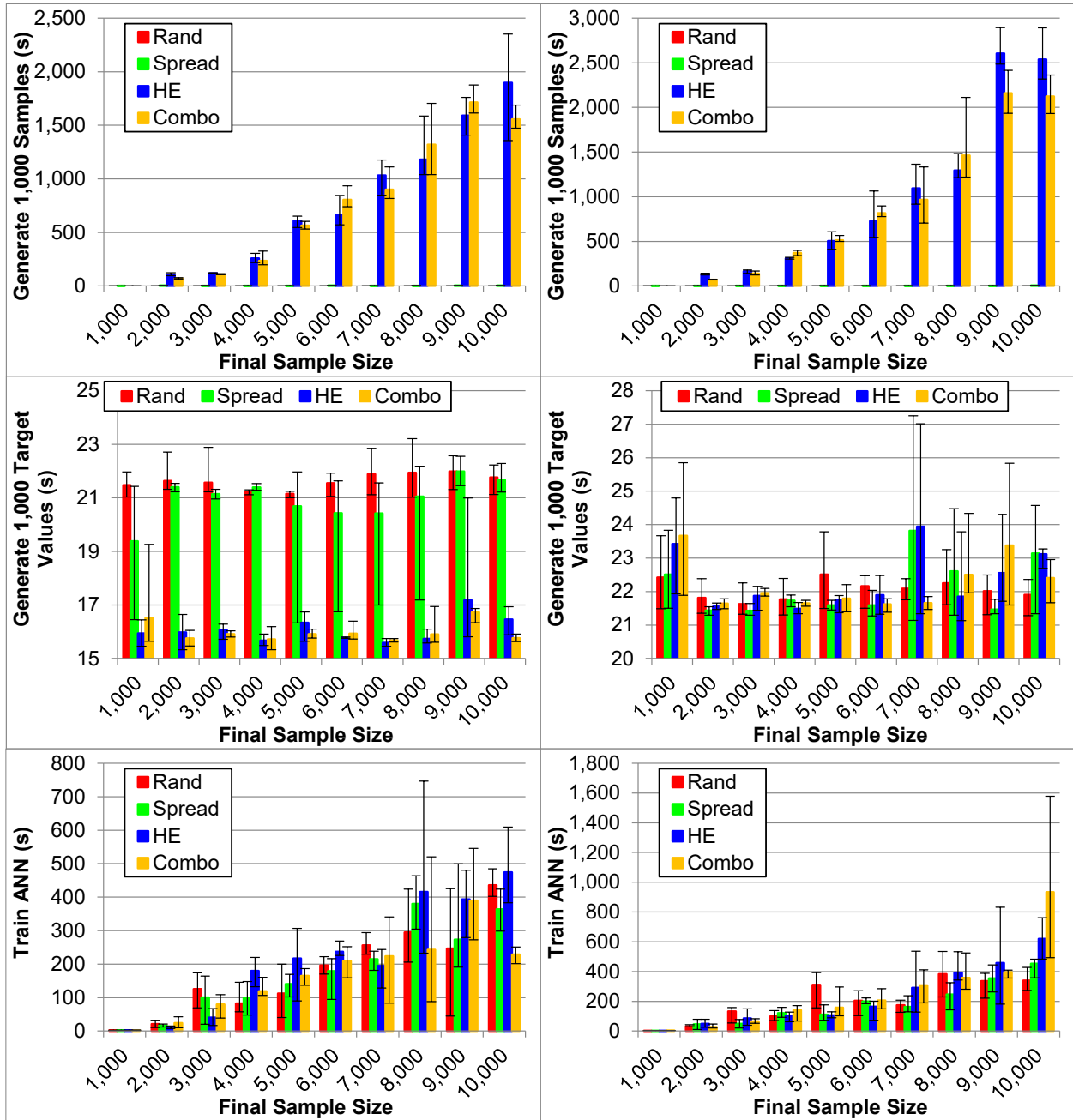


Figure D11: Sample generation, target value generation, and ANN training time for 50-node Maya (left) and Bow (right) proxy models

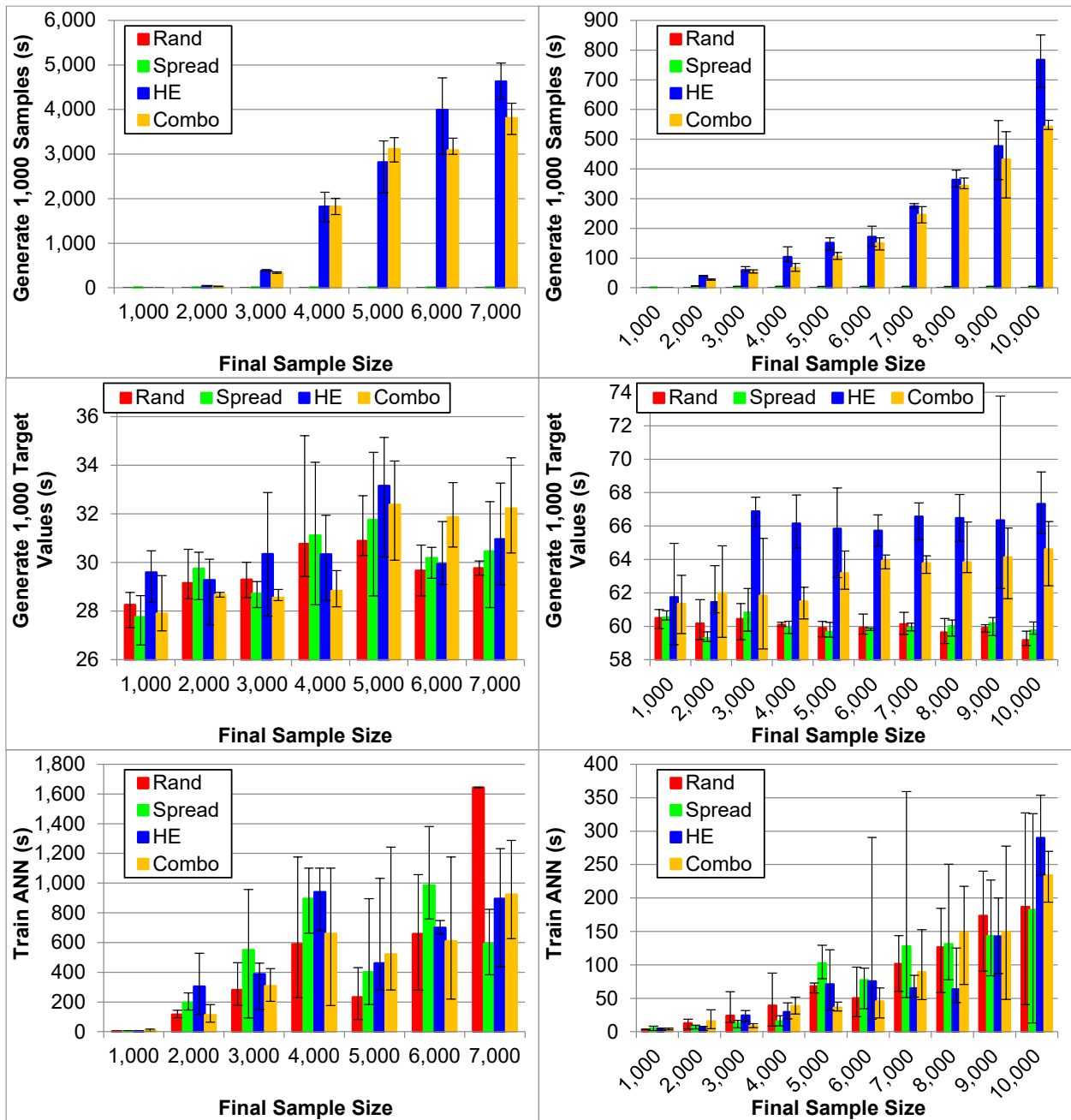


Figure D12: Sample generation, target value generation, and ANN training time for 50-node MB (left) and NGTL (right) proxy models

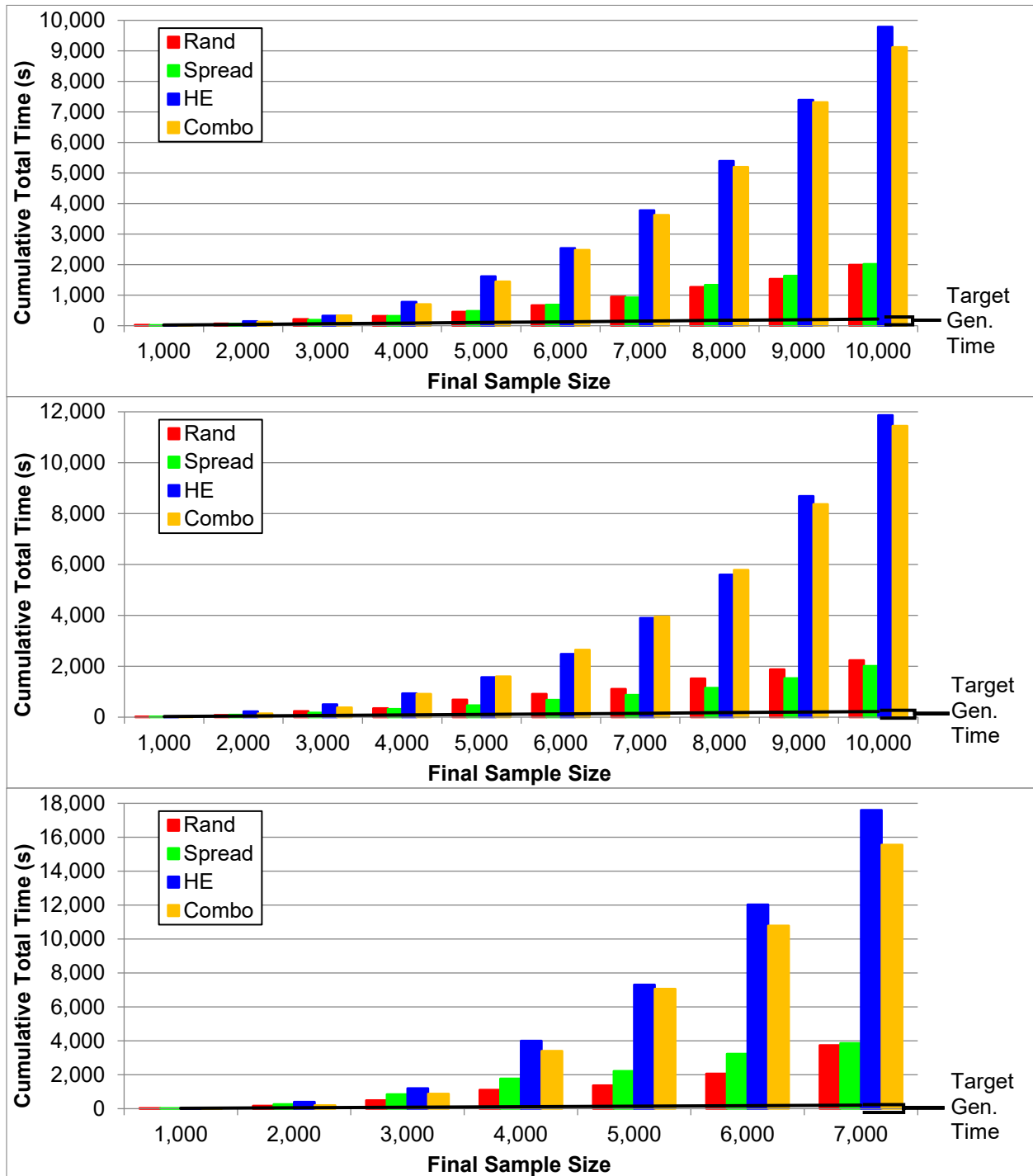


Figure D13: Cumulative total time to produce proxy models for Maya (top), Bow (middle), and MB (bottom)

## D.5. Summary of High Error and Combo Sampling Methods for NGTL

**Table D2: Cumulative combo vs. cumulative he sampling results [(Combo – HE)/HE]**

# Samples	2k	3k	4k	5k	6k	7k	8k	9k	10k
<b>Max</b>	68%	4%	57%	0%	-14%	17%	5%	0%	-2%
<b>Avg</b>	-8%	8%	-9%	-5%	-17%	0%	-20%	-8%	-18%
<b>P50</b>	-12%	2%	-14%	-10%	-22%	-6%	-24%	-14%	-22%
<b>Time</b>	-2%	-9%	-12%	-18%	-18%	-14%	-7%	-7%	-12%

**Table D3: Cumulative combo vs. one-shot rand sampling results [(Combo – Rand)/Rand]**

# Samples	2k	3k	4k	5k	6k	7k	8k	9k	10k
<b>Max</b>	137%	0%	20%	-29%	-45%	-44%	-53%	-57%	-63%
<b>Avg</b>	474%	306%	172%	152%	103%	108%	49%	52%	28%
<b>P50</b>	535%	364%	216%	194%	139%	145%	76%	77%	53%
<b>Time</b>	-78%	-63%	-41%	-15%	17%	68%	139%	221%	328%

**Table D4: Cumulative HE vs. one-shot rand sampling results [(HE – Rand)/Rand]**

# Samples	2k	3k	4k	5k	6k	7k	8k	9k	10k
<b>Max</b>	41%	-4%	-23%	-29%	-36%	-52%	-55%	-57%	-62%
<b>Avg</b>	522%	278%	199%	164%	146%	108%	87%	65%	56%
<b>P50</b>	622%	357%	266%	226%	205%	159%	132%	106%	95%
<b>Time</b>	-78%	-59%	-33%	3%	43%	94%	157%	244%	387%

## D.6. Sampling Algorithms Explained

In high dimensional space, the Manhattan distance is used instead of the Euclidian distance as it provides better representation in high dimensional space.<sup>191</sup> The distance to nearest neighbor (dNN) is calculated for each sample and plotted as a histogram to evaluate sample spread. The spread algorithm was developed iteratively to address shortcomings of the previous versions.

### D.6.1. Brute force spread algorithm

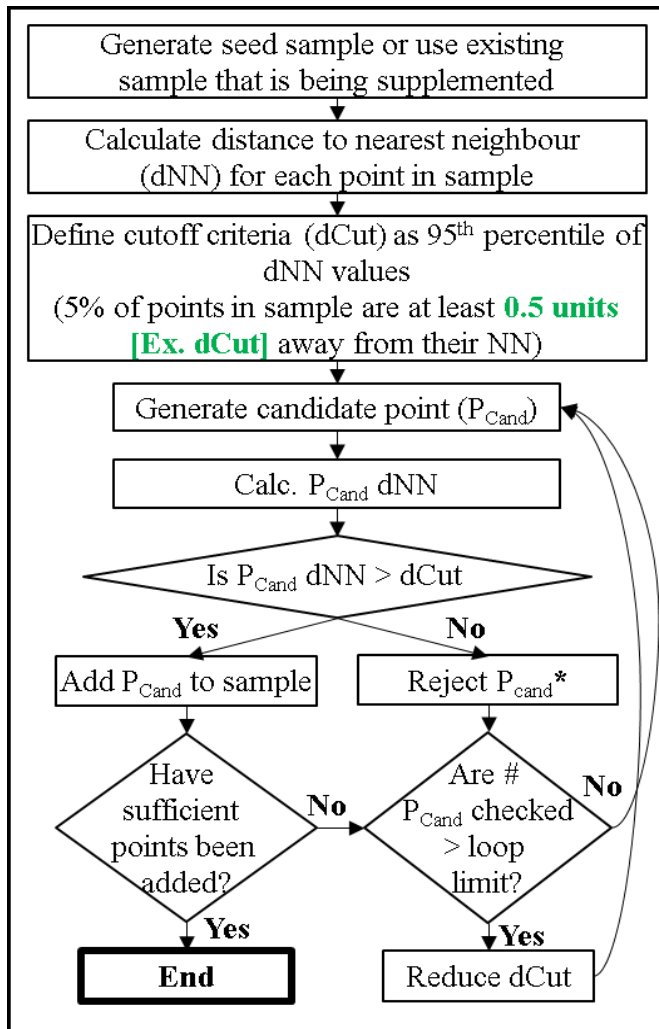


**Figure D14: Brute force spread algorithm (S-Brute), \*Rejected candidates are rechecked when dCut is reduced**

The first version used a brute force approach (S-Brute), shown in Figure D14. A small seed sample ( $n$  samples) is generated using a Monte Carlo simulation with uniform distributions for each input. The minimum distance between each point and its nearest neighbor is calculated; the 95th percentile value is then used as the cutoff criteria (dCut). Random candidates are generated, and if their nearest neighbor distance is greater than dCut, the candidate is added to the sample. If insufficient new samples have not been found after  $N_c$  candidate samples have been checked, dCut is relaxed using a step criteria, and the process is repeated. To speed up the process, candidate points with dNN lower than dCut but higher than the relaxed dCut are saved and rechecked once dCut is lowered. See Chapter D.8 for the base code used for this research.

### D.6.2. Optimized spread algorithm (S-Opt1)

Calculating the nearest neighbor distance (dNN) between the newly generated point and the existing sample is time consuming and becomes longer as the total sample size increases. An optimization method was introduced (Figure D15). The dNN is increased by moving the candidate sample away from its close neighbors. Rather than using all previous  $n$  samples,  $N_{CN}$  samples were used to determine what direction and how far to move the candidate sample. Using only  $N_{CN}$  samples reduces the computational burden while still improving the sample spacing.

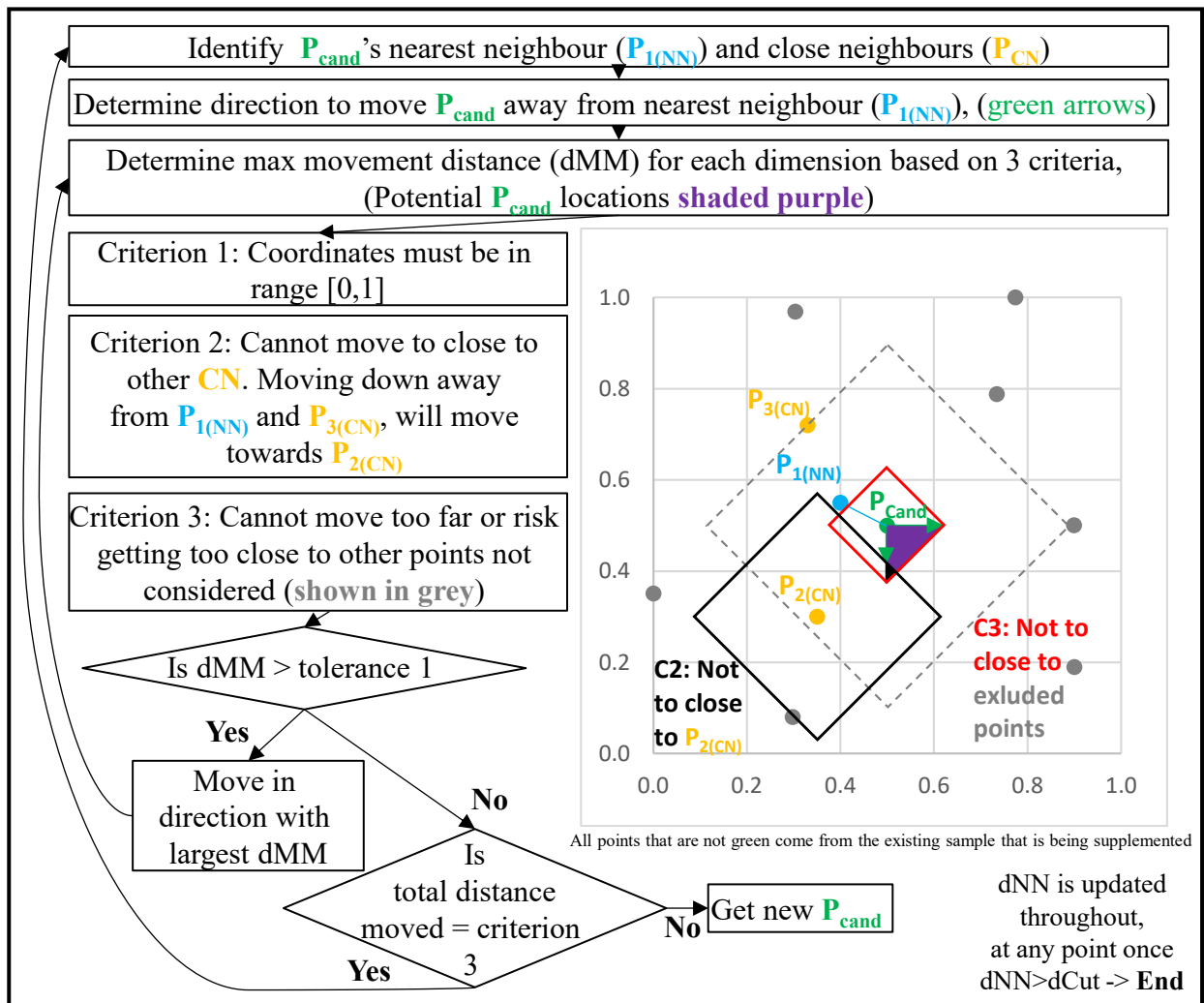


**Figure D15: Optimized Spread Algorithm**

The number of close neighbors (CNs) to include in the analysis is unclear. Including too many CNs increases the computing time to calculate dNN. Including too few CNs will cause the

algorithm to terminate once criterion 3 is reached; the criterion 3 distance is dependent on the distance to the farthest CN. If the solver is forced to terminate by criterion 3, the algorithm must recalculate the dNN for all the samples and identify new CNs, increasing computing time. In this work we assumed  $N_{CN}=2*p$ ; this was found to be acceptable for between 10 and 14 inputs. Further study is needed to determine if this relationship holds true for models with more inputs.

On average S-Brute, S-Opt1a and S-Opt1b increased the average dNN by 34, 43%, and 45%, respectively, while also reducing the 90% confidence interval by 72%, 72%, and 83%, respectively (Figure D16). In S-Opt1b, the starting dCut value was set to the average dNN from S-Opt1a, which increased computing time by setting a higher standard but also increased the average dNN. The performance boost between S-Brute and S-Opt1 depends on the sample size and initial dCut used.

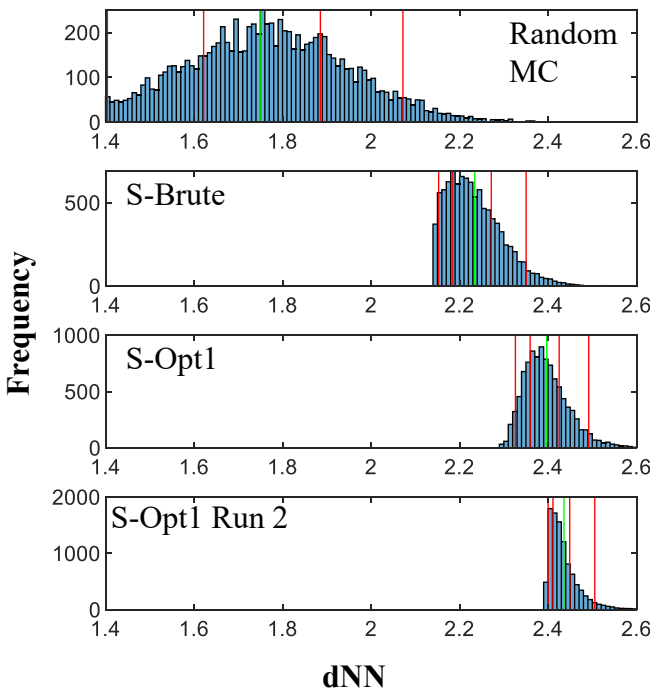


**Figure D16: dNN distributions for random and spread sampling; 10,000 samples and 10 inputs (red lines represent 5th, 25th, 75th, and 95th percentiles, respectively; green line represents average)**

### D.6.3. Optimized spread algorithm, preventing edge clustering (S-Opt2&3)

When S-Opt1 was used to train the ANN, it was found to have no statistically significant impact on model accuracy compared to random sampling. In some scenarios, the spread algorithm performed worse than the random method. Unlike the random method, the spread sample favored points that had extreme values (<0.1 or >0.9) and under-sampled the center region (Figure D19). Therefore, to improve the spread algorithm, modifications were made to increase the number of samples in the center region and produce a uniform distribution of input values to match those found in the random sample. Figure D19 was generated by starting with 1,000 randomly generated samples and then adding 1,000 samples/iterations using the specified algorithm until the final sample contained 10,000 samples. The S-Brute Algorithm had a similar spread profile as S-Opt1.

In S-Opt2, the first criterion (Figure D15) was modified to limit the bounds used to avoid extreme values. The maximum move distance for each input was reduced by multiplying the original distances by a random number between zero and 1. S-Opt2 only minorly reduced extreme spread values.

In S-Opt3, the first criterion was modified like S-Opt2, and the region where the starting candidate point was generated was restricted. In previous versions, the candidate point was generated randomly within the entire parameter space. In S-Opt3, Equations D1 & 2 are used to restrict the starting region close to the center. For each parameter, a value will be randomly generated and modified as follows:

$$Restrictor = \min \left[ \left( \frac{N_{Added} + 10}{N_{Needed} + 10} \right) + Throttler, 1 \right] \quad (\text{Eq. D1})$$

$$Cand_p = 0.5 + rand[-0.5,0.5] * Restrictor \quad (\text{Eq. D2})$$

where  $N_{Added}$  is the number of samples that have already been added,  $N_{Needed}$  is the number of samples needed, and  $Throttler$  is a tunable parameter. The restrictor percentage reflects how close to the center the candidate starting point needs to be; a value of 50% means the input

values must range between 0.25 and 0.75. By forcing the candidate to be selected near the center, we first ensure the central region is adequately sampled. As more samples are added and it is more difficult to find points near the center, the restrictor is relaxed. The throttle value controls how quickly the restrictor is relaxed. Using a throttler of 1 makes S-Opt3 equivalent to S-Opt2. The restrictor is plotted in Figure D17. The effect of the throttler on sample spacing is shown in Figure D18 for throttle values between 0.2 and 1.

While S-Opt3 could provide a near uniform spread, it requires the user to provide the tunable throttler parameter, which varies depending on the number of inputs in the sample. S-Opt4 removes the need to have a tunable parameter by instead evaluating the sample distribution throughout the sampling process and modifying the restrictor equation as:

$$Restrictor = \min \left[ \left( \frac{N_{Added} * OffsetSpeed + 10}{N_{Needed} + 10} \right) + OffsetStart, OffsetEnd \right] \quad (Eq. D3)$$

The offset speed, start, and end were calculated automatically by evaluating the spread of the current sample. Offset values are updated every time 50 new samples are added. See the SpreadOptimized4.m file for further information on how offset values are determined.

While the modifications to the optimized spread algorithms helped reduce oversampling the extreme tails, it did not improve the ANN accuracy. All S-Opt methods provided no statistically significant improvement compared to random sampling.

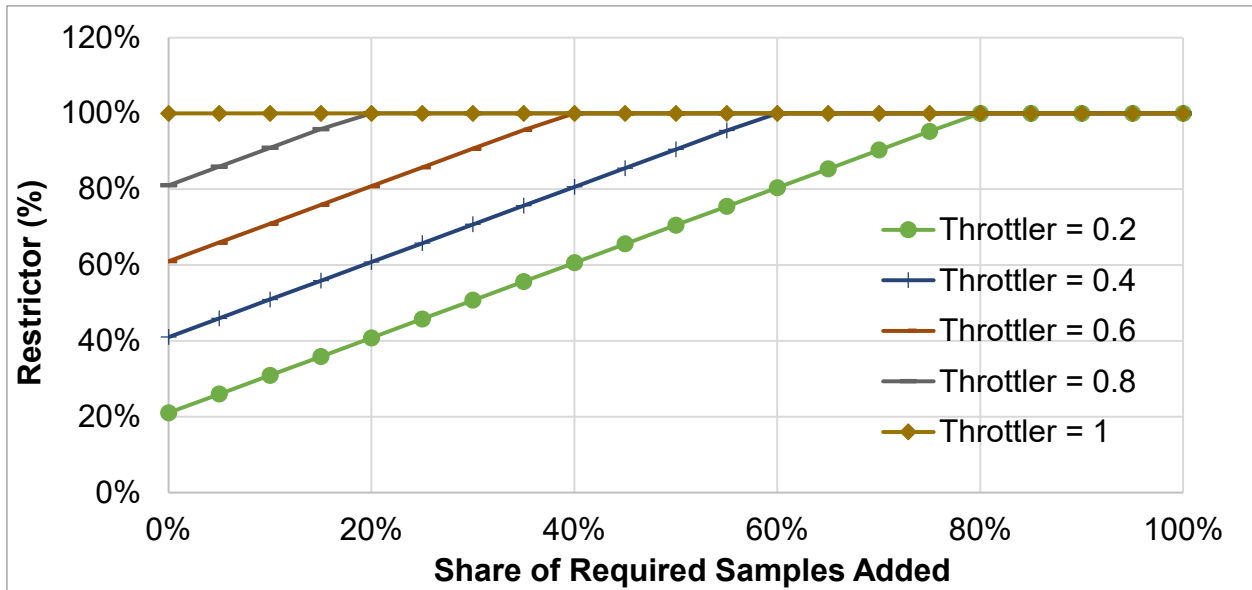


Figure D17: Restrictor as a function of throttler and share of required samples added

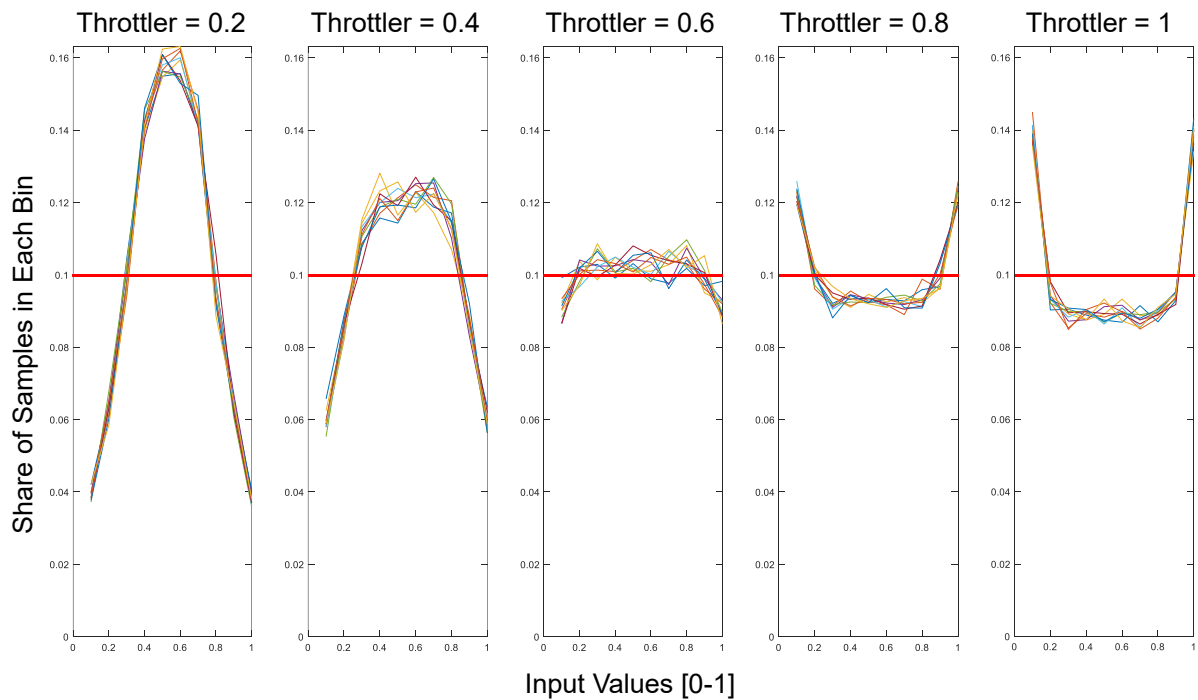
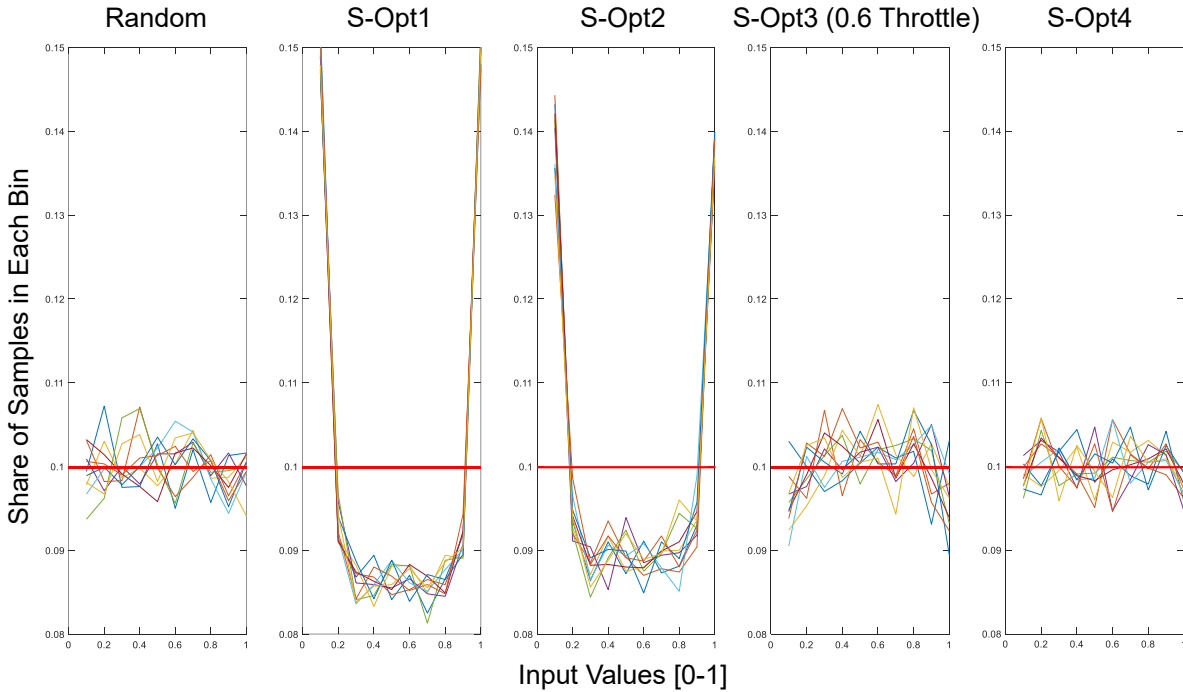


Figure D18: Impact of S-Opt3 throttler on sample distribution (bold red line represents ideal uniform distribution, colored lines represent different inputs [p=10], 10,000 samples total)



**Figure D19: Input distributions for various S-Opt algorithms (bold red line represents ideal uniform distribution, colored lines represent different inputs [p=10], 10,000 samples total)**

### D.7. MATLAB code modifications

In order to save the ANN weights and biases from the best epoch rather than the default last epoch, we modified the `trainlm` and `trainNetwork` codes. The best epoch weights are saved as “weightRecord.” “trainlm” is used with a single computer core, and “trainNetwork” is used with multiple cores. The best epoch weights are not currently available if a gpu is used.

The `trainlm` code is found on the following path: `C:\Program Files\MATLAB\R2019a\toolbox\nnet\nnet\nntrain\trainlm.m`

Starting on line 291, the modified code is highlighted in yellow:

```

% Track Best Network
[worker.perf,worker.vperf,worker.tperf,worker.je,worker.jj,worker.gradient] =
calcLib.perfsJEJJ(calcNet);
if calcLib.isMainWorker
    [worker.best,worker.tr,worker.val_fail] = nnet.train.trackBestNetwork(...
worker.best,worker.tr,worker.val_fail,calcNet,worker.perf,worker.vperf,worker
.epoch);
    %%%modified to export the weights for the best fit model instead of

```

```
    %%%the final epoch weights
    try
        wr = evalin('base','weightRecord');
    catch
        wr = {};
    end
    wr = calcLib.getwb(calcNet);
    assignin('base','weightRecord',wr);
    %%%%%%%%%%%
end
```

The trainNetwork code is found along the following path:

sdwtrainNetwork.m

Starting on line 178, the modified code is highlighted in yellow:

```
% Update feedback (using values got from main worker)
    main = mainC{mainWorkerInd
```